Universidade de Aveiro Departamento de Ciências Médicas

Universidade NOVA de Lisboa Faculdade de Ciências Médicas

2017

Roberto Alexandre dos Santos Dias

Caracterização do papel da Gαo na neuritogénese: um destaque para o complexo Gαo-Proteina Precursora de Amilóide

Characterization of Gαo role on neuritogenesis: a focus on the Gαo-Amyloid Precursor Protein complex

Universidade de Aveiro Departamento de Ciências Médicas

Universidade NOVA de Lisboa Faculdade de Ciências Médicas

2017

Roberto Alexandre dos Santos Dias

Caracterização do papel da Gαo na neuritogénese: um destaque para o complexo Gαo-Proteina Precursora de Amilóide

Characterization of Gαo role on neuritogenesis: a focus on the Gαo-Amyloid Precursor Protein complex

Tese apresentada à Universidade de Aveiro para cumprimento dos requisitos necessários à obtenção do grau de Doutor em Biomedicina, realizada sob a orientação científica da Doutora Sandra Isabel Moreira Pinto Vieira, Professora Auxiliar Convidada do Departamento de Ciências Médicas da Universidade de Aveiro e da Doutora Odete Abreu Beirão da Cruz e Silva, Professora Auxiliar Convidada com Agregação do Departamento de Ciências Médicas da Universidade de Aveiro

Este trabalho é financiado por Fundos FEDER através do Programa Operacional Factores de Competitividade – COMPETE e por Fundos Nacionais através da FCT – Fundação para a Ciência e a Tecnologia no âmbito do projeto «PTDC/SAU-NMC/111980/2009»; por Fundos da FCT e do programa POPH/FSE no âmbito da bolsa individual «SFRH/BD/90996/2012»; e pelo Instituto de Biomedicina – iBiMED «UID/BIM/04501/2013».

Dedico este trabalho aos meus pais por acreditarem sempre em mim

o júri

presidente

Doutor João Carlos Matias Celestino Rocha
professor Catedrático do Departamento de Química da Universidade de Aveiro

Doutor Carlos Jorge Alves Miranda Bandeira Duarte
professor Associado com Agregação do Departamento de Ciências da Vida da Universidade de Coimbra

Doutora Fernanda Cristina Gomes de Sousa Marques
investigadora Auxiliar do Instituto de Investigação em Ciências da Vida e Saúde da Universidade do Minho

Doutora Sandra Maria da Costa Tavares Rebelo
professora Auxiliar Convidada do Departamento de Ciências Médicas da Universidade de Aveiro

Doutora Sandra Isabel Moreira Pinto Vieira
professora Auxiliar Convidada do Departamento de Ciências Médicas da Universidade de Aveiro

agradecimentos

À professora Sandra Vieira e à professora Odete da Cruz e Silva pela orientação e apoio durante a elaboração deste trabalho

À Joana Rocha, Regina Cerqueira e Bruno Gonçalves, sem os quais este trabalho não teria sido possível.

Aos meus colegas do CBC e iBiMED que fizeram parte deste percurso, em especial à Ana Marote, Catarina Pinho, Filipa Martins, Joana Oliveira, Joana Serrano, Liliana Carvalho, Luisa Bastos, Mariana Santos, Marlene Marafona, Patricia Tenreiro e Soraia Martins.

À Juliana, Joana, Miguel e Tiago.

Ao Hugo, João, Marco e Fred.

Ao Joni, João, Ana Isabel, Denise e Patricia.

To Hideo Kojima, Hidetaka Miyazaki, Neil Gaiman, Andrzej Sapkowski, Stephen King, and many others that, without knowing, made this journey so much easier.

À minha família pelo apoio que sempre me deram.

E à Maria, por nunca se fartar de me ouvir dizer dispartes.

palavras-chave

diferenciação neuronal, fosforilação, STAT3, ERK1/2, proteassoma, lisossoma, degradação de proteínas, ImageJ, células SH-SY5Y

resumo

Gαo é a subunidade Gα mais abundante no cérebro, no entanto, as suas funções especificas ainda estão longe de serem claras. Estudos das vias de sinalização moduladas pela Gαo têm exposto potenciais papéis para a Gαo no desenvolvimento do sistema nervoso, especialmente em neuritogénese. A caracterização do interactoma da Gαo também tem sido crucial para uma melhor compreensão das funções desta proteína. Uma das proteínas interatoras da Gαo é a proteina precursora de amiloide (APP), uma proteina que se encontra envolvida em várias funções fisiológicas, como sobrevivência celular, migração neuronal, e diferenciação neuronal. APP também é mais conhecida pelo seu envolvimento da Doença de Alzheimer (AD). APP liga-se e ativa a Gαo, uma interação que tem sido associada com migração neuronal e AD. No entanto, até agora, não existem estudos publicados que investiguem a interação APP-Gαo na neuritogénese. O principal objetivo deste trabalho foi então caracterizar o papel da Gαo na neuritogénese através do foco na investigação dos efeitos neuritogénico do complexo Gαo-APP.

Primeiro, através do uso de células de neuroblastoma SH-SY5Y, estudámos o impacto da fosforilação da serina 655 (S655) da APP na interação APP-Gαo. Através do uso de dois mutantes da APP que mimetizam o estado fosforilado e desfosforilado da S655, SE e SA APP respetivamente, demonstrámos que a fosforilação da S655 aumenta a eficiência da APP em ligar e ativar a Gαo. Além disso, apresentamos provas de que a APP modula os efeitos neuritogénicos da Gαo num mecanismo fosfo-dependente. Neste mecanismo neuritogénico, a sinalização da STAT3 e ERK1/2 exibiram uma ativação sequencial, com a STAT3 participando na formação de novos processos e a ERK1/2 na elongação dos mesmos. Apresentamos ainda dados que suportam um papel da APP-Gαo na dendritogénese em culturas neuronais primárias.

A segunda parte deste trabalho focou-se na investigação de mecanismos envolvidos no controlo dos níveis proteicos celulares da APP e Gαo. Identificámos o lisossoma como um novo processo pelo qual a Gαo é degradada em consequência da sobre expressão da SA APP. Também mostramos provas de que este mecanismo pode fazer parte de autofagia mediada por chaperonas, através do qual a sinalização da APP-Gαo poderá estar a ser regulada.

Finalmente, devido ao nosso interesse em estudar diferenciação neuronal e à falta de ferramentas para este estudo em imagens de contraste de fase, criámos o NeuronRead, uma macro do ImageJ capaz de analisar de forma semiautomática imagens neuronais de contraste de fase e fluorescência. NeuronRead foi extensivamente validado, e usado para monitorizar a diferenciação de células SH-SY5Y após modulação da atividade da Gαo.

Com este trabalho contribuímos com novos dados que ajudam na compreensão da função e regulação do complexo Gαo-APP, e disponibilizamos para a comunidade cientifica uma nova ferramenta para o estudo da diferenciação neuronal

keywords

neuronal differentiation, phosphorylation, STAT3, ERK1/2, proteasome, lysosome, protein degradation, ImageJ, SH-SY5Y cells

abstract

Gαo is the most abundant Gα subunit present in the brain, however, its specific functions are still far from clear. Studies of the signaling pathways modulated by Gαo have uncovered potential roles for Gαo in the development of the nervous system, especially in neuritogenesis. The characterization of Gαo interactome has also been crucial for the better understanding of this protein's functions. One of the Gαo interacting proteins is the amyloid precursor protein (APP), a protein that is involved in several physiological functions, such as cell survival, neuronal migration, and neuronal differentiation. APP is also best known for its involvement in Alzheimer's Disease (AD). APP binds and activates Gαo, an interplay that was associated with neuronal migration and AD. However, so far, no published study has investigated the effects of the APP-Gαo interaction on neuritogenesis. The main goal of this work was thus to characterize Gαo role on neuritogenesis by focusing the research on the neuritogenic effects of the Gαo-APP complex.

First, by using SH-SY5Y neuroblastoma cells, we studied the impact of APP serine 655 (S655) phosphorylation on the APP-Gαo interaction. Through the use of two APP mutants mimicking the phosphorylated and dephosphorylated state of S655, SE and SA APP respectively, we have demonstrated that S655 phosphorylation increases APP efficiency to bind and activate Gαo. Moreover, we present evidence that APP modulates Gαo neuritogenic effects in a phospho-dependent mechanism. STAT3 and ERK1/2 signaling displayed a sequential activation on this neuritogenic mechanism, with STAT3 being mainly involved in the formation of new processes, while ERK1/2 was more involved in neuritic elongation. We also present data supporting a role for the APP-Gαo complex on dendritogenesis in rat primary neuronal cultures.

The second part of this work focused on unraveling the mechanisms involved in the control of APP and Gαo cellular protein levels. We identified the lysosome as a new pathway by which Gαo is degraded, as an effect of SA APP overexpression. We also provide evidence that this degradation mechanism might be part of chaperone-mediated autophagy, through which APP-Gαo signaling might be regulated.

Finally, due to our interest in studying neuronal differentiation and a lack of reliable tools to analyze phase contrast images, we developed NeuronRead, an ImageJ macro capable of semi-automated analysis of both phase contrast and fluorescence neuronal images. NeuronRead was extensively validated and used to monitor SH-SY5Y differentiation upon modulation of Gαo activity.

With this work, we delivered new data that advances knowledge on the function and regulation of the Gαo-APP complex in a neuronal context, and provided the scientific community with a new tool for the study of neuronal differentiation.

Table of contents

Table of Figures

Table of Supplementary Material

Abbreviations

5-HT	Serotonin
AD	Alzheimer's disease
ADF	Actin depolymerizing factor
ADP	Adenosine diphosphate
AICD	APP intracellular C-terminal domain
ANOVA	Analysis of variance
AP	Adaptor protein
APLP	Amyloid precursor-like protein
APP	Amyloid precursor protein
APPL	β-amyloid-like protein
Arp	Actin-related protein
Aβ	Amyloid β-peptide
BACE	β-site APP-cleaving enzyme
BCA	Bicinchoninic acid
BDNF	Brain-derived neurotrophic factor
BSA	Bovine serum albumin
CA	Constitutively active
CaMKII	calcium-calmodulin-dependent protein kinase II
cAMP	cyclic adenosine monophosphate
CB1R	Type 1 cannabinoid receptor
cdc42	Cell division control protein 42
CMA	Chaperone-mediated autophagy
CQ	Chloroquine
CREB	cAMP response element binding protein
CTF	C-terminal fragment
DAPI	4',6-diamidino-2-phenylindole
DIV	Days in vitro
DN	Dominant negative
DoG	Difference of Gaussians
ECL	Enhanced chemiluminescence

EGF	Epidermal growth factor
EGFR	Epidermal growth factor receptor
ERK	Extracellular signal-regulated kinase
FAD	Familial Alzheimer's Disease
FBS	Fetal bovine serum
FC	Fold change
FGF	Fibroblast growth factor
Fluor	Fluorescence
GAP	GTPase-accelerating protein
GAP43	Growth-associated protein 43
GDI	Guanosine dissociation inhibitor
GDP	Guanosine diphosphate
GEF	Guanine nucleotide exchange factor
GFP	Green fluorescent protein
GNAO1	Gαo gene
GPCR	G protein-coupled receptor
GR	Golgi region
GRIN	G protein-regulated inducer of neurite outgrowth
GSK3	Glycogen Synthase Kinase 3
GTP	Guanosine triphosphate
holoAPP	Full length APP
Hsc70	Heat shock cognate protein 70
Hsp90	Heat shock protein 90
ICC	Immunocytochemistry
IGF	Insulin-like growth factor
IL-6	interleukin-6
JAK	Janus kinase
JNK	c-Jun N-terminal kinase
KO	Knockout
KPI	Kunitz-type protease inhibitor
Lac	Lactacystin
LAMP2	Lysosome-associated membrane protein 2
LTD	Long-term depression

LTP	Long-term potentiation
M1AChR	Muscarinic acetylcholine receptor M1
MAP	Microtubule-associated protein
MAPK	Mitogen-activated protein kinase
MCH	Melanin-concentrating hormone
MEK	MAPK/ERK kinase
MIS	Müllerian inhibiting substance
NGF	Nerve growth factor
NMJ	Neuromuscular junction
NT	Neurotrophin
O/N	Overnight
ORL	Opioid receptor-like
p75NTR	Neurotrophic receptor p75
PACAP	Pituitary adenylate cyclase-activating peptide
PAGE	Polyacrylamide gel electrophoresis
pAPP	Phosphorylated APP
PAR	Protease-activated receptor
PBS	Phosphate buffered saline
PDBu	Phorbol 12,13-dibutyrate
PDK1	phosphoinositide-dependent kinase 1
PhC	Phase contrast
PI3K	Phosphatidylinositol 3-kinase
PIP3	phosphatidylinositol (3,4,5)-tri-phosphate
PKA	Protein kinase A
PKC	Protein kinase C
PM	Plasma membrane
PSD-95	Postsynaptic density protein 95
PSI	Proteasome inhibitor I
PTX	Pertussis toxin
RA	Retinoic acid
RGS	Regulator of G-protein signaling
ROI	Region of interest
S&P	Salt and pepper

S655	Serine 655
sAPP	secreted or soluble APP
SDS	Sodium dodecyl sulfate
SE	Structuring element
SEM	Standard error of the mean
STAT	Signal transducer and activator of transcription
TAG	Transient axonal glycoprotein
TBS-T	Tris-buffered saline with Tween 20
Tf	Transfection
TGFβ	Transforming growth factor β
TGN	Trans-Golgi network
Trk	Tyrosine receptor kinase
WB	Western blot
Wt	Wild-type

A. General Introduction and Aims

A1. Neuronal Differentiation

The brain is a complex organ made of different types of highly specialized cells. The main "unit" of the brain is the neuron, a cell with a very characteristic morphology. The neuron is composed of a long process called the axon, that can grow for longer than 1 meter, and several shorter but highly branched processes called dendrites. The mechanism by which neurons acquire this morphology has been the subject of intense study in neurosciences. From the initial morphological changes that undifferentiated cells suffer when they start to form new processes to the formation of synapses between mature neurons, and all the signaling pathways underlying these different steps in neuronal differentiation, these are mechanisms that researchers have explored to better understand how neurons work. Understanding neuronal differentiation has also shed light on other mechanisms, such as neuronal regeneration, that can prove essential to the understanding and treatment of several neuropathologies.

A1.1. Neuritogenesis and Acquisition of Neuronal Polarity

Early embryonic neurons are spherical cells, so the first step of neuronal differentiation involves the formation of membrane extensions that will become neurites. This step is designated by neuritogenesis, but is also usually called neurite outgrowth or neurite initiation/extension, and is accompanied by an extensive reorganization of the cytoskeleton [1, 2]. After the initial formation of neurites, these have to differentiate into axons and dendrites, in a phenomenon called neuronal polarization [3, 4]. Both neuritogenesis and neuronal polarization are highly dynamic mechanisms and must occur in tandem so that neuronal differentiation is properly developed. Earlier research has established the different developmental stages that cultured hippocampal neurons go through (Figure A1.1) [5]. In stage 1, which *in vitro* occurs during the first hours after plating, cells extend their membranes around them, creating the lamellipodium. This is a filamentous actin (F-actin) structure that makes cells strongly adhere to the cell plates. Several small finger-like F-actin processes start to appear at the edge of the membrane, named filopodia. In stage 2, that occurs throughout the first day of differentiation, the filopodia start to enlarge, giving rise to several neurites. At this point, all neurites are virtually indistinguishable, with each one having the potential to further elongate and develop into the axon. These two first stages encompass the bulk of neuritogenesis. Stage 3 sees the beginning of neuronal polarity, with one neurite starting to grow

significantly faster than the rest (5-10x faster), eventually becoming the axon. Stage 4 occurs 2-3 days after the initial axon growth, usually around 4 days after cells plating, and it is characterized by the growth and branching of the remaining neurites that will make the dendritic tree. At this time, the axon continues to elongate, although to a slightly lower rate (but still at least 5x faster than dendrites). Stage 5 is the maturation of the neuron, characterized by the formation dendritic spines, where cell-to-cell contacts are made in the form of synapses [6]. Several other studies have been published describing neuronal differentiation both *in vitro* and *in vivo*, and looking at different types of neurons. Neuritogenesis and neuronal polarization occur roughly the same in cortical neurons *in vivo*, with a few differences [4, 7, 8]. For example, excitatory cortical neurons start their differentiation in the cortical ventricular zone of the developing embryo by forming several neurites, thus becoming a multipolar cell. One of these neurites suffers elongation and becomes a trailing process, that further develops into the axon, while another neurite becomes the leading process, defining the neuron's first dendrite. The remaining neurites suffer a retraction, thus turning the cell into a bipolar neuron. At this stage these neurons migrate through the cortical plate into the marginal zone. That is why the future dendrite is called the leading process (the process that "guides" the migration) whereas the future axon is called the trailing process (the process that follows behind the migratory neuron) [9–11]. Upon reaching the marginal zone of the cortical plane, the neuron matures, with the leading process suffering further elongation and ramification to become the dendritic tree.

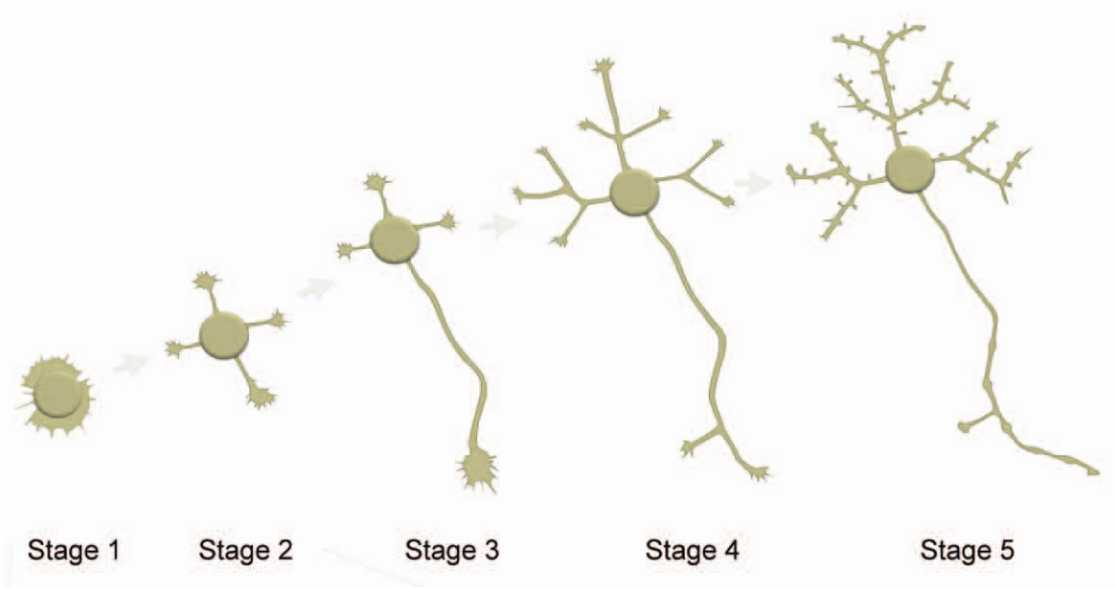

Figure A1.1. Stages of Neuronal Differentiation. Stage 1: Formation of Lamellipodia; Stage 2: Neurite outgrowth; Stage 3: Axon specification and elongation; Stage 4: Dendritic growth; Stage 5: Neuronal maturation and synaptogenesis. Image adapted from [2].

A1.2. Cytoskeleton remodeling during neuronal differentiation

A1.2.1. Lamellipodia and Filopodia formation

Neuritogenesis starts with the assembly of actin filaments on the edge of the differentiating neuron (Stage 1). These actin filaments, a result of actin polymerization, form two distinct structures: the lamellipodium, a sheet-like extension of the plasma membrane all around the cell; and the filopodia, several thin protrusions, comprising bundles of actin filaments, that arise from the lamellipodium [12, 13]. The exact mechanism that leads to the formation of filopodia it is still not completely clear. Some studies describe the formation of branches of actin filaments within the lamellipodium by association of proteins to the filaments barbed end (the fast-growing end, or plus-end). Subsequent recruitment of fascin to the barbed ends culminates in the bundling of different actin filaments and the filopodia formation [1, 14, 15]. This is called the convergent model. The *de novo* nucleation model, or tip nucleation model, describes filopodia formation as actin filaments present in the lamellipodium that are nucleated by formin proteins, thus growing and protruding out and that are later crosslinked together by fascin [16, 17]. The presence of common players (e.g. fascin) between both models indicates that the real formation of filopodia might comprise a mix of both mechanisms [1, 17]. As evidenced by both models, actin dynamics are the main force behind neurite initiation and elongation. Continuous polymerization/depolymerization of actin filaments is required for the elongation of the filopodia, in a "treadmilling" mechanism [14]. In this mechanism, there is an exchange of actin subunits (globular actin, G-actin) between the pointed end (minus end) and the barber end (plus end) of the actin filament. Polymerization occurs at the barber end (addition of G-actin), while depolymerization occurs at the pointed end (removal of G-actin) [2, 14]. This mechanism allows the actin filament to "push" against the plasma membrane and thus elongate the filopodia [18].

A1.2.2. Neurite stabilization and maturation

Filopodia are highly dynamic structures, suffering continuous formation and retraction. To stabilize these processes and form neurites (Stage 2), it is required the involvement of another component of the cell cytoskeleton, the microtubules [1, 19]. The microtubule subunit is a heterodimer of two types of tubulin, α and β. Of the several known α and β subunits, β-III tubulin is the only isoform specific to neurons and its expression is increased during neurite outgrowth [1, 20, 21]. After the formation of the filopodia, microtubules formed at the centrosome start to extend into the

filopodia. This extension occurs either by re-distribution of stable microtubules into the actin filopodia or through polymerization of new microtubules [1, 19, 22]. The stabilization of the microtubules and maturation of the first neurite normally results in the commitment of this neurite to axon specification [23, 24].

Lamellipodia and filopodia remain present at the extremity of the growing neurite, in a structure called growth cone. This structure is present in all neurites, but it is especially dynamic and active in the first neurite, contributing to its faster extension and eventual differentiation into the neuronal axon (Figure A1.2) [4, 25]. Filopodia are also formed during dendritic and axonal growth, and, if matured, give rise to dendritic and axonal branches, an essential step in neuronal differentiation that allows a single neuron to make contact with thousands of other cells [26].

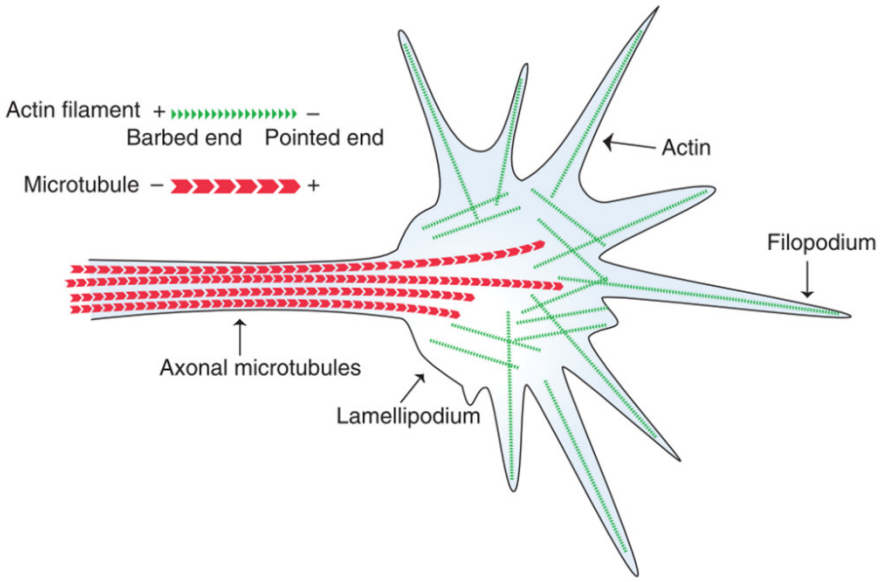

Figure A1.2. Growth cone structure. Actin (Green) forms lamellipodia and filopodia at the extremity of the growth cone, while microtubules (red) extend through the neurite into the growth cone to stabilize it. Adapted from [3].

A1.2.3. Control of Actin and Microtubules Dynamics

Several proteins are involved in the control of actin polymerization/depolymerization, and in the control of microtubules transport and stabilization. The Arp2/3 complex is one of the main factors involved in actin nucleation (assembly of actin monomers) [15], being essential in the formation of actin filaments, and plays a role in the formation of the lamellipodia [1, 3, 12]. Its exact role on neurite outgrowth it is still not completely clear, though, with different studies pointing to either a role of Arp2/3 in neurite formation [27, 28], or Arp2/3 inhibition having no impact on the formation of filopodia [29]. Cofilin I and ADF (actin depolymerizing factor) are two members of the cofilin

family abundantly present in the growth cone. They act by binding to the pointed end of the actin filaments and thus promoting the depolymerization of actin, driving neurite elongation [3, 30]. Other proteins that influence actin dynamics include WAVE, Ena/VASP, and profilin [1, 3].

The main regulators of microtubules dynamics are the MAPs (microtubule-associated proteins). MAP1b promotes microtubule nucleation, polymerization and stabilization, and is believed to be a bridge between actin and microtubules, regulating both neurite elongation and branching [1, 26, 31]. MAP2 also stabilizes microtubules but has the additional function of binding to actin and participate in the formation of the actin bundles [22, 26]. MAP2 and MAP tau are also specially interesting because of their differentially localization in mature neurons, with MAP2 being specific to the dendrites, and MAP tau being enriched in the axon, highlighting possible specific functions for the different MAPs during neuronal polarization [22, 32].

A1.3. Axon specification

As previously mentioned, an early neuron starts its differentiation by protruding several equivalent neurites (Stage 1-2). However, one of these neurites at one point starts to elongate much faster than the remaining ones, and eventual becomes the axon (Stage 3-4) [5]. The extensive reorganization the cytoskeleton suffers during neuronal differentiation is especially evident in the growth cone of the future axon, with a high degree of actin instability and the stabilization of microtubules being key in this mechanism [24, 33, 34], however there is still little information about what triggers one neurite to elongate in detriment of the rest. One model explaining the beginning of neuronal polarization is the “Touch & Go” model. In this model, cell-to-cell interactions between the pioneering axon of a pyramidal neuron and the neurite of a multipolar cell triggers the cytoskeleton remodeling in the neurite of the latter that leads to its elongation into an axon, a mechanism dependent on the cell-adhesion molecule transient axonal glycoprotein 1 (TAG1) (the signaling pathways underling this mechanism will be discussed further ahead) [4, 8, 35]. Cell-cell interactions mediated by N-cadherin are also important to trigger axonal specification, since knockdown of this protein disrupts the efficient transformation of a multipolar cell into a bipolar cell [4, 36].

Several extracellular cues are also involved in axon specification and growth, such as the brain-derived neurotrophic factor (BDNF), neurotrophin 3 (NT3), Reelin, transforming growth factor (TGFβ), insulin-like growth factor 1 (IGF1), semaphorins and Wnts [4, 6, 8]. Prevailing theories

suggest that these factors might act in an autocrine or paracrine way not only to trigger axon specification but to also maintain its elongation (Figure A1.3) [6, 8]. Differential distribution of these factors in vivo, such is the case of TGFβ, could also help explain the axon specification on different areas of the developing brain [4]. The gradient of neurotrophic factors existing in the medium could also explain why only one neurite develops into an axon. Accumulation of these factors on the growing axon location could mean a lack of stimuli on the other neurites, resulting in an inhibition of their growth [37].

The activation of different intracellular signaling pathways also regulates axon initiation and extension, but these will be discussed in a later section.

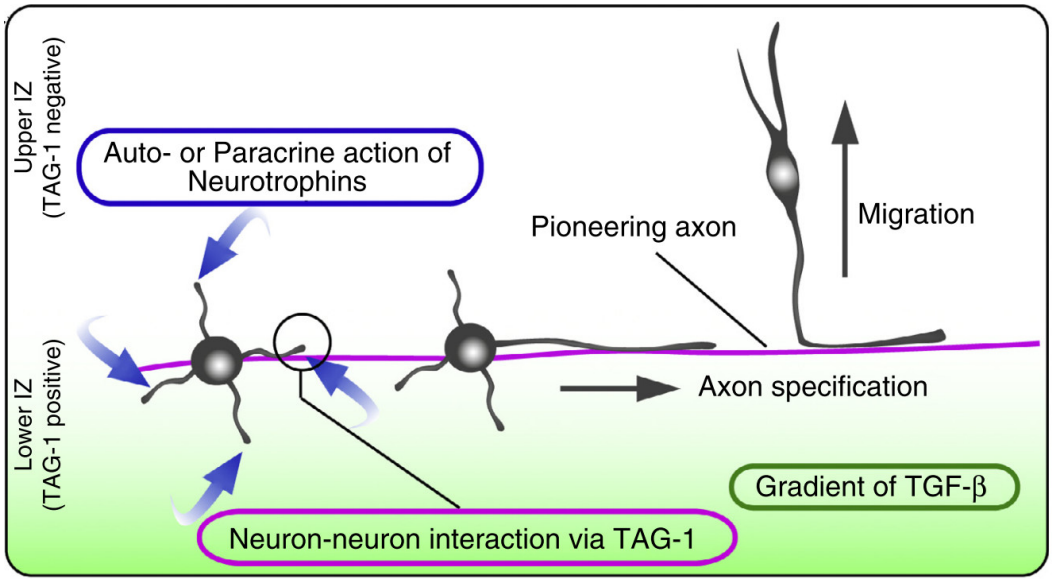

Figure A1.3. Different factors that influence axon specification in vivo. Neurotrophins released by neuronal cells act in a paracrine and autocrine to activate intracellular signaling pathways (Blue). Similar signaling pathways are activated by cell-to-cell contacts (purple). Gradients of extracellular molecules drive both axonal polarization as well as neuronal migration. Adapted from [8].

A1.4. Dendritic vs Axonal structure

Though at first glance dendrites are just shorter and more ramified versions of the axon, there are key structural differences between both type of neuronal processes. As mentioned above, after filopodia elongation through actin remodeling, microtubules invade the filopodia to mature it into a neurite. While in the axon the microtubules are densely packed and are uniaxially orientated (their minus end is always facing the cell body and their plus end is always facing the growth cone, Figure A1.2), in the dendrites microtubules have both orientations [23]. While is not completely clear why these differences arise, MAP2 and tau different localizations to the dendrites and axon, respectively, could play a role in the microtubule orientation [24].

A1.5. Synaptogenesis

Neuronal differentiation culminates with the formation of cell-cell contacts defined as synapses (Stage 5). Synapses are the main place of data transmission between neurons and are one of the most dynamic structures of the adult brain [38]. A synapse consists of a presynaptic terminal (axonal side), a postsynaptic terminal (dendritic side) and a synaptic cleft separating both [39] (this defines the chemical synapses, electrical synapses will not be explored here). There are reports of two ways neurons establish synapses[40]. In the postsynaptic spine hypothesis, filopodia developed in the dendrites establish contact with presynaptic neurons, which triggers the filopodia maturation into dendritic spines and consequently the formation of the synapse [26, 40]. In the presynaptic hypothesis, it is the axon who initiates the synapse formation. The axon continues to grow until it reaches near a postsynaptic terminal. At this point, a signal terminates the axonal growth cone elongation and starts its maturation into a presynaptic terminal[40]. This signal might be mediated by collapsins [41], with the activation of the Wnt-7a signaling playing a part in the maturation of the presynaptic terminal[42]. The differences in both models could relate to the synaptogenesis in different types of neurons. Moreover, synaptogenesis in the adult brain seems to be regulated by different mechanisms, related to neuronal activity [43].

A1.6. Signaling during neuronal differentiation

While neuronal differentiation is ultimately a result of an extreme reorganization of the cell cytoskeleton, there are several signaling pathways that control this remodeling. From extracellular cues, like BDNF, to intracellular proteins, such as the Rho family or the MAPK/ERK pathway, there are a lot of factors that intervene in the different steps, from the initial filopodia formation to the acquisition of the neuronal polarity and formation of synapses.

A1.6.1. Brain Derived Neurotrophic Factor (BDNF)

BDNF is a neurotrophin produced and secreted by neurons that has been for a long time implicated in the promotion of several aspects of neuronal differentiation [44]. Upon secretion, it can bind to the Tyrosine receptor kinase B (TrkB), as well as to the neurotrophic receptor p75 (p75NTR). Recent experiments show that BDNF induces axonal growth in *in vitro* conditions, while *in vivo* its role seems to be more on promoting the branching of the elongating axon [45]. Studies with Xenopus showed that expressing a dominant negative TrkB on retinal ganglion cells did not affect the ability

of the axons to reach their target, but significantly altered the growth cone morphology and impaired the formation of axonal branches [45, 46]. The axonal branching promoted by BDNF relies upon the activation of the ERK1/2 signaling pathway [47]. BDNF is able to influence correct wiring of the brain not only by extending new axonal branches, but also by pruning unnecessary ones through the activation of the p75NTR [47, 48]. BDNF also modulates the dendritic tree morphology, especially in aiding the formation of dendritic spines, and consequently synapses. BDNF activation of TrkB promotes dendritic filopodia motility in a PI3K-dependent way [45, 47]. BDNF also stimulates the increase of PSD-95 in dendritic filopodia [26, 45], thus promoting the maturation of the postsynaptic terminal.

BDNF role in neuronal differentiation is also highlighted by its common use as a neurotrophic factor in the differention of SH-SY5Y neuroblastoma cells [49–52]. Pre-incubation of these cells with retinoic acid leads to the expression of TrkB, with follow-up treatment with BDNF resulting in the differentiation of SH-SY5Y cells into neuron-like cells, expressing neuronal markers such as MAP2 and tau [49]. BNDF effects on these cells are mediated by activation of both the ERK1/2 and PI3K signaling pathways [51], which will be discussed ahead.

A1.6.2. Rho small GTPases

The three main members of the Rho protein family are RhoA, Cdc42 and Rac1. These are small GTPases that act as molecular switches in several signaling pathways. All three have been associated with neuronal differentiation: Cdc42 and Rac1 have mainly a positive role in neurite outgrowth, while RhoA has negative role [53]. Cdc42 knockout in mice leads to the development of smaller brains, with a reduced number of axons, that results in death at birth, thus highlighting a fundamental role of Cdc42 in axon specification [54, 55]. Cdc42 modulates the actin cytoskeleton, promoting the formation and elongation of filopodia [56]. Rac1 activation promotes axonal branching and formation of dendrites, while its inactivation leads to a decrease in the number of primary dendrites, and also affects axon growth and guidance [54]. Interestingly, Rac1 activation has to be tightly controlled during neuronal differentiation, since some experiments showed that expressing a constitutively active (CA) form of Rac1 or a dominant negative Rac1 both resulted in a decrease in neurite outgrowth [54, 57]. Similarly, a cyclic activation of Cdc42 is required for it to promote neuronal polarization [58]. RhoA seems to act as a limiting factor in neuronal differentiation [54]. Activating RhoA in hippocampal neurons and neuronal models, such as PC12, inhibits the growth of small processes or even promotes the retraction of neurites, respectively,

while its inactivation greatly enhances neurite outgrowth [4, 53]. It has been hypothesized that RhoA role *in vivo* is to control axon elongation and neuronal polarization by inhibiting the formation of extra axons [4]. This is supported by the evidence that RhoA activity is higher in growth cones of smaller neurites when compared to the axonal growth cone [59].

While these opposing roles between Cdc42/Rac1 and RhoA have been well established, normal neuronal differentiation is a result of a coordinated interplay between the three proteins, with defects in any of them seriously affecting the proper formation of axons and dendrites [53].

A1.6.3. PI3K / Akt pathway

The phosphatidylinositol 3-kinase (PI3K) and Akt signaling can be activated by different membrane receptors during neuronal differentiation, including TrkA and TrkB, as well as G-protein coupled receptors [1, 60, 61]. Activation of PI3K leads to the increase of PIP3 (phosphatidylinositol (3,4,5)-tri-phosphate), which in turn promotes Akt phosphorylation via phosphoinositide-dependent kinase (PDK1). For instance, BDNF signaling through TrkB increases filopodia motility and its number in hippocampal dendrites through the activation of PI3K signaling [1], while the neuritogenic effects of the Nerve Growth Factor (NGF) in dorsal root ganglion neurons involves the activation of a TrkA-PI3K-Akt signaling [60]. In both cases, PI3K/Akt translates its effects to the cell cytoskeleton by mediating the activation of the Rho GTPases proteins. Indeed, a possible positive signaling mechanism mediating neuronal polarization has been described involving PI3K, Cdc42 and Rac1 [8]. Signaling of BDNF through PI3K-Akt has also been shown to be involved in regulating the complexity of the dendritic tree as well as the formation of dendritic spines, with chronic inhibition of PI3K resulting in a decrease in the formation of dendritic spines and filopodia [62]. Interestingly, this study also showed a cooperation between PI3K-Akt and MAPK signaling in regulating dendritic morphology.

Besides directly inducing neurite formation, the PI3K/Akt signaling also promotes differentiation by inhibiting the GSK3 signaling [63]. Activation of PI3K/Akt in NGF signaling results in the phosphorylation of GSK3β, thus inactivating it, and this inactivation is essential in the promotion of NGF neuritogenic effects [64]. Moreover, activation of the 5-HT_{1A} GPCR potentiates NGF neuritogenic output in a signaling dependent on PI3K and Akt activation [61]. Taking together, these different reports indicate that PI3K/Akt seems to be one of the main signaling pathways where several extracellular cues converge to induce neuronal differentiation.

A1.6.4. ERK1/2 pathway

The extracellular regulated kinases 1 and 2 (ERK1/2) are part of the main pathway of the MAPK (mitogen-activated protein kinase) signaling. Different receptors translate their intracellular signaling through the activation of small GTPases of the Ras family. These activate a kinase signaling cascade that starts with the Raf kinases, which in turn activate the MAPK kinases (MEK1/2) and culminates in the activation of ERK1/2. Several reports have put ERK1/2 has a main player in neuronal development [65]. Treatment with different neurotrophic factors, usually NGF and BDNF, lead to neuritic outgrowth *in vitro* as a result of increased ERK1/2 activity [51, 66–68]. In PC12 cells, ERK1/2 is especially important, being able to induce different outcomes depending on the duration of its signaling. Sustained activation, as the one induced by NGF, results in neurite outgrowth, while temporary activation leads to cell proliferation, normally as a result of EGF incubation [68]. ERK1/2 seems to be especially involved in the axon specification mechanism. Studies involving the Rit GTPase showed that its activation led to axonal elongation in detriment of dendritic growth, and inhibition of ERK activation blocked Rit effects [69]. Another study also showed that ERK2 phosphorylation of Par3 modulated neuronal polarization[70].

In vivo, knockout studies have been essential not only to identify potential ERK functions, but also to differentiate between ERK1 and ERK2. ERK2 deletion results in a 50% reduction in axonal length, as well as a reduction in dendritic branching on mice cortex [71]. ERK2 deletion also led to embryonic cell death, contrary to ERK1 knockout, revealing a crucial role for this isoform on normal development[72].

A1.6.5. STAT3 pathway

The signal transducer and activator of transcription 3 (STAT3) is a transcriptional factor involved in innumerous cellular functions, as well as a key factor in the genesis of different cancer types. STAT3 is activated by phosphorylation by tyrosine kinase signals, with its canonical activator being the Janus kinase 2 (JAK2), but being also activated by the Src kinase or directly phosphorylated by tyrosine kinase receptors such as the Epidermal Growth Factor Receptor (EGFR) [73–75]. Although STAT3 function has been mainly studied in a context of carcinogenesis, a possible role in neuronal differentiation has been unveiled through the last years. Treatment of PC12-E2 cells with interleukin-6 (IL-6) induces neuronal-like morphological changes similar to the incubation of these cells with NGF. However, while NGF treatment is accompanied by a substantial increase in ERK1/2 activation, IL-6 leads to STAT3 activation[76]. Moreover, blocking STAT3 activity, but not blocking

of ERK1/2, significantly decreased IL-6 induced neurite outgrowth, showing that STAT3 activation in these cells is sufficient to induce neuronal-like differentiation [77]. Notwithstanding these results, the STAT3 role on neuronal differentiation *in vivo* is still not clear. In the adult nervous system, STAT3 has been implicated in the organism response to neuronal injury, being activated in cases of brain ischemia and spinal cord injury [78, 79]. STAT3 is also important in synaptic plasticity, for its activation in the postsynaptic terminal is required for long-term depression (LTD) to take place [80].

Interestingly, activation of STAT3 by the Src kinase also leads to neurite outgrowth in Neuro-2A cells, in a signaling mechanism mediated by Gαo [81]. This pathway will be explored in more detail in the following section.

Over the years, several other players in neuronal differentiation have been uncovered. A detailed scheme of the main signaling pathways involved in neuritogenesis and neuronal polarization is displayed on figure A1.4, adapted from [8].

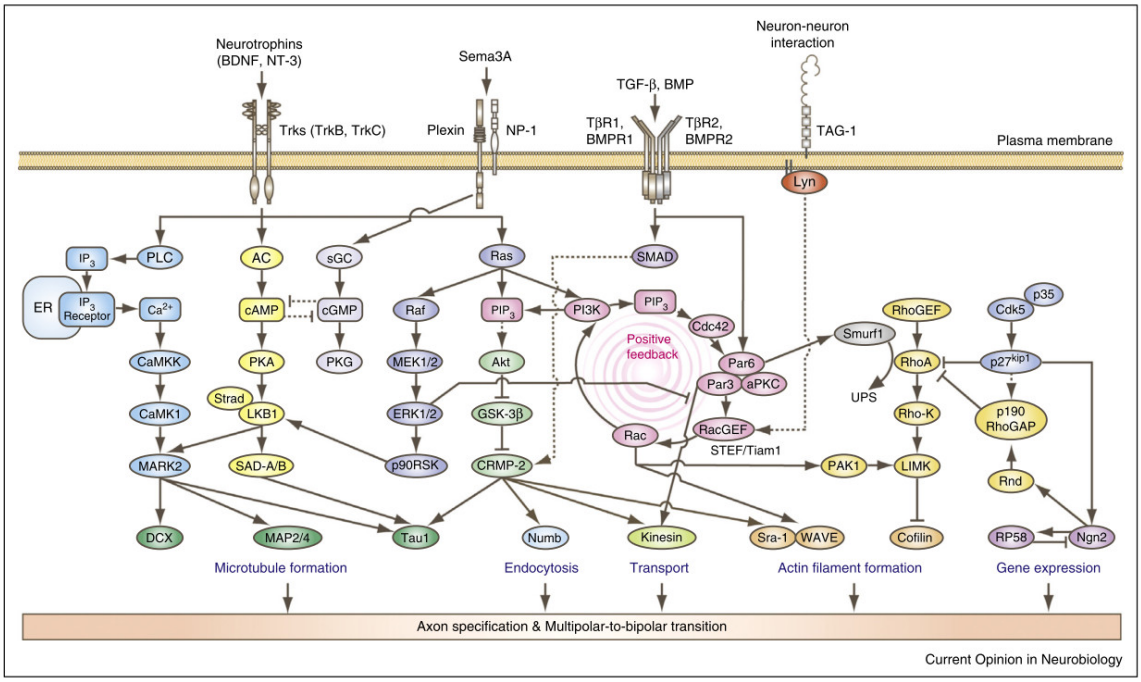

Figure A1.4. Signaling in neuronal differentiation. The different signaling pathways described here have to cross-talk with each other to successfully induce neuronal differentiation. Adapted from [8].

A2. The Other G protein (Go)

Heterotrimeric G proteins are one of the main components of intracellular signal transduction. They consist of three subunits, the α, β, and γ, with the latter two usually tightly bound together into the βγ complex. G proteins are divided according to their alpha subunit into 4 major families: Gs, Gi/o, G12/13, and Gq/11 [82]. One of the most intriguing G proteins is one of the members of the Gi/o family, the Go protein. Its alpha (α) subunit, Gαo, got its name due to being discovered after both Gs and Gi: Gs was named for being able to stimulate the adenylate cyclase activity, while Gi inhibits it. Since the new G protein had no specific function or attribute, it was named the "other" G protein [83, 84].

Similar to the small G proteins, heterotrimeric G proteins work as molecular switches of intracellular signal transduction. When inactive, Gαo is bound to GDP (guanosine diphosphate), and forms a trimeric complex with the βγ subunit. To be activated, Gαo must release the GDP and bind GTP (guanosine triphosphate). This is promoted by the binding of Guanine Nucleotide Exchange Factors (GEFs) to the G protein, with the most common GEFs being the G protein-coupled receptors (GPCRs). The activation of a GPCR by an extracellular ligand results in a conformational change that allows the binding of the receptor to the G protein. This in turn causes a second conformational change on the α subunit that results in the exchange of GDP for GTP, and the separation of the α and βγ subunits. At this point the G protein is active, and both the α and βγ subunits interact with downstream effectors to modulate different signaling pathways. What characterizes the G proteins as molecular switches is the intrinsic GTPase activity that the α subunits possess (as well as the small G proteins). Thus, G proteins only stay active for short periods of time, after which the GTP is hydrolyzed to GDP, the α and βγ subunits reconnect, and Go returns to its inactive state. Members of the Regulators of G-protein Signaling (RGS) family can bind to the α subunit and drastically increase the rate of GTP hydrolysis, thus terminating the G protein signaling faster. RGS proteins are also known as GTPase-accelerating proteins (GAPs), however this term is more commonly used to proteins that interact and regulate small monomeric G proteins, such as Ras and Rho family proteins [85–87]. As a member of the Gi/o family, Gαo is also inhibited by the Pertussis Toxin (PTX). PTX ADP-ribosylates the cysteine located four residues from the carboxyl terminus of Gαo, thus blocking Gαo interaction with its activators [88].

Although it has been intensively studied for the last 3 decades, Gαo specific function in the human organism is still not completely clear. Some data regarding Gαo physiological function has come out from a few published knockout reports. General knockout of Gαo in mice results in viable animals but that have a lifespan of only 7 weeks. The animals are small, hyperactive, hyperalgesic and have severe motor control impairments, exhibiting a turning behavior that result in the mice going around in circles for long periods of time. At a cellular level, there was a decrease in the ability of opioid receptors to inhibit Ca^{2+} channel currents in dorsal root ganglion cells, indicating a role for Gαo in translating the intracellular signaling of these receptors [89].

Since Gαo is the most expressed Gα subunit in the brain, accounting for around 1% of the total membrane protein [90], most of the studies have been devoted to try uncover the Gαo role in the brain physiology.

A2.1. Gαo genetics

The Gαo protein is highly conserved across several species, including human, rat, bovine, fly, nematode, among others, sharing over 80% identity between proteins of the different species [90].

In humans, the Gαo gene (GNAO1) is located on chromosome 16, comprising over 100 kb and containing 11 exons [91]. Analysis of the GNAO1 gene detected that exon 7 and exon 8 are duplicated, and mechanisms of alternative splicing give rise to two different isoforms, Gαo1 (aka GαoB) containing the exons 7A and 8A, and Gαo2 (aka GαoB) containing the exons 7B and 8B [91–93]. These isoforms are almost identical, with differences appearing only in 20 amino acids of the last portion of the protein (C-terminal), and since this region is essential to receptor and effector binding, Gαo1 and Gαo2 could have different functions in the brain [91, 94].

A third isoform, Gαo3, has been identified as a result of a posttranslational modification, where an asparagine at residue 346 of Gαo1 is converted through deamidation into an aspartate [95, 96]. However, there is still no description of this modification occurring in human Gαo.

A2.2. Gαo expression and distribution

Although Gαo can be found a little all over the human body, it is greatly enriched in the brain [97]. Initial immunohistochemical studies in rat brain showed that Gαo is mainly present in neuropil (regions with abundance of dendrites and axons, and consequently rich in synapses) and absent

from cell bodies [98]. The study also detected a differential distribution of Gαo along the rat central nervous system: Gαo is enriched in cerebral cortex, especially in the molecular layer (layer 1), in neuropil of the hippocampal formation, striatum, subtstantia nigra pars reticulate, molecular layer of the cerebellum, substantia gelatinosa of the spinal cord, and posterior pituitary [98]. Current data retrieved from the database Expression Atlas shows that Gαo also has a differential expression in the human nervous system, being enriched in the cerebral cortex and the basal ganglia (putamen, nucleus accumbens, caudate nucleus, globus pallidus and substantia nigra) (Figure A2.1) [97, 99–102].

At a cellular level, mouse Gαo is located in striatal neurons, cortical neurons, cerebellar granular cells, as well as striatal glial cells, cerebral cortex and colliculi glial cells. At a subcellular level, neuronal Gαo is present on the plasma membrane, mainly at cell-cell contacts, and in neurite arborization. It is also present at low levels in the cytoplasm and is absent from the nucleus [103]. During neuronal development, Gαo is especially present on the growth cones of elongating neurites [104]. In glial cells, Go is present throughout the cell in low levels, with specially strong staining around the nucleus [103].

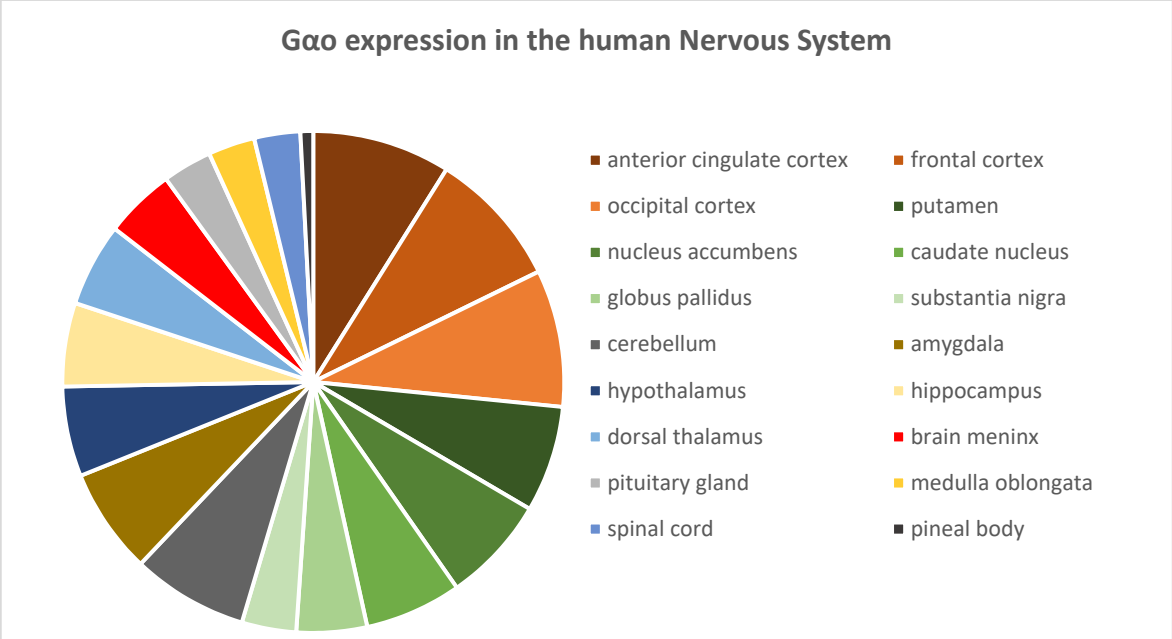

Figure A2.1. Gαo expression in the different regions of the human nervous system. Data was retrieved from four studies present in the Expression Atlas database, and the values were normalized to each study. The studies analyzed were The FANTOM5 project, The Human Protein Atlas and two studies from the Genotype-Tissue Expression (GTEx) Project [97, 99–102].

Gαo expression suffers distinct variations during neuronal development. Initial studies showed that differentiation of neuroblastoma cells (NG 108-15 and N1E-115 cells) induced different expression profiles on both Gαo isoforms: Gαo1 expression was either absent (N1E-115) or very low (NG108-15) in undifferentiated cells, with differentiation greatly increasing its protein levels; Gαo2 was already present in undifferentiated cells and its protein levels did not change substantially during differentiation [105, 106]. However, analysis of primary cultures of matured neurons showed that Gαo2 was almost absent [106], indicating that neuronal differentiation is accompanied by an increase in Gαo1 and a decrease in Gαo2 protein levels. Moreover, analysis of Gαo metabolism showed a significant increase in the protein half-life with differentiation, being around 28h in undifferentiated neuroblastoma cells, 58h in differentiated cells, and 154h in primary culture of cerebellar granule cells [107]. Adding the results that showed that mRNA levels on cerebellar cortex of mice did not suffer significant alterations during cerebellum development [108], the increase in Gαo levels with differentiation could be a result of a decrease in Gαo degradation rather than an increase in Gαo gene expression.

Interestingly, while differentiation of PC12 cell also correlates with an increase of Gαo levels [109], differentiation of the neuroblastoma cell line SH-SY5Y with retinoic acid (RA) gave opposing results, with Gαo levels suffering a slight decrease, although not significant [110]. Of note, the study did not distinguish between Gαo1 and Gαo2. Nevertheless, this could indicate that distinct differentiation mechanisms on different cell types affect Gαo expression differently.

Rat primary neuronal cultures have also evidenced an increase in Gαo expression during the differentiation of mesencephalon and hypothalamus neurons, with Gαo levels being barely detectable for the first 2 days *in vitro*, but rapidly increasing after 4 days and stabilizing 2-3 weeks after plating [111]. This increase in Gαo levels was associated with a significant increase of Gαo presence in neuronal processes, dendrites and axons. Also, in the case of mesencephalon neurons, increasing the cell density also resulted in an increase in Gαo levels, which could be an effect of the increase in cell-cell contacts [111]. A study using rat brain extracts also showed that Gαo protein levels not only increases during development, but continues to increase for several days after birth [112].

A2.3. Gαo signaling in the brain

As mentioned before, although intensively studied, Gαo role in the brain is still not completely clear. The discovery of the receptors that activate intracellular signaling through Gαo, as well as its downstream effectors have helped to establish Gαo signaling pathways, as well as deciphering potential functions of Gαo, particularly in neuritogenesis [90, 113, 114].

A2.3.1. Necdin

Necdin is a neuronal protein highly expressed on post-mitotic neurons, where it functions by blocking cell cycle progression, thus maintaining the neurons in the G0 phase of cell cycle [115]. It is also expressed during brain development, opening a potential role in regulating neuronal differentiation. A recent study by Ghil's group as identified Necdin has an interactor of Gαo [116]. Using co-immunoprecipitation assays followed by quantitative western-blot, the authors showed that Necdin interacted preferentially with the activated Gαo, thus putting Necdin as a downstream effector of Gαo. Overexpression of a constitutively active (CA) form of Gαo with Necdin enhanced the Necdin-induced blocking of cell proliferation, while co-transfection of Necdin with either wild-type or Gαo CA increased of the number of cells with neurites (this work stablishes a neurite as being a process longer than the cell body length). Furthermore, Gαo activation of Necdin signaling was promoted by activation of the type 1 Cannabinoid Receptor (CB1R), and culminated on the inhibition of the transcription factor E2F1.

A2.3.2. Src-STAT3 pathway

As mentioned above, the STAT3 pathway is a prominent player in brain development and function [77, 80], and while JAK2 is known as STAT3's canonical activator, some signaling pathways involve STAT3 activation by the Src kinase [73]. Initial studies using NIH-3T3 fibroblasts showed that overexpressing a Gαo CA resulted in proliferation and neoplastic transformation of these cells [117, 118]. This transformation was accompanied by an increase in STAT3 activity, with no alterations in ERK1/2 activity. Moreover, the Gαo-induced transformation was a result of STAT3 phosphorylation by the Src kinase rather than by JAK2. The authors had already hypothesized a possible role for the Gαo-Src-STAT3 pathway in differentiation by stating that mechanisms that induce NIH-3T3 transformation sometimes translate to other cell types as differentiation mechanisms, with their follow-up work supporting this statement. Using Neuro2A cells as a model, the research shows that

stimulating the CB1R significantly increases the number of cells with neurites (this work stablishes a neurite as being a process at least 2x longer than the cell body diameter), a mechanism mediated by the activation of the Gαo-Src-STAT3 pathway [81, 119]. CB1R activation causes Gαo to bind to Rap1GAP, a Rap1 negative regulator protein. This binding results in the targeting of Rap1GAP to proteasomal degradation, thus eliminating the blockage upon Rap1 activity [119, 120]. Rap1 activates Ral, which in turn activates the Src kinase, culminating in STAT3 phosphorylation. Besides phosphorylating STAT3 directly, the study also showed that Src kinase can activate STAT3 via an alternate pathway, where it activates Rac1-c-Jun N-terminal kinase (JNK) signaling. Activation of both signaling pathways by CB1R-Gαo are essential in inducing neurite outgrowth (Figure A2.2).

Interestingly, although G protein effectors tend to bind with more affinity to the activated forms of the Gα subunits, Rap1GAP binds preferentially to the wild-type form of Gαo when compared to the Gαo CA. Since stimulation of the CB1R leads to the activation of Gαo, it is unexpected that this mechanism would lead to the binding of Gαo to Rap1GAP. The authors try to explain these events as a possible sequential mechanism [119]. Go activation by CB1R leads to the separation of the Gα and Gβγ subunits. This separation allows Rap1GAP to bind to Gαo, since Rap1GAP binds to the same region as the βγ subunit, through the GoLoco motif. The binding of Gαo to Rap1GAP is initially weak, but it is strengthened when GTP is hydrolyzed to GDP. At this point, Rap1GAP would act as a guanosine nucleotide dissociation inhibitor (GDI), maintaining Gαo in its inactivation state until Rap1GAP could be targeted to degradation. Although no direct evidences are shown to support this theory, the idea that Gαo proper function relies on an activation/deactivation cycle is supported by similar mechanisms described in small G proteins, as the aforementioned Cdc42 [58].

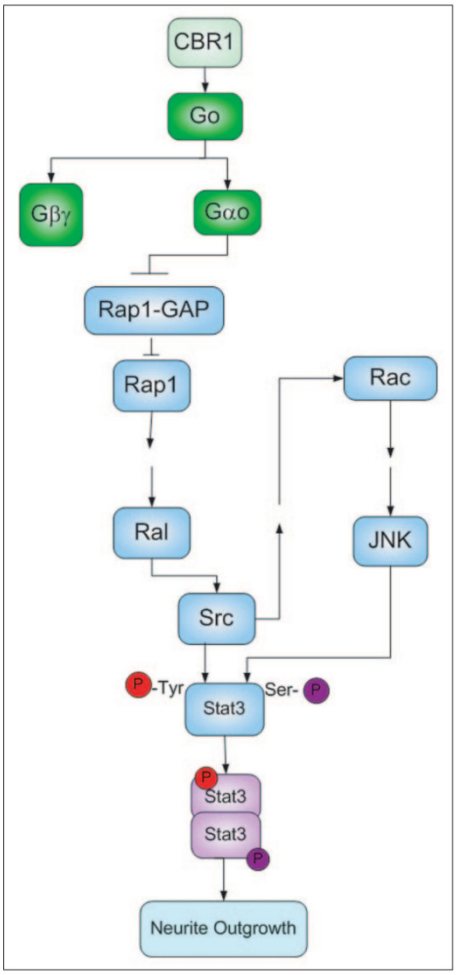

Figure A2.2. CB1R-Gαo-STAT3 signaling in neurite outgrowth. Image reproduced from [81].

An interplay between Gαo and the Src kinase has also been described downstream of Reelin [121]. As mentioned before, Reelin is an extracellular factor known to participate in neuronal polarization, as well as in the control of neuronal migration [8, 122]. Treatment of primary cultures of

hippocampal neurons with Reelin increased both the total neuritic length as well as neuritic branching. Treatment with PTX blocked Reelin neuritogenic effects on hippocampal neurons, while knockdown of Gαo did the same in F11 cells [121], thus demonstrating that Reelin activates an intracellular pathway dependent on Gαo. By trying to fully comprehend the complete signaling pathway involved in Reelin effects, the authors identified the Src kinase as a player in this signaling. Co-immunoprecipitation assays showed that Src and Gαo interact with each other, and that this interaction is strengthened by treatment with Reelin. Gαo activation in this pathway was accompanied by an increased activation of JNK, while Akt and GSK3β (other common players in Reelin signaling) were unaffected. Interestingly, activation of Src and JNK was also seen in the cannabinoid-induced signaling [81], which could implicate some cross talk between both pathways. However, the authors did not check for STAT3 activity, so is not certain that the interaction of Gαo-Src in Reelin-treated cells leads to same outcome that in cannabinoid-treated cells. Also, surprisingly, in this study Src seems to be acting upstream Gαo in the Reelin signaling pathway, rather than downstream as seen before. This was demonstrated by showing that inhibiting Gαo with PTX did not significantly inhibited Src kinase. Combining both studies [81, 121], one could hypothesize that Gαo and Src kinase could be involved in a positive loop, where Src activates Gαo, which in turn activates a signaling pathway (Rap1-Ral) that further activates Src. Such positive loop has already been described as an important mechanism of neuronal polarization, where activation of PI3K by Trk receptors leads to the activation of a cascade involving Cdc42→Par-complex→Rac1 that feedbacks into further activation of PI3K (Figure A1.4) [8], opening the possibility for Gαo-Src also participating in a similar process. Nevertheless, further research is required to better understand the inner works of Gαo-Src signaling

A2.3.3. GAP-43

Although G proteins are mostly known to be activated by GPCRs, one of the first known activators of Gαo was the growth associated protein 43 (GAP-43 aka neuromodulin) [104]. GAP-43 is protein highly enriched in neurite growth cones and is commonly used as marker for neuronal differentiation [123, 124]. The presence of both GAP-43 and Gαo in growth cones raised the question if these proteins could functionally interact in the regulation of the growth cone dynamics. Indeed, GAP-43 can bind to Gαo and stimulate the exchange of GDP for GTP, thus acting as a GPCR-like protein [104, 125]. The Gαo-activating sequence of GAP-43 was then shown to be able to induce neurite outgrowth in N1E-115 cells, an effect that was mimicked by mastoparan (an activator of

Gi/o) and inhibited by PTX, thus showing that Gαo plays a role in mediating GAP-43 neuritogenic function. The effect of GAP-43 interaction with Gαo is not always the same, however, since in dorsal root ganglia neurons this interaction leads to the collapse of the growth cones [126], indicating that the outcome of GAP-43-Gαo interaction might depend upon the cellular environment in which it occurs, and also that a tight control is required to achieve successful neurite outgrowth.

There are some contradictory reports regarding the mechanism by which GAP-43 interacts with and activates Gαo. The initial report showed that treatment with PTX did not alter the ability for GAP-43 to activate Gαo [125], contrary to what happens normally to GPCRs, which could mean that GAP-43 binds to a different region of Gαo. However, later studies showed that effects mediated by GAP-43 are sensible to PTX treatment [126]. The authors explain these differences as a possible result of GAP-43 being overabundant in the initial experiments, thus somehow being able to bypass PTX inhibition, or that the GAP-43 peptides used in the later experiments are more susceptible to PTX action than the full-length protein [126]. The interaction between GAP-43 and Gαo is also affected by palmitoylation of Gαo, a reversible post-translational modification that facilitates the attachment of Gαo to the cell membrane [127]. GAP-43 ability to activate Gαo is greatly increased when Gαo is depalmitoylated [128]. The authors point to the fact that activation of G proteins by GPCRs results in the increase of Gαo depalmitoylation, indicating that GAP-43 could function as an intracellular potentiator of GPCR signaling. Indeed, some studies have already showed that GAP-43 is able to modulate GPCR-Gαo signaling. GAP-43 and the muscarinic M2 receptor can synergistically activate Gαo in vitro, while injection of GAP-43 in *Xenopus laevis* oocytes significantly increased GPCR response to agonist stimulation [129]. More recently, a study showed that an α7 nicotinic receptor could modulate neurite outgrowth by interaction with a protein complex containing Gαo, GAP-43 and GRIN1 (another Gαo interactor that will be discussed further ahead) [130], not only adding evidence that GAP-43 is a potential intracellular positive modulator of GPCR-Gαo signaling, but also that this signaling is important in regulating neuritogenesis.

A2.3.4. ERK1/2 pathway

One of the main signaling pathways at the center of Gαo activity is the ERK1/2 signaling. Gαo was first described to activate ERK1/2 in CHO cells [131]. In these cells, stimulation of the muscarinic acetylcholine receptor M1 (M1AChR) and the platelet-activating factor receptor (PAFR) resulted in activation of ERK (note that this work only checked for the activation of p44 MAPK aka ERK1). This effect was blocked by treatment with PTX and rescued by the expression of a PTX-insensitive Gαo,

thus demonstrating that Gαo activity was required for ERK activation. Gαo activation of ERK was done by a non-canonical pathway, since Ras was not involved but the protein kinase C (PKC) was required [131]. Further work confirmed this, with PKC inactivation blocking ERK activation by Gαo [132]. The pathway by which Gαo activates ERK was further resolved, with PI3K and B-Raf linking Gαo-PKC to ERK1/2. It was also shown that Gαo activation by GPCRs could lead to the modulation of signaling activated by other receptors, such as the Epidermal growth factor receptor (EGFR), since expressing Gαo CA was not enough to activate ERK, but significantly potentiated ERK activation by EGFR [132]. The Gαo-PKC-ERK pathway has still not been seen in a neuronal setting, however, PKC-ERK signaling has already been strongly associated with neurite outgrowth [133, 134], so Gαo participation on the mediation of these effects should not be excluded.

Neuronal activation of ERK1/2 by Gαo seems to be associated with a variety of functions. In Neuro2A cells, expression of Gαo CA significantly increases the number of cells with neurites, accompanied by an increase in ERK1/2 activation [135]. This activation of ERK1/2 was mediated by a small GTPase, Rit, with transfection of a dominant negative form of Rit blocking Gαo neuritogenic effects and decreasing ERK1/2 phosphorylation. Another study also showed that Gαo neuritogenic roles in Neuro2A are possibly translated via ERK1/2 activation [136]. Focusing on the study of RGS8, the authors showed that this protein inhibits Gαo, producing several effects: it blocked the ability to Gαo activate Necdin, reduced the formation of neurites induced by Gαo transfection, and blocked ERK1/2 activation induced by a protease-activated receptor (PAR1)/Gαo signal. Of note, while these results show that Gαo has a neuritogenic effect, and it is able to activate ERK1/2, these events were evaluated in separated, so it is not clear if ERK1/2 activation induced by the PAR1/Gαo signaling can produce neuritogenic effects.

In SH-SY5Y cells, Gαo might also potentially induce neurite outgrowth via ERK1/2 [137]. Treatment of cells with melanin-concentrating hormone (MCH) led to an increase in the number of neurites per cell, as well as an increase in their length. This effect was accompanied by an increase in ERK1/2 phosphorylation, and was significantly decreased when cells were treated with PD98059, an inhibitor of MEK. MCH induction of ERK1/2 activation was blocked by treatment with PTX, indicating that the MCH receptor is coupled to either Go or Gi. Since no specific experiments were performed to differentiate between Gαo and Gαi, further studies are required to confirm the potential MCH-Gαo-ERK1/2 pathway in neurite outgrowth.

One of Gαo functions in the brain seems to be in the modulation of nociception[89], with ERK1/2 potentially playing a role in this function. Knockouts of Gαo in mice resulted in animals that suffered

from hyperalgesia when subjected to hot-plate tests [89]. The opioid receptor-like (ORL1) receptor, a potential target for pain medication, has been shown to translate intracellular signaling through Gαo. Moreover, the activation of Gαo by ORL1 leads to the phosphorylation of ERK1/2, confirmed by treating cells with PTX or overexpressing a PTX-insensitive form of Gαo [138]. Stimulation of μ-opioid receptor with morphine also activates an intracellular pathway that involves Gαo and ERK1/2 activation [139]. The involvement of Gαo in ERK1/2 activation was demonstrated by expressing Gαo mutants that were insensitive to PTX and RGSs. Further work has helped establish a critical role for Gαo in pain control, particularly in mediating supraspinal anti-nociception effects of morphine, methadone and nalbuphine, although ERK1/2 activity was not monitored in these studies [140, 141].

Finally, a Gαo-ERK1/2 pathway has been described in cell survival. Overexpressing the YWK-II transmembrane protein in CHO cells results in an increased activation of ERK1/2 induced by the Müllerian inhibiting substance (MIS). This increased ERK1/2 activation was blocked by incubation with PTX and by transfection of cDNAs encoding the C-terminal of Gαo1 and Gαo2 (with Gαoi c-terminal having no effect), thus demonstrating that MIS-YWK-II signal was translated specifically via Gαo. MIS is able to promote cell survival, and indeed in this study it was able to do so by activating the YWK-II-Gαo-ERK1/2 signaling pathway [142]. This pathway could be important in brain function since YWK-II is widely distributed throughout the human organism, including the brain, and has a high homology with the amyloid precursor-like protein 2 (APLP2), being sometimes even referred as APLP2 in rat [142–144].

A2.3.5. GRIN1

The G protein-regulated inducer of neurite outgrowth (GRIN or GPRIN) is a highly enriched protein of the human central nervous system that has two isoforms, GRIN1 and GRIN2 [145]. While it was first discovered as an interactor of Gαz, its potential biological function was brought to light by its interaction with Gαo. GRIN1 is highly enriched in neuronal growth cones, together with GAP-43 and Gαo, and initial experiments showed that GRIN1 interacts preferentially with the active form of Gαo, indicating it is as a potential effector of Gαo. Further characterization of this interaction identified the C-terminal region of GRIN1 (aa 716-746 and 797-827) as the binding point of Gαo [146]. This interaction has no effect in GTPase activity, supporting the hypothesis that GRIN1 is an effector of Gαo rather than its regulator. The outcome of this interaction is an interesting one. Expression of Gαo CA with GRIN1 in Neuro2A and MA104 cells significantly increases the formation

of neurites [145], while transfection of a mutant GRIN1 lacking the Gαo binding region, with or without Gαo present, also resulted in increased neurite extension [146]. The authors concluded that the Gαo binding region acts as a self-inhibitory domain upon GRIN1. Binding of Gαo to this domain causes a change that lifts GRIN1's inhibition, thus resulting in its ability to induce neurite extension. The interaction between Gαo and GRIN1 is also essential for the translocation of the latter from the cytosol to the plasma membrane. This work also identified Cdc42 as a possible downstream effector for this interaction, since co-expression of a dominant negative (DN) Cdc42 with Gαo and GRIN1 blocked neurite extension in Swiss3T3. Interestingly, in Neuro2a cells, expressing a DN Rac1 also blocked neurite extension induced by Gαo-GRIN1 [146], which means that this interaction can modulate different signaling pathways according to the environment in which it occurs.

A previously mentioned study has identified GRIN1 and Gαo as part of neuritogenic complex with GAP-43 [130]. This complex was co-immunoprecipitated with the α7 acetylcholine nicotinic receptor, with GRIN1 acting as the link between the receptor and Gαo and GAP-43, since downregulation of GRIN1 using siRNAs significantly decreased the α7 receptor interaction with the G protein complex. From this and the follow-up work [147] it is not completely clear if the α7 receptor is a downstream effector of a potential GAP-43-Gαo-GRIN1 pathway, or if it is a negative regulator of this pathway. Both works show that inactivation of the α7 receptor leads to an increase in neurite outgrowth, while its activation reduces the number of growth cones present in hippocampal neurons. Moreover, inactivation of the α7 receptor increases its interaction with GAP-43 and Gαo, while its activation decreases the interactions, with GRIN1 interaction being unaffected in either conditions. Also, the study detected an increase in GAP-43 phosphorylation, which is correlated with an increase in neurite outgrowth, when the receptor was inactivated, while Gαo modulation (through treatment with either PTX or Mastoparan) had a significant impact on α7 receptor effects [130]. Taking these results all together, a hypothesis emerges of a convergence of the two signaling pathways, one starting with the α7 receptor and the other with GAP-43, on GRIN1, however, further research is required to fully comprehend the inner works of this new potential signaling.

Analysis of the expression and colocalization of GRIN1 and Gαo during the development of the mouse's nervous system highlighted a possible role for this complex in the migration and differentiation of neurons during development, as well as in the maintenance of the neuronal wiring on mature brains, although future functional experiments are required to test these hypotheses [148].

The interaction between Gαo and GRIN2 has also been subjected to investigation, with some surprising results. Although previous reports have established the ability for Gαo to activate the ERK1/2 pathway [131, 135], its interaction with GRIN2 negatively regulates ERK1/2 activity [149]. The study showed that without activation of Gαo, GRIN2 is bound to Sprouty2, an inhibitor of MAPK signaling. Upon activation of Gαo through CB1R, Gαo binds to GRIN2, thus freeing Sprouty2, which in turn blocks ERK1/2 activity induced by FGF treatment. It is not clear what are the effects of this signaling, since the work thus not show any morphological output. Since ERK1/2 has already been associated with neuronal differentiation, either activated by Gαo or other pathways, its inhibition could mean a decrease in neuritic outgrowth. However, ERK1/2 output can be significantly different depending on the source of its activation [150, 151], meaning that the interference of Gαo-GRIN2 with FGF-ERK1/2 pathway could have an effect in cellular functions other than neuritogenesis.

A2.3.6. Dopamine receptors

Several dopamine receptors are coupled to Gαo. In SH-SY5Y cells, D3 receptors regulate cyclic AMP (cAMP) production and Ca^{2+} channel currents through activation of Gαo [152]. Studies on Gαo knockout mice showed that most of the dopamine D2 receptors in the central nervous system preferentially translate their signals through Gαo instead of Gαi, which could explain some of the motor control defects exhibited by these mice [89, 153]. A more recent study, besides also showing that D2 receptors activate preferentially Gαo, it advanced the hypothesis that this signaling could be important in stimulating synaptic plasticity, due to the positive effect Gαo has in neurite outgrowth [154].

A2.3.7. Wnt pathway

The Wnt signaling plays several roles in the nervous system, from participating in the neuronal differentiation to the regulation of synaptic plasticity [155]. Experiments in both *Drosophila* and mammalian cells have shown that Gαo is coupled to Frizzled receptors and is able to translate Wnt extracellular signals to a pathway that involves Dishevelled proteins, small Rho GTPases and JNK [156, 157]. Wnt-Gαo seems to be important in forming and maintaining the synaptic structure. Gαo is activated by Frizzled2 in *Drosophila*, and disturbances in this pathway leads to a reduction in the number of synaptic boutons present in the neuromuscular junction [158]. Gαo role in this signaling seems to be to bind to Ankyrin2, a protein that participates in regulating the stability of the microtubule cytoskeleton. The study also showed that the interaction between Gαo and Ankyrin is

also necessary for the neuritogenic effects of Gαo, since downregulation of Ankyrin in Neuro2a cells significantly decreased the formation of neurites induced by Gαo transfection [158]. Gαo also couples to Frizzled9 in rat hippocampal neurons [159]. Wnt-5a binding to Frizzled9 results in the activation of Gαo, which in turns activates a non-canonical pathway of Wnt signaling, involving the calcium-calmodulin-dependent protein kinase IIα, PKC, and JNK, culminating in an increase in the formation of dendritic spines, as well as the clustering of PSD-95 in the post-synaptic region (Figure A2.3). These effects were mimicked by treatment with Mastoparan-7, an activator of Gαo and Gαi, strengthening the potential role of Gαo in synaptogenesis [160].

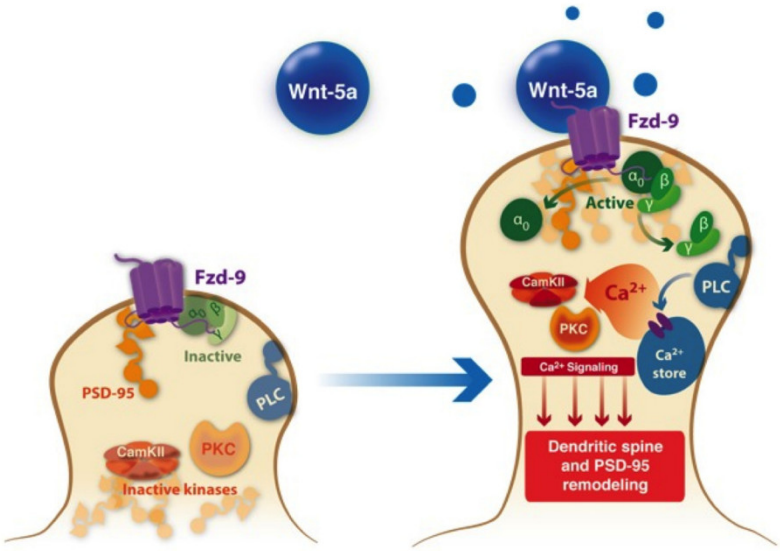

Figure A2.3. Wnt-Gαo signaling in synaptogenesis. Image reproduced from [159].

A2.3.8. Gαo2 functions

Almost every study dedicated to Gαo either focus on the Gαo1 isoform or does not distinguish between both isoforms. However, there have been a few studies that highlight specific Gαo2 functions. One of these seems to be the regulation of vesicles. Activation of Gαo2, but not of Gαo1 or Gαi, induced a significant reduction of vesicular catecholamine uptake in PC12 cells by inhibiting the catecholamine transporters [161, 162]. By using specific knockouts of Gαo2, researchers showed that Gαo2 also controls the vesicular uptake of glutamate, thus putting Gαo2 as a potential player in the control of neurotransmitter storage and release, as well as in mechanisms of synaptic plasticity [163].

Interestingly, Gαo2 seems to have opposite effects to Gαo1 on neuronal differentiation. While several reports show that Gαo activation is associated with neurite outgrowth, one study showed that deleting Gαo2 gives rise to longer axons, and with more branches, in hippocampal neurons [164]. Gαo2, like Gαo1, also binds to Rap1GAP, but while this binding in the case of Gαo1 leads to the increase in Rap1 activity through the degradation of Rap1GAP [81, 120], the deletion of Gαo2 increases Rap1 activity, which could mean that Gαo2 is redirecting Rap1GAP to inactivate Rap1, rather than targeting it for degradation. The study also showed that Gαo2 effects were mainly in axon morphology, with the dendritic outgrowth not suffering major changes with Gαo2 deletion [164]. Combining these results with the differential expression pattern of both Gαo1 and Gαo2, where Gαo2 is expressed mainly in undifferentiated cells while Gαo1 protein levels increase with differentiation, one could speculate that Gαo2 is important in maintaining cells in an undifferentiated state, with Gαo1 increase leading to the overcome of Gαo2 blockade, and thus helping promote neuronal differentiation. However, there is still a lot of research required to assess this potential mechanism.

A2.3.9. Other Gαo signaling

The continuous discovery of new Gαo interactors has been essential in the understanding of the potential Gαo roles in the brain. RGS14 is one of those interactors, a regulator of G protein signaling that binds preferentially to Gαo in comparison to Gαi, terminating its activity [165]. RGS14 has been shown to negatively regulate synaptic plasticity, and since it is highly enriched in hippocampal neurons, this could be an important function in learning and memory mechanisms [166, 167]. Moreover, this regulation is thought to be mediated by RGS14-induced inhibition of ERK1/2 signaling [166, 168]. There is still no evidence connecting these RGS14 effects to its interaction with Gαo, and ERK1/2 inhibition by RGS14 seems to be dependent on a direct interaction between RGS14 and H-Ras. Nonetheless, since both proteins have been associated with synaptic plasticity mechanisms, there could be an interplay happening between Gαo and RGS14 and controlling each other functions.

The serotonin type-1D (5-HT_{1D}) receptor is another GPCR that acts through Gαo. As mentioned above, Gαo seems to have a key role in the control of nociception, and data suggests that this could also be through its interaction with the 5-HT_{1D} receptor. Activation of this receptor leads to the increase in A-type potassium currents (I_A) in mouse trigeminal ganglion neurons, and if I_A is blocked it induces neuronal hyperexcitability and can lead to pain generation [169]. The I_A elevation was

mediated by the activation of protein kinase A (PKA) and the p38 MAPK, and was blocked by treatment with antibodies against Gαo and Gβ. Interestingly, no activation was seen of JNK and ERK, two signaling pathways modulated by Gαo, whereas blocking PKC (another Gαo signaling partner) did not affect I_A [170]. These results, coupled with the fact that antibodies against the Gβ subunit affected the 5-HT_{1D} receptor effects, could mean that Go mediates serotonin signaling mainly through its Gβγ subunit rather than through Gαo.

Interestingly, stimulation of the serotonin receptor 5-HT_{1A} can also induce neurite outgrowth through activation of a Gα-Rap1-Src-STAT3 pathway, much like CB1R [171]. The study describes Gαi as being the G protein involved in this signaling. However, they only tested this by treatment with PTX, which blocks both Gαi and Gαo, which means that Gαo could also play a role in 5-HT_{1A}-induced neurite outgrowth.

Gαo has been reported to modulate neurite outgrowth by repressing cAMP-CREB activation. While the exact mechanism that results in CREB inhibition is not known, overexpression of Gαo and Gαo CA in F11 cells resulted in a significant decrease in neurite elongation induced by cAMP activation, while increasing the number of new neurites formed [172].

Most of the studies presented here seem to indicate that Gαo is largely involved in mechanisms of neuritogenesis and synaptic plasticity, with some of the signaling mechanisms activated by Gαo being uncovered. One crucial Gαo signaling partner that was still not described here is the amyloid precursor protein (APP). APP not only interacts with Gαo but it is also involved in regulating some of the same pathways than Gαo, highlighting potential functions that could be shared by both proteins. The interaction between Gαo and APP will be the main focus of this thesis so the following introductory sections will be dedicated to APP and the published data regarding this interaction.

A3. The Amyloid Precursor Protein

The amyloid precursor protein (APP) is a Type I transmembrane protein ubiquitously expressed throughout the organism, that is best known for giving rise to the β-amyloid peptide (Aβ), one of the hallmarks of the Alzheimer's Disease. The APP gene is expressed as several isoforms, with the 3 main ones being APP695, APP751 and APP770 (the numbering represents the number of amino acids present in the protein sequence), which are a result of alternative splicing of exons 7 and 8 [173]. These 3 isoforms are all characterized by a long N-terminal extracellular domain and a short C-terminal intracellular domain, with their main structural differences being the presence of a Kunitz-type protease inhibitor (KPI) domain on APP751 and APP770, and the presence of an OX-2 domain on APP770 (Figure A3.1) [173]. APP is part of a protein family composed of two other APP-like proteins, APLP1 and APLP2. These two proteins differ from APP due to their lack of the Aβ region [174], and they seem to share essential functions with APP. Evidence for this comes from knockout studies in mice, where single knockouts of any member of the APP protein family results in viable animals, while double knockout of either APP/APLP2 or APLP1/APLP2 (but not APP/APLP1) resulted in early post-natal lethality [175, 176]. These studies show that while crucial for a normal development, APP functions can to a certain extent be compensated by the other members of its family.

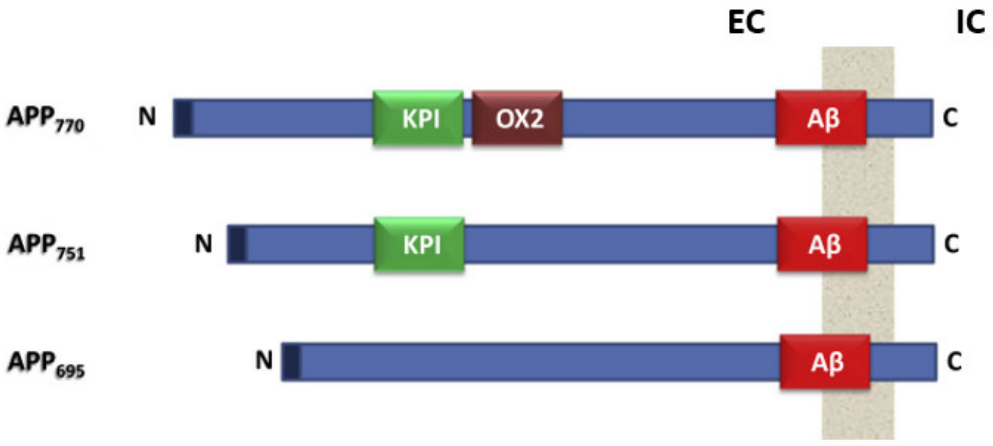

Figure A3.1. Different isoforms of APP. EC, Extracellular space; IC, Intracellular space. Adapted from [173].

The three APP isoforms have distinct expression profiles. While all three proteins are expressed in the brain, APP695 is the most abundant isoform on this tissue [177]. In the brain, APP role has been highly studied, being implicated in mechanisms of cell adhesion, neuronal migration and neuronal differentiation [173, 176, 178]. APP functions, as well as its role in the pathogenesis of Alzheimer's Disease, are strictly linked to the extremely dynamic "life" that APP takes inside the cell. This life involves posttranslational modifications, from phosphorylation to glycosylation, an intense traffic across several cell compartments, and proteolytic processing that originates different peptides (e.g. Aβ) with diverse functions.

A3.1. APP processing

A main feature of APP is its proteolytic processing into Aβ. However, Aβ is only one of the different peptides that result from APP processing. The canonic processing pathways that APP suffers are the amyloidogenic pathway and the nonamyloidogenic pathway, depending on if Aβ is produced or not (Figure A3.2) [179–182]. In the amyloidogenic pathway, APP is first cut on the β-cleavage site of its extracellular domain by a β-secretase, resulting in the shedding of sAPPβ (secreted or soluble APPβ), with the remaining c-terminal fragment (C99 or β-CTF) remaining membrane-bound. The βCTF is then cleaved by γ-secretase to originate Aβ and the APP intracellular domain (AICD). The nonamyloidogenic pathway starts with APP being cut by a α-secretase, resulting in the release of

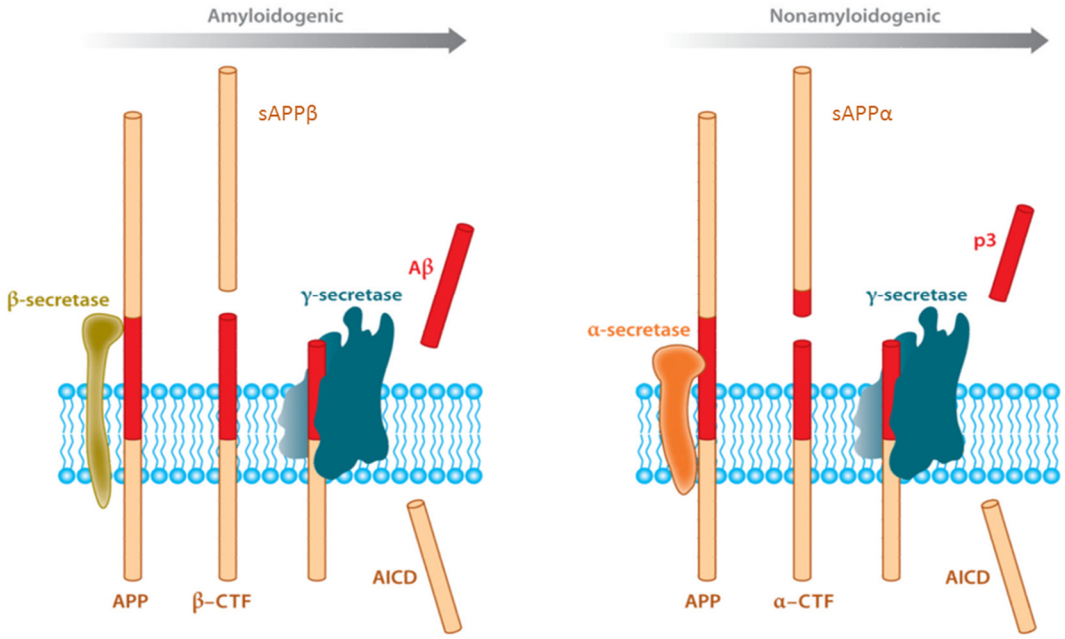

Figure A3.2. APP processing. Amyloidogenic (left) and nonamyloidogenic (right) pathways. Adapted from [182].

sAPPα and the c-terminal fragment (C83 or α-CTF), with the latter being then cut by γ-secretase to originate the p3 fragment and the AICD.

Each protein fragment originated during APP processing has been the focus of research to try to understand their potential physiological functions. Aβ interest is mainly due to its role in AD, where it accumulates and forms aggregates in the form of senile plaques in extracellular space [182, 183]. The formation of these plaques seems to be one of the main causes of neuronal death in Alzheimer's, with the amyloid cascade hypothesis still being one the most accepted theories regarding Alzheimer's pathogenesis, however the complete mechanism is still not completely clear [184]. Besides its pathological part, low levels of Aβ seem to be a positive regulator of synaptic plasticity and memory, by modulating presynaptic nicotine receptors and increasing Ca^{2+} levels [185–187].

The sAPP fragments are mostly released into the extracellular space where they are thought to act as ligands to stimulate different cellular functions, many of them through binding to the full length APP [178]. Most of the physiological roles of the soluble APP have been attributed to sAPPα. sAPPα participates in mechanisms of long term-potentiation (LTP) by regulating NMDA receptor function [188, 189]. The positive effects of sAPPα on memory formation are also dependent on its role in the formation of dendritic spines [187, 190, 191]. sAPPα is strongly involved in neuroprotection by modulating full-length APP-dependent and independent mechanisms. In the APP-dependent mechanism, sAPPα binds to APP and blocks the formation of APP dimers, leading to the protection of neuroblastoma cells against starvation [192]. In the APP-independent mechanism, the ability of mice to recover after neuronal injury is significantly impaired in APP knockout animals, but the addition of sAPPα to these animals reverts the negative effects even in the absence of full-length APP [193]. sAPPα has also been implicated on cell proliferation, with inhibition of α-secretase reducing proliferation of different types of stem cells, which could be recovered by the addition of exogenous sAPPα. Additionally, this trophic effect was associated with ERK activation [194]. A strong role of sAPPα on neurite outgrowth has also been strongly implied, and it will be discussed further ahead. sAPPβ physiological effects are more unclear, with a potential function in regulating axonal pruning and neuronal death during development, but that could also be a mechanism by which this fragment could be involved in neuronal death during Alzheimer's pathogenesis [181, 195].

The APP C-terminal fragments have different functions regarding their length. While α-CTF has still no clear role, β-CTF has been implicated in mechanisms of memory impairment and neuronal

degeneration [187]. AICD, on the other hand, has some important physiological functions, mainly in regulating transcription [187]. One of the main characteristic of AICD is the presence of the YENPTY domain, which is thought to regulate its interaction with different proteins and thus influence AICD functions. Indeed, AICD capability of gene transactivation is thought to be modulated by its interaction with the adaptor protein FE65 [196, 197]. One of the genes upregulated by AICD/FE65 is GSK3β, an effect that is thought to be important in the control of the cell cytoskeleton and cell trafficking [197]. Interestingly, AICD can also upregulate the expression of APP itself [198]. AICD can also be involved in cell death mechanisms by increasing the expression of the pro-apoptotic factor p53 [197, 199]. Regardless of these different reports showing AICD transcriptional activity, there is still some controversy over the significance of this function *in vivo* [187].

Lastly, to this day the P3 fragment has still not been implicated in any physiological or pathological mechanisms [187].

A3.2. APP trafficking

The APP processing is closely related to its intracellular trafficking (Figure A3.3) [178, 200]. APP is produced in the endoplasmic reticulum (ER) and from there it is transported by secretory pathway through the Golgi apparatus into the plasma membrane (PM) (Step 1). It is during this transport that APP suffers maturation through several post-translational modifications, mainly N- and O-linked glycosylation, phosphorylation, and tyrosine sulphation. Even though most of the nascent APP takes this secretory pathway to the PM, there is only a small portion of APP localized in the PM (≈ 10%). Most of it remains in the Golgi apparatus or in the Trans-Golgi network (TGN). Some of the APP that reaches the PM goes through the nonamyloidogenic pathway, due to the presence of α-secretases in this region, resulting in the shedding of sAPPα into the extracellular space. The remaining APP can either remain in the PM where it can act as a receptor-like protein [201], or take the endocytic pathway (Step 2). Endocytosis is triggered by the presence of the YENPTY domain, and APP is then compartmentalized into endosomes, from where it can be recycled back to the membrane (Step 3) or targeted to lysosomal degradation. It is during the endocytic pathway that APP comes into contact with β-secretases, specially β-site APP-cleaving enzyme 1 (BACE-1), either in the endosomes or in the TGN. This leads to the amyloidogenic pathway and thus the production of Aβ. There is in fact several evidence that interfering with the YENPTY domain, or with some of the proteins that interact with APP through the YENPTY domain, such as FE65 or Mint1, leads to

the reduction of Aβ production. The resulting CTFs from both amyloidogenic and nonamyloidogenic processing are cut by γ-secretases in either the endosomes or in the lysosomes [178, 200].

APP trafficking in neurons follow the pathway described above within the soma, however trafficking along dendrites and axons have a few peculiarities that are still under study. It is known that APP travels in vesicle-like structures along the axon, but is not clear at which point to they fuse with the membrane, or what signals regulate this process. The same is true to the retrograde traffic that APP goes through the axon, while the specific signals that mediate APP trafficking to either dendrites or axons are still under study [200]. Nonetheless, it is clear that APP is present in both the pre- and postsynaptic terminals [202].

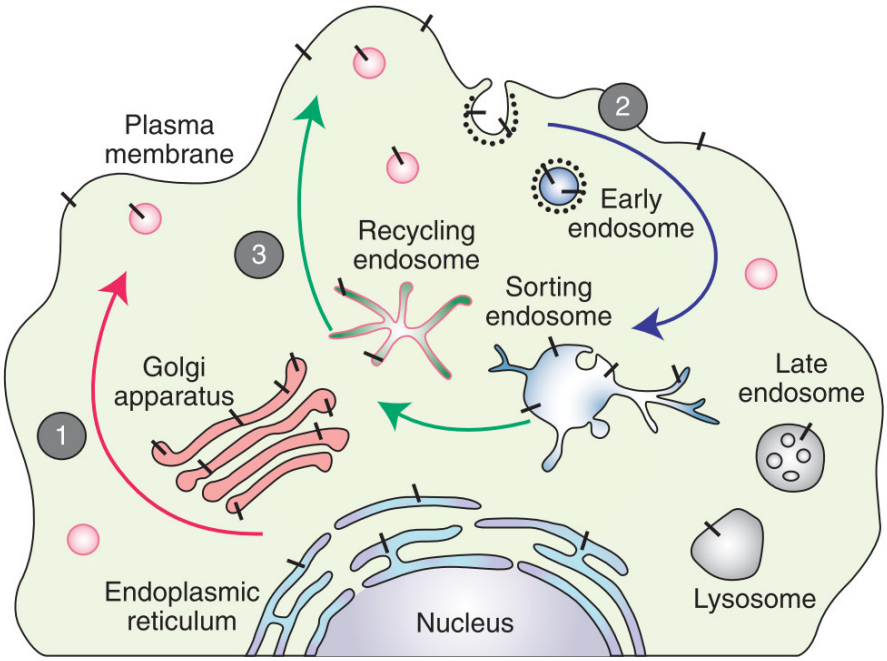

Figure A3.3. APP trafficking. Reproduced from [200].

A3.3. APP phosphorylation

APP can be subjected to phosphorylation in several of its residues, two of which are present in the ectodomain, and 8 potential sites present in the intracellular domain. The phosphorylation of the two ectodomain residues, Ser198 and Ser206, is still a matter of debate, with no specific function being attributed to these modifications so far [203, 204]. Phosphorylation of APP's intracellular domain, on the other hand, has been extensively studied, and it has potential roles in APP's trafficking, processing, and mediating interactions with other proteins. The ^{682}YENPTY^{687} domain

can be modulated by phosphorylation of its tyrosine residue, Tyr682, or phosphorylation of the upstream residue Thr668 [201]. Tyr682 can be phosphorylated by different kinases, such as TrkA, Abl, and Src, and its phosphorylation is required for APP interaction with adaptor proteins SchA and Grb2, which in turn leads to the activation of the MAPK pathway [201, 205]. Thr668 can be phosphorylated by JNK3, Cdk5, and GSK3, leading to a conformational change in the YENPTY domain. This causes an interference with the APP-Fe65 interaction, while also increasing the APP processing by BACE1 and γ-secretase, thus favoring the amyloidogenic pathway [200, 206]. However, these results are controversial, with different reports showing that Thr668 phosphorylation inhibits γ-secretase action and decreases Aβ formation [207], while it is also required for AICD interaction with Fe65 and its translocation into the nucleus [208, 209]. Phosphorylation of both YENPTY tyrosine, Tyr682 and Tyr687, also have an impact on Aβ production by directing APP to different cellular compartments, and thus promoting either α or β-secretase cleavage [209].

Ser655 is another phosphorylatable residue, which is located on the ^{653}YTSI^{656} sorting motif, and its phosphorylation, which can occur via PKC and CaMKII, has a significant impact in APP trafficking. A study using APP phosphomutants that mimic Ser655 phosphorylation (S655E) or dephosphorylation (S655A) showed that Ser655 phosphorylation increased APP secretory trafficking through the Golgi and into the plasma membrane, while also increasing sAPP production [210]. A follow-up study showed that Ser655 phosphorylation also enhanced APP recycling back to the TGN, in a process mediated by the retromer complex. Moreover, Ser655 dephosphorylation resulted in an increased targeting of APP to the lysosomes, thus showing that Ser655 phosphorylation is also important for regulating APP half-life [211]. A more recent study corroborates these results by showing that the Ser655 residue is required for the interaction between APP and AP-3 (adaptor protein 3), and that phosphorylation of Ser655 disrupts this interaction and decreases APP trafficking to the lysosome [212]. The authors also showed that Ser655 phosphorylation resulted in a decreased production of Aβ, which could be tied to the decreased targeting of phosphorylated APP to the late endosome-lysosome compartments. Of note, this study was conducted using APP phosphomutants constructs in the APP751 isoform. Ser655 phosphorylation could also be important in regulating APP interactions with other proteins, since it has been shown that it induces significant conformational changes in the intracellular domain of APP, specifically in the hydrophobic pocket downstream of Ser655, ^{656}IHHGVV^{661}, which could affect the binding of proteins to this region [213].

A3.4. APP as a neuritogenic protein

Although APP is best known for giving rise to Aβ, research has highlighted several potential roles that APP has in the normal brain, from cell adhesion to synaptogenesis, and of especially interest for this work, its role on neurite outgrowth [178, 187, 201]. Early evidence show that APP is highly enriched in developing neurites of rat neocortex and hippocampal neurons [214]. In fact, APP seems to be involved in the elongation of neurites, since increasing APP levels in PC12 cells leads to a significant increase in neuritic length and branching without affecting the number of primary neurites [215]. This effect of APP in neuritic elongation was also seen in SH-SY5Y neuroblastoma cells differentiated with RA, where a significant increase in APP levels was detected during a second phase of differentiation (4-8 days of differentiation), which is characterized by neurite elongation and stabilization [216]. The APP role on this mechanism was further confirmed by overexpressing full-length APP695 during the second phase of RA-induced differentiation, which led to a significant increase in neurites longer that 50 µm. Besides RA, APP also mediates differentiation induced by NGF. Using specific antibodies to block APP significantly reduces NGF neuritic effects on PC12 cells [215]. Moreover, APP phosphorylation seems to play a significant role on NGF effects, since APP phosphorylation of Thr668 is detected during NGF differentiation, mainly in the growth cones of PC12 cells [217]. Interestingly, NGF treatment of PC12 cells expressing an APP phosphomutant mimicking Thr668 phosphorylation resulted in the decrease of neurite extension. While this could at first indicate that phosphorylation of APP blocks its neuritogenic effects, the authors advance a model by which the phosphomutant could be competing with the endogenously phosphorylated APP for the binding to a neuritogenic molecule present in the growth cone, thus acting as a dominant negative form of APP [217]. APP effect on neuronal differentiation has also been reported on rat cortical neurons, with the decrease in APP expression leading to a decrease in both dendritic and axonal growth [218]. APP neuritogenic function could also be important in neuroregeneration mechanisms, with APP expression being significantly increased in axons after neuronal injury [176].

The mechanisms by which APP induces neurite outgrowth remain elusive; however, the study of its interacting proteins have been helpful in uncover potential signaling pathways. APP acts as an adhesion molecule through its interaction with several extracellular components, such as laminin, collagen I, and heparin, with these interactions being important to neurite outgrowth and axonal guidance [176, 219]. APP also regulates axonal guidance through interaction with netrin-1 and its receptor, DCC, and consequent activation of the ERK1/2 pathway [220]. APP interaction with Reelin, another extracellular protein involved in neuronal differentiation (see above), results in changes to

both APP trafficking and processing [221, 222]. Reelin treatment causes an increase in cell surface APP, which correlates with an increase in sAPPα shedding and a reduction in Aβ production. Moreover, Reelin neuritogenic effects seem to be dependent on its interaction with APP, since downregulation of APP blocks Reelin-induced neurite outgrowth *in vitro*. Also, knockdown of APP or Reelin significantly decreased dendritic outgrowth *in vivo* [222]. Taken together, these reports strengthen the idea that APP role in cell physiology is by acting as a receptor-like protein.

APP neuritogenic effects are not restricted to is full-length form (aka holoAPP), with several reports indicating sAPPα as a key potentiator of neuritogenesis. After secretion to the extracellular space, sAPPα can induce neurite outgrowth through the interaction with different membrane proteins, including holoAPP. sAPPα interacts directly with p75NTR, and while sAPPα induces neurite outgrowth in mouse cortical neurons, this effect is abolished when p75NTR is knockdown. This effect was mediated by activation of the PKA signaling [223]. sAPPα also induces neurite outgrowth by modulating both holoAPP and β1-integrin, with knockout of APP, or blockage of β1-integrin with antibodies, resulting in the loss of sAPPα effects. Also, this study showed that knockout of APP also induces neurite elongation, with the addition of sAPPα in this condition not having any additional effect. The model proposed indicate that holoAPP blocks neurite elongation by interacting with β1-integrin, while sAPPα acts by disrupting this interaction and thus promotes neuritogenesis [224]. sAPPα signaling is also required for activity-induced neurite outgrowth, in a mechanism mediated by activation of the ERK signaling[225]. ERK1/2 activation also occurs during axonal elongation induced by sAPPα. Interestingly, in this study, sAPPβ also induced axonal growth, although it required higher concentrations to do it significantly [226]. Besides neuronal differentiation, sAPPα can also induce glial differentiation. Treatment of human neural progenitor cells with sAPPα led to an increase in cells expressing the glial fibrillary acidic protein (GFAP, a glial marker), which correlated with an increase in the activation of STAT3. The authors show that sAPPα activates STAT3 by either increasing the levels of the gp130 receptor by an indirect mechanism, or by activating gp130 directly, thus functioning as a novel ligand for this receptor [227]. Neurite outgrowth has also been associated with other peptides originated from APP processing, such as Aβ and AICD [228, 229]. Of especial interest to this work, an interaction between a membrane-bound AICD and Gαs was found to mediate neurite outgrowth, and it will be discussed further ahead [230].

Finally, APP knockouts have shed some contradictory evidence regarding its neuritogenic function, with some showing an impact of APP knockout in dendritic extension and branching [231], while others showed that APP absence has no significant effect on neuronal differentiation [232], or even

reporting an increased elongation of neurites [224]. These contradictory results highlight the need to further investigate APP signaling to fully comprehend its function in the normal brain.

A4. The APP-Gαo complex

A4.1. APP-Gαo interaction

The interaction between the amyloid precursor protein (APP) and Gαo was first described in 1993 [233, 234]. On a first approach, the researchers identified the sequence His^{657}-Lys^{676} of the cytoplasmic region of APP_{695} as a possible interaction point with G proteins. This is due to the presence of two basic residues on the N-terminal side of this sequence (His657-His658) and a BBXXB motif on the C-terminal side of the sequence (B represents a basic residue and X represents a non-basic residue; ^{672}RHLSK^{676}), a pattern present in Gα-activating domains of several GPCRs [235–238]. Using in vitro assays, the researchers were able to confirm that a peptide with this 20 amino acid sequence increased the rate of GTP binding to Gαo, while having little to no effect on other Gα subunits. Also, this effect was blocked by incubation of Gαo with Pertussis Toxin (PTX). Immunoprecipitation assays performed in bovine brain membranes with the antibody 22C11 (antibody which recognizes the N-terminal of APP) revealed that APP interacted with Gαo but not with other G proteins, and that the His657-Lys676 sequence was essential for this interaction. Furthermore, by pre-incubating Gαo with GTPγS prior to the immunoprecipitation assays it was demonstrated that APP does not interact with the active form of Gαo [233].

APP has also been characterized as an atypical GPCR, activating Gαo in a ligand-dependent manner [239]. Phospholipid vesicles containing APP_{695} and Gαo were incubated with 22C11, which led to the increase of GTPγS binding and its turnover without altering the intrinsic GTPase activity of Gαo. This mechanism is similar to the one promoted by GPCRs, which act by increasing the rate of GTP/GDP exchange [240]. The authors hypothesize that 22C11 is acting as a possible extracellular ligand of APP, not yet identified, and it “activates” APP by promoting its dimerization, which is the mechanism present in other single membrane-spanning receptors [241–244]. Another study also showed that incubation of 22C11 had an effect in APP-Gαo interaction [245]. However, contrary to the previous results, they detected a reduction in Gαo GTPase activity. An explanation advanced by the authors for this difference was the fact that they used full membrane preparations extracted from rat brain, while the previous study was conducted in phospholipid vesicles [239]. The presence of other proteins (and potential APP/Gαo interactors) in the membranes could interfere with the APP-Gαo complex, thus resulting in a different outcome. The authors also point out that 22C11 might be acting by inducing a conformational change in the C-terminal domain of APP, or by

releasing other interactor proteins, although the latter effect could be a direct consequence of the former. Nevertheless, this study also offered more evidence for the specificity of APP-Gαo binding by showing that Gαi2 was not able to bind APP. Also, the mutation of two histidines present in the APP His^{657}-Lys^{676} sequence resulted in a loss of APP-Gαo interaction, further confirming this sequence as the Gαo binding domain.

Other regions of APP have also been associated with its interaction with Gαo. Mutations in the residue Valine642 of APP, associated with Familial Alzheimer's Disease (FAD) [246, 247], have been described to influence Go activity. Mutation of this residue to isoleucine (V642I), phenylalanine (V642F) or glycine (V642G) all lead to an increased activation of Gαo when compared to wild-type APP (Wt APP) [248]. The ability of these mutated APPs (FAD-APPs) to activate Gαo depend on the presence of the Go binding domain, and are sensible to the action of PTX. The authors hypothesize that the mutation of V642 into other amino acids causes a shift in APP conformation, in what they call a change between an inactive conformation (as in Wt APP) and an active conformation (as in FAD-APPs). The role of the C-terminal sequence downstream of the Gαo binding domain, specially the ^{682}YENPTY^{687} domain, on the APP-Gαo interaction is still not completely clear. Most of the initial studies show that deletion of the sequence encompassing this domain, or its targeting with specific antibodies, do not affect APP-Gαo interaction, nor does it affect the outcome of this interaction [233, 248–250]. However, a more recent study showed that the YENPTY domain can modulate APP-Gαo interaction. While full-length APP shows a decreased interaction with Gαo when Aβ is present, Aβ incubation with APP lacking the YENPTY domain blocks Aβ effect [251]. While this highlight a possible role for the YENPTY domain on APP-Gαo interaction, the exact mechanism behind this role still needs to be further explored.

The C-terminal domain of Gαo, more specifically the 5 C-terminal residues, has been identified has the APP binding point [252]. Using Gα chimeras with the 5 C-terminal residues from different G proteins showed that APP could only activate the Gα chimera presenting the Gαo C-terminal. This is consistent with classical binding of GPCRs to heterotrimeric G-proteins [253]. It also explains why treatment of Gαo with PTX affects Gαo activation by APP [233, 248], since PTX acts by APD-ribosylating the cysteine residue present in that 5-residue C-terminal of Gαo [254, 255].

Most of the studies done so far have not only showed that APP interacts with Gαo, but also that this interaction is specific, with other G proteins being excluded as APP interactors [233, 239, 245]. However, this specificity has been challenged by a report showing an interaction between APP and Gαs [230]. This study focused on the capability of the APP intracellular domain (AICD) to activate

signaling mechanisms that regulate neurite outgrowth. They expressed a construct of a membrane-bound AICD (mAICD) that led to an adenylate-cyclase dependent activation of PKA and inhibition of GSK3β signaling. These results raised the question of a possible involvement of the Gs heterotrimeric protein, and indeed, mAICD was co-immunoprecipitated with Gαs in N2a cells overexpressing both mAICD and wild-type Gαs. Mutation of the APP BBXXB motif blocked both the mAICD-Gαs interaction and the neuritogenic effects elicited by mAICD, thus highlighting a new potential signaling pathway involving APP and Gαs. Interestingly, besides not showing if mAICD can interact with Gαo beside Gαs, the authors did not address the fact that previous studies had excluded Gαs as an APP interactor. Also, the interaction here described was only verified for mAICD and not for the full-length APP, while previous studies of APP-Gα interaction have used mainly the full-length APP_{695}. The mAICD peptide could possibly have a different conformation that enables the binding of Gαs, a hypothesis similar to the one advanced by other authors who stated that cleavage of APP into AICD could trigger a switch in the interaction with the different G proteins. [234]. Nevertheless, further work is still required to fully comprehend the extension of the interactions between APP and G-proteins.

A4.2. APP-Gαo physiological function

Although APP interaction with Gαo as been a subject of study for over 20 years, the outcome of this interaction is still not clear. There is published data pointing to a role of this complex in both a pathological setting, such as the progress of the Alzheimer's Disease, as well as in a physiological setting, like the development and function of the human brain. APP and Gαo have been individually implicated in controlling neuronal migration [256–258], with a possible cooperation between both in this mechanism emerging recently [259]. An initial study conducted by the Copenhaver research group focused on a possible interaction between APPL, an ortholog of APP from *Manduca sexta*, and Gαo in migrating neurons [260]. Using a highly motile type of neurons, EP cells, as a model, the study showed that both APPL and Gαo colocalized in these cells in immunohistochemical preparations of *Manduca sexta* embryos. Immunoprecipitation assays further confirmed that APPL and Gαo interacted in these migrating neurons. A follow up study showed that inhibiting either APPL (by knocking down its expression) or Gαo (by incubation with PTX) resulted in very similar effects on neuronal migration, specifically a pattern of ectopic growth and migration of EP cells [261]. Although this indicates that APPL and Gαo might have similar functions and act upon the same signaling pathways, the research does not present data showing a direct effect of APPL-Gαo

binding on neuronal migration. Also, further research is required to check if these results are maintained in a mammalian model.

This study also showed that consistent with the interaction of Gαo with mammal APP_{695} [233], there is a significantly decrease of active Gαo co-immunoprecipitation with APPL. However, treatment with PTX, a toxin that inhibits Gαo and Gαi activity by blocking their activation by GPCRs, increased the interaction of APPL with Gαo. This is an unexpected result since ADP-ribosylation of G proteins by PTX is supposed to result in the uncoupling of the G protein from the GPCR [88, 262]. As previously stated, PTX treatment affects APP activation of Gαo, however, there is no published data about its impact on the direct interaction between APP-Gαo [233, 245, 248]. So, it is not clear if the increase in APPL binding to Gαo is specific to this insect ortholog or if it also occurs in mammalian cells. In APPL case, it could be that ADP-ribosylation of Gαo still allows APPL binding but somehow blocks the conformational change that APPL (and GPCRs in general) needs to elicit on Gαo to activate it, and thus APPL-Gαo remain in a complexed state.

The APP-Gαo complex also seems to play a potential role in mediating sAPPα signaling. sAPPα has already been implicated in several neuronal functions, from cell survival/protection to cell differentiation [192, 193, 223, 225]. New data shows that activation of the Akt pathway by sAPPα requires both full length APP and G protein activity [263]. Treatment with sAPPα significantly decreased cell death in both SH-SY5Y cells and mouse hippocampal neurons that were under trophic factor deprivation, an effect that was lost when APP gene was knockdown in these cells. This neuroprotective effect of sAPPα was translated inside the cell by the activation of the Akt signaling pathway, and it was blocked by treatment with PTX. Expression of an APP mutant lacking the G-protein interaction domain also blocked sAPPα and Akt signaling [263]. Taken together, these results describe a possible neuroprotective signaling pathway with sAPPα as an extracellular ligand, APP as its membrane receptor and Gαo as an intracellular signaling transducer that activates PI3K-Akt.

Notwithstanding the research presented above, the physiological significance of the APP-Gαo complex it is still not clear [234]. While potential roles in neuronal migration and neuroprotection seem promising, further research is still required to confirm these functions. There are also other potential processes where the APP-Gαo complex can participate that remain unexplored. One of those is their potential cooperation in neuritogenesis. As previously mentioned, Gαo and APP have both been strongly associated with neuritogenesis. Briefly, Gαo has been seen to activate different signaling pathways that lead to neurite outgrowth, such as the Src-STAT3 pathway [81, 113] and

the ERK1/2 pathway[135]. Also, some of Gαo interactors have neuritogenic functions, with some being attributed to their interaction with Gαo, such as Rit [135], Necdin [116], GAP-43 [126, 130] and GRIN1 [130, 146]. Likewise, full length APP interaction with Reelin also plays a part in the induction in neurite outgrowth [222], with APP also participating in the mediation of the NGF effects [215]. Moreover, APP's proteolytic fragment sAPPα induces neurite outgrowth through the Egr1 [226] and MAPK/ERK signaling [225]. Both APP and sAPPα participate in the regulation of neurite outgrowth via interactions with Integrin β1 [224], with our lab also showing a relationship between sAPP/APP expression and neuronal differentiation, in SH-SY5Y neuroblastoma cells differentiated with RA treatment [216]. There is some contradictory data showing that APP might instead have a negative impact in neurite outgrowth [264], or that it is not essential for proper neuronal differentiation [232].

Still, there is enough evidence supporting a role for both APP and Gαo in neuritogenesis that raises the possibility of these two proteins interacting and cooperating in this function. Supporting this potential role is the aforementioned study showing that AICD interacts with another G protein, Gαs, in the promotion of neurite outgrowth [230]. The authors showed that not only AICD interacted with Gαs, but that mutating the Gαs binding-motif (^{672}RHLSK^{676}) present in AICD blocked its neuritogenic effects. Since the mutated motif is also required for the APP-Gαo binding [233], this gives strength to the possibility of APP and Gαo playing a role in neuronal differentiation.

A4.3. APP-Gαo pathological function

Far more data has been published about the role of the APP-Gαo interaction in cell death and disease than its physiological function [234]. This is mainly due to the prominent part that APP plays in the pathogenesis of the Alzheimer's Disease (AD). Mutations of the residue Valine642 of APP are present in Familial Alzheimer's Disease (FAD). *In vitro* studies showed that cells expressing mutated APPs undergo apoptosis associated with DNA fragmentation, in a Go-dependent mechanism [248, 265, 266]. These APP mutants (FAD-APP) show an increased capability to activate Gαo, and FAD-APP apoptotic effects were blocked by either incubation with PTX, overexpression of a FAD-APP lacking the G-protein binding sequence, or by incubation with antibodies targeting the G-protein-binding sequence (thus blocking APP-Gαo interaction). Gαi involvement in this mechanism was excluded by co-expression of FAD-APPs with a dominant negative Gαi (G204A), which had no effect on APP-induced apoptosis. As expected, co-expression of FAD-APP with a dominant negative Gαo (G204A) blocked DNA fragmentation, further confirming Go involvement in FAD-APP apoptotic

effects. Interestingly, one study showed that Gαo activation by FAD-APP resulted in suppression of the transcriptional activity of the cAMP response element (CRE) [252]. Since activation of the cAMP-CREB signaling has been associated with synaptic plasticity and memory formation [267, 268], the authors hypothesize that CRE inhibition by FAD-APP could be a molecular event behind the memory loss that occurs during AD. Although APP interacts directly with Gαo, the βγ subunit of the heterotrimeric G-protein also seems to be important for the apoptosis induced by FAD-APP. FAD-APP co-transfection with βγ subunits induced DNA fragmentation in NK1 cells, while overexpression of Gαo alone did not have significant effects [269]. Taken together, these results show two possible roles for the APP-Gαo interaction in FAD: 1) direct activation of Gαo that leads to the blocking of the cAMP-CREB signaling and thus disrupting memory formation; or 2) releasing and activating the βγ subunit, inducing DNA fragmentation, and culminating in neuronal death [234]. Not all FAD-APP mutations lead to cell death through Gαo activation, though. For example, the Swedish mutation (K595N/M596L) induces cell death via Go activation when it is expressed at low levels, however, when expressed at high levels it leads to cell death in a way that is resistant to PTX [250].

Cell death was also detected in F11 cells and mouse primary neuronal cultures expressing Wt APP and incubated with antibodies targeting the extracellular domain of APP, an effect blocked by incubation with PTX and deletion of the His^{657}-Lys^{676} sequence [249, 270]. This correlates with previous results that showed that incubation of APP with the 22C11 antibody increased Gαo activation [239]. Further studies trying to identify the signaling downstream of the APP-induced neuronal death showed that not only was Gαo potentially involved, but that the Src kinase could also play a role, since treatment with either PTX or the Src inhibitor PP2 blocked APP effects [271]. These results are of particular interest since previous work had stablished a neuritogenic signaling pathway involving both Gαo and the Src-STAT3 [81], thus opening the possibility that APP could also participate in this pathway, and that a tight regulation is required to balance between neuronal differentiation and neuronal death.

Finally, there is still some mixed information about the role of Aβ in neuronal death induced by the APP-Gαo complex. While some reports show that Aβ does not participate in APP-Gαo neuronal death [249], others demonstrated that Aβ toxicity in neuronal cells was dependent on APP binding to Gαo (deletion of Gαo binding sequence) and Gαo activity (incubation with PTX) [251, 272]. These differences might be due the different types of studies being conducted. Sudo study tried to check if Aβ mediated the neurotoxic effect of APP upon its “activation” with specific antibodies, thus placing Aβ downstream of APP-GαO interaction, while Sola Vigo and Shaked researches placed Aβ upstream of the APP-Gαo interaction. Still, more work needs to be developed to fully understand

the interplay between Aβ and the APP-Gαo complex, and if these results have a real impact in our understandment of the AD pathology.

Analyzing the published data, one must ask how can the APP-Gαo complex have so different effects, from neuronal death to neuronal protection. There are several ways researchers can try to answer this question. One possible way is to further characterize the nature of the APP-Gαo interaction. The constitutively activation of Gαo induced by a mutant APP, such as the one occurring in FAD, in contrast with a cyclic activation of Gαo induced by Wt APP, the mechanism most likely present in healthy neurons, could be one possible explanation why so different outcomes are described. Another untapped area of APP physiology that could answer this question is the modifications that APP suffers during its cellular life. While the role of the APP proteolytic fragments have been explored (e.g. AICD), few is known about the impact of phosphorylation on APP-Gαo interaction. APP phosphorylation has several important functions, from modulation of its transport and processing, to the regulation of its protein interactome, thus it is reasonable to speculate that it might also influence APP-Gαo interaction and function.

References

[1] Sainath R, Gallo G. Cytoskeletal and signaling mechanisms of neurite formation. *Cell Tissue Res* 2015; 359: 267–78.

[2] Flynn KC. The cytoskeleton and neurite initiation. *Bioarchitecture* 2013; 3: 86–109.

[3] Tahirovic S, Bradke F. Neuronal polarity. *Cold Spring Harb Perspect Biol* 2009; 1: a001644.

[4] Takano T, Xu C, Funahashi Y, Namba T, Kaibuchi K. Neuronal polarization. *Development* 2015; 142: 2088–93.

[5] Dotti CG, Sullivan CA, Banker G a. The establishment of polarity by hippocampal neurons in culture. *J Neurosci* 1988; 8: 1454–68.

[6] Craig AM, Banker G. Neuronal Polarity. *Annu Rev Neurosci* 1994; 17: 267–310.

[7] Sakakibara A, Hatanaka Y. Neuronal polarization in the developing cerebral cortex. *Front Neurosci* 2015; 9: 116.

[8] Funahashi Y, Namba T, Nakamuta S, Kaibuchi K. Neuronal polarization in vivo: Growing in a complex environment. *Curr Opin Neurobiol* 2014; 27: 215–223.

[9] Nadarajah B, Parnavelas JG. Modes of neuronal migration in the developing cerebral cortex. *Nat Rev Neurosci* 2002; 3: 423–432.

[10] Noctor SC, Martínez-Cerdeño V, Ivic L, Kriegstein AR. Cortical neurons arise in symmetric and asymmetric division zones and migrate through specific phases. *Nat Neurosci* 2004; 7: 136–144.

[11] Rakic P. Mode of cell migration to the superficial layers of fetal monkey neocortex. *J Comp Neurol* 1972; 145: 61–83.

[12] Small JV, Stradal T, Vignal E, Rottner K. The lamellipodium: where motility begins. *Trends Cell Biol* 2002; 12: 112–20.

[13] da Silva JS, Dotti CG. Breaking the neuronal sphere: regulation of the actin cytoskeleton in neuritogenesis. *Nat Rev Neurosci* 2002; 3: 694–704.

[14] Svitkina TM, Bulanova EA, Chaga OY, Vignjevic DM, Kojima S, Vasiliev JM, Borisy GG. Mechanism of filopodia initiation by reorganization of a dendritic network. *J Cell Biol* 2003; 160: 409–421.

[15] Firat-Karalar EN, Welch MD. New mechanisms and functions of actin nucleation. *Curr Opin Cell Biol* 2011; 23: 4–13.

[16] Vignjevic D, Peloquin J, Borisy GG. In Vitro Assembly of Filopodia-Like Bundles. *Methods Enzymol* 2006; 406: 727–739.

[17] Yang C, Svitkina T. Filopodia initiation: focus on the Arp2/3 complex and formins. *Cell Adh Migr* 2011; 5: 402–8.

[18] Coles CHH, Bradke F. Coordinating Neuronal Actin–Microtubule Dynamics. *Curr Biol* 2015; 25: R677–R691.

[19] Dent EW, Kwiatkowski A V., Mebane LM, Philippar U, Barzik M, Rubinson DA, Gupton S, Van Veen JE, Furman C, Zhang J, Alberts AS, Mori S, Gertler FB. Filopodia are required for cortical neurite initiation. *Nat Cell Biol* 2007; 9: 1347–1359.

[20] Lee MK, Tuttle JB, Rebhun LI, Cleveland DW, Frankfurter A. The expression and posttranslational modification of a neuron-specific beta-tubulin isotype during chick embryogenesis. *Cell Motil Cytoskeleton* 1990; 17: 118–32.

[21] Laferrière NB, Brown DL. Expression and posttranslational modification of class III beta-tubulin during neuronal differentiation of P19 embryonal carcinoma cells. *Cell Motil Cytoskeleton* 1996; 35: 188–99.

[22] Dehmelt L, Halpain S. Actin and microtubules in neurite initiation: Are MAPs the missing link? *J Neurobiol* 2004; 58: 18–33.

[23] Georges PC, Hadzimichalis NM, Sweet ES, Firestein BL. The yin-yang of dendrite morphology: Unity of actin and microtubules. *Mol Neurobiol* 2008; 38: 270–284.

[24] Kapitein LC, Hoogenraad CC. Building the Neuronal Microtubule Cytoskeleton. *Neuron* 2015; 87: 492–506.

[25] Dent EW, Gupton SL, Gertler FB. The growth cone cytoskeleton in Axon outgrowth and guidance. *Cold Spring Harb Perspect Biol* 2011; 3: 1–39.

[26] Gallo G. Mechanisms underlying the initiation and dynamics of neuronal filopodia: from neurite formation to synaptogenesis. In: *International review of cell and molecular biology*. Elsevier, pp. 95–156.

[27] Pinyol R, Haeckel A, Ritter A, Qualmann B, Kessels MM, Small J. Regulation of N-WASP and the Arp2/3 Complex by Abp1 Controls Neuronal Morphology. *PLoS One* 2007; 2: e400.

[28] Korobova F, Svitkina T. Arp2/3 complex is important for filopodia formation, growth cone motility, and neuritogenesis in neuronal cells. *Mol Biol Cell* 2008; 19: 1561–74.

[29] Strasser GA, Rahim NA, VanderWaal KE, Gertler FB, Lanier LM. Arp2/3 Is a Negative Regulator of Growth Cone Translocation. *Neuron* 2004; 43: 81–94.

[30] Pak CW, Flynn KC, Bamburg JR. Actin-binding proteins take the reins in growth cones. *Nat Rev Neurosci* 2008; 9: 136–147.

[31] Cueille N, Blanc CT, Popa-Nita S, Kasas S, Catsicas S, Dietler G, Riederer BM. Characterization of MAP1B heavy chain interaction with actin. *Brain Res Bull* 2007; 71: 610–618.

[32] Matus A. Microtubule-associated proteins and the determination of neuronal form. *J Physiol (Paris)* 1990; 84: 134–7.

[33] Fukata Y, Kimura T, Kaibuchi K. Axon specification in hippocampal neurons. *Neurosci Res* 2002; 43: 305–15.

[34] Polleux F, Snider W. Initiating and growing an axon. *Cold Spring Harb Perspect Biol* 2010; 2: a001925.

[35] Namba T, Kibe Y, Funahashi Y, Nakamuta S, Takano T, Ueno T, Shimada A, Kozawa S, Okamoto M, Shimoda Y, Oda K, Wada Y, Masuda T, Sakakibara A, Igarashi M, Miyata T, Faivre-Sarrailh C, Takeuchi K, Kaibuchi K. Pioneering Axons Regulate Neuronal Polarization in the Developing Cerebral Cortex. *Neuron* 2014; 81: 814–829.

[36] Gärtner A, Fornasiero EF, Munck S, Vennekens K, Seuntjens E, Huttner WB, Valtorta F, Dotti CG. N-cadherin specifies first asymmetry in developing neurons. *EMBO J* 2012; 31: 1893–903.

[37] Inagaki N, Toriyama M, Sakumura Y. Systems biology of symmetry breaking during neuronal polarity formation. *Dev Neurobiol* 2011; 71: 584–593.

[38] Tavosanis G. Dendritic structural plasticity. *Dev Neurobiol* 2012; 72: 73–86.

[39] Purves D, Augustine G, Fitzpatrick D, Hall M, LaMantia A, McNamara J, White L. *Neuroscience*. 4th ed. Massachusetts: Sinauer Associates, Inchttp://www.sinauer.com/neuroscience-621.html (2008, accessed 3 May 2016).

[40] Li M, Cui Z, Niu Y, Liu B, Fan W, Yu D, Deng J. Synaptogenesis in the developing mouse visual cortex. *Brain Res Bull* 2010; 81: 107–113.

[41] Hatada Y, Wu F, Silverman R, Schacher S, Goldberg DJ. En passant synaptic varicosities form directly from growth cones by transient cessation of growth cone advance but not of actin-based motility. *J Neurobiol* 1999; 41: 242–51.

[42] Hall AC, Lucas FR, Salinas PC. Axonal remodeling and synaptic differentiation in the cerebellum is regulated by WNT-7a signaling. *Cell* 2000; 100: 525–35.

[43] Saneyoshi T, Fortin DA, Soderling TR. Regulation of spine and synapse formation by activity-dependent intracellular signaling pathways. *Curr Opin Neurobiol* 2010; 20: 108–15.

[44] Leßmann V, Brigadski T. Mechanisms, locations, and kinetics of synaptic BDNF secretion: An update. *Neurosci Res* 2009; 65: 11–22.

[45] Cohen-Cory S, Kidane AH, Shirkey NJ, Marshak S. Brain-derived neurotrophic factor and the development of structural neuronal connectivity. *Dev Neurobiol* 2010; 70: 271–88.

[46] Marshak S, Nikolakopoulou AM, Dirks R, Martens GJ, Cohen-Cory S. Cell-autonomous TrkB signaling in presynaptic retinal ganglion cells mediates axon arbor growth and synapse maturation during the establishment of retinotectal synaptic connectivity. *J Neurosci* 2007; 27: 2444–56.

[47] Deinhardt K, Chao M V. Shaping neurons: Long and short range effects of mature and proBDNF signalling upon neuronal structure. *Neuropharmacology* 2014; 76 Pt C: 603–9.

[48] Low LK, Cheng H-J. Axon pruning: an essential step underlying the developmental plasticity of neuronal connections. *Philos Trans R Soc Lond B Biol Sci* 2006; 361: 1531–44.

[49] Encinas M, Iglesias M, Liu Y, Wang H, Muhaisen A, Ceña V, Gallego C, Comella JX. Sequential treatment of SH-SY5Y cells with retinoic acid and brain-derived neurotrophic factor gives rise to fully differentiated, neurotrophic factor-dependent, human neuron-like cells. *J Neurochem* 2000; 75: 991–1003.

[50] Kaplan DR, Matsumoto K, Lucarelli E, Thielet CJ. Induction of TrkB by retinoic acid mediates biologic responsiveness to BDNF and differentiation of human neuroblastoma cells. *Neuron* 1993; 11: 321–331.

[51] Encinas M, Iglesias M, Llecha N, Comella JX. Extracellular-regulated kinases and phosphatidylinositol 3-kinase are involved in brain-derived neurotrophic factor-mediated survival and neuritogenesis of the neuroblastoma cell line SH-SY5Y. *J Neurochem* 1999; 73: 1409–1421.

[52] Agholme L, Lindström T, Kågedal K, Marcusson J, Hallbeck M, Kgedal K, Marcusson J, Hallbeck M. An in vitro model for neuroscience: Differentiation of SH-SY5Y cells into cells with morphological and biochemical characteristics of mature neurons. *J Alzheimer's Dis* 2010; 20: 1069–1082.

[53] Koh C-G. Rho GTPases and their regulators in neuronal functions and development. *Neurosignals* 2007; 15: 228–37.

[54] Auer M, Hausott B. Rho GTPases as regulators of morphological neuroplasticity. *Ann Anat - Anat Anzeiger* 2011; 193: 259–266.

[55] Garvalov BK, Flynn KC, Neukirchen D, Meyn L, Teusch N, Wu X, Brakebusch C, Bamburg JR, Bradke F. Cdc42 regulates cofilin during the establishment of neuronal polarity. *J Neurosci* 2007; 27: 13117–29.

[56] Chen C, Wirth A, Ponimaskin E. Cdc42: An important regulator of neuronal morphology. *Int J Biochem Cell Biol* 2012; 44: 447–451.

[57] Nikolic M. The role of Rho GTPases and associated kinases in regulating neurite outgrowth. *Int J Biochem Cell Biol* 2002; 34: 731–745.

[58] Schwamborn JC, Püschel AW. The sequential activity of the GTPases Rap1B and Cdc42 determines neuronal polarity. *Nat Neurosci* 2004; 7: 923–929.

[59] Gonzalez-Billault C, Muñoz-Llancao P, Henriquez DR, Wojnacki J, Conde C, Caceres A. The role of small GTPases in neuronal morphogenesis and polarity. *Cytoskeleton (Hoboken)* 2012; 69: 464–85.

[60] Read DE, Gorman AM. Involvement of Akt in neurite outgrowth. *Cell Mol Life Sci* 2009; 66: 2975–2984.

[61] Ishima T, Iyo M, Hashimoto K. Neurite outgrowth mediated by the heat shock protein Hsp90α: a novel target for the antipsychotic drug aripiprazole. *Transl Psychiatry* 2012; 2: e170.

[62] Kumar V, Zhang M-X, Swank MW, Kunz J, Wu G-Y. Regulation of dendritic morphogenesis by Ras-PI3K-Akt-mTOR and Ras-MAPK signaling pathways. *J Neurosci* 2005; 25: 11288–99.

[63] Jiang H, Guo W, Liang X, Rao Y. Both the establishment and the maintenance of neuronal polarity require active mechanisms: critical roles of GSK-3beta and its upstream regulators. *Cell* 2005; 120: 123–35.

[64] Zhou F-Q, Zhou J, Dedhar S, Wu Y-H, Snider WD. NGF-induced axon growth is mediated by localized inactivation of GSK-3beta and functions of the microtubule plus end binding protein APC. *Neuron* 2004; 42: 897–912.

[65] Samuels IS, Saitta SC, Landreth GE. MAP'ing CNS Development and Cognition: An ERKsome Process. *Neuron* 2009; 61: 160–167.

[66] Olsson A-K, Vadhammar K, Nånberg E. Activation and Protein Kinase C-Dependent Nuclear Accumulation of ERK in Differentiating Human Neuroblastoma Cells. *Exp Cell Res* 2000; 256: 454–467.

[67] Huang X, Zhu L, Zhao T, Wu L, Wu K, Schachner M, Xiao Z-C, Fan M. CHL1 negatively regulates the proliferation and neuronal differentiation of neural progenitor cells through activation of the ERK1/2 MAPK pathway. *Mol Cell Neurosci* 2011; 46: 296–307.

[68] Vaudry D, Stork PJS, Lazarovici P, Eiden LE. Signaling pathways for PC12 cell differentiation: making the right connections. *Science* 2002; 296: 1648–9.

[69] Lein PJ, Guo X, Shi G-X, Moholt-Siebert M, Bruun D, Andres DA. The novel GTPase Rit differentially regulates axonal and dendritic growth. *J Neurosci* 2007; 27: 4725–36.

[70] Funahashi Y, Namba T, Fujisue S, Itoh N, Nakamuta S, Kato K, Shimada A, Xu C, Shan W, Nishioka T, Kaibuchi K. ERK2-mediated phosphorylation of Par3 regulates neuronal polarization. *J Neurosci* 2013; 33: 13270–85.

[71] Pucilowska J, Puzerey PA, Karlo JC, Galán RF, Landreth GE. Disrupted ERK signaling during cortical development leads to abnormal progenitor proliferation, neuronal and network excitability and behavior, modeling human neuro-cardio-facial-cutaneous and related syndromes. *J Neurosci* 2012; 32: 8663–77.

[72] Aouadi M, Binetruy B, Caron L, Le Marchand-Brustel Y, Bost F. Role of MAPKs in development and differentiation: lessons from knockout mice. *Biochimie* 2006; 88: 1091–8.

[73] Haura EB. SRC and STAT pathways. *J Thorac Oncol* 2006; 1: 403–5.

[74] Yuan J, Zhang F, Niu R, Zhou Z, Jing N. Multiple regulation pathways and pivotal biological functions of STAT3 in cancer. *Sci Rep* 2015; 5: 17663.

[75] Rawlings JS, Rosler KM, Harrison DA. The JAK/STAT signaling pathway. *J Cell Sci* 2004; 117: 1281–3.

[76] Wu YY, Bradshaw RA. Induction of neurite outgrowth by interleukin-6 is accompanied by activation of Stat3 signaling pathway in a variant PC12 cell (E2) line. *J Biol Chem* 1996; 271: 13023–32.

[77] Wu YY, Bradshaw RA. Activation of the Stat3 Signaling Pathway Is Required for Differentiation by Interleukin-6 in PC12-E2 Cells. *J Biol Chem* 2000; 275: 2147–2156.

[78] Yamauchi K, Osuka K, Takayasu M, Usuda N, Nakazawa A, Nakahara N, Yoshida M, Aoshima C, Hara M, Yoshida J. Activation of JAK/STAT signalling in neurons following spinal cord injury in mice. *J Neurochem* 2006; 96: 1060–1070.

[79] Dziennis S, Alkayed NJ. Role of signal transducer and activator of transcription 3 in neuronal survival and regeneration. *Rev Neurosci* 2008; 19: 341–61.

[80] Nicolas CS, Peineau S, Amici M, Csaba Z, Fafouri A, Javalet C, Collett VJ, Hildebrandt L, Seaton G, Choi S-LL, Sim S-EE, Bradley C, Lee K, Zhuo M, Kaang B-KK, Gressens P, Dournaud P, Fitzjohn SM, Bortolotto ZA, Cho K, Collingridge GL. The JAK/STAT Pathway Is Involved in Synaptic Plasticity. *Neuron* 2012; 73: 374–390.

[81] He JC, Gomes I, Nguyen T, Jayaram G, Ram PT, Devi LA, Iyengar R. The G alpha(o/i)-coupled cannabinoid receptor-mediated neurite outgrowth involves Rap regulation of Src and Stat3. *J Biol Chem* 2005; 280: 33426–34.

[82] Milligan G, Kostenis E. Heterotrimeric G-proteins: a short history. *Br J Pharmacol* 2006; 147 Suppl: S46-55.

[83] Sternweis PC, Robishaw JD. Isolation of two proteins with high affinity for guanine nucleotides from membranes of bovine brain. *J Biol Chem* 1984; 259: 13806–13.

[84] Neer EJ, Lok JM, Wolf LG. Purification and properties of the inhibitory guanine nucleotide regulatory unit of brain adenylate cyclase. *J Biol Chem* 1984; 259: 14222–9.

[85] Rasmussen SGF, DeVree BT, Zou Y, Kruse AC, Chung KY, Kobilka TS, Thian FS, Chae PS, Pardon E, Calinski D, Mathiesen JM, Shah STA, Lyons JA, Caffrey M, Gellman SH, Steyaert J, Skiniotis G, Weis WI, Sunahara RK, Kobilka BK. Crystal structure of the β2 adrenergic receptor-Gs protein complex. *Nature* 2011; 477: 549–55.

[86] Baltoumas FA, Theodoropoulou MC, Hamodrakas SJ. Interactions of the α-subunits of heterotrimeric G-proteins with GPCRs, effectors and RGS proteins: a critical review and analysis of interacting surfaces, conformational shifts, structural diversity and electrostatic

potentials. *J Struct Biol* 2013; 182: 209–18.

[87] Kimple AJ, Bosch DE, Giguère PM, Siderovski DP. Regulators of G-protein signaling and their Gα substrates: promises and challenges in their use as drug discovery targets. *Pharmacol Rev* 2011; 63: 728–749.

[88] Mangmool S, Kurose H. Gi/o protein-dependent and -independent actions of pertussis toxin (ptx). *Toxins (Basel)* 2011; 3: 884–899.

[89] Jiang M, Gold MS, Boulay G, Spicher K, Peyton M, Brabet P, Srinivasan Y, Rudolph U, Ellison G, Birnbaumer L. Multiple neurological abnormalities in mice deficient in the G protein Go. *Proc Natl Acad Sci U S A* 1998; 95: 3269–74.

[90] Jiang M, Bajpayee NS. Molecular mechanisms of go signaling. *Neurosignals* 2009; 17: 23–41.

[91] Tsukamoto T, Toyama R, Itoh H, Kozasa T, Matsuoka M, Kaziro Y. Structure of the human gene and two rat cDNAs encoding the alpha chain of GTP-binding regulatory protein Go: two different mRNAs are generated by alternative splicing. *Proc Natl Acad Sci U S A* 1991; 88: 2974–8.

[92] Lang J. Purification and characterization of subforms of the guanine-nucleotide-binding proteins G alpha i and G alpha o. *Eur J Biochem* 1989; 183: 687–92.

[93] Murtagh JJ, Eddy R, Shows TB, Moss J, Vaughan M. Different forms of Go alpha mRNA arise by alternative splicing of transcripts from a single gene on human chromosome 16. *Mol Cell Biol* 1991; 11: 1146–55.

[94] The UniProt Consortium. UniProt: the universal protein knowledgebase. *Nucleic Acids Res* 2017; 45: D158–D169.

[95] McIntire WE, Dingus J, Schey KL, Hildebrandt JD. Characterization of the major bovine brain Go alpha isoforms. Mapping the structural differences between the alpha subunit isoforms identifies a variable region of the protein involved in receptor interactions. *J Biol Chem* 1998; 273: 33135–41.

[96] Exner T, Jensen ON, Mann M, Kleuss C, Nürnberg B. Posttranslational modification of Galphao1 generates Galphao3, an abundant G protein in brain. *Proc Natl Acad Sci U S A* 1999; 96: 1327–32.

[97] Uhlén M, Fagerberg L, Hallström BM, Lindskog C, Oksvold P, Mardinoglu A, Sivertsson Å,

Kampf C, Sjöstedt E, Asplund A, Olsson I, Edlund K, Lundberg E, Navani S, Szigyarto CA-K, Odeberg J, Djureinovic D, Takanen JO, Hober S, Alm T, Edqvist P-H, Berling H, Tegel H, Mulder J, Rockberg J, Nilsson P, Schwenk JM, Hamsten M, von Feilitzen K, Forsberg M, Persson L, Johansson F, Zwahlen M, von Heijne G, Nielsen J, Pontén F. Proteomics. Tissue-based map of the human proteome. *Science* 2015; 347: 1260419.

[98] Worley PF, Baraban JM, Van Dop C, Neer EJ, Snyder SH. Go, a guanine nucleotide-binding protein: immunohistochemical localization in rat brain resembles distribution of second messenger systems. *Proc Natl Acad Sci U S A* 1986; 83: 4561–5.

[99] Petryszak R, Keays M, Tang YA, Fonseca NA, Barrera E, Burdett T, Füllgrabe A, Fuentes AM-P, Jupp S, Koskinen S, Mannion O, Huerta L, Megy K, Snow C, Williams E, Barzine M, Hastings E, Weisser H, Wright J, Jaiswal P, Huber W, Choudhary J, Parkinson HE, Brazma A. Expression Atlas update--an integrated database of gene and protein expression in humans, animals and plants. *Nucleic Acids Res* 2016; 44: D746-52.

[100] Lizio M, Harshbarger J, Shimoji H, Severin J, Kasukawa T, Sahin S, Abugessaisa I, Fukuda S, Hori F, Ishikawa-Kato S, Mungall CJ, Arner E, Baillie JK, Bertin N, Bono H, de Hoon M, Diehl AD, Dimont E, Freeman TC, Fujieda K, Hide W, Kaliyaperumal R, Katayama T, Lassmann T, Meehan TF, Nishikata K, Ono H, Rehli M, Sandelin A, Schultes EA, 't Hoen PAC, Tatum Z, Thompson M, Toyoda T, Wright DW, Daub CO, Itoh M, Carninci P, Hayashizaki Y, Forrest ARR, Kawaji H, FANTOM consortium. Gateways to the FANTOM5 promoter level mammalian expression atlas. *Genome Biol* 2015; 16: 22.

[101] GTEx Consortium. The Genotype-Tissue Expression (GTEx) project. *Nat Genet* 2013; 45: 580–5.

[102] GTEx Consortium. Human genomics. The Genotype-Tissue Expression (GTEx) pilot analysis: multitissue gene regulation in humans. *Science* 2015; 348: 648–60.

[103] Brabet P, Dumuis A, Sebben M, Pantaloni C, Bockaert J, Homburger V. Immunocytochemical localization of the guanine nucleotide-binding protein Go in primary cultures of neuronal and glial cells. *J Neurosci* 1988; 8: 701–8.

[104] Strittmatter SM, Valenzuela D, Kennedy TE, Neer EJ, Fishman MC. Go is a major growth cone protein subject to regulation by GAP-43. *Nature* 1990; 344: 836–41.

[105] Mullaney I, Milligan G. Identification of two distinct isoforms of the guanine nucleotide binding protein G0 in neuroblastoma X glioma hybrid cells: independent regulation during

cyclic AMP-induced differentiation. *J Neurochem* 1990; 55: 1890–8.

[106] Brabet P, Pantaloni C, Rodriguez M, Martinez J, Bockaert J, Homburger V. Neuroblastoma differentiation involves the expression of two isoforms of the alpha-subunit of Go. *J Neurochem* 1990; 54: 1310–20.

[107] Brabet P, Pantaloni C, Bockaert J, Homburger V. Metabolism of two Go alpha isoforms in neuronal cells during differentiation. *J Biol Chem* 1991; 266: 12825–8.

[108] Schüller U, Lamp EC, Schilling K. Developmental expression of heterotrimeric G-proteins in the murine cerebellar cortex. *Histochem Cell Biol* 2001; 116: 149–159.

[109] Asano T, Morishita R, Sano M, Kato K. The GTP-binding proteins, Go and Gi2, of neural cloned cells and their changes during differentiation. *J Neurochem* 1989; 53: 1195–8.

[110] Ammer H, Schulz R. Retinoic acid-induced differentiation of human neuroblastoma SH-SY5Y cells is associated with changes in the abundance of G proteins. *J Neurochem* 1994; 62: 1310–8.

[111] Granneman JG, Kapatos G. Developmental expression of Go in neuronal cultures from rat mesencephalon and hypothalamus. *J Neurochem* 1990; 54: 1995–2001.

[112] Asano T, Kamiya N, Semba R, Kato K. Ontogeny of the GTP-binding protein Go in rat brain and heart. *J Neurochem* 1988; 51: 1711–6.

[113] Bromberg KD, Iyengar R, He JC. Regulation of neurite outgrowth by G(i/o) signaling pathways. *Front Biosci* 2008; 13: 4544–57.

[114] Ma'ayan A, Jenkins SL, Barash A, Iyengar R. Neuro2A Differentiation by G i/o Pathway. *Sci Signal* 2009; 2: cm1-cm1.

[115] Yoshikawa K. Cell cycle regulators in neural stem cells and postmitotic neurons. *Neurosci Res* 2000; 37: 1–14.

[116] Ju H, Lee S, Kang S, Kim S-S, Ghil S. The alpha subunit of Go modulates cell proliferation and differentiation through interactions with Necdin. *Cell Commun Signal* 2014; 12: 39.

[117] Kroll SD, Chen J, De Vivo M, Carty DJ, Buku A, Premont RT, Iyengar R. The Q205LGo-alpha subunit expressed in NIH-3T3 cells induces transformation. *J Biol Chem* 1992; 267: 23183–8.

[118] Ram PT, Horvath CM, Iyengar R. Stat3-mediated transformation of NIH-3T3 cells by the

constitutively active Q205L Galphao protein. *Science (80-)* 2000; 287: 142–144.

[119] Jordan JD, He JC, Eungdamrong NJ, Gomes I, Ali W, Nguyen T, Bivona TG, Philips MR, Devi LA, Iyengar R. Cannabinoid receptor-induced neurite outgrowth is mediated by Rap1 activation through G(alpha)o/i-triggered proteasomal degradation of Rap1GAPII. *J Biol Chem* 2005; 280: 11413–11421.

[120] Jordan JD, Carey KD, Stork PJ, Iyengar R. Modulation of rap activity by direct interaction of Galpha(o) with Rap1 GTPase-activating protein. *J Biol Chem* 1999; 274: 21507–10.

[121] Cho S-K, Choi J-M, Kim J-M, Cho JY, Kim S-S, Hong S, Suh-Kim H, Lee Y-D. AKT-independent Reelin signaling requires interactions of heterotrimeric Go and Src. *Biochem Biophys Res Commun* 2015; 467: 1063–9.

[122] Lee GH, D'Arcangelo G. New Insights into Reelin-Mediated Signaling Pathways. *Front Cell Neurosci* 2016; 10: 122.

[123] Oestreicher AB, De Graan PN, Gispen WH, Verhaagen J, Schrama LH. B-50, the growth associated protein-43: modulation of cell morphology and communication in the nervous system. *Prog Neurobiol* 1997; 53: 627–86.

[124] Donnelly CJ, Park M, Spillane M, Yoo S, Pacheco A, Gomes C, Vuppalanchi D, McDonald M, Kim HKHKH, Kim HKHKH, Merianda TT, Gallo G, Twiss JL. Axonally synthesized β-actin and GAP-43 proteins support distinct modes of axonal growth. *J Neurosci* 2013; 33: 3311–22.

[125] Strittmatter SM, Valenzuela D, Sudo Y, Linder ME, Fishman MC. An intracellular guanine nucleotide release protein for G0. GAP-43 stimulates isolated alpha subunits by a novel mechanism. *J Biol Chem* 1991; 266: 22465–71.

[126] Strittmatter SM, Igarashi M, Fishman MC. GAP-43 amino terminal peptides modulate growth cone morphology and neurite outgrowth. *J Neurosci* 1994; 14: 5503–5513.

[127] Linder ME, Middleton P, Hepler JR, Taussig R, Gilman AG, Mumby SM. Lipid modifications of G proteins: alpha subunits are palmitoylated. *Proc Natl Acad Sci U S A* 1993; 90: 3675–9.

[128] Yang H, Wan L, Song F, Wang M, Huang Y. Palmitoylation modification of Galpha(o) depresses its susceptibility to GAP-43 activation. *Int J Biochem Cell Biol* 2009; 41: 1495–501.

[129] Strittmatter SM, Cannon SC, Ross EM, Higashijima T, Fishman MC. GAP-43 augments G protein-coupled receptor transduction in Xenopus laevis oocytes. *Proc Natl Acad Sci U S A*

1993; 90: 5327–5331.

[130] Nordman JC, Kabbani N. An interaction between α7 nicotinic receptors and a G-protein pathway complex regulates neurite growth in neural cells. *J Cell Sci* 2012; 125: 5502–13.

[131] van Biesen T, Hawes BE, Raymond JR, Luttrell LM, Koch WJ, Lefkowitz RJ. G(o)-protein alpha-subunits activate mitogen-activated protein kinase via a novel protein kinase C-dependent mechanism. *J Biol Chem* 1996; 271: 1266–9.

[132] Antonelli V, Bernasconi F, Wong YH, Vallar L. Activation of B-Raf and regulation of the mitogen-activated protein kinase pathway by the G(o) alpha chain. *Mol Biol Cell* 2000; 11: 1129–42.

[133] Choe Y, Lee BJ, Kim K. Participation of protein kinase C alpha isoform and extracellular signal-regulated kinase in neurite outgrowth of GT1 hypothalamic neurons. *J Neurochem* 2002; 83: 1412–22.

[134] Liao K-KK, Wu M-JJ, Chen P-YY, Huang S-WW, Chiu S-JJ, Ho C-TT, Yen J-HH. Curcuminoids promote neurite outgrowth in PC12 cells through MAPK/ERK- and PKC-dependent pathways. *J Agric Food Chem* 2012; 60: 433–443.

[135] Kim SH, Kim S, Ghil SH. Rit contributes to neurite outgrowth triggered by the alpha subunit of Go. *Neuroreport* 2008; 19: 521–5.

[136] Lee J, Ghil S. Regulator of G protein signaling 8 inhibits protease-activated receptor 1/Gi/o signaling by forming a distinct G protein-dependent complex in live cells. *Cell Signal* 2016; 28: 391–400.

[137] Cotta-Grand N, Rovère C, Guyon A, Cervantes A, Brau F, Nahon J-L. Melanin-concentrating hormone induces neurite outgrowth in human neuroblastoma SH-SY5Y cells through p53 and MAPKinase signaling pathways. *Peptides* 2009; 30: 2014–24.

[138] Tso PH, Wong YH. Opioid receptor-like (ORL1) receptor utilizes both G(oA) and G(oB) for signal transduction. *Protein Pept Lett* 2006; 13: 437–41.

[139] Clark MJ, Harrison C, Zhong H, Neubig RR, Traynor JR. Endogenous RGS protein action modulates mu-opioid signaling through Galphao. Effects on adenylyl cyclase, extracellular signal-regulated kinases, and intracellular calcium pathways. *J Biol Chem* 2003; 278: 9418–25.

[140] Lamberts JT, Jutkiewicz EM, Mortensen RM, Traynor JR. Mu-Opioid Receptor Coupling to

Gαo Plays an Important Role in Opioid Antinociception. *Neuropsychopharmacology* 2011; 36: 2041–2053.

[141] Lamberts JT, Smith CE, Li M-H, Ingram SL, Neubig RR, Traynor JR. Differential control of opioid antinociception to thermal stimuli in a knock-in mouse expressing regulator of G-protein signaling-insensitive Gαo protein. *J Neurosci* 2013; 33: 4369–77.

[142] Yin X, Ouyang S, Xu W, Zhang X, Fok KL, Wong HY, Zhang J, Qiu X, Miao S, Chan HC, Wang L. YWK-II protein as a novel G(o)-coupled receptor for Müllerian inhibiting substance in cell survival. *J Cell Sci* 2007; 120: 1521–8.

[143] Wu W, Song W, Li S, Ouyang S, Fok KL, Diao R, Miao S, Chan HC, Wang L. Regulation of apoptosis by Bat3-enhanced YWK-II/APLP2 protein stability. *J Cell Sci* 2012; 125: 4219–29.

[144] Shariati SAM, Lau P, Hassan BA, Müller U, Dotti CG, De Strooper B, Gärtner A. APLP2 regulates neuronal stem cell differentiation during cortical development. *J Cell Sci* 2013; 126: 1268–77.

[145] Chen LT, Gilman AG, Kozasa T. A candidate target for G protein action in brain. *J Biol Chem* 1999; 274: 26931–8.

[146] Nakata H, Kozasa T. Functional characterization of Galphao signaling through G protein-regulated inducer of neurite outgrowth 1. *Mol Pharmacol* 2005; 67: 695–702.

[147] Nordman JC, Phillips WS, Kodama N, Clark SG, Del Negro CA, Kabbani N. Axon targeting of the alpha 7 nicotinic receptor in developing hippocampal neurons by Gprin1 regulates growth. *J Neurochem* 2014; 129: 649–662.

[148] Masuho I, Mototani Y, Sahara Y, Asami J, Nakamura S, Kozasa T, Inoue T. Dynamic expression patterns of G protein-regulated inducer of neurite outgrowth 1 (GRIN1) and its colocalization with Galphao implicate significant roles of Galphao-GRIN1 signaling in nervous system. *Dev Dyn* 2008; 237: 2415–29.

[149] Hwangpo A, Jordan JD, Premsrirut PK, Jayamaran G, Licht JD, Iyengar R, Neves SR. G protein-regulated inducer of neurite outgrowth (GRIN) modulates sprouty protein repression of mitogen-activated protein kinase (MAPK) activation by growth factor stimulation. *J Biol Chem* 2012; 287: 13674–13685.

[150] Lu Z, Xu S. ERK1/2 MAP kinases in cell survival and apoptosis. *IUBMB Life* 2006; 58: 621–31.

[151] Zhang K, Duan L, Ong Q, Lin Z, Varman PM, Sung K, Cui B. Light-mediated kinetic control

reveals the temporal effect of the Raf/MEK/ERK pathway in PC12 cell neurite outgrowth. *PLoS One* 2014; 9: e92917.

[152] Zaworski PG, Alberts GL, Pregenzer JF, Im W Bin, Slightom JL, Gill GS. Efficient functional coupling of the human D3 dopamine receptor to G(o) subtype of G proteins in SH-SY5Y cells. *Br J Pharmacol* 1999; 128: 1181–8.

[153] Jiang M, Spicher K, Boulay G, Wang Y, Birnbaumer L. Most central nervous system D2 dopamine receptors are coupled to their effectors by Go. *Proc Natl Acad Sci U S A* 2001; 98: 3577–3582.

[154] Möller D, Kling RCR, Skultety M, Leuner K, Hübner H, Gmeiner P. Functionally Selective Dopamine D2, D3 Receptor Partial Agonists. *J Med Chem* 2014; 57: 4861–75.

[155] Ciani L, Salinas PC. WNTs in the vertebrate nervous system: from patterning to neuronal connectivity. *Nat Rev Neurosci* 2005; 6: 351–362.

[156] Katanaev VL, Ponzielli R, Sémériva M, Tomlinson A. Trimeric G protein-dependent frizzled signaling in Drosophila. *Cell* 2005; 120: 111–22.

[157] Bikkavilli RK, Feigin ME, Malbon CC. G alpha o mediates WNT-JNK signaling through dishevelled 1 and 3, RhoA family members, and MEKK 1 and 4 in mammalian cells. *Journal of cell science* 2008; 121: 234–245.

[158] Lüchtenborg A-M, Solis GP, Egger-Adam D, Koval A, Lin C, Blanchard MG, Kellenberger S, Katanaev VL. Heterotrimeric Go protein links Wnt-Frizzled signaling with ankyrins to regulate the neuronal microtubule cytoskeleton. *Development* 2014; 141: 3399–409.

[159] Ramírez VT, Ramos-Fernández E, Henríquez JP, Lorenzo A, Inestrosa NC. Wnt-5a/Frizzled9 Receptor Signaling through the Gαo-Gβγ Complex Regulates Dendritic Spine Formation. *J Biol Chem* 2016; 291: 19092–107.

[160] Ramírez VT, Ramos-Fernández E, Inestrosa NC. The Gαo Activator Mastoparan-7 Promotes Dendritic Spine Formation in Hippocampal Neurons. *Neural Plast* 2016; 2016: 4258171.

[161] Ahnert-Hilger G, Nurnberg B, Exner T, Schafer T, Jahn R. The heterotrimeric G protein Go2 regulates catecholamine uptake by secretory vesicles. *EMBO J* 1998; 17: 406–413.

[162] Höltje M, von Jagow B, Pahner I, Lautenschlager M, Hörtnagl H, Nürnberg B, Jahn R, Ahnert-Hilger G. The neuronal monoamine transporter VMAT2 is regulated by the trimeric GTPase Go(2). *J Neurosci* 2000; 20: 2131–41.

[163] Winter S. G o2 Regulates Vesicular Glutamate Transporter Activity by Changing Its Chloride Dependence. *J Neurosci* 2005; 25: 4672–4680.

[164] Baron J, Blex C, Rohrbeck A, Rachakonda SK, Birnbaumer L, Ahnert-Hilger G, Brunk I. The α-subunit of the trimeric GTPase Go2 regulates axonal growth. *J Neurochem* 2013; 124: 782–94.

[165] Traver S, Bidot C, Spassky N, Baltauss T, De Tand MF, Thomas JL, Zalc B, Janoueix-Lerosey I, Gunzburg JD. RGS14 is a novel Rap effector that preferentially regulates the GTPase activity of galphao. *Biochem J* 2000; 350 Pt 1: 19–29.

[166] Lee SE, Simons SB, Heldt SA, Zhao M, Schroeder JP, Vellano CP, Cowan DP, Ramineni S, Yates CK, Feng Y, Smith Y, Sweatt JD, Weinshenker D, Ressler KJ, Dudek SM, Hepler JR. RGS14 is a natural suppressor of both synaptic plasticity in CA2 neurons and hippocampal-based learning and memory. *Proc Natl Acad Sci U S A* 2010; 107: 16994–8.

[167] Evans PR, Dudek SM, Hepler JR. Regulator of G Protein Signaling 14: A Molecular Brake on Synaptic Plasticity Linked to Learning and Memory. *Prog Mol Biol Transl Sci* 2015; 133: 169–206.

[168] Shu F, Ramineni S, Hepler JR. RGS14 is a multifunctional scaffold that integrates G protein and Ras/Raf MAPkinase signalling pathways. *Cell Signal* 2010; 22: 366–76.

[169] Xu G-Y, Winston JH, Shenoy M, Yin H, Pasricha PJ. Enhanced excitability and suppression of A-type K+ current of pancreas-specific afferent neurons in a rat model of chronic pancreatitis. *Am J Physiol Gastrointest Liver Physiol* 2006; 291: G424-31.

[170] Zhao X, Zhang Y, Qin W, Cao J, Zhang Y, Ni J, Sun Y, Jiang X, Tao J. Serotonin type-1D receptor stimulation of A-type K(+) channel decreases membrane excitability through the protein kinase A- and B-Raf-dependent p38 MAPK pathways in mouse trigeminal ganglion neurons. *Cell Signal* 2016; 28: 979–88.

[171] Fricker AD, Rios C, Devi LA, Gomes I. Serotonin receptor activation leads to neurite outgrowth and neuronal survival. *Mol Brain Res* 2005; 138: 228–235.

[172] Ghil SH, Kim BJ, Lee YD, Suh-Kim H. Neurite outgrowth induced by cyclic AMP can be modulated by the alpha subunit of Go. *J Neurochem* 2000; 74: 151–8.

[173] Nalivaeva NN, Turner AJ. The amyloid precursor protein: A biochemical enigma in brain development, function and disease. *FEBS Lett* 2013; 587: 2046–2054.

[174] Zhang Y, Xu H. Molecular and Cellular Mechanisms for Alzheimers Disease:Understanding APP Metabolism. *Curr Mol Med* 2007; 7: 687–696.

[175] Heber S, Herms J, Gajic V, Hainfellner J, Aguzzi A, Rülicke T, von Kretzschmar H, von Koch C, Sisodia S, Tremml P, Lipp HP, Wolfer DP, Müller U. Mice with combined gene knock-outs reveal essential and partially redundant functions of amyloid precursor protein family members. *J Neurosci* 2000; 20: 7951–63.

[176] Dawkins E, Small DH. Insights into the physiological function of the β-amyloid precursor protein: beyond Alzheimer's disease. *J Neurochem* 2014; 129: 756–769.

[177] Tanaka S, Shiojiri S, Takahashi Y, Kitaguchi N, Ito H, Kameyama M, Kimura J, Nakamura S, Ueda K. Tissue-specific expression of three types of β-protein precursor mRNA: Enhancement of protease inhibitor-harboring types in Alzheimer's disease brain. *Biochem Biophys Res Commun* 1989; 165: 1406–1414.

[178] van der Kant R, Goldstein LSB. Cellular Functions of the Amyloid Precursor Protein from Development to Dementia. *Dev Cell* 2015; 32: 502–515.

[179] Thinakaran G, Koo EH. Amyloid precursor protein trafficking, processing, and function. *J Biol Chem* 2008; 283: 29615–29619.

[180] Cole SL, Vassar R. The role of amyloid precursor protein processing by BACE1, the beta-secretase, in Alzheimer disease pathophysiology. *J Biol Chem* 2008; 283: 29621–29625.

[181] Chow VW, Mattson MP, Wong PC, Gleichmann M. An overview of APP processing enzymes and products. *Neuromolecular Med* 2010; 12: 1–12.

[182] O'Brien RJ, Wong PC. Amyloid precursor protein processing and Alzheimer's disease. *Annu Rev Neurosci* 2011; 34: 185–204.

[183] Marotta CA, Majocha RE, Tate B. Molecular and cellular biology of Alzheimer amyloid. *JMolNeurosci* 1992; 3: 111–125.

[184] Selkoe DJ, Hardy J. The amyloid hypothesis of Alzheimer's disease at 25 years. *EMBO Mol Med* 2016; 8: 595–608.

[185] Puzzo D, Privitera L, Fa' M, Staniszewski A, Hashimoto G, Aziz F, Sakurai M, Ribe EM, Troy CM, Mercken M, Jung SS, Palmeri A, Arancio O. Endogenous amyloid-β is necessary for hippocampal synaptic plasticity and memory. *Ann Neurol* 2011; 69: 819–830.

[186] Lawrence JLM, Tong M, Alfulaij N, Sherrin T, Contarino M, White MM, Bellinger FP,

Todorovic C, Nichols RA. Regulation of presynaptic Ca2+, synaptic plasticity and contextual fear conditioning by a N-terminal β-amyloid fragment. *J Neurosci* 2014; 34: 14210–8.

[187] Müller UC, Deller T, Korte M. Not just amyloid: physiological functions of the amyloid precursor protein family. *Nat Rev Neurosci* 2017; 18: 281–298.

[188] Taylor CJ, Ireland DR, Ballagh I, Bourne K, Marechal NM, Turner PR, Bilkey DK, Tate WP, Abraham WC. Endogenous secreted amyloid precursor protein-α regulates hippocampal NMDA receptor function, long-term potentiation and spatial memory. *Neurobiol Dis* 2008; 31: 250–260.

[189] Hoe HS, Lee HK, Pak DTS. The upside of APP at synapses. *CNS Neurosci Ther* 2012; 18: 47–56.

[190] Weyer SW, Zagrebelsky M, Herrmann U, Hick M, Ganss L, Gobbert J, Gruber M, Altmann C, Korte M, Deller T, Müller UC. Comparative analysis of single and combined APP/APLP knockouts reveals reduced spine density in APP-KO mice that is prevented by APPsα expression. *Acta Neuropathol Commun* 2014; 2: 36.

[191] Fol R, Braudeau J, Ludewig S, Abel T, Weyer SW, Roederer J-P, Brod F, Audrain M, Bemelmans A-P, Buchholz CJ, Korte M, Cartier N, Müller UC. Viral gene transfer of APPsα rescues synaptic failure in an Alzheimer's disease mouse model. *Acta Neuropathol* 2016; 131: 247–266.

[192] Gralle M, Botelho MG, Wouters FS. Neuroprotective secreted amyloid precursor protein acts by disrupting amyloid precursor protein dimers. *J Biol Chem* 2009; 284: 15016–25.

[193] Corrigan F, Vink R, Blumbergs PC, Masters CL, Cappai R, Van Den Heuvel C. SAPPα rescues deficits in amyloid precursor protein knockout mice following focal traumatic brain injury. *J Neurochem* 2012; 122: 208–220.

[194] Demars MP, Bartholomew A, Strakova Z, Lazarov O. Soluble amyloid precursor protein: a novel proliferation factor of adult progenitor cells of ectodermal and mesodermal origin. *Stem Cell Res Ther* 2011; 2: 36.

[195] Nikolaev A, McLaughlin T, O'Leary DDM, Tessier-Lavigne M. APP binds DR6 to trigger axon pruning and neuron death via distinct caspases. *Nature* 2009; 457: 981–9.

[196] Nakaya T, Suzuki T. Role of APP phosphorylation in FE65-dependent gene transactivation mediated by AICD. *Genes Cells* 2006; 11: 633–45.

[197] Pardossi-Piquard R, Checler F. The physiology of the β-amyloid precursor protein intracellular domain AICD. *J Neurochem* 2012; 120: 109–124.

[198] von Rotz RC, Kohli BM, Bosset J, Meier M, Suzuki T, Nitsch RM, Konietzko U. The APP intracellular domain forms nuclear multiprotein complexes and regulates the transcription of its own precursor. *J Cell Sci* 2004; 117: 4435–48.

[199] Ozaki T, Li Y, Kikuchi H, Tomita T, Iwatsubo T, Nakagawara A. The intracellular domain of the amyloid precursor protein (AICD) enhances the p53-mediated apoptosis. *Biochem Biophys Res Commun* 2006; 351: 57–63.

[200] Haass C, Kaether C, Thinakaran G, Sisodia S. Trafficking and proteolytic processing of APP. *Cold Spring Harb Perspect Med* 2012; 2: a006270.

[201] Deyts C, Thinakaran G, Parent AT. APP Receptor? To Be or Not To Be. *Trends Pharmacol Sci* 2016; 37: 390–411.

[202] Musardo S, Saraceno C, Pelucchi S, Marcello E. Trafficking in neurons: Searching for new targets for Alzheimer's disease future therapies. *Eur J Pharmacol* 2013; 719: 84–106.

[203] Walter J, Capell A, Hung AY, Langen H, Schnolzer M, Thinakaran G, Sisodia SS, Selkoe DJ, Haass C. Ectodomain phosphorylation of beta-amyloid precursor protein at two distinct cellular locations. *J Biol Chem* 1997; 272: 1896–1903.

[204] da Cruz e Silva EF, da Cruz e Silva OA. Protein phosphorylation and APP metabolism. *Neurochem Res* 2003; 28: 1553–1561.

[205] Tamayev R, Zhou D, D'Adamio L. The interactome of the amyloid beta precursor protein family members is shaped by phosphorylation of their intracellular domains. *Mol Neurodegener* 2009; 4: 28.

[206] Lee M-S, Kao S-C, Lemere CA, Xia W, Tseng H-C, Zhou Y, Neve R, Ahlijanian MK, Tsai L-H. APP processing is regulated by cytoplasmic phosphorylation. *J Cell Biol* 2003; 163: 83–95.

[207] Feyt C, Pierrot N, Tasiaux B, Van Hees J, Kienlen-Campard P, Courtoy PJ, Octave J-N. Phosphorylation of APP695 at Thr668 decreases gamma-cleavage and extracellular Abeta. *Biochem Biophys Res Commun* 2007; 357: 1004–10.

[208] Chang K-A, Kim H-S, Ha T-Y, Ha J-W, Shin KY, Jeong YH, Lee J-P, Park C-H, Kim S, Baik T-K, Suh Y-H. Phosphorylation of amyloid precursor protein (APP) at Thr668 regulates the nuclear translocation of the APP intracellular domain and induces neurodegeneration. *Mol*

Cell Biol 2006; 26: 4327–38.

[209] Schettini G, Govoni S, Racchi M, Rodriguez G. Phosphorylation of APP-CTF-AICD domains and interaction with adaptor proteins: signal transduction and/or transcriptional role - relevance for Alzheimer pathology. *J Neurochem* 2010; 115: 1299–1308.

[210] Vieira SI, Rebelo S, Domingues SC, da Cruz e Silva EF, da Cruz e Silva OA. S655 phosphorylation enhances APP secretory traffic. *Mol Cell Biochem* 2009; 328: 145–154.

[211] Vieira SI, Rebelo S, Esselmann H, Wiltfang J, Lah J, Lane R, Small SA, Gandy S, da Cruz ESEF, da Cruz ESOA. Retrieval of the Alzheimer's amyloid precursor protein from the endosome to the TGN is S655 phosphorylation state-dependent and retromer-mediated. *Mol Neurodegener* 2010; 5: 40.

[212] Tam JHK, Rebecca Cobb M, Seah C, Pasternak SH. Tyrosine binding protein sites regulate the intracellular trafficking and processing of amyloid precursor protein through a novel lysosome-directed pathway. *PLoS One* 2016; 11: 1–24.

[213] Ramelot TA, Nicholson LK. Phosphorylation-induced structural changes in the amyloid precursor protein cytoplasmic tail detected by NMR. *J Mol Biol* 2001; 307: 871–84.

[214] Masliah E, Mallory M, Ge N, Saitoh T. Amyloid precursor protein is localized in growing neurites of neonatal rat brain. *Brain Res* 1992; 593: 323–328.

[215] Milward EA, Papadopoulos R, Fuller SJ, Moir RD, Small D, Beyreuther K, Masters CL. The amyloid protein precursor of Alzheimer's disease is a mediator of the effects of nerve growth factor on neurite outgrowth. *Neuron* 1992; 9: 129–137.

[216] da Rocha JF, da Cruz E Silva OAB, Vieira SI. Analysis of the amyloid precursor protein role in neuritogenesis reveals a biphasic SH-SY5Y neuronal cell differentiation model. *J Neurochem* 2015; 134: 288–301.

[217] Ando K, Oishi M, Takeda S, Iijima K, Isohara T, Nairn AC, Kirino Y, Greengard P, Suzuki T. Role of phosphorylation of Alzheimer's amyloid precursor protein during neuronal differentiation. *J Neurosci* 1999; 19: 4421–7.

[218] Allinquant B, Hantraye P, Mailleux P, Moya K, Bouillot C, Prochiantz A. Downregulation of amyloid precursor protein inhibits neurite outgrowth in vitro. *J Cell Biol* 1995; 128: 919–927.

[219] Sosa LJ, Bergman J, Estrada-Bernal A, Glorioso TJ, Kittelson JM, Pfenninger KH. Amyloid

Precursor Protein Is an Autonomous Growth Cone Adhesion Molecule Engaged in Contact Guidance. *PLoS One* 2013; 8: 1–16.

[220] Rama N, Goldschneider D, Corset V, Lambert J, Pays L, Mehlen P. Amyloid precursor protein regulates netrin-1-mediated commissural axon outgrowth. *J Biol Chem* 2012; 287: 30014–30023.

[221] Hoe H-S, Tran TS, Matsuoka Y, Howell BW, Rebeck GW. DAB1 and Reelin effects on amyloid precursor protein and ApoE receptor 2 trafficking and processing. *J Biol Chem* 2006; 281: 35176–85.

[222] Hoe HS, Lee KJ, Carney RS, Lee J, Markova A, Lee JY, Howell BW, Hyman BT, Pak DT, Bu G, Rebeck GW. Interaction of reelin with amyloid precursor protein promotes neurite outgrowth. *J Neurosci* 2009; 29: 7459–7473.

[223] Hasebe N, Fujita Y, Ueno M, Yoshimura K, Fujino Y, Yamashita T. Soluble β-amyloid Precursor Protein Alpha binds to p75 neurotrophin receptor to promote neurite outgrowth. *PLoS One* 2013; 8: e82321.

[224] Young-Pearse TL, Chen AC, Chang R, Marquez C, Selkoe DJ. Secreted APP regulates the function of full-length APP in neurite outgrowth through interaction with integrin beta1. *Neural Dev* 2008; 3: 15.

[225] Gakhar-Koppole N, Hundeshagen P, Mandl C, Weyer SW, Allinquant B, Muller U, Ciccolini F. Activity requires soluble amyloid precursor protein alpha to promote neurite outgrowth in neural stem cell-derived neurons via activation of the MAPK pathway. *Eur J Neurosci* 2008; 28: 871–882.

[226] Chasseigneaux S, Dinc L, Rose C, Chabret C, Coulpier F, Topilko P, Mauger G, Allinquant B. Secreted Amyloid Precursor Protein β and Secreted Amyloid Precursor Protein α Induce Axon Outgrowth In Vitro through Egr1 Signaling Pathway. *PLoS One* 2011; 6: e16301.

[227] Kwak YD, Dantuma E, Merchant S, Bushnev S, Sugaya K. Amyloid-beta precursor protein induces glial differentiation of neural progenitor cells by activation of the IL-6/gp130 signaling pathway. *Neurotox Res* 2010; 18: 328–338.

[228] Whitson JS, Glabe CG, Shintani E, Abcar A, Cotman CW. Beta-amyloid protein promotes neuritic branching in hippocampal cultures. *Neurosci Lett* 1990; 110: 319–24.

[229] Zhou F, Gong K, Song B, Ma T, van Laar T, Gong Y, Zhang L. The APP intracellular domain

(AICD) inhibits Wnt signalling and promotes neurite outgrowth. *Biochim Biophys Acta - Mol Cell Res* 2012; 1823: 1233–1241.

[230] Deyts C, Vetrivel KS, Das S, Shepherd YM, Dupré DJ, Thinakaran G, Parent AT. Novel GαS-protein signaling associated with membrane-tethered amyloid precursor protein intracellular domain. *J Neurosci* 2012; 32: 1714–29.

[231] Wang S, Bolós M, Clark R, Cullen CL, Southam KA, Foa L, Dickson TC, Young KM. Amyloid β precursor protein regulates neuron survival and maturation in the adult mouse brain. *Mol Cell Neurosci* 2016; 77: 21–33.

[232] Bergmans BA, Shariati SAM, Habets RLP, Verstreken P, Schoonjans L, MÃ¼ller U, Dotti CG, De Strooper B. Neurons Generated from APP/APLP1/APLP2 Triple Knockout Embryonic Stem Cells Behave Normally In Vitro and In Vivo : Lack of Evidence for a Cell Autonomous Role of APP in Neuronal Differentiation. *Stem Cells* 2009; 28: N/A-N/A.

[233] Nishimoto I, Okamoto T, Matsuura Y, Takahashi S, Murayama Y, Ogata E. Alzheimer amyloid protein precursor complexes with brain GTP-binding protein G(o). *Nature* 1993; 362: 75–79.

[234] Copenhaver PF, Kögel D. Role of APP Interactions with Heterotrimeric G Proteins: Physiological Functions and Pathological Consequences. *Front Mol Neurosci* 2017; 10: 3.

[235] Pauwels PJ, Gouble A, Wurch T. Activation of constitutive 5-hydroxytryptamine(1B) receptor by a series of mutations in the BBXXB motif: positioning of the third intracellular loop distal junction and its G(o)alpha protein interactions. *Biochem J* 1999; 343 Pt 2: 435–42.

[236] Timossi C, Ortiz-Elizondo C, Pineda DB, Dias JA, Conn PM, Ulloa-Aguirre A. Functional significance of the BBXXB motif reversed present in the cytoplasmic domains of the human follicle-stimulating hormone receptor. *Mol Cell Endocrinol* 2004; 223: 17–26.

[237] Okamoto T, Katada T, Murayama Y, Ui M, Ogata E, Nishimoto I. A simple structure encodes G protein-activating function of the IGF-II/mannose 6-phosphate receptor. *Cell* 1990; 62: 709–717.

[238] Pauwels PJ, Tardif S, Colpaert FC. Differential signalling of both wild-type and Thr(343)Arg dopamine D(2short) receptor by partial agonists in a G-protein-dependent manner. *Biochem Pharmacol* 2001; 62: 723–32.

[239] Okamoto T, Takeda S, Murayama Y, Ogata E, Nishimoto I. Ligand-dependent G protein coupling function of amyloid transmembrane precursor. *J Biol Chem* 1995; 270: 4205–4208.

[240] McCudden CR, Hains MD, Kimple RJ, Siderovski DP, Willard FS, Stanley RJ, Thomas GMH, Chung KY, Rasmussen SGF, Liu T, Li S, DeVree BT, Chae PS, Calinski D, Kobilka BK, Woods VL, Sunahara RK, Kamp ME, Liu Y, Kortholt A, Rangel Serrano A, Milligan G, Kostenis E, Cabrera-Vera TM, Vanhauwe J, Thomas TO, Medkova M, Preininger A, Mazzoni MR, Hamm HE, Chabre M, Maire M, Navarro G, Cordomí A, Zelman-Femiak M, Brugarolas M, Moreno E, Aguinaga D, Perez-Benito L, Cortés A, Casadó V, Mallol J, Canela EI, Lluís C, Pardo L, García-Sáez AJ, McCormick PJ, Franco R, Wettschureck N, Offermanns S, Aittaleb M, Boguth C, Khan SM, Sleno R, Gora S, Zylbergold P, Laverdure J-P, Labbé J-C, Miller GJ, Hébert TE, Us C, Siderovski DP, Willard FS, Flock T, Ravarani CNJ, Sun D, Venkatakrishnan AJ, Kayikci M, Tate CG, Veprintsev DB, Babu MM. Universal allosteric mechanism for Gα activation by GPCRs. *Nature* 2005; 77: 1159–1204.

[241] Watowich SS, Hilton DJ, Lodish HF. Activation and inhibition of erythropoietin receptor function: role of receptor dimerization. *Mol Cell Biol* 1994; 14: 3535–49.

[242] Kovacs E, Zorn JA, Huang Y, Barros T, Kuriyan J. A Structural Perspective on the Regulation of the Epidermal Growth Factor Receptor. *Annu Rev Biochem* 2015; 84: 739–764.

[243] Khalifa N Ben, Van Hees J, Tasiaux B, Huysseune S, Smith SO, Constantinescu SN, Octave J-N, Kienlen-Campard P. What is the role of amyloid precursor protein dimerization? *Cell Adh Migr* 2010; 4: 268–72.

[244] Schlessinger J, Feng XH, Derynck R, Trible RP, Samelson LE, Vos AM de, Shelly M, Henis S, Eisenstein M, Raskin BJ, Al. E. Cell signaling by receptor tyrosine kinases. *Cell* 2000; 103: 211–25.

[245] Brouillet E, Trembleau A, Galanaud D, Volovitch M, Bouillot C, Valenza C, Prochiantz A, Allinquant B. The amyloid precursor protein interacts with Go heterotrimeric protein within a cell compartment specialized in signal transduction. *J Neurosci* 1999; 19: 1717–27.

[246] Hardy J. Framing beta-amyloid. *Nat Genet* 1992; 1: 233–4.

[247] Karlinsky H, Vaula G, Haines JL, Ridgley J, Bergeron C, Mortilla M, Tupler RG, Percy ME, Robitaille Y, Noldy NE, et al. Molecular and prospective phenotypic characterization of a pedigree with familial Alzheimer's disease and a missense mutation in codon 717 of the

beta-amyloid precursor protein gene. *Neurology* 1992; 42: 1445–1453.

[248] Okamoto T, Takeda S, Giambarella U, Murayama Y, Matsui T, Katada T, Matsuura Y, Nishimoto I. Intrinsic signaling function of APP as a novel target of three V642 mutations linked to familial Alzheimer's disease. *EMBO J* 1996; 15: 3769–77.

[249] Sudo H, Hashimoto Y, Niikura T, Shao Z, Yasukawa T, Ito Y, Yamada M, Hata M, Hiraki T, Kawasumi M, Kouyama K, Nishimoto I. Secreted Aβ Does Not Mediate Neurotoxicity by Antibody-Stimulated Amyloid Precursor Protein. *Biochem Biophys Res Commun* 2001; 282: 548–556.

[250] Hashimoto Y, Niikura T, Ito Y, Nishimoto I. Multiple mechanisms underlie neurotoxicity by different types of Alzheimer's disease mutations of amyloid precursor protein. *J Biol Chem* 2000; 275: 34541–34551.

[251] Shaked GM, Chauv S, Ubhi K, Hansen LA, Masliah E. Interactions between the amyloid precursor protein C-terminal domain and G proteins mediate calcium dysregulation and amyloid beta toxicity in Alzheimer's disease. *FEBS J* 2009; 276: 2736–2751.

[252] Ikezu T, Okamoto T, Komatsuzaki K, Matsui T, Martyn JA, Nishimoto I. Negative transactivation of cAMP response element by familial Alzheimer's mutants of APP. *EMBO J* 1996; 15: 2468–75.

[253] Herrmann R, Heck M, Henklein P, Henklein P, Kleuss C, Hofmann KP, Ernst OP. Sequence of Interactions in Receptor-G Protein Coupling. *J Biol Chem* 2004; 279: 24283–24290.

[254] Locht C, Coutte L, Mielcarek N. The ins and outs of pertussis toxin. *FEBS J* 2011; 278: 4668–4682.

[255] Reisine T. Pertussis toxin in the analysis of receptor mechanisms. *Biochem Pharmacol* 1990; 39: 1499–1504.

[256] Horgan AM, Copenhaver PF. G protein-mediated inhibition of neuronal migration requires calcium influx. *J Neurosci* 1998; 18: 4189–200.

[257] Young-Pearse TL, Bai J, Chang R, Zheng JB, LoTurco JJ, Selkoe DJ. A critical function for beta-amyloid precursor protein in neuronal migration revealed by in utero RNA interference. *J Neurosci* 2007; 27: 14459–69.

[258] Pinho AC, Dias R, Cerqueira AR, da Cruz e Silva OAB, Vieira SI. APP and its secreted fragment sAPP in SH-SY5Y neuronal-like migration. *Microsc Microanal* 2015; 21: 36–37.

[259] Ramaker JM, Copenhaver PF. Amyloid Precursor Protein family as unconventional Go-coupled receptors and the control of neuronal motility. *Neurogenes (Austin, Tex)* 2017; 4: e1288510.

[260] Swanson TL, Knittel LM, Coate TM, Farley SM, Snyder MA, Copenhaver PF. The insect homologue of the amyloid precursor protein interacts with the heterotrimeric G protein Go alpha in an identified population of migratory neurons. *Dev Biol* 2005; 288: 160–78.

[261] Ramaker JM, Swanson TL, Copenhaver PF. Amyloid precursor proteins interact with the heterotrimeric G protein Go in the control of neuronal migration. *J Neurosci* 2013; 33: 10165–81.

[262] Locht C, Antoine R. A proposed mechanism of ADP-ribosylation catalyzed by the pertussis toxin S1 subunit. *Biochimie* 1995; 77: 333–340.

[263] Milosch N, Tanriöver G, Kundu A, Rami A, François J-C, Baumkötter F, Weyer SW, Samanta A, Jäschke A, Brod F, Buchholz CJ, Kins S, Behl C, Müller UC, Kögel D. Holo-APP and G-protein-mediated signaling are required for sAPPα-induced activation of the Akt survival pathway. *Cell Death Dis* 2014; 5: e1391.

[264] Billnitzer AJ, Barskaya I, Yin C, Perez RG. APP independent and dependent effects on neurite outgrowth are modulated by the receptor associated protein (RAP). *J Neurochem* 2013; 124: 123–132.

[265] Yamatsuji T, Okamoto T, Takeda S, Murayama Y, Tanaka N, Nishimoto I. Expression of V642 APP mutant causes cellular apoptosis as Alzheimer trait-linked phenotype. *Embo J* 1996; 15: 498–509.

[266] Yamatsuji T, Matsui T, Okamoto T, Komatsuzaki K, Takeda S, Fukumoto H, Iwatsubo T, Suzuki N, Asami-Odaka A, Ireland S, Kinane TB, Giambarella U, Nishimoto I. G protein-mediated neuronal DNA fragmentation induced by familial Alzheimer's disease-associated mutants of APP. *Science* 1996; 272: 1349–52.

[267] Frank DA, Greenberg ME. CREB: a mediator of long-term memory from mollusks to mammals. *Cell* 1994; 79: 5–8.

[268] Serita T, Fukushima H, Kida S. Constitutive activation of CREB in mice enhances temporal association learning and increases hippocampal CA1 neuronal spine density and complexity. *Sci Rep* 2017; 7: 42528.

[269] Giambarella U, Yamatsuji T, Okamoto T, Matsui T, Ikezu T, Murayama Y, Levine MA, Katz A, Gautam N, Nishimoto I. G protein betagamma complex-mediated apoptosis by familial Alzheimer's disease mutant of APP. *EMBO J* 1997; 16: 4897–4907.

[270] Sudo H, Jiang H, Yasukawa T, Hashimoto Y, Niikura T, Kawasumi M, Matsuda S, Takeuchi Y, Aiso S, Matsuoka M, Murayama Y, Nishimoto I. Antibody-Regulated Neurotoxic Function of Cell-Surface β-Amyloid Precursor Protein. *Mol Cell Neurosci* 2000; 16: 708–723.

[271] Xu Y-X, Wang H-Q, Yan J, Sun X-B, Guo J-C, Zhu C-Q. Antibody binding to cell surface amyloid precursor protein induces neuronal injury by deregulating the phosphorylation of focal adhesion signaling related proteins. *Neurosci Lett* 2009; 465: 276–281.

[272] Sola Vigo F, Kedikian G, Heredia L, Heredia F, Anel AD, Rosa AL, Lorenzo A. Amyloid-beta precursor protein mediates neuronal toxicity of amyloid beta through Go protein activation. *Neurobiol Aging* 2009; 30: 1379–1392.

Aims

The major goal of this work was to perform a systematic research of the role of Gαo on neuritogenesis. We approached this goal by studying the effects of Gαo interaction with the Amyloid Precursor Protein (APP) on the mechanisms behind neurite formation and elongation. To this end, we defined the following specific aims:

- Study the impact of APP Serine 655 phosphorylation on the ability to APP bind and activate Gαo.
- Characterize the neuritogenic effects of Gαo and determine how APP modulates these effects.
- Identify potential mechanisms by which APP and Gαo regulate each other protein levels.

Additionally, our interest in studying the mechanisms of neuronal differentiation led us to the development of a new tool that would assist us in this research. To achieve this goal, we defined the following aim:

- Develop and validate an ImageJ macro for morphological analysis of Phase Contrast and Fluorescence images of neuronal cells.

B. Results

B1. The APP-Gαo interaction is modulated by APP S655 phosphorylation and impacts neuritogenesis via STAT3 and ERK activation

Roberto A. Dias[1,2], Ana R. Cerqueira[1], Joana F. da Rocha[1,2], Odete A. B. da Cruz e Silva[1], Sandra I. Vieira*[1,2]

[1]Neurosciences and Signalling Laboratory, Institute of Biomedicine (iBiMED), Department of Medical Sciences, University of Aveiro, Campus de Santiago, 3810-193 Aveiro, Portugal;

[2]Cell Differentiation and Regeneration Laboratory, Institute of Biomedicine (iBiMED), Department of Medical Sciences, University of Aveiro, Campus de Santiago, 3810-193 Aveiro, Portugal.

*E-mail: sivieira@ua.pt; Tlf:(+351) 234 247 256; Fax:(+351) 234 372 587

Acknowledgements

This work was supported by the Universidade de Aveiro, Fundação para a Ciência e Tecnologia (Portuguese Ministry of Science and Technology), QREN, and the European Union (Fundo Europeu de Desenvolvimento Regional, FEDER and COMPETE): scholarships SFRH/BD/90996/2012 and SFRH/BD/78507/2011, research project PTDC/SAU-NMC/111980/2009, research unit program iBiMED (UID/BIM/04501/2013). We would like to acknowledge Filipa Martins (iBiMED, University of Aveiro), Prof. Dr. Carlos Duarte and Ivan Lalanda (Centre for Neurosciences and Cell Biology, CNC, Universidade de Coimbra) for all the kind assistance with the rat brain and primary neuronal cultures, respectively.

B1.1. Abstract

Neuritogenesis comprises the generation, elongation, and maturation of neurites, the pillars of neural networks. Various neuritogenic molecules have been discovered through the last couple of decades, including the main cerebral G-alpha subunit Gαo, and the amyloid precursor protein (APP), central to the Alzheimer's disease (AD) pathogenesis. APP binding to Gαo increase its activation but, despite their high relevance in neurophysiology and pathophysiology, the functions of the APP-Gαo complex are still unclear. We here demonstrate that the APP ability to bind and activate Gαo is dependent on the phosphorylation state of the APP Serine 655 residue, and that this interaction plays a role on neurite outgrowth. APP phosphorylation influences the formation of new processes and their elongation. Evaluation of the STAT3 and ERK1/2 pathways provided evidence that these pathways are sequential activated during Gαo-APP driven neuritogenesis. While STAT3 mainly mediates the generation of new processes, ERK1/2 is more involved in neuritic elongation. Unraveling APP-Gαo neuritogenic functions not only adds knowledge to the mechanisms of neuronal differentiation and neuritic plasticity but may also spur future therapeutic strategies on neuroregeneration, and on AD itself.

B1.2. Introduction

Neuronal differentiation is a key embryonic event that is recalled during neuroregeneration in adulthood. Early neuronal differentiation comprises neuritogenesis, the formation of processes that will elongate into neurites. These arise from the neuronal body, elongate and specialize into dendrites and axon [1]. Neuritogenesis initiates from the contact between adhesion molecules on the neuron's membrane and the extracellular matrix, which triggers cytoskeleton remodeling [2–4]. Various signaling pathways are subsequently activated in neurons and neuronal-like cells such as PC12 and SH-SY5Y, including the extracellular signal-regulated kinase (ERK) and the signal-transducer-and-activator-of-transcription 3 (STAT3) cascades [5–8].

The complete mechanism underlying neuritogenesis is not yet fully understood and, as the list of key neuritogenic players increases [9], new promising molecules with potential therapeutic value emerge, namely the amyloid precursor protein (APP) and the alpha subunit of the heterotrimeric G Protein Go, Gαo. Albeit best known for its role in Alzheimer's disease (AD) [10], APP's biological functions are a current focus of interest. APP is a type-I transmembrane glycoprotein, and its secreted form (sAPP), which results from APP processing by α-secretases such as ADAM10 [11], has growth factor-like neurotrophic functions and induces neuritic elongation in cultured neurons [12, 13]. Both full-length and secreted APP have been associated with neuritogenesis, potentially via Integrin beta1 [13, 14]. APP and its cleavage into sAPP also have been linked to neuronal differentiation induced by neurotrophins such as NGF and BDNF [14–16], with APP being shown to increase NGF-induced neuritic length and branching in PC12 cells [17]. sAPP is also required for activity-induced neuritogenesis that occurs in differentiating neurons, via ERK pathway activation [18]. Although it is clear that APP behaves as a neurotrophic signal transducer, its mode of action has not been fully elucidated. APP neurotrophic functions rely not only on its sAPP extracellular domain but also in its short intracellular domain (AICD), responsible for APP binding to several proteins. Gαo, the most abundant alpha subunit of G proteins in the central nervous system [19], is such an APP binding protein [20, 21].

Although the object of extensive study, due to the major role that G-protein-coupled receptors (GPCRs) play in human physiology, it was the discovery of some Gαo interactors that shed light on its neuritogenic functions. Activated Gαo binds to and activates G protein-regulated inducer of neurite outgrowth 1 (GRIN1), inducing neuritic elongation in Neuro2a cells [22]. Gαo can also induce neuritic outgrowth through the STAT3 pathway. In Neuro2a cells, ligand binding to the CB1

cannabinoid receptor (CB1R) activates Gαo, which binds Rap1GAPII thus activating Rap1. This culminates in Src kinase activation and STAT3 phosphorylation [23–25]. Although mainly associated with cellular proliferation, the STAT3 cascade mediates neuronal differentiation induced by ligands such as IL-6 and PACAP in PC12 cells [26, 27]. Gαo has also been shown to modulate neurite outgrowth by interfering with the cAMP pathway [28] and by interacting with Rit , leading to ERK1/2 activation [29].

The group of Nishimoto and Ogata first described an APP/Gαo physical interaction and reported that APP increased Gαo activation [20, 21, 30]. APP binding to Gαo increases the Gαo activation state, either by activating it (increased Gαo-binding to GTP) or by decreasing the Gαo GTPase activity [21, 31]. A potential role for APP-Gαo interaction in the AD pathogenesis has also been investigated [32, 33] and an effect of the APP insect-homologue in Gαo-mediated neuronal motility was described in *Manduca sexta´s* developing enteric nervous system [34, 35]. Notwithstanding these results, the physiological role of this interaction is still not clear.

In the work here presented we advance knowledge on the physical and functional interaction between Gαo and APP, including the effects of APP phosphorylation at Serine 655 (S655) on APP-Gαo binding. PKC-mediated APP S655 phosphorylation alters the conformation of the ^{653}YTSI^{656} sorting motif and of a hydrophobic pocket immediately downstream [36–39]. This hydrophobic pocket is a part of the APP's ^{657}His-Lys^{676} C-terminal domain to which Gαo binds [20, 37, 38]. APP S655 phosphomutants were used to demonstrate that APP interaction with Gαo can be modulated by phosphorylation of APP Serine 655 residue, with also having an impact in the ability of APP to activate Gαo. Moreover, we demonstrate that APP and Gαo cooperate in the sequential activation of the STAT3 and ERK pathways, with S655 phosphorylation influencing the outcome of this interaction, and presenting different neuritogenic outcomes.

B1.3. Materials and Methods

B1.3.1. Antibodies

Primary antibodies used in Western Blot (WB) and Immunocytochemistry (ICC) assays: mouse 22C11 monoclonal anti-APP N-terminus (Chemicon; WB-1:250; ICC-1:50); rabbit anti-Gαo/GNAO1 polyclonal (Upstate; WB-1:5000; ICC-1:250; Thermo; WB-1:2000; ICC-1:200); rabbit anti-phosphoTyr705-STAT3 (monoclonal (Millipore; WB-1:3000); mouse anti-STAT3 monoclonal (Cell Signaling Technology; WB-1:2000); rabbit anti-phosphoThr185/Tyr187-ERK1/2 monoclonal (Millipore; WB-1:1000); rabbit anti-ERK1/2 polyclonal (Millipore; WB-1:1000); mouse anti-βIII-tubulin C-terminus (Millipore; ICC-1:250); mouse anti-MAP2 (Sigma-Aldrich; ICC-1:200). Secondary antibodies used: horseradish peroxidase-labeled goat antibodies (GE Healthcare) for enhanced chemiluminescence (ECL) detection; Alexa Fluor 405, 488 or 594-conjugated goat antibodies (Molecular Probes) for ICC analysis. Antibodies were prepared in 3% BSA in phosphate buffer saline (PBS) for ICC, and in either 3-5% milk or BSA for WB, per the manufacturers' instructions.

B1.3.2. Chemicals

The JAK2 inhibitor AG490 (Tyrphostin B42; Selleck Chemicals), the Src kinase inhibitor PP1 (1-(1,1-dimethylethyl)-3-(4-methylphenyl)-1H-pyrazolo[3,4-d]pyrimidin-4-amine) (Enzo Life Sciences), and the EGFR inhibitor PD168393 (Santa Cruz Biotechnology) were used at 10 µM [40–42]. SH-SY5Y cells were incubated for 6h with each inhibitor before being harvested in 1% SDS. Neurons were incubated for 18h before being subject to ICC or collected for WB. To stimulate PKC and thus increase APP S655 phosphorylation [43], SH-SY5Y cells were incubated with 1 µM phorbol-12,-14-di-butyrate (PDBu) for 2h prior harvesting [38].

B1.3.3. Gαo and APP cDNA constructs

Wild-type and constitutively active cDNAs of human G-protein alpha o, isoform A, (Gαo and GαoCA, respectively), cloned into a pcDNA3.1+ vector, were from Missouri S&T cDNA Resource Center. The GαoCA cDNA has a Q205L mutation that hinders its GTPase activity [44]. The empty pcDNA3 vector ('V1'; Invitrogen) was used to control Gαo transfections. APP cDNAs (human isoform 695), Wild-type (Wt) and Serine 655 (S655) point mutated to Alanine ('SA') or to Glutamate ('SE'), already N-

terminally fused to GFP (Green Fluorescent Protein) were previously constructed. Due to the amino acids characteristics, the SE and SA APP mutants mimic a constitutively phosphorylated and dephosphorylated S655 state, respectively. The pEGFP-N1 empty vector ('V2'; Clontech) was used to control the APP-GFP cDNAs transfections [38, 45].

B1.3.4. SH-SY5Y cells and primary neuronal cultures

Human neuroblastoma SH-SY5Y cells (ATCC CRL-2266) were grown in Minimal Essential Medium (MEM) supplemented with F-12, 10% FBS, 0.5 mM L-glutamine, 100 U/ml penicillin and 100 mg/ml streptomycin (Gibco, Invitrogen). Cells were maintained at 37°C/5% CO_2. APP-GFP (Wt, SA, and SE) and Gαo (Wt, CA) cDNAs were transiently transfected using TurboFect (Fermentas), according to the manufacturer. After 6 or 24h of transfection, cells were either harvested with 1% SDS for WB, or fixed with 4% paraformaldehyde for ICC.

Rat cortical primary neuronal cultures were established from E18 Wistar rat embryos as previously described [46]. Briefly, following dissociation with trypsin and deoxyribonuclease I, cells were plated onto poly-D-lysine coated 6-well plates ($0.75x10^6$ cells/well) in Neurobasal medium (Gibco, Invitrogen) supplemented with B27, 0.5 mM glutamine and 60 µg/ml gentamicin. Neuronal cultures, maintained at 37ºC/5% CO_2 for 3 days, were transfected with Gαo and APP-GFP cDNAs using Lipofectamine® 2000 (Invitrogen Life Technologies). 18 hours before cell fixation, neurons were incubated with 10 µM of the EGFR inhibitor PD168393 or the Src inhibitor PP1. Upon 24h of transfection, cells were harvested with 4% paraformaldehyde or 1% SDS for ICC and WB analyses, respectively. A minimum number of pregnant female Wistar rats (9-12 weeks; Harlan Interfaune Ibérica, SL) was used, and all steps were taken to ameliorate animal suffering. All experimental procedures complied the ARRIVE guidelines, observed the European legislation for animal experimentation (EU Directive 2010/63/EU) and were approved and supervised by our Institutional Animal Care and Use Committee: Comissão Responsável pela Experimentação e Bem-Estar Animal, CREBEA).

B1.3.5. Immunocytochemistry, microscopy and image software

Fixed cells were permeabilized (0.2% Triton), washed with PBS, blocked (3% BSA/PBS), and incubated with primary antibodies for 2h. Following 3 washes with PBS, cells were incubated with secondary antibodies for 1h, washed with PBS and deionised water, and mounted onto glass slides

(Vectashield mounting medium with or without DAPI; Vector Labs). Microphotographs were acquired on a LSM 510 META confocal microscope (Zeiss), as before [38], and image analysis was carried out using ImageJ Fiji [47]. The JaCoP plugin [48] was used to obtain the percentage of proteins co-localization, using the Manders' method. The number of processes/cell was determined by counting any membrane projection arising from the cell body. The length of the processes was determined with the NeuronJ plugin; processes with lengths between 20-35 µm were categorized as 'pre-neurites'; if longer than 35 µm, as 'neurites' [14, 49].

B1.3.6. SDS-PAGE and Western Blot

Total protein mass-normalized (BCA protein assay; Pierce) cell aliquots were subjected to SDS-PAGE and WB. Ponceau-S staining of the transferred proteins was used as loading control, as an alternative to actin or tubulin, since these proteins vary with our experimental conditions [14, 50]. For this, nitrocellulose membranes were immersed in Ponceau-S solution (Sigma-Aldrich; 0.1 % [w/v] in 5% acetic acid), further washed with distilled water, and scanned (GS-800 calibrated densitometer, Bio-Rad). Following their wash with TBS-T, membranes were subject to WB analysis. Briefly, membranes were blocked with 5% milk or BSA in TBS-T, incubated with primary antibodies for 2h or overnight (O/N), and with horseradish peroxidase-linked secondary antibodies for 2h, and subject to ECL detection. X-ray films (Amersham) were scanned and protein bands quantified with the Quantity One 1-D Analysis Software (Bio-Rad).

B1.3.7. APP/Gαo co-Immunoprecipitation and pull-down assays

APP/Gαo were co-immunoprecipitated with Protein-G Dynabeads (Novex, Life Technologies) pre-complexed with the 22C11 antibody. Briefly, rat neurons were collected in lysis buffer (50 mM Tris-HCl pH 8.0, 120 mM NaCl, 4% CHAPS) containing a protease inhibitors cocktail (Sigma-Aldrich). Lysates were precleared for 1h with dynabeads and further incubated O/N at 4°C with the 22C11-dynabeads complexes. The immunoprecipitate was washed 3x with PBS, and the protein complexes eluted with Laemli buffer. Samples were boiled and subjected to WB [38].

APP-GFP proteins were pulled-down with GFP-Trap® (Chromotek) following the manufacturer's protocol with adaptations: SH-SY5Y cells, co-transfected with the APP-GFPs and Gαo/GαoCA cDNAs for 12 h, were incubated for 45 min/RT in-plate with the cross-linker DSP [Dithiobis(succinimidyl propionate); Sigma-Aldrich]. Cells were washed with PBS, harvested in cold 1 mM PMSF/PBS,

centrifuged for 5 min/4ºC, and resuspended in 200 µl Lysis buffer [10 mM Tris/Cl pH 7.5, 150 mM NaCl, 0.5 mM EDTA, 0.5% NP-40, 1 mM PMSF, protease inhibitor cocktail (Sigma-Aldrich)]. Samples were lysed on ice for 30 min, with extensively pipetting every 10 min. Following centrifugation (5 min at 10,000 g/4ºC), a 25 µl supernatant aliquot was taken ('Lysates'), and 300 µl Wash buffer (NP-40-free Lysis buffer) was added to the remaining supernatant. Mass-normalized samples were incubated with 20 µl GFP-TRAP® beads (pre-washed in Wash buffer) with orbital shaking O/N at 4ºC. Samples were subsequently centrifuged (5 min at 10,000 g/4ºC) and the pellet washed 3x with 1 ml Wash buffer. Pulled-down proteins were recovered in 50 µl Laemmli's buffer, boiled and sonicated, and subjected to WB.

B1.3.8. Gαo activation assay

The Gαo activation assay (NewEast Biosciences) was performed according to the manufacturer's instructions. Briefly, SH-SY5Y cells were transfected for 6h with the APP-GFPs cDNAs (or V2 as control), and lysed. In the last 2h before lysis, a set of Wt APP-GFP transfected cells was incubated with 1 µM PDBu to activate PKC and induce APP S655 phosphorylation [37, 39]. Cellular lysates were incubated for 1h with an anti-active Gαo monoclonal antibody and 20 µl protein A/G-agarose beads; the primary antibody/active Gαo complexes were recovered by centrifugation. Following 3 washes with lysis buffer, pulled-down active Gαo proteins were extracted with Laemli buffer and subjected to WB. For positive and negative controls, non-transfected cellular lysates were pre-incubated for 90 min with GTPγS and GDP, respectively.

B1.3.9. Statistical analysis

Data is expressed as mean ± SEM (standard error of the mean) of at least three different experiments. Statistical analysis was conducted by one-way ANOVA followed by the Tukey test, or by one-sample t-test, using the GraphPad Prism® software. Three levels of significance were used, depending if the p-value was under 0.05, 0.01 or 0.001.

B1.4. Results

B1.4.1. PhosphoS655 APP preferentially interacts with and activates Gαo

Gαo is known to interact and be activated by APP [20, 21, 30, 31]. This interaction was here verified in rat cortex lysates by immunoprecipitating APP using the anti-APP N-terminus 22C11 antibody. Cortical Gαo co-immunoprecipitated with APP, as expected (Figure B1.1A). Although the APP-Gαo interaction has been well established, with the specific region of APP known to interact with Gαo already identified, the influence of APP phosphorylation in said interaction is still unknown. We thus investigated if APP phosphorylation at Serine 655 (S655) could modulate the APP-Gαo interaction, since phosphorylation of this residue affects the conformation of the APP's hydrophobic pocket that binds Gαo [20, 36]. SH-SY5Y neuroblastoma cells were transfected with APP-GFP cDNAs (human isoform 695) expressing the Wild type form of APP (Wt APP), and two phosphomutants mimicking the unphosphorylated S655 (SA) and the phosphorylated S655 (SE) APP [38, 45]. APP-GFP proteins were then pulled-down using a GFP-trap® assay (Figure B1.1B). Albeit the three APP-GFP forms pulled-down Gαo, their binding efficiencies were quite different. Gαo was pulled-down in similar amounts with Wt and SE APP-GFP, although slightly higher with the phosphomimicking mutant (Figure B1.1B-C). Conversely, SA APP-GFP showed a 50% decrease in its ability to pull-down Gαo ($p<0.01$) (Figure B1.1B-C).

Following, the effect of APP S655 phosphorylation in the reported ability of APP to activate Gαo was analyzed. For that, active Gαo levels were monitored in APP-overexpressing SH-SY5Y cells ('Gαo activation assay', Figure B1.1D). Taking APP-GFP transfection levels into account, the SE APP-GFP mutant activated Gαo at the highest level, followed by the Wt form, while SA poorly activated Gαo (Figure B1.1D, left panel). This assay was also performed in Wt APP-overexpressing cells pre-exposed for 2h to PDBu, a PKC activator that increases APP S655 phosphorylation [43]. In the cells incubated with PDBu, the levels of active Gαo also increased over control (Figure B1.1D, right panel), supporting the model that APP phosphorylation modulates Gαo interaction and activation.

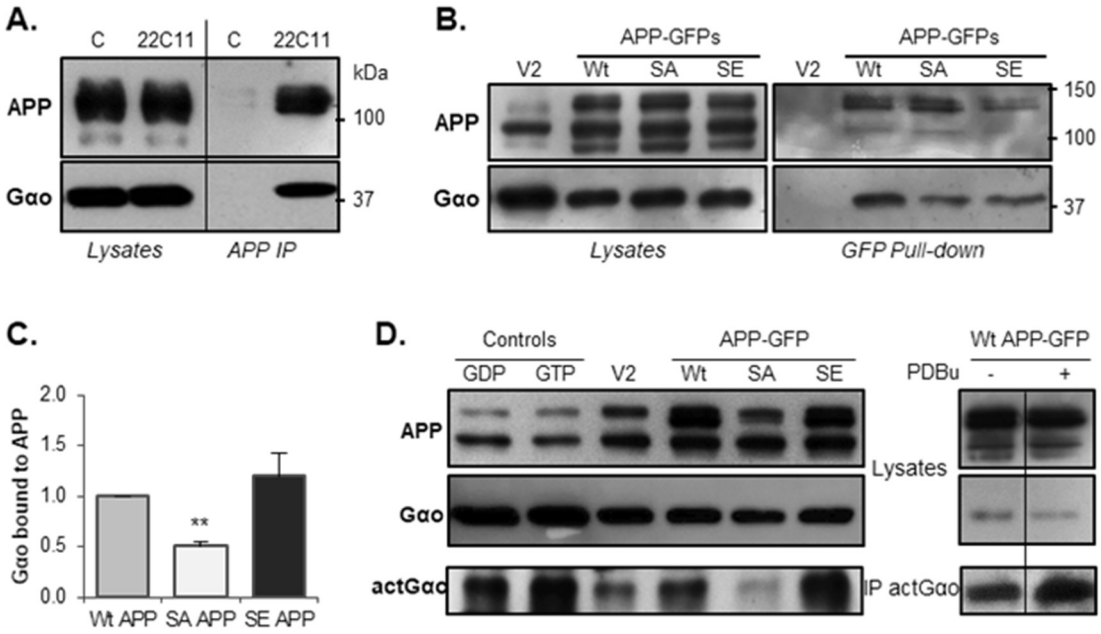

Figure B1.1. APP-Gαo interaction and Gαo activation are potentiated by APP S655 phosphorylation. **A.** Gαo was co-immunoprecipitated with APP from rat neuronal cortex, using the anti-APP 22C11 antibody; 'C', control (without 22C11). **B.** Gαo was co-pulled down with the APP-GFP proteins (Wt, SA and SE) by GFP-Trap®, in SH-SY5Y cells co-transfected with APP-GFPs and Gαo. **C.** The levels of co-precipitated Gαo were quantified and expressed as fold changes over the Wt APP-GFP condition (taken as 1). These values were corrected to the amount of APP-GFP pulled-down in each assay. **D.** Gαo activation assay: active Gαo ('actGαo') was immunoprecipitated in SH-SY5Y cells transfected with the APP-GFPs proteins. 'GDP' and 'GTP': negative and positive controls, respectively. Right panel: Gαo activation assay of Wt APP-GFP expressing cells pre-incubated in the last 2h with 1 µM PDBu to increase the levels of APP S655 phosphorylation.

B1.4.2. APP modulation of early Gαo-induced neuritogenesis

Gαo role in neural differentiation has been a focus of research for quite some time [22–24, 29, 51–54]. After establishing that APP phosphorylation modulates Gαo activity, we analyzed if this could translate into altered Gαo-induced neuritogenesis.

A morphological analysis of SH-SY5Y cells overexpressing wild-type Gαo or a constitutively active Gαo (Gαo CA) during 6h (a time-point at which protein overexpression was already significant) detected neuritogenic alterations in transfected cells (Figure B1.2A). Gαo overexpression significantly increased the number of cellular processes (2.2-fold change over the empty vector; $p<0.01$), with Gαo CA also increasing the number of processes, slightly higher than Gαo (4.9±0.5 and 5.6±0.5 processes/cell, respectively) (Figure B1.2C). Gαo overexpression also had an effect on the processes' length by increasing the percentage of cells presenting at least one pre-neurite (process longer than 20 µm) (1.45-fold change over the empty vector, $p<0.05$). Interestingly, GαoCA also increased the percentage of cells with pre-neurites, but to a lower extent than Gαo (Figure B1.2D). A similar result had already been described in F11 cells [28], where transfection with Gαo

and Gαo CA led to a decrease in average neurite length when compared to control, but had a significant increase in the number of processes. Taken together, these results indicate that Gαo activation has mainly an immediate effect in the formation of new processes rather than in the elongation of pre-existing ones.

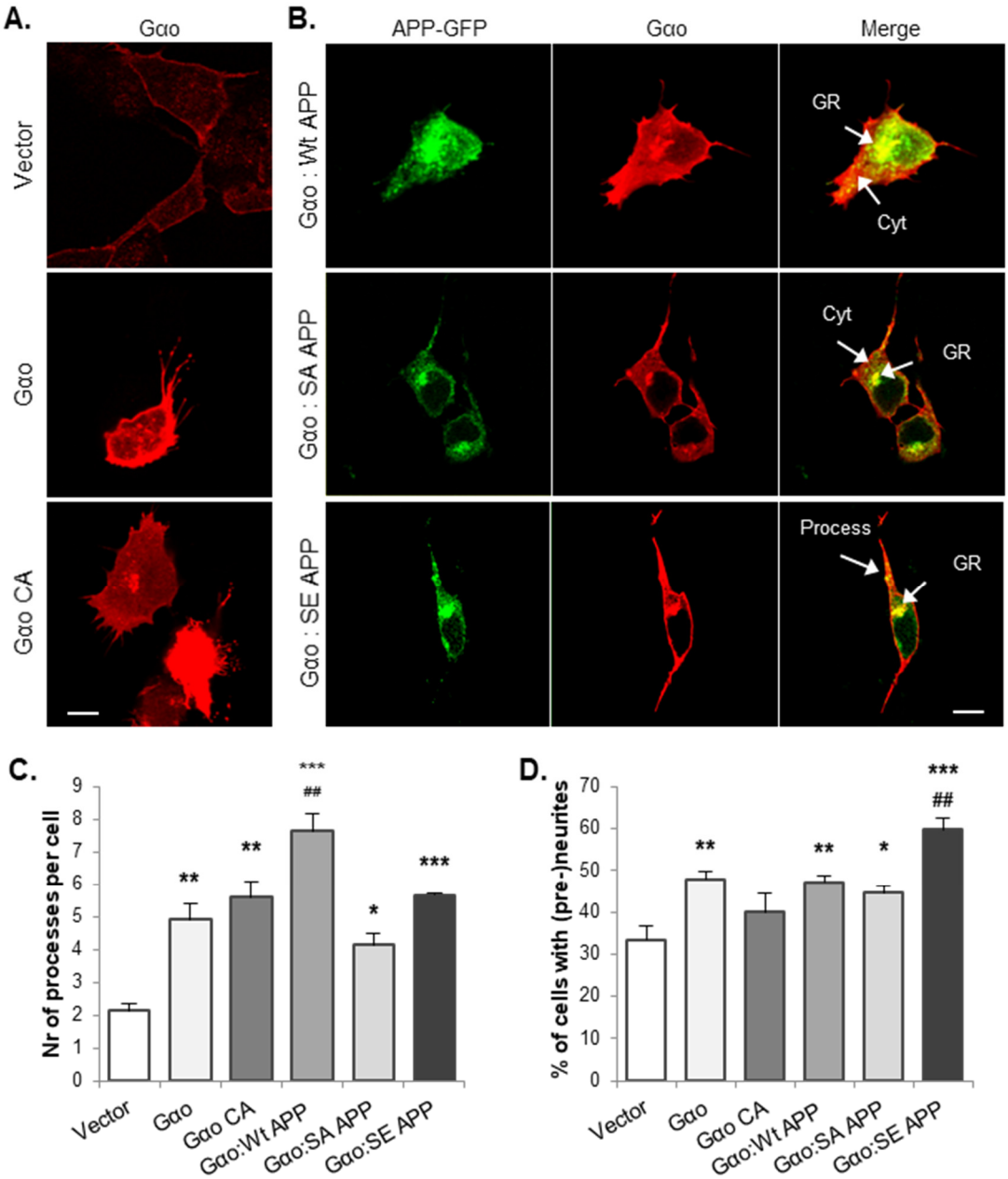

Figure B1.2. Gαo:APP functionally cooperate in neuritogenesis. **A**. Microphotographs of SH-SY5Y cells transfected with the empty vector pcDNA3 ('Vector'), Gαo, and Gαo CA cDNAs. Endogenous and transfected Gαo proteins were detected by immunofluorescence (red). Scale bar: 10 µm. **B**. Microphotographs of SH-SY5Y cells co-transfected with either Wt, SA or SE APP-GFPS (green) and Gαo (red). 'GR' – Golgi region; 'Cyt' – cytoplasm. Scale bar: 10 µm. Morphometric analyses were performed on these cells: **C**. Number of processes arising from the cell body; **D**. Percentage of cells presenting at least one pre-neurite or neurite, termed '(pre-)neurite', and representing processes longer than 20 µm. Symbols '*' and '#' represent a statistical significance relative to the empty vector and to the Gαo single transfection condition, respectively. */#, $p<0.05$; **/##, $p<0.01$; ***/###, $p<0.001$.

To investigate the effects of APP and its phosphorylation on Gαo-induced neuritogenesis, the different cDNA forms of APP (Wt, SA, SE) were co-transfected with wild-type Gαo (Figure B1.2B). Gαo:Wt APP-GFP co-expression had a strong effect on the formation of new processes, higher than Gαo alone (Figure B1.2C; 7.6±0.5 vs 4.9±0.5 processes/cell respectively, $p<0.01$). Neither Gαo:SA (4.1±0.4) nor Gαo:SE (5.7±0.1) combinations were able to significantly alter the number of Gαo-induced processes. Nevertheless, SE tended to increase this number to a level similar to Gαo CA alone (5.7±0.1 vs 5.6±0.5 for Gαo CA), while SA tended to decrease it (4.1±0.4). Comparatively, at 6h of transfection, none of the APP-GFP proteins alone increased the number of processes (Supplementary Figure B1.1).

Regarding the capacity to elongate processes (Figure B1.2D), Gαo:SE APP significantly increased the percentage of cells with at least one pre-neurite or neurite over Gαo alone (60±3% vs 48±2%, $p<0.01$), while no significant variations occurred for both Gαo:Wt APP and Gαo:SA APP co-transfections. Therefore, combined Gαo overexpression with sustained APP S655 phosphorylation results in processes' elongation (in detriment to their generation). Of note, 6h of sole SE APP expression did not promote neuritic elongation (Supplementary Figure B1.1).

Our results show that APP indeed modulates Gαo-induced neuritogenesis, and that APP's S655 phosphorylation has an impact on the outcome of this interaction.

B1.4.3. APP enhances the Gαo-induced STAT3 activation involved in neuritogenesis

As aforementioned, Gαo is able to induce neurite outgrowth by activation of the STAT3 signaling pathway [23, 24]. So, to evaluate the potential role of the STAT3 pathway in APP-Gαo induced neuritogenesis, we examined STAT3 phosphorylation at Tyr705 (pSTAT3) in cells overexpressing the different forms of Gαo and APP (Figure B1.3).

Upon 6h of transfection (Figure B1.3A), both Gαo forms increased pSTAT3 (2.4±0.7-fold change for Gαo and 1.9±0.5-fold change for GαoCA). Regarding Gαo:APP co-transfections, co-transfection of Gαo with Wt APP, the condition where the highest number of processes was observed, was the only one where an increase in pSTAT3/STAT3 was detected, though to slightly lower levels than Gαo and Gαo CA (1.7±0.7-fold change). It has already been reported that activated STAT3 remains phosphorylated for only short time periods, followed by a negative feedback mechanism of dephosphorylation [55]. Our data indicates that this might be occurring earlier/faster for GαoCA and Gαo:Wt APP co-transfection. Moreover, there was a high degree of variability between

experiments, evidenced by the high standard errors. This gives strength to the idea that in these conditions a fast cycle of STAT3 phosphorylation/dephosphorylation was occurring. To test this hypothesis, a time-course analysis of STAT3 phosphorylation was performed at 3, 4, 5 and 6 hours of transfection (Figure B1.3B). The levels of pSTAT3 and STAT3 were compared to control levels (transfection of empty vectors) and the pSTAT3/STAT3 ratio plotted as fold changes over control levels with time. Figure B1.3B shows that both Gαo and Gαo:Wt APP transfections activate STAT3 and are indeed associated with a phosphorylation/dephosphorylation cycle of STAT3. These cycles, however, seem to be slightly out of phase with each other. Gαo alone shows an increase from 3 to 4h followed by a decrease at 5h (1.24, 1.44, 1.05-fold changes), while its co-transfection with Wt APP shows an already higher STAT3 phosphorylation status at 3h, which decreases at 4h, followed by an increase at 5h (1.40, 1.10, 1.30-fold changes). These results corroborate our initial idea that STAT3 signaling is occurring faster when both Gαo and Wt APP are overexpressed. Comparatively, Gαo CA overexpression also led to an initial increased STAT3 phosphorylation, but this decrease for the next 2 hours, only increasing back at 6h of transfection. This seems to indicate that a constant activation of GαoCA activates STAT3 but elicits a stronger feedback mechanism, while a cyclic Gαo activation, such as the one occurring when Wt APP and Gαo are expressed, leads to a faster cycle of STAT3 activity with less/shorter inhibition periods.

The time-course experiment showed again that there is a highly dynamic modulation of the STAT3 pathway during transfection of Gαo and APP, evidenced by the variability between experiments. This data is strong evidence that the STAT3 pathway is activated by APP-Gαo and that this pathway could be the main drive for the formation of new processes. To further confirm this, STAT3 phosphorylation was pharmacologically inhibited with either 10 µM of AG490 or PP1, drug inhibitors of Janus Kinase-2 (JAK2) and Src kinase, respectively (Figure B1.3C). Morphometric analyses proved that STAT3 activation is indeed a main pathway mediating Gαo:Wt APP-induced neuritic outgrowth. While the incubation with either of the inhibitors significantly impacted the number of cell processes, Src inhibition led to a steeper reduction of this score (Figure B1.3C, left graph). This indicates that Gαo:Wt APP, as Gαo [23], induces the formation of cellular processes mainly via the Src-STAT3 pathway. Regarding elongation in Gαo-overexpressing cells, while the Src PP1 inhibitor decreased it to 34±4% ($p<0.05$), JAK2 inhibition markedly increased the percentage of (pre-)neurites from 48±2% in control to 69±3% ($p<0.01$). Indeed, JAK2 inhibition led to a dose-dependent neuritic elongation in a Gαo-overexpression background (Supplementary Figure B1.2A-C). This suggests that Src-STAT3 also participates in the mild Gαo-induced neuritic elongation, with the JAK2-STAT3 pathway competing for this role, probably by deviating STAT3 for other functions.

Remarkably, pSTAT3 inhibitors had no effects on processes' elongation in an APP overexpression background (Figure B1.3C, right graph). Hence, APP-Gαo seem to be elongating processes by mechanisms that use signaling molecules other than STAT3. Concordantly, SE APP is the APP form that more strongly activates Gαo (Figure B1.1) and that leads to the greatest percentage of cells with pre-neurites (Figure B1.2), but does not seem to have an impact in STAT3 activity (Figure B1.3A).

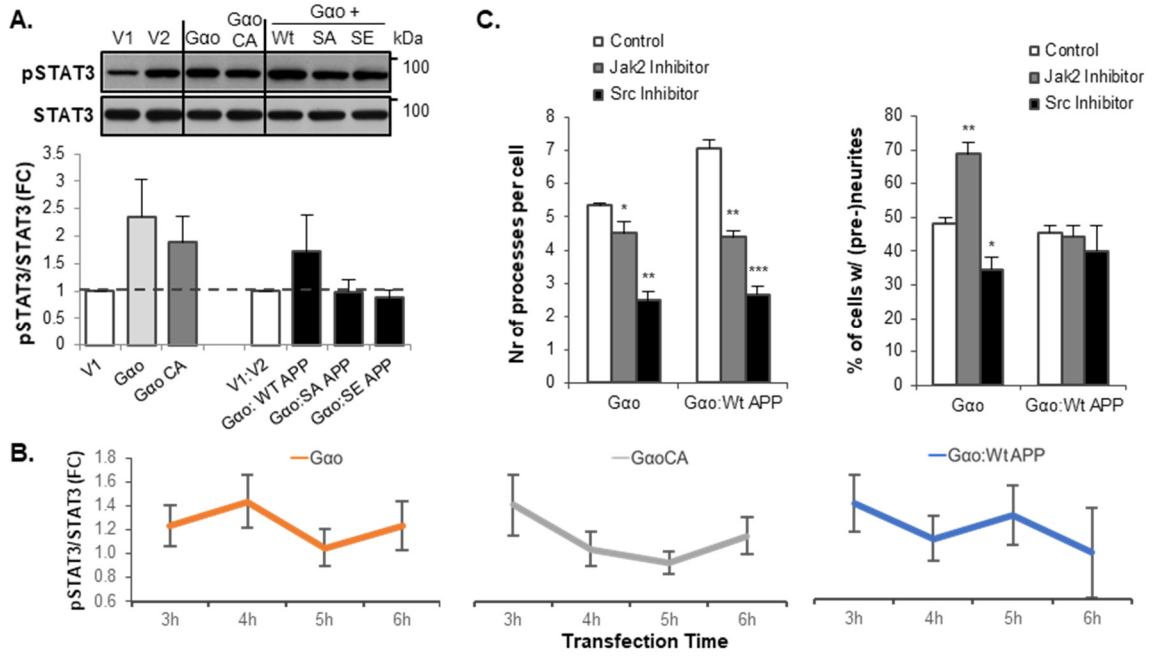

Figure B1.3. APP and Gαo modulation of the STAT3 signaling pathway. A. WB analysis of STAT3 phosphorylation (pSTAT3) at 6h of transfection of the different Gαo and APP-GFP cDNAs. The fold changes (FC) of the pSTAT3/STAT3 ratios were calculated, taking the ratios of the respective controls (V1 and V1:V2) as 1. **B.** Time-course analysis of STAT3 phosphorylation after 3, 4, 5 and 6h of transfection with Gαo, GαoCA and Gαo:Wt APP. STAT3 phosphorylation was compared to the transfection of the empty vector at each time-point. N=4 **C.** Morphometric analyses in conditions of STAT3 inhibition with 10 µM of JAK2 inhibitor (AG490) and Src inhibitor (PP1), for 6h. '(pre-)neurites', pre-neurites and neurites (processes longer than 20 µm). The '*' symbol represents statistical significance relative to control. *, p<0,05; **, p<0,01; ***, p<0,001.

The MAPK/ERK pathway could be a possible signaling pathway modulated by APP-Gαo, since Gαo is able to activate ERK1/2 [29, 56–58], and activation of this pathway has also been associated with sAPP [18]. Further, JAK2 inhibition resulted in a dose-dependent increase in ERK1/2 phosphorylation (pERK1/2), supporting the role of this pathway (together with the STAT3 one) in Gαo-mediated neurite elongation (Supplementary Figure B1.3D). However, after 6h of transfection we could not observe increases in pERK1/2 in any of the conditions analyzed (data not shown). APP-Gαo might be mediating early elongation via other effectors and/or ERK1/2 activation might be occurring even faster than STAT3, as observed elsewhere [59].

B1.4.4. APP modulation of late Gαo-induced neuritic elongation

After confirming that APP and Gαo cooperate in a fast signaling mechanism that induces neuritogenesis, we further analyzed if this effect was maintained for a longer time period. SH-SY5Y cells were thus transfected for 24h with Gαo alone or co-transfected with the different APP-GFPs, and morphological changes were evaluated and compared to control conditions (cells co-transfected with empty vectors) and with the results obtained at 6h of transfection (Figure B1.4). Control cells increase their number of processes with time, until what appears to be a maximum steady level common to most conditions at 24h (~5 processes/cell), but do not alter their number of neurites (Figure B1.4A-C 'Vector'). Cells overexpressing wild-type Gαo showed no alterations in the number of processes per cell between 6h and 24h, but presented a significant higher percentage of cells with at least one pre-neurite (48±2% at 6h vs 65%±4% at 24h of transfection, $p<0.05$) (Figure B1.4C). For the Wt APP:Gαo co-transfection, the number of processes decreased with time (from 7.6±0.5 at 6h to 4.7±0.5 at 24h, $p<0.05$), to values similar to control and Gαo alone conditions (Figure B1.4A-B), and the percentage of cells with pre-neurites only slightly increased (Figure B1.4C). SE APP co-transfection with Gαo had a similar effect than Wt APP: it decreased the number of processes per cell to the lowest value (from 5.7±01 at 6h to 4.1±0.3 at 24h of transfection, $p<0.01$), and a slight not significant increase in the percentage of cells with pre-neurites (compared to Gαo alone values). On the other hand, co-transfection of Gαo with SA APP resulted in a slight increase in the number of processes (to Vector control levels) and in a significant increase in the percentage of cells with pre-neurites (45±2% at 6h vs 74±8% at 24h of transfection, $p<0.05$). A take-away message from these results is that after the initial burst of processes formation, Gαo overexpressing cells stop this mechanism in favor of elongating at least one process. At this time, the elongation effect is more favored by Gαo co-transfection with SA APP.

Following, the activation state of the STAT3 and ERK1/2 signaling pathways was also analyzed, and revealed a shift in their activity after 24h of APP and Gαo overexpression. While there is an activation of the STAT3 pathway at 6h of transfection (Figure B1.3), at 24h no increased activity over control cells was detected on the conditions tested (Figure B1.4D). On the other hand, an increase in the pERK/ERK ratio was observed for Gαo alone but more significant when Gαo was co-transfected with Wt and SE APP (2.1±0.2-fold change for Gαo:Wt APP, $p<0.05$; and 3.3±0.3-fold change for Gαo:SE APP, $p<0.01$) (Figure B1.4E). These pERK1/2 results correlate well with the ability of these two forms of APP to bind and activate Gαo (Figure B1.1).

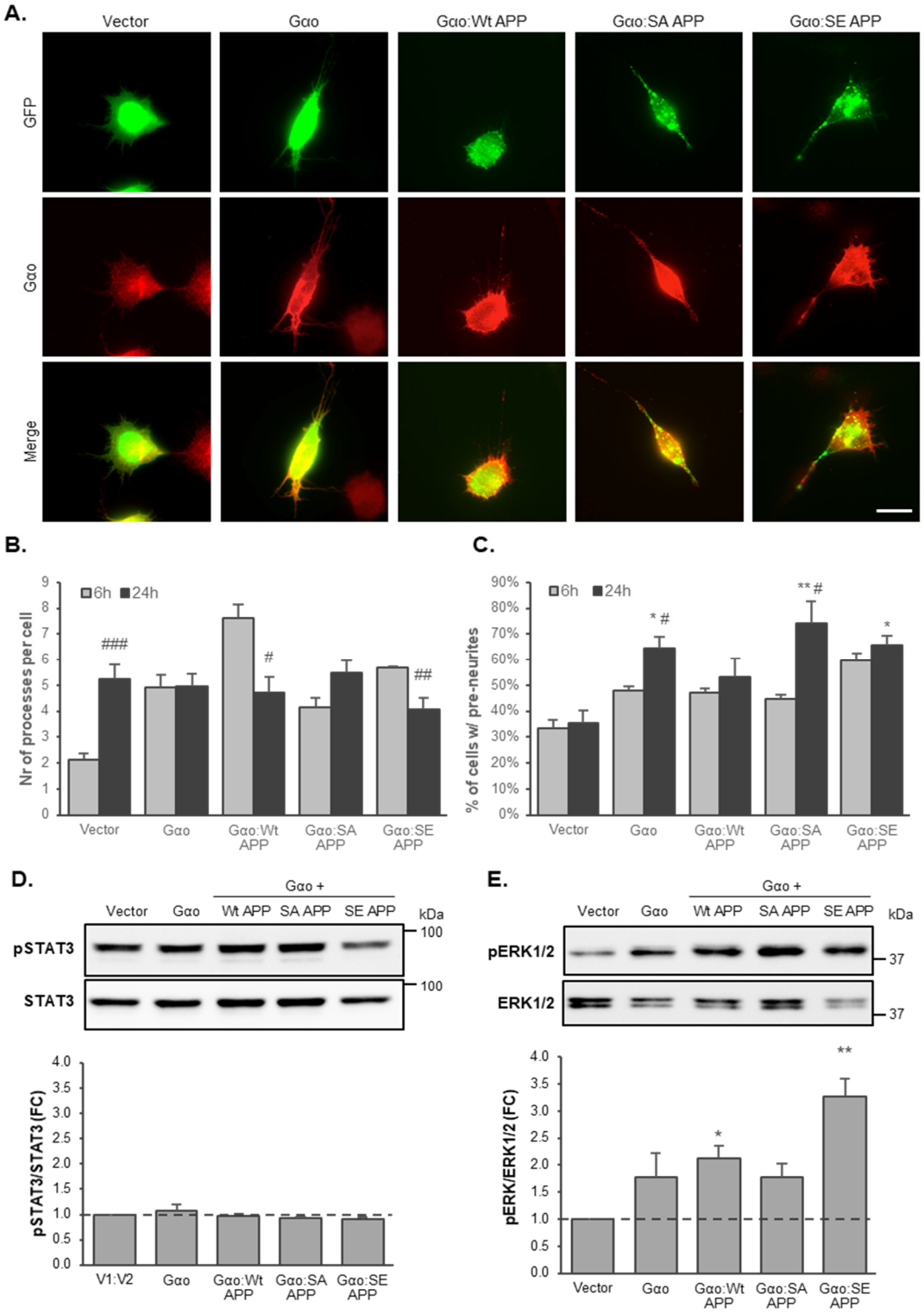

Figure B1.4. Gαo:APP morphological and signaling effects after 24h of transfection. **A.** Microphotographs of SH-SY5Y cells transfected during 24h with either the empty vector, Gαo, Gαo:Wt APP, Gαo:SA APP or Gαo:SE APP cDNAs. Gαo: red; APP: green. Scale bar: 20 µm. Morphometric analyses were performed and compared to the results obtained at 6h of transfection: **B.** Number of processes arising from the cell body; **C.** Percentage of cells presenting at least one pre-neurite or neurite, termed '(pre-)neurite' (processes longer than 20µm). **D.** Western blot analyses of STAT3 and E. ERK1/2 phosphorylation levels at 24h of transfection. The fold changes (FC) of the pSTAT3/STAT3 and pERK/ERK1/2 ratios were calculated, taking the ratios of the empty vector ("Vector") as 1. Symbols '*' and '#' represent a statistical significance relative to the empty vector and to the 6h of transfection, respectively. */#, p<0.05; **/##, p<0.01; ***/###, p<0.001.

Combined, these data suggest that part of the later Gαo-induced neuritic elongation is mediated by ERK1/2 activation. Arguing in favour of this idea is the fact that inhibition of the Epidermal Growth Factor Receptor (EGFR) by PD168393 decreased the percentage of cells with processes longer than 20 μm (and the number of processes), in both Gαo alone and Gαo:SE APP conditions (Supplementary Figure B1.3). Nevertheless, ERK1/2 can not be the only mechanism by which Gαo induces neuritic elongation, since the conditions where there is a highest level of ERK1/2 activation (Gαo:Wt APP and Gαo:SE APP) are not the ones where there is the highest number of cells with pre-neurites (Gαo:SA APP). These indicate that ERK1/2 activation might be necessary but not sufficient for the maximum efficiency in neuritic elongation, and that other molecules can be into play, whose action is favored by the presence of SA APP. Also, the increased ERK1/2 activation detected in Gαo:Wt APP and Gαo:SE APP conditions might be playing a role in other cellular functions not addressed in this work [60–62].

B1.4.5. Gαo and APP interplay on neuronal differentiation

After studying the neuritogenic role of the APP-Gαo in SH-SY5Y cells, the effect of this complex was analyzed in rat cortical neurons. Primary neuronal cultures, differentiated for 3 days in vitro (DIV), were transfected for 24h with the Gαo cDNA, alone or together with the Wt and SE APP-GFPs (or V1:V2 vectors, for control). Noteworthy, GαoCA transfection for 24h was highly deadly to neurons (data not shown). The 3-4 DIV period was chosen due to its ongoing axonal growth and onset of dendritic outgrowth [63, 64]. At this time period, the longest neurite is the axon, practically negative for the Microtubule-Associated Protein 2 (MAP2), while the much shorter dendrites are MAP2-positive (Supplementary Figure B1.4) and easy to identify. Cells analyzed were positive for the neuronal βIII-tubulin marker (Figure B1.5-6).

Gαo was found abundant not only at the neuronal soma, but also at both dendrites and axons; it highly colocalized with transfected APP-GFP at the soma and dendrites, and at the axonal proximal region (Figure B1.5A). Gαo overexpression increased dendritic outgrowth by ~50% (226±18 μm in V1:V2 to 372±33 μm, $p<0.05$), at the expense of axonal elongation (Figure B1.5A-B; zoom-ins). The number of primary neurites is maintained (6.6±0.6 for V1:V2 and 6.5±0.2 for Gαo). Gαo:Wt APP co-transfection had similar effects that Gαo in total dendritic outgrowth but, notably, it had a lesser detrimental effect on axonal elongation than Gαo alone (Figure B1.5A zoom-ins, 5B). Both Gαo and Gαo:Wt APP increased the total length per dendrite (Figure B1.5C and B1.5D), but Gαo:Wt APP (and Gαo:SE APP) increase dendritic branching at a higher extent than Gαo alone (Figure B1.5D), while

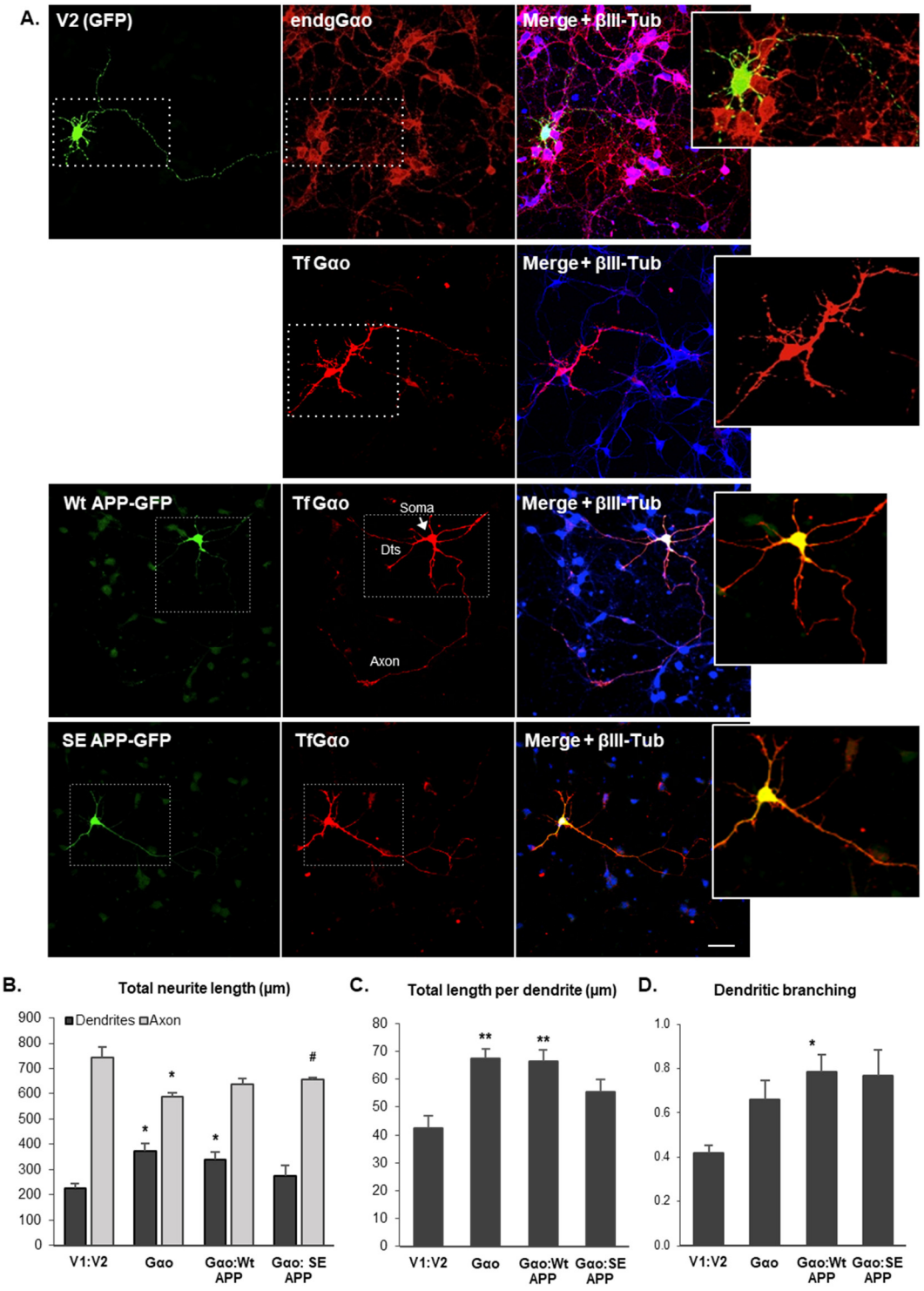

Figure B1.5. Gαo:APP neuritogenic effects in primary neurons. A. Microphotographs of rat embryonic cortical neurons at 4 days in vitro (DIV), a time point when the axon is highly elongated and the dendrites have started to elongate. At 3 DIV, neurons were transfected for 24h with the empty vectors ('V1:V2'), Gαo alone, Gαo:Wt APP-GFP or Gαo:SE APP-GFP cDNAs. APP-GFP (green), Gαo (red); βIII-tubulin (blue) is shown to confirm the cells as neurons. Zoom-ins are shown at right to highlight neuronal morphology aspects and the proteins co-distribution. Bar: 50 µm. EndgGαo, Endogenous Gαo; TfGαo, Transfected Gαo. **B.** Total dendritic and axon lengths (including branches) **C.** Average primary dendritic length **D.** Number of branches per primary dendrite. Symbols '*' and '#' represent a statistical significance relative to the empty vectors and to the Gαo alone, respectively. */#, $p<0.05$. For each condition, at least 50 different neurons were analyzed, from 2 different experiments.

slightly decreasing the number of primary neurites (6.2±0.4 for Gαo:Wt APP and 6.0±0.4 for Gαo:SE APP). SE APP co-expression with Gαo significantly protected the axon from the effects of Gαo alone (658±7 µm for Gαo:SE APP vs 587±17 µm for Gαo, $p<0.05$). This higher commitment to elongation of the longest neurite occurred at the expense of the elongation of the novel dendrites (Figure B1.5A and B1.5B).

These results show that the formation of new processes induced by Gαo and Gαo:Wt APP in SH-SY5Y cells is translated to 4 DIV neurons as an increase in dendritic elongation and branching. A role for the STAT3 pathway in this dendritogenic effect is suggested by WB analyses, that reveal increased phospho and total STAT3 levels only for Gαo and Gαo:Wt APP neurons, in accordance with their dendritogenic profile (Figure B1.6A).

Pharmacological inhibition of the Src-STAT3 pathway confirmed the involvement of this cascade in basal and in Gαo-induced neuronal differentiation (Figure B1.6B). Exposure for 18h to the Src inhibitor PP1 decreased dendritic outgrowth in control (V1:V2) and in Gαo expressing neurons. Surprisingly, co-expression of Gαo with APP (Wt or SE) in neurons protected these from the PP1 negative effects and allowed dendritic elongation (Figure B1.6B). Interestingly, pERK2 (lower band in the immunoblot) and total ERK levels also remarkably increased in Gαo and Gαo:APP expressing neurons (Figure B1.6C). Nevertheless, the EGFR inhibitor PD168393 only decreased dendritic length in Gαo overexpressing neurons (and not in basal cells), with APP co-expression again protecting from the detrimental effect (Supplementary Figure B1.5).

Therefore, Gαo has a major role in dendritic elongation, mainly via Src-STAT3 but also via EGFR. Interestingly, APP (particularly SE APP) co-overexpression with Gαo protected neurites from the detrimental effects of Src-STAT3 and EGFR inhibition (Figure B1.6A and Supplementary Figure B1.5). Taken together, when alone neuronal Gαo primarily acts via Src-STAT3 and the ERK pathway, but when in the presence of APP, the Gαo:APP complex might be acting on alternative routes to Src and EGFR or acting on these cascades downstream of Src/EGFR.

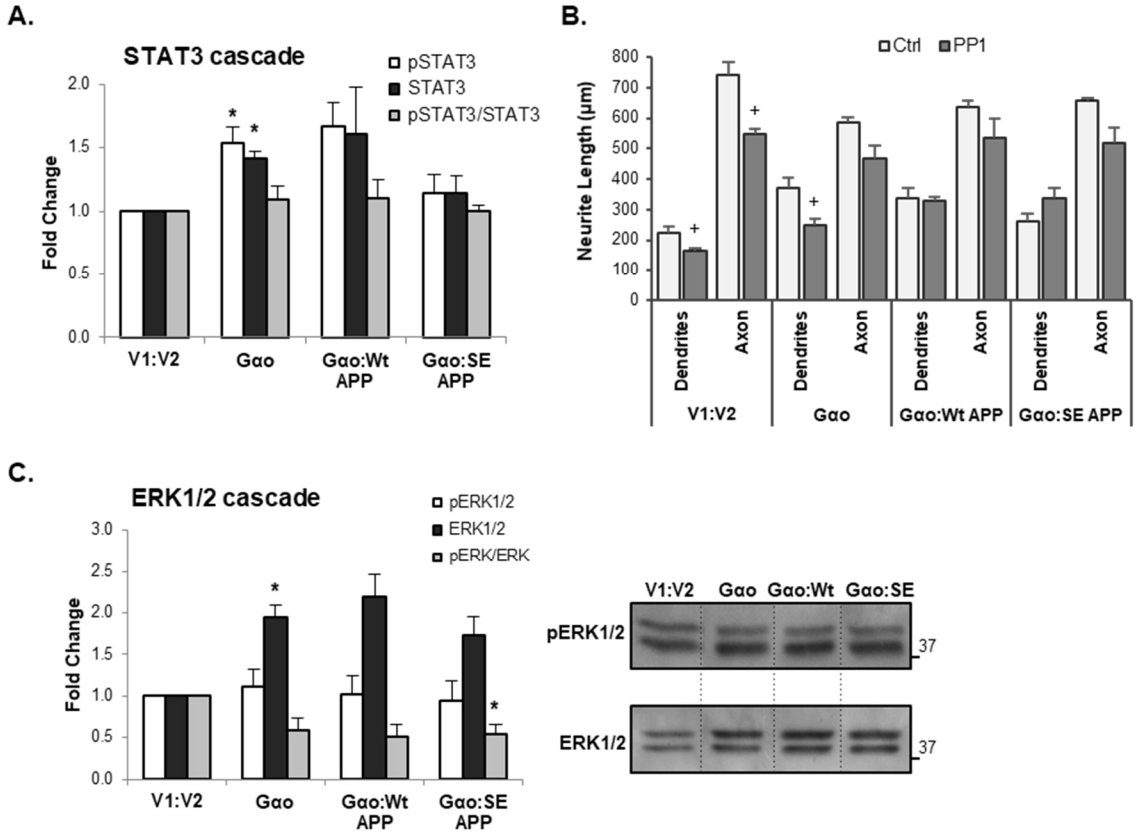

Figure B1.6. STAT3 and ERK1/2 signaling on APP-Gαo effects in primary neurons. A. Levels of phospho and total STAT3 were determined in WB of neuronal lysates. **B.** Morphometric analysis of total dendritic and axonal lengths (including branches) upon Src inhibition. Neuronal cultures were transfected with V1:V2, Gαo, Gαo:Wt APP-GFP and Gαo:SE APP-GFP cDNAs at 3 DIV, and exposed to 10 µM of the Src inhibitor in the last 18h. PP1, Src inhibitor; Ctrl, control unexposed neurons. For each condition, at least 50 different neurons were analysed, from 2 different experiments. **C.** Levels of phospho and total ERK1/2 were determined in WB of neuronal lysates. Left: graphical analyses; right: ERK1/2 blots. Symbols '*' and '+' represent a statistical significance relative to the empty vectors ('V1:V2') and to control without Src inhibitor ('Ctrl'), respectively. */+, $p<0.05$.

B1.5. Discussion

In the 90's an interaction between APP and Gαo, the major neuronal G-alpha subunit, was first described [20]. APP was discovered not only to bind but also to activate Gαo in a GPCR-like manner [21, 31, 35]. This opened new perspectives to understand how APP, a protein central to the Alzheimer's pathology, functions in the brain. It also advanced knowledge on Gαo, a much more elusive protein with potential roles in brain plasticity and memory [65, 66]. However, albeit their relevance in the brain, the role for the APP-Gαo protein-protein complex is still not clear. With our work, we further characterized how APP and Gαo interact and uncovered a new role for this interaction on neuritogenesis, a process very important to the human brain during developmental and regenerating conditions. Further, we have demonstrated that APP and Gαo activate signaling pathways (STAT3 and ERK1/2) central to various cellular processes and that may underlie other APP-Gαo functions in cell proliferation and neuronal plasticity, for example.

We first characterized the APP and Gαo physical interaction. Since Serine 655 phosphorylation induces backbone conformational changes on the APP C-terminal Gαo-binding pocket [20, 36], we hypothesized that it interfered with Gαo-APP binding strength. In fact, Gαo strongly binds to and is activated by the phosphomimetic SE APP (Figure B1.1). APP was described to effectively activate Gαo when bound to 22C11. This anti-APP N-terminal antibody was suggested to mimic ligand-mediated APP activation and induce APP C-terminal conformational changes that facilitated Gαo activation [21, 31]. We postulate that APP S655 phosphorylation has a similar conformational effect as 22C11 does, and that pAPP (APP S655 phosphorylated) is an "activated" form, mediating extracellular signaling to Gαo.

Following, we investigated a role for the APP-Gαo complex in neuritogenesis, a biological process to which both proteins had been previously associated in separate. Wt Gαo and Gαo CA constructs were used in an attempt to differentiate between active and non-active Gαo effects. Nevertheless, in various neuritogenic parameters analyzed, there were no significant differences between Gαo and Gαo CA conditions. This was previously observed in F11 cells [28], and might result from both a higher amount of Gαo being available to be activated by its upstream interactors, and from the higher levels of Gαo compared to its endogenous negative regulators. These regulators belong to a class of proteins called Regulators of G-protein Signaling (RGS) that accelerate the GTPase activity of Gα subunits, resulting in the conversion of GTP to GDP and G protein signaling termination [67–

70]. Thus, a deficit in RGS control upon the overabundant Gαo could result in Gαo remaining in its GTP-bound form for longer periods of time, behaving similarly to Gαo CA.

Neuritogenesis involves both the formation and extension of cellular processes that eventually elongate into neurites. These two mechanisms appear to be competitive, and are regulated by different signaling cascades that share common molecular players [14]. Our results support this idea, showing that Gαo (and APP) plays a part on both phases of neuritogenesis.

Phase I, the formation of new processes, occurs earlier and is promoted by Gαo and activation of the Src-STAT3 signaling (Figure B1.2-3). APP cooperates with Gαo in this function; however, its role does not seem to be restricted to activating Gαo since our results show that overexpressing both APP and Gαo increases the number of processes beyond the effect of overexpressing a constitutively active mutant of Gαo. One possibility relates to the cyclic nature of Gαo activity. In a case that Gαo is in a continuous cycle of activation/deactivation (such as when it is co-expressed with Wt APP), this might maintain the formation of new processes for longer periods of time without eliciting a negative feedback response. Contrarily, a constant activation of Gαo (as in transfection with Gαo CA) might result in a faster/stronger feedback inactivation of the mechanism. A similar hypothesis has been raised by other authors regarding the function of some small GTPases; for example, the constitutively activation of Rac1 and Cdc42 gave opposite results to the established roles of these proteins in neurite outgrowth [71, 72]. A different study even showed that a GTP-GDP cycle was essential for Cdc42 to induce neuronal polarity [73]. This hypothesis is corroborated by our results regarding STAT3 signaling, where Gαo overexpression leads to an apparent cyclic activation of Gαo that results in a cyclic activation of STAT3, while a constant activation of Gαo (Gαo CA) results in a longer period of STAT3 inactivity after an initial earlier activation (Figure B1.3). Alternatively, APP might be acting by targeting Gαo to zones of neurite formation and/or by potentiating Gαo binding to the Rap1GAP protein by bridging means, since binding of Gαo to Rap1GAP prevents this last from inhibiting Rap1 and leads to Src-STAT3 activation [23, 24]. Indeed, our results corroborate the already published data that Gαo is able to activate the STAT3 pathway [23, 44], and adds that this signaling is primarily involved in the formation of new processes rather than in their elongation, with APP being able to modulate this event. APP may also function by bringing to the mix other neuritogenic molecules, such as GAP43, Reelin, and Rit. These proteins are known functional interactors of either Gαo or APP, and have all already been implicated in neuritogenesis [29, 53, 74–77], so APP and Gαo overexpression might act by bringing together a complex involving these proteins.

Phase II, the elongation phase, occurs after the formation of new processes, with the cell shifting its machinery to the elongation of at least one process. This mechanism occurs when Gαo is overexpressed and correlates with an increase in ERK1/2 activity (Figure B1.4). These results are in continuity with previous studies showing that Gαo is not only capable of activating the ERK1/2 pathway [56, 58] but that this pathway can translate Gαo neuritogenic effects [29]. This delayed activation of ERK1/2 signaling (no activitation detected at 6h of transfection, data not shown) has also been observed in mevastatin-differentiated Neuro2a cells [78]. Moreover, ERK1/2 has already been associated with neurite elongation instead of neurite formation [79]. In this study, light-stimulation of the Raf/MEK/ERK signaling in PC12 cells resulted in a significant increase on neurite length accompanied by a decrease in the number of neurites formed. Hynds et al [80] also demonstrated that neurite initiation and elongation are two events regulated by separate signaling pathways. However, contrary to ours and to Zheng et al results [79], Hynds et al observed that inhibition of MEK blocked Rit-induced ERK1/2 phosphorylation and consequent neurite initiation, but not elongation nor branching. Rit is a G protein that can function in neuritogeneis downstream NGF or Gαo [29, 81]. One explanation for these differences could arise from differences in ERK1 and ERK2 functions. While our results show a preferentially increase in ERK2 phosphorylation (42 kDa protein), Hynds et al paper show an equal increase in both ERK1 (44kDa protein) and ERK2 phosphorylation. Either way, further analyses are required to fully comprehend the role of Gαo-ERK1/2 signaling in neurite outgrowth.

APP role on this phase of neuritogenesis is not completely clear. Our results show that initially, APP co-expression with Gαo can increase processes' length, in a S655 phosphorylation dependent manner (Figure B1.2). However, this early effect did not correlate with an increase in either STAT3 or ERK1/2 activation (Figure B1.3). Moreover, after 24h, SE APP further increased Gαo-induced ERK1/2 activation but this did not result in a significant increase in neuritic elongation (Figure B1.4). This could mean that the initial increase in neuritic elongation could be occurring by either a faster activation of the ERK1/2 pathway not detected in our experiments, or by the participation of other neuritogenic molecules, similar to what might be happening during neurite formation. Of the aforementioned proteins that could play a role in this, GAP-43 is a suitable candidate since it is able to activate Gαo in neuronal cells, leading to neurite outgrowth [75, 77], and it co-localizes with APP in growing neurites during brain development, as well as in pathological conditions [82, 83]. Moreover, it has been shown that GAP-43 can modulate GPCRs signal transduction [84]. This strengthens the hypothesis that GAP-43 could do the same in an APP-Gαo signaling pathway. GRIN1 is also a potential candidate for a role in this mechanism. Gαo is able to interact with GRIN1

in a pathway that leads to Cdc42 activation and culminates in neurite extension [22]. More recently, both GRIN1 and GAP-43 were associated with a Gαo complex present in PC12 cells and rat cortical neurons [54]. This complex acted downstream of the α7 nicotinic receptor on the regulation of neural differentiation. While this model is still incomplete, with the signaling pathways acting downstream of Gαo remaining unknown, the existence of a complex between Gαo/GRIN1/GAP-43 in our model could also be possible, since both GRIN1 and GAP-43 are expressed in SH-SY5Y cells [85]. This does not exclude future research of other proteins involved in the APP-Gαo signaling pathway, such as Rit [29] and Necdin [86], as well as the importance of APP proteolytic fragments, sAPP[18, 87] and AICD[88, 89], in APP-Gαo induced neuritogenesis. Nevertheless, one conclusion that we can take from our results is that APP can indeed cooperate with Gαo in the activation of the ERK1/2 pathway, with phosphorylation of S655 enhancing this effect. ERK1/2 activation seems directly involved in neuritogenesis since the use of an EGFR inhibitor decreased the proccesses' length (Supplementary Figure B1.3). This has still to be further explored by using a MEK inhibitor, but Gαo has already been described to activate ERK1/2 by modulation of the Epidermal Growth Factor Receptor (EGFR) pathway [56], and a relationship between APP neuritogenic role, ERK1/2 activation and EGFR activation state in SH-SY5Y cells is being established in our lab (data not published). Nevertheless, the ERK1/2 pathway is only part of the elongation mechanism, since SA APP was able to further elongate cells at 24h of co-transfection with Gαo, and did not increase pERK activation over Gαo (Figure B1.4). In our lab, we are also observing that SA APP is more associated to actin cytoskeleton remodeling in late neuritogenic phases (unpublished data). Per se, SA APP cannot elongate neurites over Wt or SE APP, but it might be favoring elongation in a Gαo overexpression background.

Our data corroborate previous reports stating that the formation and elongation of processes are two competitive mechanisms. The ERK pathway would be primarily involved in the elongation of neurites [79], while other pathways as the Src-STAT3 cascade are required for their genesis. Final evidence supporting this hypothesis of Gαo-STAT3 signaling being involved in neurite formation/initiation and Gαo-ERK1/2 signaling being involved in neurite elongation comes from the results with the JAK2 inhibitor. Inhibition of this kinase led to a slight decrease in the number of processes per cell while increasing the percentage of cells with at least one pre-neurite (Figure B1.3), an effect that was Gαo-dependent since there was no increase in control cells. Increased concentrations of the inhibitor enhanced this effect and was accompanied by an increase in ERK1/2 phosphorylation (Supplementary Figure B1.2). While it is not clear what is the exact mechanism beyond JAK2 inhibition that leads to increased ERK1/2 activation, this gives strength to the dual role

of Gαo in neurite initiation and neurite elongation, and to the STAT3 and ERK1/2 signaling involvement in these neuritogenic phases.

Finally, in differentiating neurons, Gαo main role seems to be in dendritogenesis, with its overexpression significantly increasing dendritic length, and having a negative effect on axonal elongation (Figure B1.5). This is in accordance with our (and other groups) data on neuritogenesis sharing molecular players both involved in neuritic initiation, elongation, branching, and thus competing. Wt APP maintains this Gαo dendritogenic effect, although partial shifting the focus from dendritic elongation to dendritic branching (Figure B1.5). STAT3 and ERK1/2 pathways are altered in Gαo and Gαo-Wt APP conditions (Figure B1.6). However, while Src-STAT3 and EGFR-ERK1/2 are indeed involved in Gαo-induced dendritogenic effects, as confirmed by their pharmacological inhibition, surprisingly APP co-expression protected from the detrimental effects of these pathways inhibition (Figure B1.6). Hence, in neurons, APP might be either activating STAT3 and ERK1/2 via other means than Src and EGFR, or modulating other signaling pathways. Importantly, SE APP appears to be also very involved in elongation of longer or more stable neurites, as it was much less detrimental to axonal elongation (at the expense of decreasing its effect on dendritic arborization).

In conclusion, we have demonstrated that Gαo and APP physically and functionally interact in an APP S655 phosphorylation mode. The APP-Gαo complex has roles in both neuritic formation and elongation. Additionally, APP phosphorylation state and the orchestrated activation of the STAT3 and ERK1/2 signaling pathways helps to determine the outcome of APP-Gαo interaction [90, 91]. Importantly, the disruption of these signaling pathways could potential play a role on the involvement of the APP and Gαo proteins in Alzheimer's Disease [92, 93]. Therefore, the characterization of the dual neuritogenic effects and signaling activation of Gαo, and the role of APP role on its modulation, not only sheds new light on the mechanisms of neuronal differentiation and physiology, but might also provide new groundwork to advance the knowledge on AD pathogenesis.

B1.6. References

[1] da Silva JS, Dotti CG. Breaking the neuronal sphere: regulation of the actin cytoskeleton in neuritogenesis. *Nat Rev Neurosci* 2002; 3: 694–704.

[2] Gupton SL, Gertler FB. Integrin signaling switches the cytoskeletal and exocytic machinery that drives neuritogenesis. *Dev Cell* 2010; 18: 725–36.

[3] Rathjen FG. Neural cell contact and axonal growth. *Curr Opin Cell Biol* 1991; 3: 992–1000.

[4] Hansen SM, Berezin V, Bock E. Signaling mechanisms of neurite outgrowth induced by the cell adhesion molecules NCAM and N-cadherin. *Cell Mol Life Sci* 2008; 65: 3809–21.

[5] Wu H, Ichikawa S, Tani C, Zhu B, Tada M, Shimoishi Y, Murata Y, Nakamura Y. Docosahexaenoic acid induces ERK1/2 activation and neuritogenesis via intracellular reactive oxygen species production in human neuroblastoma SH-SY5Y cells. *Biochim Biophys Acta* 2009; 1791: 8–16.

[6] Sumimoto S, Muramatsu R, Yamashita T. Thromboxane A2 stimulates neurite outgrowth in cerebral cortical neurons via mitogen activated protein kinase signaling. *Brain Res*. Epub ahead of print 7 August 2014. DOI: 10.1016/j.brainres.2014.07.048.

[7] Sarina, Yagi Y, Nakano O, Hashimoto T, Kimura K, Asakawa Y, Zhong M, Narimatsu S, Gohda E. Induction of neurite outgrowth in PC12 cells by artemisinin through activation of ERK and p38 MAPK signaling pathways. *Brain Res* 2013; 1490: 61–71.

[8] Wu YY, Bradshaw RA. Activation of the Stat3 Signaling Pathway Is Required for Differentiation by Interleukin-6 in PC12-E2 Cells. *J Biol Chem* 2000; 275: 2147–2156.

[9] Curtis I De. *Intracellular Mechanisms for Neuritogenesis*. Boston, MA: Springer US. Epub ahead of print 2007. DOI: 10.1007/978-0-387-68561-8.

[10] Sommer B. Alzheimer's disease and the amyloid cascade hypothesis: ten years on. *Curr Opin Pharmacol* 2002; 2: 87–92.

[11] Chow VW, Mattson MP, Wong PC, Gleichmann M. An overview of APP processing enzymes and products. *Neuromolecular Med* 2010; 12: 1–12.

[12] Demars MP, Bartholomew A, Strakova Z, Lazarov O. Soluble amyloid precursor protein: a novel proliferation factor of adult progenitor cells of ectodermal and mesodermal origin. *Stem Cell Res Ther* 2011; 2: 36.

[13] Young-Pearse TL, Chen AC, Chang R, Marquez C, Selkoe DJ. Secreted APP regulates the function of full-length APP in neurite outgrowth through interaction with integrin beta1. *Neural Dev* 2008; 3: 15.

[14] da Rocha JF, da Cruz E Silva OAB, Vieira SI. Analysis of the amyloid precursor protein role in neuritogenesis reveals a biphasic SH-SY5Y neuronal cell differentiation model. *J Neurochem* 2015; 134: 288–301.

[15] Ruiz-León Y, Pascual A. Induction of tyrosine kinase receptor B by retinoic acid allows brain-derived neurotrophic factor-induced amyloid precursor protein gene expression in human SH-SY5Y neuroblastoma cells. *Neuroscience* 2003; 120: 1019–1026.

[16] Holback S, Adlerz L, Iverfeldt K. Increased processing of APLP2 and APP with concomitant formation of APP intracellular domains in BDNF and retinoic acid-differentiated human neuroblastoma cells. *J Neurochem* 2005; 95: 1059–68.

[17] Milward EA, Papadopoulos R, Fuller SJ, Moir RD, Small D, Beyreuther K, Masters CL. The amyloid protein precursor of Alzheimer's disease is a mediator of the effects of nerve growth factor on neurite outgrowth. *Neuron* 1992; 9: 129–137.

[18] Gakhar-Koppole N, Hundeshagen P, Mandl C, Weyer SW, Allinquant B, Muller U, Ciccolini F. Activity requires soluble amyloid precursor protein alpha to promote neurite outgrowth in neural stem cell-derived neurons via activation of the MAPK pathway. *Eur J Neurosci* 2008; 28: 871–882.

[19] Sternweis PC, Robishaw JD. Isolation of two proteins with high affinity for guanine nucleotides from membranes of bovine brain. *J Biol Chem* 1984; 259: 13806–13.

[20] Nishimoto I, Okamoto T, Matsuura Y, Takahashi S, Murayama Y, Ogata E. Alzheimer amyloid protein precursor complexes with brain GTP-binding protein G(o). *Nature* 1993; 362: 75–79.

[21] Okamoto T, Takeda S, Murayama Y, Ogata E, Nishimoto I. Ligand-dependent G protein coupling function of amyloid transmembrane precursor. *J Biol Chem* 1995; 270: 4205–4208.

[22] Nakata H, Kozasa T. Functional characterization of Galphao signaling through G protein-regulated inducer of neurite outgrowth 1. *Mol Pharmacol* 2005; 67: 695–702.

[23] He JC, Gomes I, Nguyen T, Jayaram G, Ram PT, Devi LA, Iyengar R. The G alpha(o/i)-coupled

cannabinoid receptor-mediated neurite outgrowth involves Rap regulation of Src and Stat3. *J Biol Chem* 2005; 280: 33426–34.

[24] Jordan JD, He JC, Eungdamrong NJ, Gomes I, Ali W, Nguyen T, Bivona TG, Philips MR, Devi LA, Iyengar R. Cannabinoid receptor-induced neurite outgrowth is mediated by Rap1 activation through G(alpha)o/i-triggered proteasomal degradation of Rap1GAPII. *J Biol Chem* 2005; 280: 11413–11421.

[25] Ma'ayan A, Jenkins SL, Barash A, Iyengar R. Neuro2A differentiation by Galphai/o pathway. *Sci Signal* 2009; 2: cm1.

[26] Wu YY, Bradshaw RA. Induction of neurite outgrowth by interleukin-6 is accompanied by activation of Stat3 signaling pathway in a variant PC12 cell (E2) line. *J Biol Chem* 1996; 271: 13023–32.

[27] Ishido M. Activation of STAT3 by pituitary adenylate cyclase-activating polypeptide (PACAP) during PACAP-promoted neurite outgrowth of PC12 cells. *J Mol Neurosci* 2010; 42: 349–58.

[28] Ghil SH, Kim BJ, Lee YD, Suh-Kim H. Neurite outgrowth induced by cyclic AMP can be modulated by the alpha subunit of Go. *J Neurochem* 2000; 74: 151–8.

[29] Kim SH, Kim S, Ghil SH. Rit contributes to neurite outgrowth triggered by the alpha subunit of Go. *Neuroreport* 2008; 19: 521–5.

[30] Copenhaver PF, Kögel D. Role of APP Interactions with Heterotrimeric G Proteins: Physiological Functions and Pathological Consequences. *Front Mol Neurosci* 2017; 10: 3.

[31] Brouillet E, Trembleau A, Galanaud D, Volovitch M, Bouillot C, Valenza C, Prochiantz A, Allinquant B. The amyloid precursor protein interacts with Go heterotrimeric protein within a cell compartment specialized in signal transduction. *J Neurosci* 1999; 19: 1717–27.

[32] Yamatsuji T, Okamoto T, Takeda S, Murayama Y, Tanaka N, Nishimoto I. Expression of V642 APP mutant causes cellular apoptosis as Alzheimer trait-linked phenotype. *Embo J* 1996; 15: 498–509.

[33] Sola Vigo F, Kedikian G, Heredia L, Heredia F, Anel AD, Rosa AL, Lorenzo A. Amyloid-beta precursor protein mediates neuronal toxicity of amyloid beta through Go protein activation. *Neurobiol Aging* 2009; 30: 1379–1392.

[34] Swanson TL, Knittel LM, Coate TM, Farley SM, Snyder MA, Copenhaver PF. The insect

homologue of the amyloid precursor protein interacts with the heterotrimeric G protein Go alpha in an identified population of migratory neurons. *Dev Biol* 2005; 288: 160–78.

[35] Ramaker JM, Swanson TL, Copenhaver PF. Amyloid precursor proteins interact with the heterotrimeric G protein Go in the control of neuronal migration. *J Neurosci* 2013; 33: 10165–81.

[36] Ramelot TA, Nicholson LK. Phosphorylation-induced structural changes in the amyloid precursor protein cytoplasmic tail detected by NMR. *J Mol Biol* 2001; 307: 871–84.

[37] Vieira SI, Rebelo S, Domingues SC, da Cruz e Silva EF, da Cruz e Silva OA. S655 phosphorylation enhances APP secretory traffic. *Mol Cell Biochem* 2009; 328: 145–154.

[38] Vieira SI, Rebelo S, Esselmann H, Wiltfang J, Lah J, Lane R, Small SA, Gandy S, da Cruz ESEF, da Cruz ESOA. Retrieval of the Alzheimer's amyloid precursor protein from the endosome to the TGN is S655 phosphorylation state-dependent and retromer-mediated. *Mol Neurodegener* 2010; 5: 40.

[39] da Cruz e Silva OAB, Rebelo S, Vieira SI, Gandy S, da Cruz e Silva EF, Greengard P. Enhanced generation of Alzheimer's amyloid-beta following chronic exposure to phorbol ester correlates with differential effects on alpha and epsilon isozymes of protein kinase C. *J Neurochem* 2009; 108: 319–30.

[40] Nicolas CS, Peineau S, Amici M, Csaba Z, Fafouri A, Javalet C, Collett VJ, Hildebrandt L, Seaton G, Choi S-LL, Sim S-EE, Bradley C, Lee K, Zhuo M, Kaang B-KK, Gressens P, Dournaud P, Fitzjohn SM, Bortolotto ZA, Cho K, Collingridge GL. The JAK/STAT Pathway Is Involved in Synaptic Plasticity. *Neuron* 2012; 73: 374–390.

[41] Lund TC, Coleman C, Horvath E, Sefton BM, Jove R, Medveczky MM, Medveczky PG. The Src-family kinase Lck can induce STAT3 phosphorylation and DNA binding activity. *Cell Signal* 1999; 11: 789–96.

[42] Pu Y-S, Hsieh M-W, Wang C-W, Liu G-Y, Huang C-Y, Lin C-C, Guan J-Y, Lin S-R, Hour T-C. Epidermal growth factor receptor inhibitor (PD168393) potentiates cytotoxic effects of paclitaxel against androgen-independent prostate cancer cells. *Biochem Pharmacol* 2006; 71: 751–60.

[43] Oishi M, Nairn AC, Czernik AJ, Lim GS, Isohara T, Gandy SE, Greengard P, Suzuki T. The cytoplasmic domain of Alzheimer's amyloid precursor protein is phosphorylated at Thr654, Ser655, and Thr668 in adult rat brain and cultured cells. *Mol Med* 1997; 3: 111–23.

[44] Ram PT, Horvath CM, Iyengar R. Stat3-mediated transformation of NIH-3T3 cells by the constitutively active Q205L Galphao protein. *Science (80-)* 2000; 287: 142–144.

[45] da Cruz e Silva OA, Iverfeldt K, Oltersdorf T, Sinha S, Lieberburg I, Ramabhadran T V, Suzuki T, Sisodia SS, Gandy S, Greengard P. Regulated cleavage of Alzheimer beta-amyloid precursor protein in the absence of the cytoplasmic tail. *Neuroscience* 1993; 57: 873–7.

[46] Martins F, Rebelo S, Santos M, Cotrim CZ, da Cruz e Silva EF, da Cruz e Silva OAB. BRI2 and BRI3 are functionally distinct phosphoproteins. *Cell Signal* 2016; 28: 130–144.

[47] Schindelin J, Arganda-Carreras I, Frise E, Kaynig V, Longair M, Pietzsch T, Preibisch S, Rueden C, Saalfeld S, Schmid B, Tinevez J-Y, White DJ, Hartenstein V, Eliceiri K, Tomancak P, Cardona A. Fiji: an open-source platform for biological-image analysis. *Nat Methods* 2012; 9: 676–82.

[48] Bolte S, Cordelières FP. A guided tour into subcellular colocalization analysis in light microscopy. *J Microsc* 2006; 224: 213–32.

[49] Meijering E, Jacob M, Sarria J-CF, Steiner P, Hirling H, Unser M. Design and validation of a tool for neurite tracing and analysis in fluorescence microscopy images. *Cytometry A* 2004; 58: 167–76.

[50] Romero-Calvo I, Ocon B, Martinez-Moya P, Suarez MD, Zarzuelo A, Martinez-Augustin O, de Medina FS. Reversible Ponceau staining as a loading control alternative to actin in Western blots. *Anal Biochem* 2010; 401: 318–320.

[51] Bromberg K, Iyengar R, Cijiang He J. Regulation of neurite outgrowth by Gi/o signalling pathways. 2008; 4544–4557.

[52] Xie R, Li L, Goshima Y, Strittmatter SM. An activated mutant of the alpha subunit of G(o) increases neurite outgrowth via protein kinase C. *Brain Res Dev Brain Res* 1995; 87: 77–86.

[53] Cho S-K, Choi J-M, Kim J-M, Cho JY, Kim S-S, Hong S, Suh-Kim H, Lee Y-D. AKT-independent Reelin signaling requires interactions of heterotrimeric Go and Src. *Biochem Biophys Res Commun* 2015; 467: 1063–9.

[54] Nordman JC, Kabbani N. An interaction between α7 nicotinic receptors and a G-protein pathway complex regulates neurite growth in neural cells. *J Cell Sci* 2012; 125: 5502–13.

[55] Braun DA, Fribourg M, Sealfon SC. Cytokine response is determined by duration of receptor and signal transducers and activators of transcription 3 (STAT3) activation. *J Biol*

Chem 2013; 288: 2986–93.

[56] Antonelli V, Bernasconi F, Wong YH, Vallar L. Activation of B-Raf and regulation of the mitogen-activated protein kinase pathway by the G(o) alpha chain. *Mol Biol Cell* 2000; 11: 1129–42.

[57] Bratton MR, Antoon JW, Duong BN, Frigo DE, Tilghman S, Collins-Burow BM, Elliott S, Tang Y, Melnik LI, Lai L, Alam J, Beckman BS, Hill SM, Rowan BG, McLachlan JA, Burow ME. Gαo potentiates estrogen receptor α activity via the ERK signaling pathway. *J Endocrinol* 2012; 214: 45–54.

[58] van Biesen T, Hawes BE, Raymond JR, Luttrell LM, Koch WJ, Lefkowitz RJ. G(o)-protein alpha-subunits activate mitogen-activated protein kinase via a novel protein kinase C-dependent mechanism. *J Biol Chem* 1996; 271: 1266–9.

[59] Zorina Y, Iyengar R, Bromberg KD. Cannabinoid 1 receptor and interleukin-6 receptor together induce integration of protein kinase and transcription factor signaling to trigger neurite outgrowth. *J Biol Chem* 2010; 285: 1358–70.

[60] Samuels IS, Saitta SC, Landreth GE. MAP'ing CNS Development and Cognition: An ERKsome Process. *Neuron* 2009; 61: 160–167.

[61] Yang K, Cao F, Sheikh AM, Malik M, Wen G, Wei H, Ted Brown W, Li X. Up-regulation of Ras/Raf/ERK1/2 signaling impairs cultured neuronal cell migration, neurogenesis, synapse formation, and dendritic spine development. *Brain Struct Funct* 2013; 218: 669–682.

[62] Ryu H-H, Lee Y-S. Cell type-specific roles of RAS-MAPK signaling in learning and memory: Implications in neurodevelopmental disorders. *Neurobiol Learn Mem* 2016; 135: 13–21.

[63] Fukata Y, Kimura T, Kaibuchi K. Axon specification in hippocampal neurons. *Neurosci Res* 2002; 43: 305–15.

[64] Flynn KC. The cytoskeleton and neurite initiation. *Bioarchitecture* 2013; 3: 86–109.

[65] Jiang M, Bajpayee NS. Molecular mechanisms of go signaling. *Neurosignals* 2009; 17: 23–41.

[66] Ramírez VT, Ramos-Fernández E, Inestrosa NC. The Gαo Activator Mastoparan-7 Promotes Dendritic Spine Formation in Hippocampal Neurons. *Neural Plast* 2016; 2016: 4258171.

[67] Milligan G, Kostenis E. Heterotrimeric G-proteins: a short history. *Br J Pharmacol* 2006; 147 Suppl: S46-55.

[68] Traver S, Bidot C, Spassky N, Baltauss T, De Tand MF, Thomas JL, Zalc B, Janoueix-Lerosey I, Gunzburg JD. RGS14 is a novel Rap effector that preferentially regulates the GTPase activity of galphao. *Biochem J* 2000; 350 Pt 1: 19–29.

[69] Hollinger S, Hepler JR. Cellular regulation of RGS proteins: modulators and integrators of G protein signaling. *Pharmacol Rev* 2002; 54: 527–59.

[70] Kach J, Sethakorn N, Dulin NO. A finer tuning of G-protein signaling through regulated control of RGS proteins. *Am J Physiol Heart Circ Physiol* 2012; 303: H19-35.

[71] Sainath R, Gallo G. Cytoskeletal and signaling mechanisms of neurite formation. *Cell Tissue Res* 2015; 359: 267–78.

[72] Allen MJ, Shan X, Murphey RK. A Role for Drosophila Drac1 in Neurite Outgrowth and Synaptogenesis in the Giant Fiber System. *Mol Cell Neurosci* 2000; 16: 754–765.

[73] Schwamborn JC, Püschel AW. The sequential activity of the GTPases Rap1B and Cdc42 determines neuronal polarity. *Nat Neurosci* 2004; 7: 923–929.

[74] Hoe HS, Lee KJ, Carney RS, Lee J, Markova A, Lee JY, Howell BW, Hyman BT, Pak DT, Bu G, Rebeck GW. Interaction of reelin with amyloid precursor protein promotes neurite outgrowth. *J Neurosci* 2009; 29: 7459–7473.

[75] Strittmatter SM, Igarashi M, Fishman MC. GAP-43 amino terminal peptides modulate growth cone morphology and neurite outgrowth. *J Neurosci* 1994; 14: 5503–5513.

[76] Tułodziecka K, Czeredys M, Nałęcz KA. Palmitoylcarnitine affects localization of growth associated protein GAP-43 in plasma membrane subdomains and its interaction with Gαo in neuroblastoma NB-2a cells. *Neurochem Res* 2013; 38: 519–529.

[77] Strittmatter SM, Valenzuela D, Sudo Y, Linder ME, Fishman MC. An intracellular guanine nucleotide release protein for G0. GAP-43 stimulates isolated alpha subunits by a novel mechanism. *J Biol Chem* 1991; 266: 22465–71.

[78] Evangelopoulos ME, Weis J, Krüttgen A. Mevastatin-induced neurite outgrowth of neuroblastoma cells via activation of EGFR. *J Neurosci Res* 2009; 87: 2138–44.

[79] Zhang K, Duan L, Ong Q, Lin Z, Varman PM, Sung K, Cui B. Light-mediated kinetic control reveals the temporal effect of the Raf/MEK/ERK pathway in PC12 cell neurite outgrowth. *PLoS One* 2014; 9: e92917.

[80] Hynds DL, Spencer ML, Andres D a, Snow DM. Rit promotes MEK-independent neurite

branching in human neuroblastoma cells. *J Cell Sci* 2003; 116: 1925–35.

[81] Shi G, Andres DA. Rit Contributes to Nerve Growth Factor-Induced Neuronal Differentiation via Activation of B-Raf–Extracellular Signal-Regulated Kinase and p38 Mitogen-Activated Protein Kinase Cascades. *Microbiology* 2005; 25: 830–846.

[82] Masliah E, Mallory M, Hansen L, Alford M, DeTeresa R, Terry R, Baudier J, Saitoh T. Localization of amyloid precursor protein in GAP43-immunoreactive aberrant sprouting neurites in Alzheimer's disease. *Brain Res* 1992; 574: 312–6.

[83] Masliah E, Mallory M, Ge N, Saitoh T. Amyloid precursor protein is localized in growing neurites of neonatal rat brain. *Brain Res* 1992; 593: 323–328.

[84] Strittmatter SM, Cannon SC, Ross EM, Higashijima T, Fishman MC. GAP-43 augments G protein-coupled receptor transduction in Xenopus laevis oocytes. *Proc Natl Acad Sci U S A* 1993; 90: 5327–5331.

[85] Uhlén M, Fagerberg L, Hallström BM, Lindskog C, Oksvold P, Mardinoglu A, Sivertsson Å, Kampf C, Sjöstedt E, Asplund A, Olsson I, Edlund K, Lundberg E, Navani S, Szigyarto CA-K, Odeberg J, Djureinovic D, Takanen JO, Hober S, Alm T, Edqvist P-H, Berling H, Tegel H, Mulder J, Rockberg J, Nilsson P, Schwenk JM, Hamsten M, von Feilitzen K, Forsberg M, Persson L, Johansson F, Zwahlen M, von Heijne G, Nielsen J, Pontén F. Proteomics. Tissue-based map of the human proteome. *Science* 2015; 347: 1260419.

[86] Ju H, Lee S, Kang S, Kim S-S, Ghil S. The alpha subunit of Go modulates cell proliferation and differentiation through interactions with Necdin. *Cell Commun Signal* 2014; 12: 39.

[87] Milosch N, Tanriöver G, Kundu A, Rami A, François J-C, Baumkötter F, Weyer SW, Samanta A, Jäschke A, Brod F, Buchholz CJ, Kins S, Behl C, Müller UC, Kögel D. Holo-APP and G-protein-mediated signaling are required for sAPPα-induced activation of the Akt survival pathway. *Cell Death Dis* 2014; 5: e1391.

[88] Deyts C, Vetrivel KS, Das S, Shepherd YM, Dupré DJ, Thinakaran G, Parent AT. Novel GαS-protein signaling associated with membrane-tethered amyloid precursor protein intracellular domain. *J Neurosci* 2012; 32: 1714–29.

[89] Zhou F, Gong K, Song B, Ma T, van Laar T, Gong Y, Zhang L. The APP intracellular domain (AICD) inhibits Wnt signalling and promotes neurite outgrowth. *Biochim Biophys Acta - Mol Cell Res* 2012; 1823: 1233–1241.

[90] Vaudry D, Stork PJS, Lazarovici P, Eiden LE. Signaling pathways for PC12 cell differentiation: making the right connections. *Science* 2002; 296: 1648–9.

[91] Kiu H, Nicholson SE. Biology and significance of the JAK/STAT signalling pathways. *Growth Factors* 2012; 30: 88–106.

[92] Chiba T, Yamada M, Sasabe J, Terashita K, Shimoda M, Matsuoka M, Aiso S. Amyloid-β causes memory impairment by disturbing the JAK2/STAT3 axis in hippocampal neurons. *Mol Psychiatry* 2009; 14: 206–222.

[93] Feld M, Krawczyk MC, Sol Fustiñana M, Blake MG, Baratti CM, Romano A, Boccia MM. Decrease of ERK/MAPK Overactivation in Prefrontal Cortex Reverses Early Memory Deficit in a Mouse Model of Alzheimer's Disease. *J Alzheimer's Dis* 2014; 40: 69–82.

B1.7. Supplementary Material

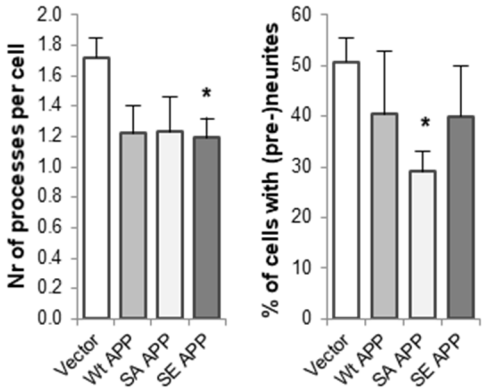

Supplementary Figure B1.1. Morphometric analysis of SH-SY5Y cells transfected with the different APP-GFPs for 6h. Number of processes arising from the cell body (left graph) and the percentage of cells presenting at least one pre-neurite or neurite, termed '(pre-)neurites' (right graph) (processes longer than 20µm). '*' represents a statistical significance relative to the empty vector. *, p<0.05.

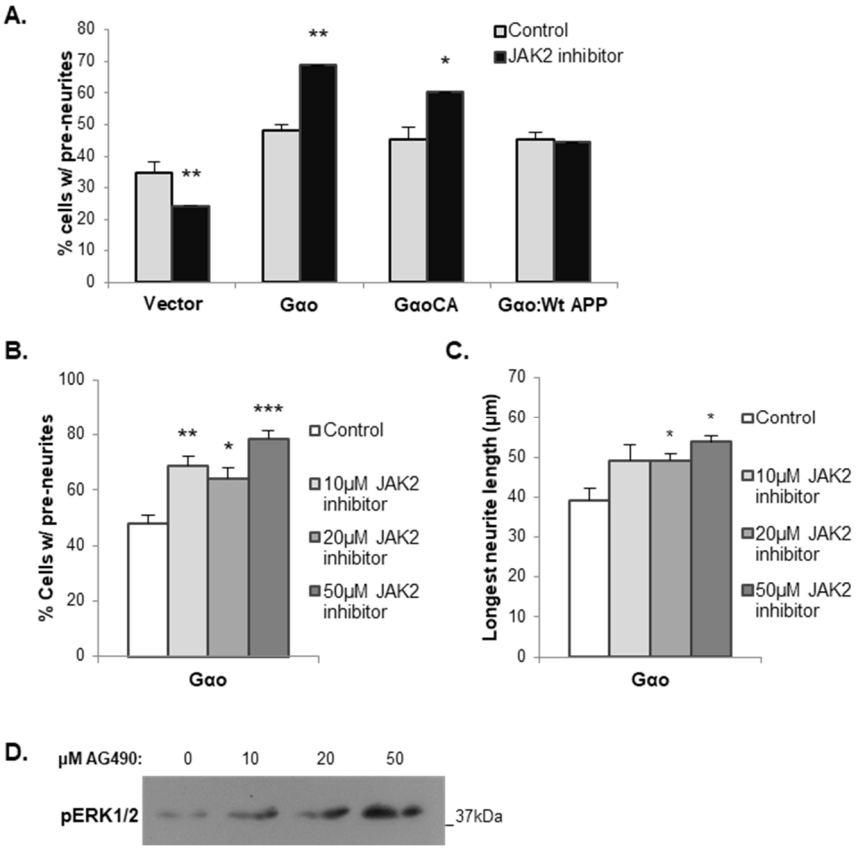

Supplementary Figure B1.2. JAK2-STAT3 inhibition. **A)** Percentage of cells presenting at least one pre-neurite or neurite, termed '(pre-)neurites' (processes longer than 20µm). Cells were treated with 10 µM of AG490 ("JAK2 inhibitor") or left untreated ("Control"). **B)** and **C)** Effects of increasing concentrations of AG490 on Gαo-induced neuritogenic effects. The percentage of cells with at least one pre-neurite was accounted for (B) and the longest process of each cell was measured (C). '*' represents a statistical significance relative to the untreated cells ("control"). *, p<0.05; **, p<0.01; ***, p<0.001. **D.** Immunoblot of pERK levels in cells transfected with Gαo and treated with increasing concentrations of AG490.

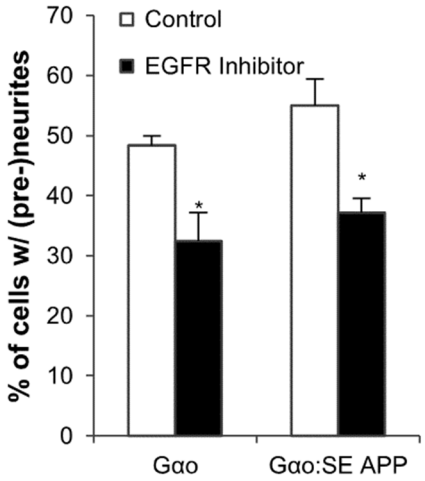

Supplementary Figure B1. 3. EGFR inhibition in SH-SY5Y cells. SH-SY5Y cells were transfected with the Gαo cDNA alone or both Gαo and SE APP cDNAs, and exposed to 10 μM PD168393, an EGFR inhibitor. Morphometric analysis revealed that, in Gαo transfected cells, EGFR inhibition significantly reduced the percentage of cells with at least one (pre)-neurite (processes longer than 20 μm, including pre-neurites and neurites) from 48±2% to 32±5%. In Gαo:SE APP-expressing cells EGFR inhibition reduced it from 53±4% to 37±2% ($p<0.05$). The EGFR-ERK1/2 pathway is thus important in Gαo and Gαo:SE APP-induced neuritic elongation.

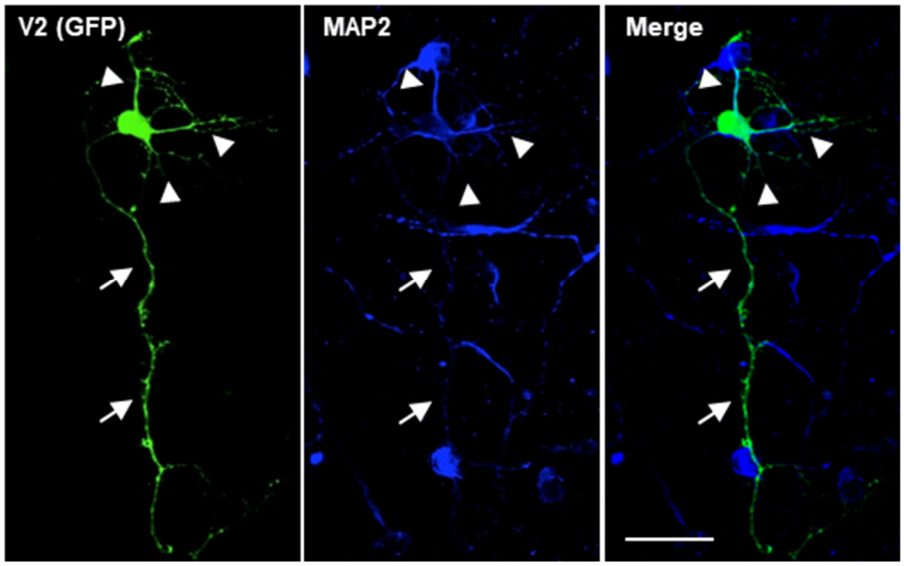

Supplementary Figure B1.4. Confirmation of the neuritic nature in 4 DIV neurons. 3DIV rat embryonic cortical neurons were transfected with empty vector (V2-GFP) for 24h. At 4DIV, cells were fixed and immunolabeled for MAP2 (blue), a dendritic marker. Scale bar = 20 μm. Dendrites can be identified by a strong MAP2 signal (arrowheads), while the axon exhibits little to no MAP2 labelling (arrows).

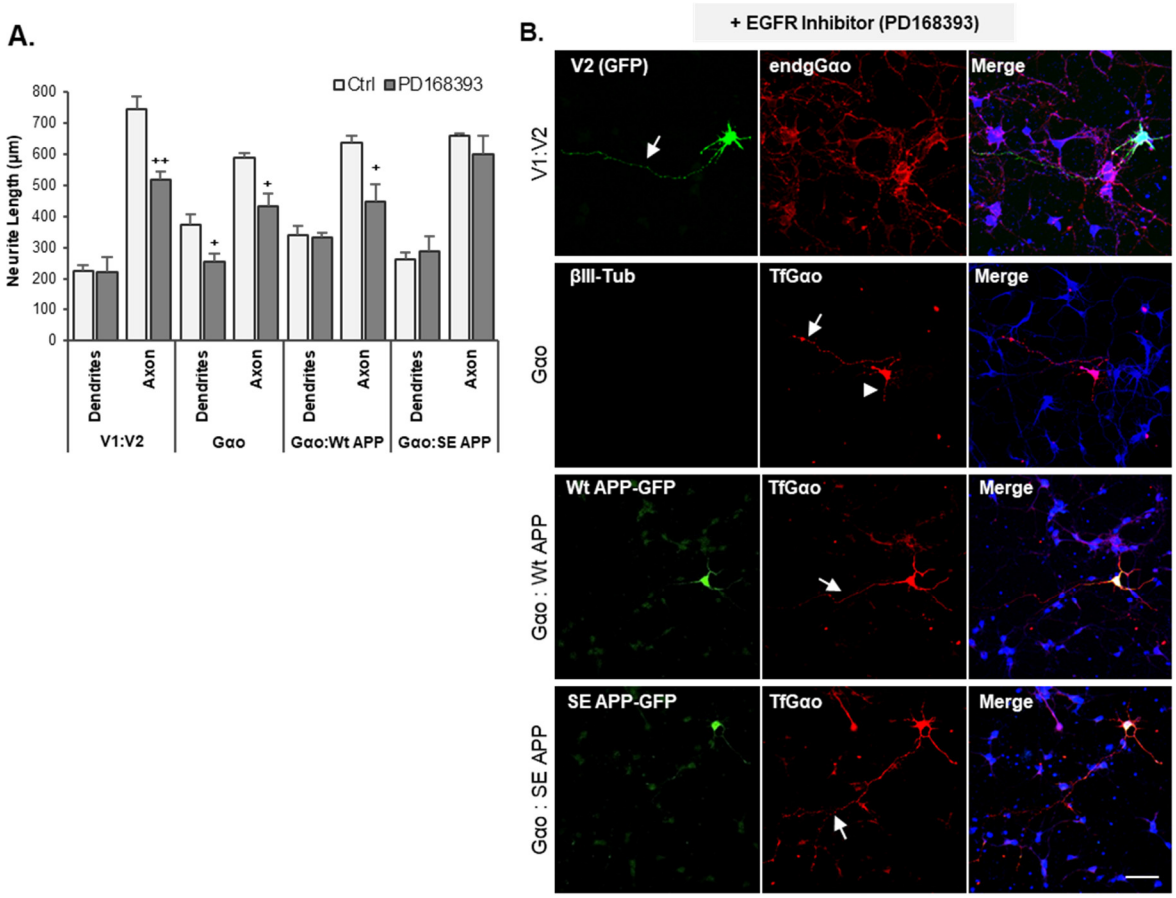

Supplementary Figure B1.5. Impact of EGFR inhibition on APP-Gαo effects in primary neurons. B. Morphometric analysis of total dendritic and axonal lengths (including branches) upon EGFR inhibition. Neuronal cultures were transfected with V1:V2, Gαo, Gαo:Wt APP-GFP and Gαo:SE APP-GFP cDNAs at 3 DIV, and exposed to 10 µM of the EGFR inhibitor in the last 18h. PD168393, EGFR inhibitor; Ctrl, control unexposed neurons. For each condition, at least 50 different neurons were analysed, from 2 different experiments. Symbol '$^{+}$' represents statistical significance relative to control without inhibtor. $^{+}$, $p<0.05$; $^{++}$, $p<0.01$. **B.** Representative microphotographs of the neuritogenic effects of EGFR inhibition. Gαo (red); APP and βIII-tubulin (green); arrows, axon; arrowheads, dendrites. EndgGαo, Endogenous Gαo; TfGαo, Transfected Gαo. Scale bar = 50 µm.

B2. Regulation of Gαo and APP protein levels

Roberto A. Dias[1,2], Ana R. Cerqueira[1], João V. Ferreira[3], Joana F. da Rocha[1,2], Paulo Pereira[3], Odete A. B. da Cruz e Silva[1], Sandra I. Vieira[1,2]

[1] Neurosciences and Signalling Laboratory, Institute of Biomedicine (iBiMED), Department of Medical Sciences, University of Aveiro, Campus de Santiago, 3810-193 Aveiro, Portugal;

[2] Cell Differentiation and Regeneration Laboratory, Institute of Biomedicine (iBiMED), Department of Medical Sciences, University of Aveiro, Campus de Santiago, 3810-193 Aveiro, Portugal.

[3] Centro de Estudos de Doenças Crónicas (CEDOC), NOVA Medical School, Faculdade de Ciências Médicas, Universidade Nova de Lisboa, Lisboa, Portugal

Acknowledgements

This work was supported Fundação para a Ciência e Tecnologia (Portuguese Ministry of Science and Technology), the COMPETE program, QREN, and the European Union (FEDER): Institute for Biomedicine iBiMED UID/BIM/04501/2013; PTDC/SAU-NMC/111980/2009, SFRH/BD/90996/2012, SFRH/BD/78507/2011.

B2.1. Abstract

One of the mechanisms that cells use to control signaling responses is by regulating protein levels. This can be achieved either by modulation of gene expression or by modulation of protein degradation. Interaction between APP and Gαo has been under study for the last decades. Some potential crucial functions that have been attributed to this interaction include the (co)-activation of signaling pathways involved in cell migration and neuronal differentiation. Nevertheless, it is not known how APP-Gαo signaling is terminated. By using SH-SY5Y neuroblastoma cells transfected with either APP or Gαo, we show that APP downregulates Gαo protein levels, and that this effect is dependent on APP phosphorylation at S655. Moreover, this downregulation occurs primarily via lysosomal degradation, in a mechanism that appears to involve chaperone-mediated autophagy (CMA). Treatment of cells with pertussis toxin (PTX), a known inhibitor of Gαo, triggers Gαo proteasomal degradation under basal conditions, while also affecting APP protein levels, further indicating that control of APP and Gαo is interconnected. APP overexpression, in its turn, targets PTX-inactive Gαo to a degradation pathway other than the proteasome, potentially CMA. The work here presented uncovers new mechanisms by which APP and Gαo protein levels are controlled, thus broadening our understanding of APP/Gαo signaling.

B2.2. Introduction

Inside human cells, G protein signaling is widely used for many important cellular processes and is maintained under tight control. One of the mechanisms by which cells implement this control is by direct termination of their signaling. G proteins are mainly negatively modulated by a family of proteins called Regulators of G Protein Signaling (RGS) [1–3]. RGS bind to the α subunit of G proteins and increase their GTPase activity. This leads to the conversion of GTP to GDP, and subsequent recoupling of the Gα subunit with the βγ complex, thus terminating their intracellular signaling. Nevertheless, the targeting of G proteins to degradation is also a control mechanism used by cells [4]. Another mechanism by which cells implement this control is by modulating the protein levels of G proteins and their G-Protein Coupled Receptors (GPCRs). Several GPCRs have already been described to suffer ubiquitination after their activation [1, 5]. For instance, both the β2-Adrenergic receptor [6–8] and the chemokine receptor CXCR4 [9] are ubiquitinated upon activation, leading to the receptor's internalization and trafficking to lysosomal degradation. GPCRs can also be subjected to proteasomal degradation, in a general mechanism by which cells eliminate misfolded receptors, that is not dependent on the receptor activation [10, 11]. Several lines of evidence show that various α-subunits of heterotrimeric G proteins also suffer ubiquitination [12–14]. In rats, polyubiquitination of Gαi2 occurs after intense exercise, resulting in the α-subunit being targeted to proteasomal degradation, a mechanism that is dependent on receptor activation [15]. G protein degradation also occurs as an effect of certain toxins. For instance, prolonged treatment with cholera toxin, a known activator of Gαs, leads to the down-regulation of this α-subunit [16, 17].

The Gαo protein is the most expressed Gα subunit in neurons, though its main function in the brain it is still not clear. Several studies have indicated possible roles in neuronal differentiation and migration [18–23]. Some RGS proteins that act upon Gαo to control its activity have already been described [24–26], however, few is known regarding the regulation of Gαo protein levels. One study has shown that the protein levels of Gαo are controlled by its interaction with the heat shock protein 90 (hsp90) [27]. The authors demonstrated that the disruption of the Gαo-hsp90 complex by incubating cells with Geldanamycin, a ligand of hsp90, led to a decrease of Gαo levels. Furthermore, this decrease occurred via degradation of Gαo by the proteasome [27]. As with other G proteins, certain toxins also affect the levels of Gαo. The Pertussis toxin (PTX) is known to inhibit Gαo by ADP-ribosylating its C-terminal [28], and treatment of LA-N-5 neuroblastoma cells with PTX

leads to reduced Gαo levels [29]. The consequence of this response, however, was not addressed in a Gαo signaling context.

Our group has been studying Gαo signaling pathways, with a particular focus on Gαo neuritogenic functions and on Gαo cooperation with one of its interactors, APP (Amyloid Precursor Protein). APP is a type 1 transmembrane protein, mostly known for its role in the Alzheimer's Disease (AD) [30–32], but that also plays a part in neuronal differentiation and migration, as well as in cell survival [18–20, 33–37]. The interaction between APP and Gαo has been well documented, with APP being described to bind and activate Gαo, acting as a GPCR-like protein [18, 38–40]. The outcome of this interaction, however, is still not completely clear. Initial studies showed that a mutated form of APP, present in Familial Alzheimer's Disease, is able to increase Gαo activation when compared to Wild-type APP, resulting in increased cell death [41, 42]. Further studies have shown that the APP-Gαo interaction could also have a role in Aβ-induced toxicity [43, 44], thus complementing the idea that Gαo might have a central role in AD. A physiological role in cell migration has been implied to this interaction. Using an insect homolog of APP, APPL, researchers showed that inhibition of either APPL or Gαo resulted in erratic neuronal migration of enteric neurons in a *Manduca sexta* model [18]. They also demonstrated that APP acts upstream Gαo, similarly to a GPCR. In our studies on the nature of this interaction we have observed that APP interaction with Gαo leads to the activation of the STAT3 and ERK1/2 signaling pathways in neuroblastoma SH-SY5Y cells, resulting in increased neuritogenesis (Chapter B1). Furthermore, we showed that this interaction is modulated by APP phosphorylation at Serine 655 (S655, APP695 isoform numbering), a residue of the YTSI sorting domain. Upon S655 phosphorylation, the YTSI domain changes its conformation, as well as the conformation of the downstream hydrophobic pocket, where Gαo binds [38, 45]. Phosphorylation of this residue was already associated by us with the control of APP trafficking. By using phosphomimicking mutants of APP (SA APP and SE APP) we have shown that phosphorylation of S655 directs APP trafficking to the secretory pathway, increasing the rate of APP cleavage to soluble APP (sAPP) [46]. Further, in the endo-lysosomal pathway, APP S655 phosphorylation rescues APP from degradation by redirecting it to the trans-Golgi network [47]. On the other hand, APP internalization from the plasma membrane in a unphosphorylated state targets it for lysosomal degradation [47, 48].

Since APP is able to activate Gαo in a GPCR-like manner, while also being subjected to similar mechanisms of protein level's control as GPCRs, this raises the hypothesis that the cell could be modulating APP-Gαo interaction and signaling by tightly regulating their protein levels. The work presented here addresses the possible role of APP and its phosphorylation on the regulation of Gαo

levels, and investigates the potential for Gαo activity acting as a feedback mechanism affecting APP degradation. Finally, the degradation mechanisms involved in the modulation of the APP-Gαo complex that might play an important role on the control of their functions are identified.

B2.3. Materials and Methods

B2.3.1. Antibodies

Primary antibodies used in Western Blot (WB) and Immunocytochemistry (ICC) assays: mouse 22C11 monoclonal anti-APP N-terminus (Chemicon; WB-1:250; ICC-1:50); rabbit anti-Gαo/GNAO1 polyclonal (Upstate; WB-1:5000; ICC-1:250; Thermo; WB-1:2000; ICC-1:200); mouse anti-LAMP2 (abcam; ICC-1:50); rat anti-Hsc70 (kindly provided by Dr. Paulo Pereira; WB-1:2000; ICC-1:200). Secondary antibodies used: horseradish peroxidase-labeled goat antibodies (GE Healthcare) for enhanced chemiluminescence (ECL) detection; Alexa Fluor 405, 488, 568 or 594-conjugated goat antibodies (Molecular Probes) for ICC analysis. Antibodies were prepared in 3% BSA in phosphate buffer saline (PBS) for ICC, and in either 3-5% milk or BSA for WB, per the manufacturers' instructions.

B2.3.2. Chemicals

Chloroquine (CQ) (N4-(7-Chloro-4-quinolinyl)-N1,N1-dimethyl-1,4-pentanediamine diphosphate salt; Sigma) was used at a concentration of 50 µM to inhibit lysosomal degradation [47]. Proteasomal degradation was inhibited by using Lactacystin (Lac; Millipore) and Proteasome Inhibitor I (PSI; Millipore), each at 10 µM [27, 49]. Cells were incubated with either a proteasomal or a lysosomal inhibitor for 18h before being subjected to ICC, or collected for WB analyses. Pertussis toxin (PTX; Calbiochem) was used at a concentration of 100 ng/mL to inhibit Gαo [50].

B2.3.3. Gαo and APP cDNA constructs

Wild-type and constitutively active cDNAs of human G-protein alpha o, isoform A, (Gαo and GαoCA, respectively), cloned into a pcDNA3.1+ vector, were obtained from Missouri S&T cDNA Resource Center. The GαoCA cDNA has a Q205L mutation that hinders its GTPase activity [51]. The empty pcDNA3 vector (Invitrogen) was used to control Gαo transfections. APP cDNAs (human isoform 695), Wt and Serine 655 (S655) point mutated to Alanine (SA) or to Glutamate (SE), already N-terminally fused to GFP (Green Fluorescent Protein) were previously constructed . Due to the amino acids characteristics, S655E and S655A mimic a constitutively phosphorylated and

dephosphorylated S655 state, respectively. The pEGFP-N1 empty vector (Clontech) was used to control the APP-GFP cDNAs transfections [47, 52–54].

B2.3.4. SH-SY5Y cells culture and transfection

Human neuroblastoma SH-SY5Y cells (ATCC CRL-2266) were grown in Minimal Essential Medium (MEM) supplemented with F-12, 10% FBS, 0.5 mM L-glutamine, 100 U/ml penicillin and 100 mg/ml streptomycin (Gibco, Invitrogen). Cells were maintained at 37°C/5% CO_2. APP-GFP (Wt, SA, and SE) and Gαo (Wt, CA) cDNAs were transiently transfected using TurboFect (Fermentas), according to the manufacturer. After 24h of transfection, cells were either harvested with 1% SDS for WB analyses, or fixed with 4% paraformaldehyde for ICC.

B2.3.5. Immunocytochemistry, microscopy and image software

Fixed cells were permeabilized (0.2% Triton), washed with PBS, blocked (3% BSA/PBS), and incubated with primary antibodies for 2h. Following 3 washes with PBS, cells were incubated with secondary antibodies for 1h, washed with PBS and deionised water, and mounted onto glass slides (Vectashield mounting medium with or without DAPI; Vector Labs). Microphotographs were acquired on a LSM 510 META confocal microscope (Zeiss), as before [47], and image analysis was carried out using ImageJ Fiji [55]. For the co-localization analysis, z-stacks of individual cells were acquired by confocal microscopy, and analyzed with the JaCoP plugin [56] to obtain the percentage of proteins co-localization, using the Manders' method.

B2.3.6. SDS-PAGE and Western Blot

Total protein mass-normalized (BCA protein assay; Pierce) cell aliquots were subjected to SDS-PAGE and WB. Ponceau-S staining of the transferred proteins was used as loading control, as an alternative to actin or tubulin, since these proteins vary with our experimental conditions [19, 57]. For this, nitrocellulose membranes were immersed in Ponceau-S solution (Sigma-Aldrich; 0.1 % [w/v] in 5% acetic acid), further washed with distilled water, and scanned (GS-800 calibrated densitometer, Bio-Rad). Following their wash with TBS-T, membranes were subject to WB analysis. Briefly, membranes were blocked with 5% milk or BSA in TBS-T, incubated with primary antibodies for 2h or overnight, and with horseradish peroxidase-linked secondary antibodies for 2h, and

subject to ECL detection. X-ray films (Amersham) were scanned and protein bands quantified with the Quantity One 1-D Analysis Software (Bio-Rad).

B2.3.7. Statistical analysis

Data is expressed as mean ± SEM (standard error of the mean) of at least three different experiments. Statistical analysis was conducted by one-way ANOVA followed by the Tukey test, or by one-sample t-test, using the GraphPad Prism® software. Three levels of significance were used, depending if the p-value was under 0.05, 0.01 or 0.001.

B2.4. Results

B2.4.1. APP and Gαo regulation of each other's protein levels depends on the APP phosphorylation and Gαo activation states

Our previous work has focused on characterizing the APP-Gαo interaction, as well as characterizing the neuritogenic role of this complex (Chapter B1). When analyzing the distribution of these two proteins in neuroblastoma SH-SY5Y cells, we detected a distinct contrast between APP and Gαo labeling. In cells where APP was present in high quantities Gαo protein levels were low, and cells with high levels of Gαo had low levels of APP (Figure B2.1). While some cells presented low levels of both proteins, there was an almost complete absence of cells whit high levels of both proteins.

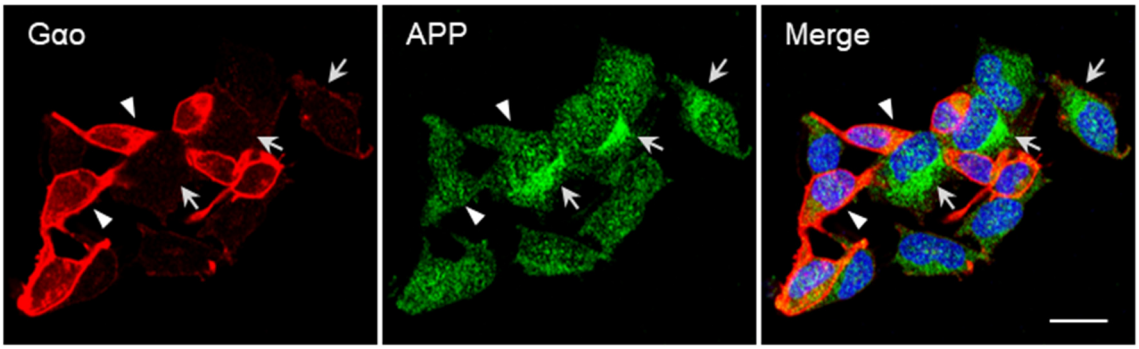

Figure B2.1. APP and Gαo distribution in SH-SY5Y cells. Endogenous Gαo (red) and APP (green) immunolabelled in SH-SY5Y cells. Nuclei were labelled with DAPI (blue). The population includes cells expressing high levels of APP and low levels of Gαo (arrows) and cells expressing high levels of Gαo and low levels of APP (arrowheads). Scale bar = 20μm.

Since APP has been described has a GPCR-like protein [58], we hypothesized that its interaction with Gαo could be subjected to similar regulatory mechanisms that control GPCR signaling, mainly the regulation of the signaling protein's levels. To test this hypothesis, we first transfected SH-SY5Y cells for 24h with increasing amounts of either Gαo or APP-GFP cDNAs (Figure B2.2). Since our previous work had already described a role of Serine 655 (S655) phosphorylation on APP-Gαo interaction, cells were also transfected with two phosphomutants mimicking either S655 phosphorylation (SE APP-GFP) or S655 dephosphorylation (SA APP-GFP). Transfection of low and medium amounts of Gαo cDNA had no effect on APP protein levels, as the transfection of a high amount of Gαo cDNA led to a slight increase in APP levels, although not significant (1.16±0.13-fold change over the empty vector at the maximum 2 μg cDNA/10 cm^2 dose) (Figure B2.2A – left blots and light gray graph). A Gαo cDNA mutant that expresses a constitutively active form of Gαo (Gαo

CA) was also transfected. Interestingly, while transfection of a low amount of Gαo CA resulted in a non-significant increase in APP protein levels (1.13±0.24-fold change over the empty vector), transfecting higher concentrations led to a decrease in APP levels (0.80±0.14-fold change over the empty vector at the maximum 2 μg cDNA/10 cm^2 dose) (Figure B2.2A – right blots and black graph). In both cases there was a high variability between experiments.

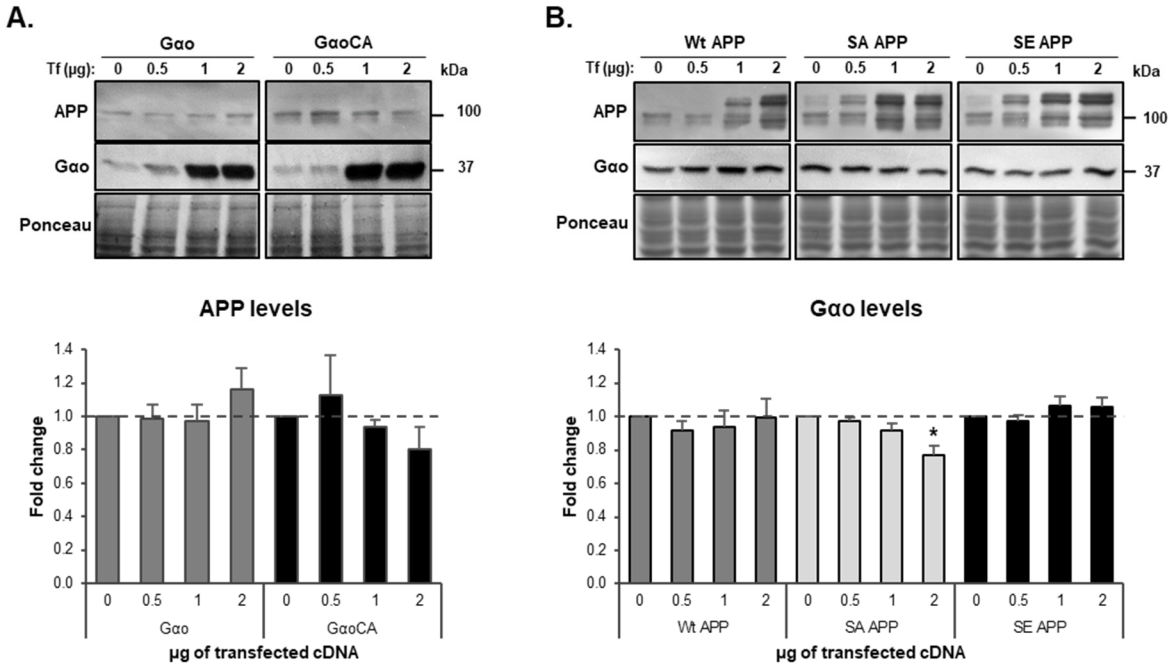

Figure B2.2. Effects of APP and Gαo on each other's protein levels. A. Effects of Gαo overexpression on endogenous APP protein levels, by transfection of SH-SY5Y cells for 24h with increasing amounts of Gαo or GαoCA (constitutively active Gαo Q205L mutant). Transfection of 2 μg of pcDNA3, the Gαo empty vector, was used as control. N=5. **B.** Effects of APP overexpression on endogenous Gαo protein levels, by transfection of SH-SY5Y cells for 24h with increasing amounts of APP-GFP cDNAs: wild-type APP (Wt APP) or APP phosphomutants mimicking S655 dephospho- or phosphorylation state (SA APP and SE APP, respectively). Transfection of 2 μg of pEGFP-N1, the APP empty vector, was used as control. N=5. Symbol '*' represents statistical significance relative to the transfection of the empty vector. *, $p<0.05$.

On the other hand, overexpressing increasing amounts of SA APP-GFP did produce a consistent effect on endogenous Gαo (Figure B2.2B). Overexpression of a high concentration of SA APP (2 μg cDNA) led to a significant decrease in Gαo protein levels (0.77±0.06-fold change over transfection of empty vector, $p<0.05$), while neither Wt nor SE APP had a significant impact on Gαo levels. This is an interesting result, since our previous data showed that S655 phosphorylation is important for APP interaction with Gαo, and its activation. Indeed, while every form of APP-GFP can bind Gαo, the dephosphomimicking mutant SA APP is the least efficient in binding and activating Gαo (Chapter

B1). These results show a correlation between high amounts of an 'inactive' APP form (in terms of inefficiency to bind/activate Gαo) and a decrease in Gαo protein levels.

B2.4.2. Proteasomal and lysosomal Gαo degradation

Degradation of Gαo seems to be an important mechanism in regulating its activity in neuronal cells. After observing the above effect of SA APP on Gαo levels, we decided to focus on the mechanisms by which APP constitutive dephosphorylation was decreasing Gαo protein levels.

Gαo high neuronal levels have been reported as a result of not only increased synthesis of the protein but also due to a significant increase in its half-life (from 28h to 58h) during differentiation of N1E-115 neuroblastoma cells [59]. Notwithstanding its low degradation rate, Gαo has already been described as a substrate of proteasomal degradation [27], and SA APP could be targeting Gαo to proteasomal degradation. We transfected cells with SA APP and treated them with two different proteasome inhibitors, Proteasome Inhibitor I (PSI) and Lactacystin (Lac) (Figure B2.3). Unexpectedly, treatment with both proteasome inhibitors led to a decrease in Gαo protein levels, instead of the expected increase (Figure B2.3B). This decrease was especially pronounced for cells expressing the empty vector (control cells), with Gαo in SA APP cells being less affected by PSI and Lac due to their already decreased Gαo protein levels.

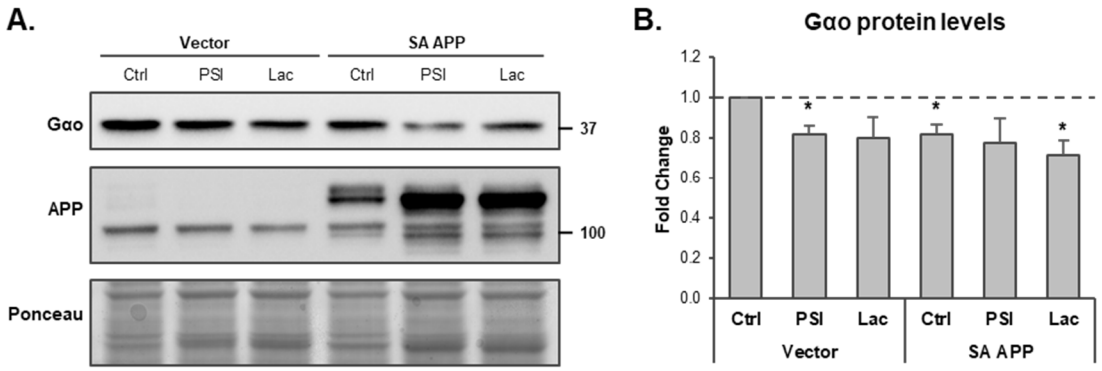

Figure B2.3. Effects of proteasome inhibition on Gαo protein levels. SH-SY5Y cells were transfected with SA APP or its empty vector (pGFP, as control), and treated with two different proteasome inhibitors, Proteasome Inhibitor I (PSI) and Lactacystin (Lac), at 10 μM each. **A.** Immunoblots of Gαo and APP, and Ponceau staining as the loading control. **B.** Variations in Gαo protein levels were evaluated by assessing Gαo signal in each condition and comparing it to the signal in cells transfected with the empty vector and left untreated ("Vector – Ctrl"; dashed line). The '*' symbol represents statistical significance of cells treated with PTX relative to the untreated condition (dashed line). *, $p<0.05$. N=4.

These results suggest that either 1) mass-normalized WB is not able to detect differences in protein levels of proteins with low degradation rates such as Gαo, under proteasome inhibition conditions,

2) that Gαo is degraded by the proteasome in altered conditions but not in basal cellular conditions, or 3) Gαo is being downregulated by other mechanisms. To gather some clues we analyzed Gαo co-localization with endogenous APP and the different APP forms (Figure B2.4). Both Gαo and Gαo CA forms colocalized with endogenous APP at the Golgi region, where APP is abundant, and at the plasma membrane (PM). Gαo also co-localized with APP at small cytoplasmic vesicles, more than Gαo CA, which is more enriched at the PM and the Golgi (Figure B2.4A). In APP-GFP transfected cells (Figure B2.4B), endogenous Gαo co-localizes with SA APP mainly in the cytoplasm (Golgi area and cytoplasmic vesicles), while its co-localization with SE APP occurs almost exclusively in cellular processes, with less Gαo being present in the cytoplasm. Co-localization with Wt APP is intermediate to these two, occurring at all these subcellular regions.

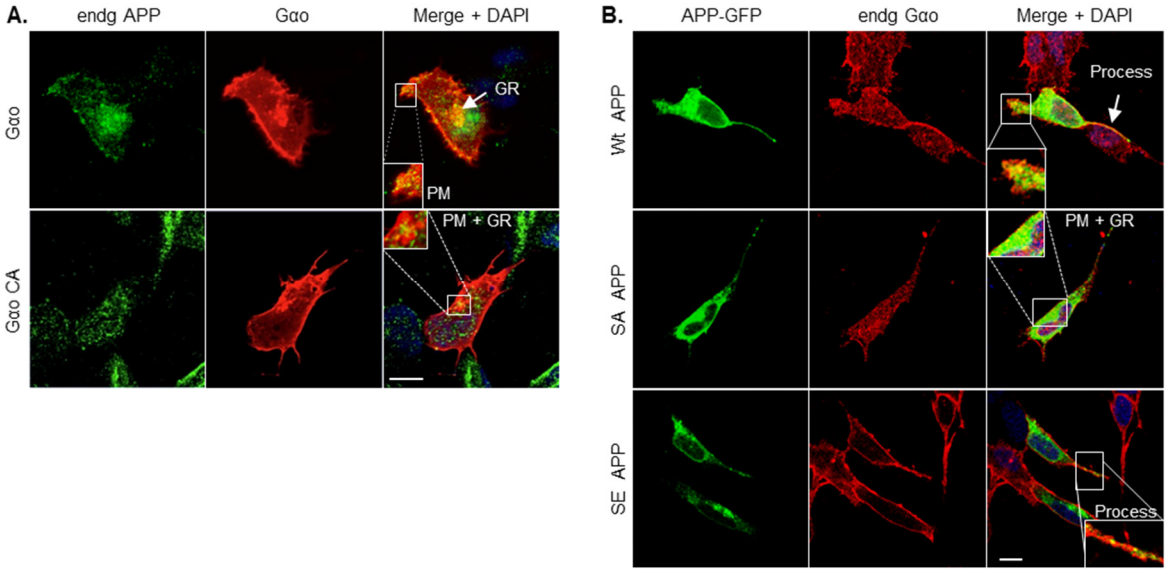

Figure B2.4. Gαo and APP colocalization in SH-SY5Y cells. A. Cells were transfected with Gαo or Gαo CA (red) and endogenous APP ('endg APP') was detected by immunocytochemistry (ICC) means (22C11 antibody, green). **B.** Cells were transfected with the Wt, SA or SE APP-GFP cDNAs (green) and endogenous Gαo ('endg Gαo') was detected by ICC means (red). DAPI was used to counterstain the nuclei (blue). Scale bar: 10 µm. PM, plasma membrane; Golgi R.. Golgi region, where APP is concentrated; Process, cellular projection, including its plasma membrane where both proteins co-localize.

Taken together, these results and the ones above on Figure B2.2 on higher effects of active Gαo on APP levels, and SA APP on Gαo levels, suggest a degradation route where phosphorylated APP activates Gαo, potentially near the PM, and that upon APP dephosphorylation both proteins are targeted to degradation. Given that SA APP endocytosed from the PM is preferentially degraded by the lysosome (while SE APP is not) [47, 48], we subsequently investigated if Gαo could be degraded by the lysosome. To test if the SA APP trafficking could also be leading Gαo to degradation, we inhibited the lysosome with Chloroquine (CQ) in cells overexpressing the three APP-GFP species and monitored Gαo protein levels through western blot (WB) (Figure B2.5). Confirming our

hypothesis, a small amount of Gαo (≈20%, as in Figure B2.3) was recovered in SA APP expressing cells (1.22±0.07-fold change, p<0.05) when lysosomal degradation was inhibited with CQ (Figure B2.5A). This did not occur for the other conditions (Vector, Wt and SE APP). Indeed, similar to the results of the proteasomal inhibition, there was even a slight (although not significant) decrease in Gαo levels when the lysosome was inhibited in Wt and SE APP overexpressing cells. Co-localization of Gαo with LAMP2, a lysosomal marker, in basal conditions, also corroborates the CQ results (Figure B2.5B). Gαo co-localization with LAMP2 is generally low but significantly higher in SA APP transfected cells when compared to Wt and S655E APP (5.6±0.8%, p<0.05 vs ~3.3% for Wt and SE APP). In the same cells, SA APP also co-localized more with LAMP2 than Wt and SE APP, confirming, as expected, that S655 dephosphorylation increases APP targeting to the lysosome.

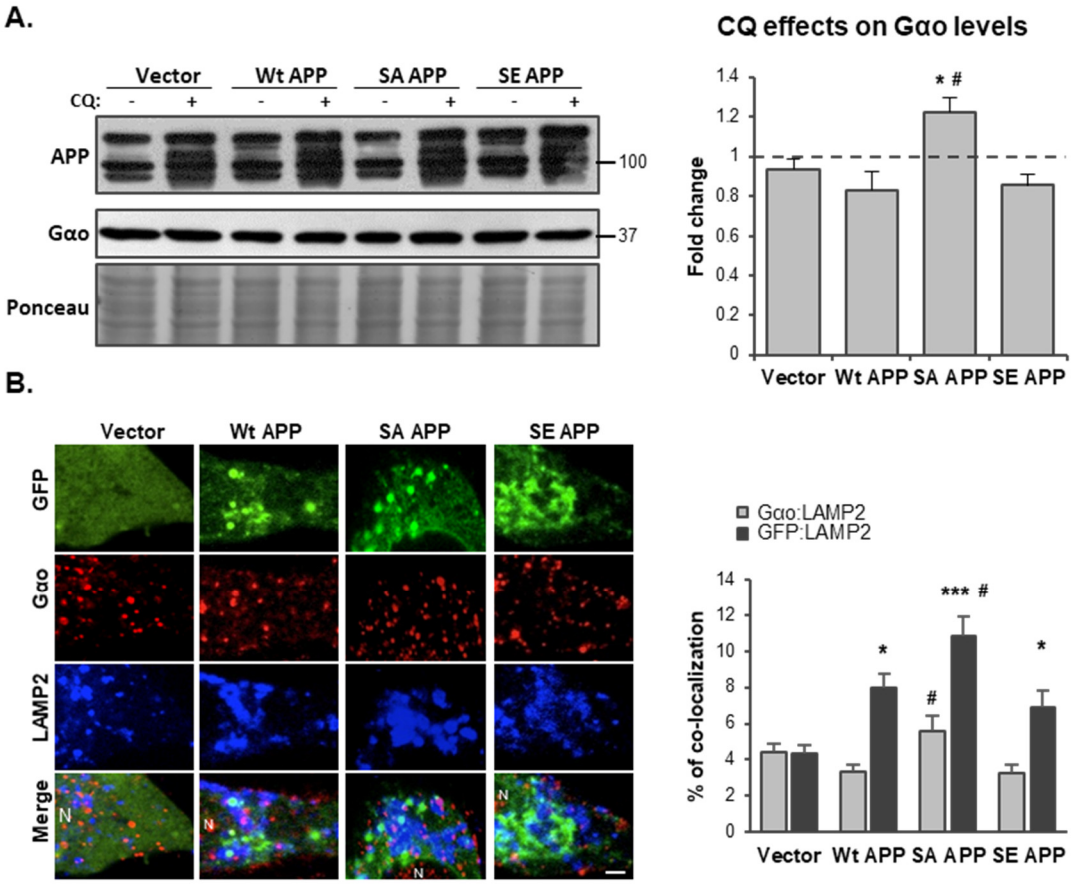

Figure B2.5. APP and Gαo degradation in lysosomes. A. Western blot and quantitative analysis of Gαo protein levels when in SH-SY5Y cells transfected with empty vector, Wt, SA, or SE APP (APP-GFP constructs), and treated with 50 µM of chloroquine (CQ). Ponceau-S staining was used as loading control. Variations in protein content were evaluated by assessing Gαo signal in each V/APP condition treated with CQ ("+") and comparing it to the respective condition without CQ ("-"). '*' represents statistical significance relative to the untreated condition (dashed line), and "#" represents statistical significance relatively to Wt APP. */#, p<0,05. N=3. **B.** Maximum intensity projections of Z-stacks from SH-SY5Y cells transfected with pEGFP-N1 vector ("Vector") and APP-GFP (Wt, SA, SE), and immunolabeled for Gαo (red) and the lysosomal marker LAMP2 (blue). Scale bar = 2 µm. Graph: percentage of co-localization of endogenous Gαo and APP proteins with LAMP2 ('Gαo:LAMP2' and 'GFP:LAMP2', respectively), quantified using the Manders' method. A minimum of 30 z-stacks from SH-SY5Y cells were analyzed for each condition. Symbols * and # represent a statistical significance relative to the empty vector and Wt APP, respectively. */#, p<0.05; **/##, p<0.01; ***/###, p<0.001.

B2.4.3. Chaperone-mediated autophagy as a potential mechanism of Gαo control

Taking together the above results suggest that SA APP decreases Gαo levels in a mechanism involving Gαo targeting to lysosomes, alone or combined with SA APP. Besides Serine 655, APP targeting to the lysosome is also regulated by an APP "KFERQ" targeting motif. This motif is an essential component of chaperone-mediated autophagy (CMA), also being called CMA-targeting motif [60, 61], and it has already been reported that deletion of the APP's KFERQ-like motif results in a decrease of APP co-localization with the lysosome [62]. Since no data exists linking Gαo and lysosomal degradation, we first tried to identify possible KFERQ motifs in the Gαo amino acid sequence. Considering the properties that a sequence must comply to be considered a potential KFERQ motif [60, 61], we have identified the ^{173}QDILR^{177} sequence has a KFERQ-like motif (Figure B2.6).

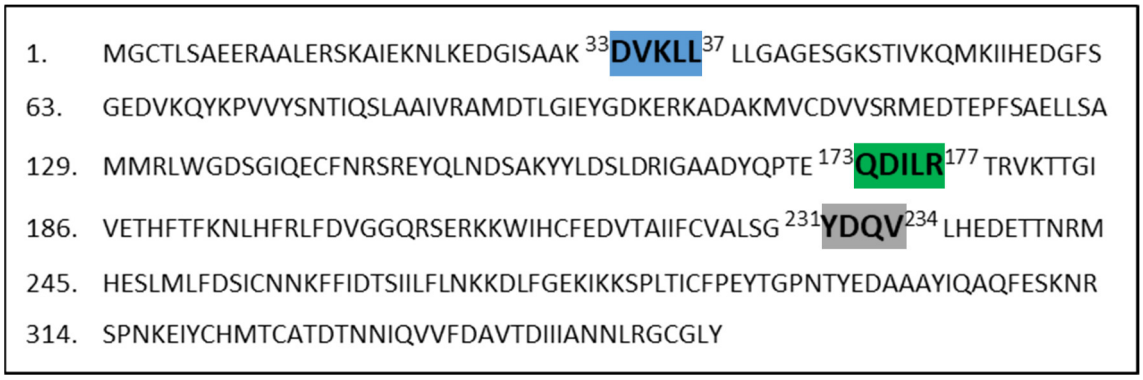

Figure B2.6. Presence of lysosomal-targeting motifs in the Gαo sequence. The ^{173}QDILR^{177} sequence (green) was identified as a potential KFERQ-like motif. A "KFERQ" motif is a pentapeptide consisting of a glutamine in either side of the motif, a positively and a negatively charged amino acid, a hydrophobic amino acid, and a fifth amino acid that can either be positively charged of hydrophobic [60, 61]. By using the ELM resource [63], we also identified the ^{33}DVKLL^{37} sequence (blue) as a putative Endosome-Lysosome-Basolateral sorting signal, and the ^{231}YDQV^{234} sequence (gray) as a putative tyrosine-based sorting signal.

By using the ELM resource [63], the ^{33}DVKLL^{37} sequence was identified as a putative Endosome-Lysosome-Basolateral sorting signal. This motif, however, is mostly associated with the sorting and trafficking of transmembrane receptors to the endosome and lysosome and so its presence in a G protein might not be relevant [64]. The ^{231}YDQV^{234} sequence was also identified as a putative tyrosine-based sorting signal, which mediates intracellular trafficking through the binding to Adaptor Proteins (AP) [65, 66]. Interestingly, a version of this motif is also present on APP, the ^{653}YTSI^{656} sequence, which includes Serine 655 [46, 67].

The targeting of KFERQ-containing proteins to the lysosome occurs through their interaction with the Hsc70 protein (Heat shock cognate protein 70). Cytosolic Hsc70 recognizes and binds to

cytosolic KFERQ-containing target proteins, and mediates their lysosomal uptake via a lysosomal hsc70 counterpart and LAMP2 [61, 68]. To further validate a possible role of CMA in Gαo control, Gαo co-localization with Hsc70 in SH-SY5Y cells was investigated (Figure B2.7A).

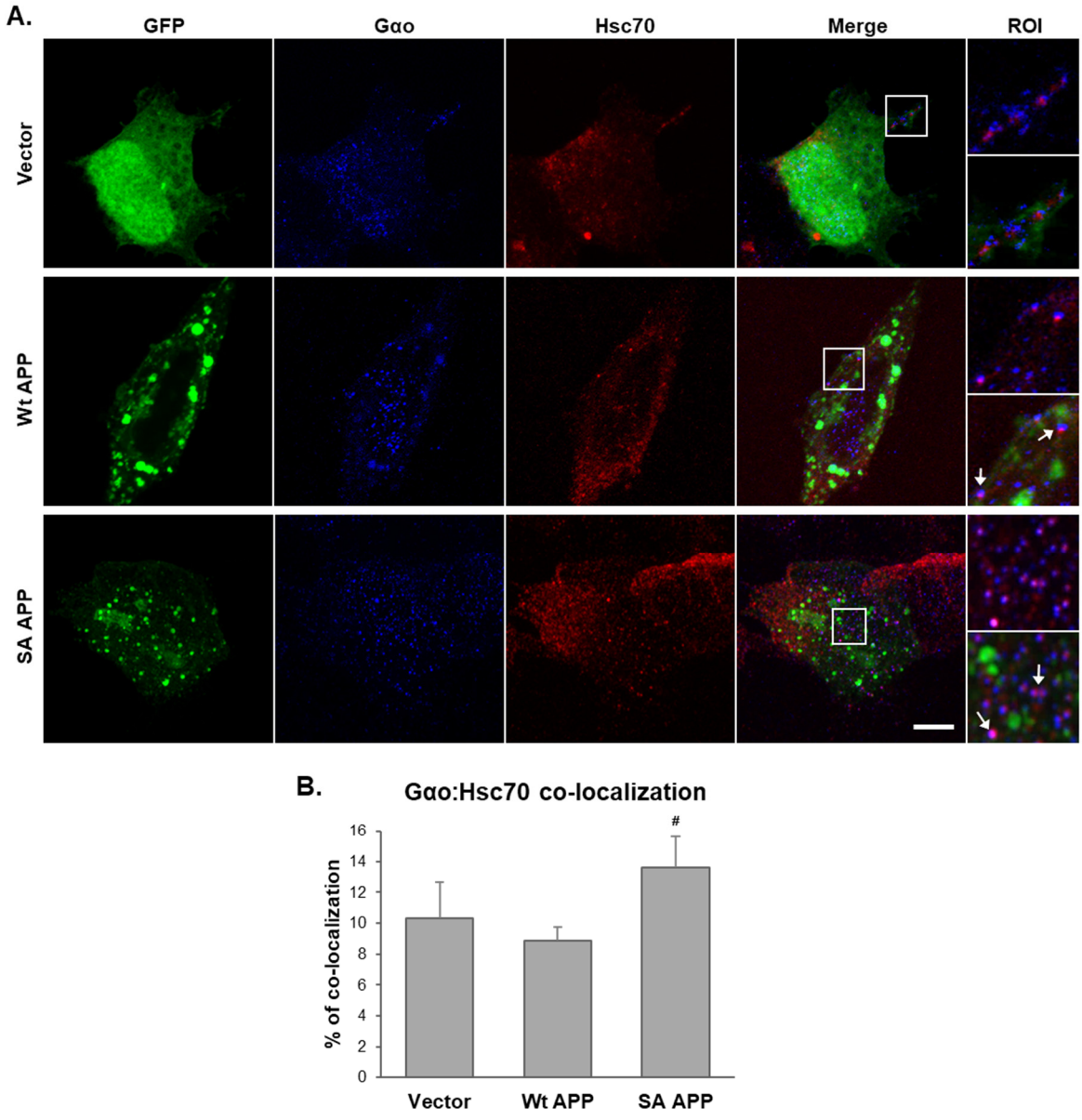

Figure B2.7. Gαo and Hsc70 co-localize in SH-SY5Y cells. SH-SY5Y cells were transfected for 24h with pEGFP-N1 empty vector ('Vector'), Wt APP-GFP ('Wt APP') and SA APP-GFP ('SA APP') (green). **A.** Maximum intensity projections of Z-stacks from SH-SY5Y cells immunolabelled for Gαo (blue) and Hsc70 (red). For each condition, a region of interest (ROI) was digitally amplified, showing either the combination of Gαo and Hsc70 labeling (upper ROI) or a combination of Gαo, Hsc70, and APP (lower ROI). Scale bar = 5 µm. **B.** Percentage of co-localization of Gαo and Hsc70 signals, quantified using the Manders' method. A minimum of 25 z-stacks from SH-SY5Y cells were analyzed for each condition. "#" represents a statistical significance relative to Wt APP. #, $p<0.05$

Gαo had a very interesting juxtaposed co-localization with Hsc70 in small vesicles/puncta throughout the cytosol, including near the membrane (Figure B2.7A). As expected, co-localization between both proteins increased when SA APP was overexpressed; microphotographs reveal what appears to be a higher merge of the Hsc70/Gαo signals in these cells (Figure B2.7A ROIs and B2.7B). Nevertheless, even though the co-localization between Gαo and Hsc70 changed with APP expression, the three proteins were rarely detected together (Figure B2.7A, arrows).

The correlation between Gαo increased degradation in SA APP-overexpressing cells and its increased localization with Hsc70 points to CMA as a possible regulatory mechanism of Gαo levels. Still, further tests need to be conducted in order to verify if Gαo interacts directly with Hsc70, and if this potential interaction is required for the SA APP-induced Gαo degradation.

B2.4.4. Effect of Gαo inhibition on Gαo and APP protein levels

As aforementioned, the effect of APP on Gαo levels seems to be dependent on its ability to first bind and activate Gαo. To test this hypothesis, we treated cells overexpressing the different APP-GFPs with Pertussis Toxin (PTX), a known inhibitor of Gαo/i proteins. ADP-ribosylation by pertussis toxin blocks G protein interaction with GPCRs [28], and it has already been described to hinder Gαo activation by APP [33, 38]. SH-SY5Y cells were transfected with 2 μg of each APP construct or with an empty vector and, after 6h of transfection, PTX was added to the cell media for additional 18 hours. Gαo successful inhibition can be confirmed by observing its slower migration through the SDS-PAGE (Figure B2.8A, arrows), a phenomenon previously described as a consequence of ADP-ribosylation [69].

Analysis of Gαo protein levels after PTX treatment showed a significant decrease when compared to cells left untreated, both in cells overexpressing the empty vector as well as in cells overexpressing APP (Figure B2.8A). Moreover, there were no significant differences in Gαo reduction levels between the different forms of APP (0.60±0.04-fold change for Wt APP, 0.62±0.06-fold change for SA APP, and 0.57±0.03-fold change for SE APP). A similar reduction had already been reported in other type of neuroblastoma cells, LA-N-5 cells; however, no specific mechanism has been described to explain this downregulating effect [29].

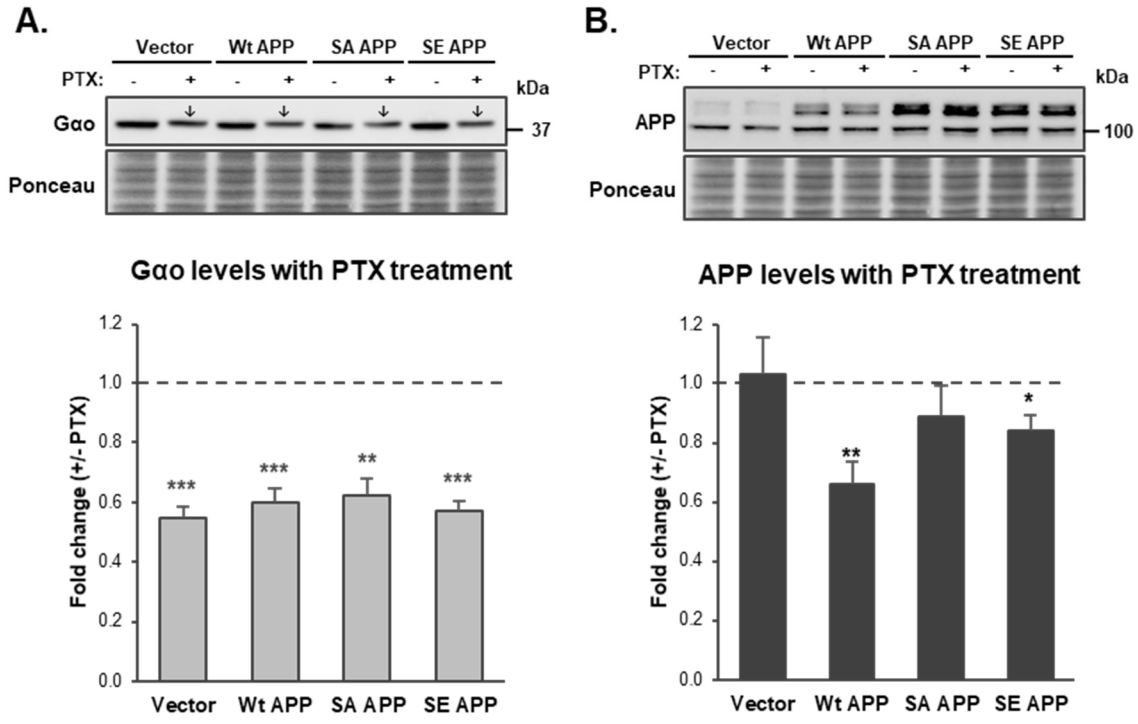

Figure B2.8. Impact of PTX treatment on Gαo and APP protein levels. SH-SY5Y cells were transfected with 2 µg of either pEGFP-N1 empty vector or the Wt, SA or SE APP-GFP cDNAs. After 6h of transfection, PTX was added to the cell media to a final concentration of 100 ng/mL, for additional 18 hours. Variations in protein content were evaluated by assessing **A.** Gαo and **B.** APP protein levels in PTX treated cells ("+") compared to the respective condition without PTX ("-"). The '*' symbol represents statistical significance relative to the untreated condition (dashed line). *, p<0,05; **, p<0,01; ***, p<0,001. N=6. Of note, ADP-ribosylation by PTX results in a slower migration of the Gαo protein through the SDS-PAGE gel (arrows in the immunoblot).

The APP protein levels were also analyzed after PTX treatment (Figure B2.8B). While endogenous APP did not seem to be affected by PTX (1.03±0.13-fold change for Vector), both exogenous Wt and SE APP suffered significant decreases with PTX treatment (0.66±0.08-fold change for Wt APP, $p<0.01$; 0.84±0.05 for SE APP, $p<0.05$). SA APP also decreased with PTX treatment, although not significantly (0.89±0.11-fold change). It is important to notice that in most experiments performed Wt APP transfection efficiency was lower than SA and SE APP (Figure B2.8B, APP immunoblot). These differences of transfection could be a factor playing in APP response to PTX treatment, and thus explain why Wt APP is more affected than the APP phosphomutants. Nevertheless, the data indicates a correlation between S655 phosphorylation and PTX effect on APP levels.

Taking together, these results offer two new pieces of information regarding the manner APP and Gαo are regulated: a) inhibition of Gαo causes a reduction in its protein levels that is independent of APP expression and/or phosphorylation state; and b) inhibition of Gαo triggers a concomitant

downregulation of APP protein levels, a process more dependent on the APP S655 phosphorylation status. In turn, it also opens several questions, such as which mechanisms are behind these alterations in protein levels.

To try and answer this question, the role that proteasomal degradation could be playing in Gαo and APP decrease in response to PTX treatment was addressed. SH-SY5Y cells transfected with the different APPs were treated with PTX in combination with the proteasome inhibitor Lactacystin (Lac), and compared to cells treated with PTX alone (Figure B2.9). Evaluation of Gαo levels revealed that the Gαo decrease in PTX control cells (transfected with empty vector) was partly reversed by the proteasome inhibition (Figure B2.9A-B and Supplementary Figure B2.1A). However, this effect was lost in cells overexpressing APP. Regarding APP, Lac treatment significantly increased transfected APP levels, even past control levels (Figure B2.9A and B2.9C, and Supplementary Figure B2.1B). This pronounced effect indicates that proteasomal inhibition leads to the accumulation of overexpressed APP (mainly immature APP) which would otherwise be targeted to proteasomal degradation to control APP cellular levels [70]. Based on this result, however, we cannot determine if PTX effect on Wt and SE APP protein levels is a result of increased proteasomal degradation of these proteins.

This data indicates that, under basal conditions, Gαo inhibition by PTX triggers its degradation through the proteasome. Under an APP overexpression background, however, inhibited Gαo molecules are also downregulated by other routes. Further testing will be necessary to comprehend APP role in this effect. Since we have detected a link between APP overexpression and Gαo CMA/lysosomal degradation (Figure B2.5-7), this pathway is a potential promising candidate.

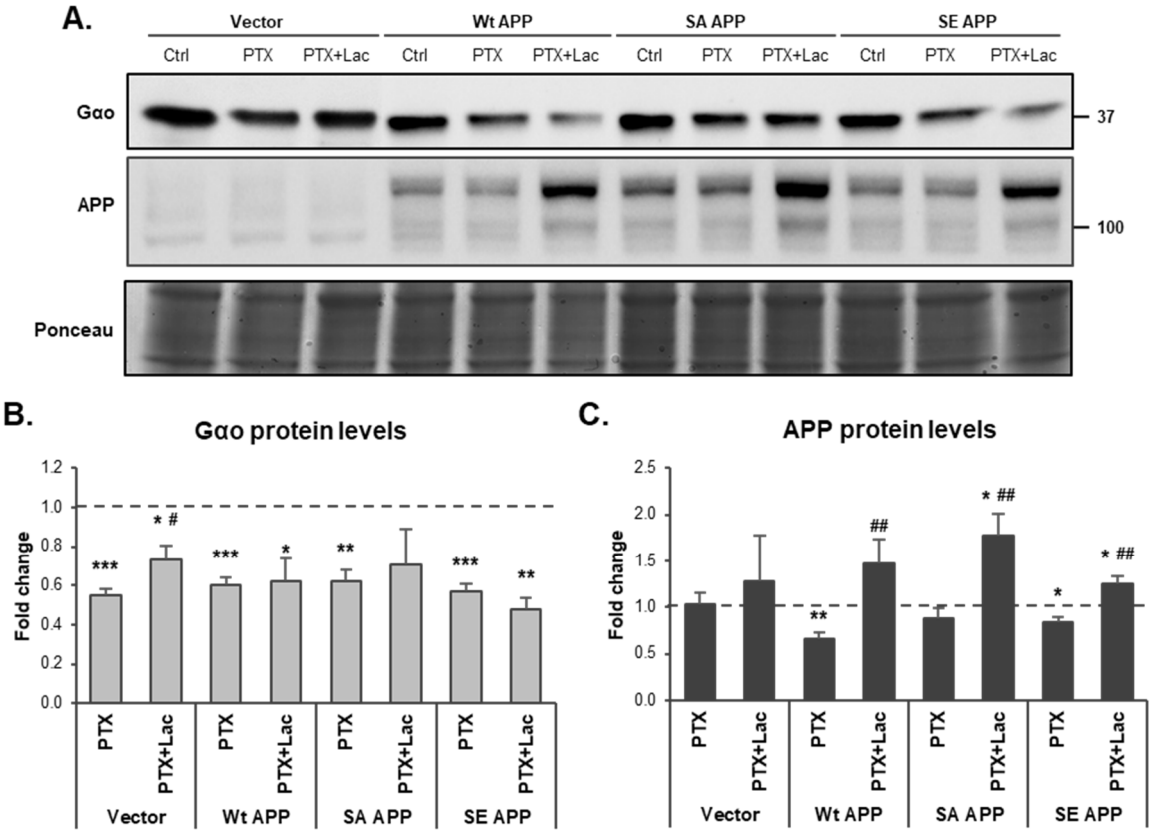

Figure B2.9. Effect of proteasome inhibition on PTX treatment. SH-SY5Y cells were transfected with 2 µg of either pEGFP-N1 empty vector or the Wt, SA or SE APP-GFP cDNAs. After 6h of transfection, PTX was added to the cell media to a final concentration of 100 ng/mL, for additional 18 hours. To test the role of the proteasome on PTX-induced degradation, the proteasome inhibitor Lactacystin (Lac) was added to cells in combination with PTX. **A.** Immublots of Gαo and APP; Ponceau staining was used as loading control. **B-C.** Variations in Gαo and APP protein content were evaluated by comparing cells treated with PTX ("PTX"), or PTX in combination with Lac ("PTX+Lac"), to the respective control condition without PTX (dashed line). The '*' symbol represents statistical significance of cells treated with PTX relative to the untreated condition (dashed line). The "#" symbol represents statistical significance of cells treated with PTX+Lac relative to PTX alone. */#, p<0.05; **/##, p<0.01; ***/###, p<0.001. N=3.

B2.5. Discussion

The interaction between Gαo and APP has been a challenging subject. It is known that APP is able to bind and activate Gαo [38, 40], however, the physiological role that this interaction plays in the human brain is still unclear [71]. Moreover, the mechanisms that regulate this interaction inside the cell have remained unexplored. The work presented here revealed that APP and Gαo protein levels can be controlled reciprocally.

Previous work conducted by us (Chapter B1) showed that the APP's ability to bind and activate Gαo is enhanced by APP phosphorylation at Serine 655. Our results presented here show that APP (de)phosphorylation also has an impact on Gαo protein levels. Overexpression of an APP mutant mimicking S655 constitutive dephosphorylation led to the reduction of Gαo protein levels through lysosomal degradation (Figure B2.2 and Figure B2.5), while inhibition of proteasomal degradation did not recover Gαo levels (Figure B2.3). This is surprising, since the only report of Gαo degradation explores Gαo proteasomal cleavage [27]. Although unexpected, there have been reports of other G proteins being degraded through the lysosome [72, 73], making it more plausible that APP could be targeting Gαo to this degradation pathway.

Even though our experiments showed no Gαo recovery upon proteasomal inhibition, this pathway should not be completely ruled out in the control of APP/Gαo signaling. The further decrease in Gαo levels detected upon proteasomal inhibition could be an artifact from the mass-normalized Western Blot samples. Since proteasomal inhibition might lead to the accumulation of mainly proteins with a fast turnover [74], proteins with a slow turnover, such as Gαo, might have reduced relative abundance in the loaded sample, even if being affected by the proteasome. Other works have found Western blot unreliable in the study of proteins changes after proteasomal inhibition [75]. One way of overcoming this issue might be to normalize the Western Blot samples to the number of cells rather than to the total protein, or to use immunofluorescence to evaluate protein expression in each condition [76].

The decrease of Gαo protein levels upon proteasome inhibition could also be a result of increased protein degradation by other pathways. As described by us, Gαo is subjected to lysosomal degradation when SA APP is overexpressed. Since SA APP levels greatly increase upon proteasomal inhibition (Figure B2.3), this could result in an increased Gαo targeting to the lysosome. This could also explain why APP overexpression blocks Gαo recovery upon treatment with PTX and Lactacystin

(Figure B2.9). However, since Gαo levels are also downregulated when cells are transfected with the empty vector and treated with Lactacystin (Figure B2.3), or endogenous APP also highly increases, or a different/additional mechanism by which Gαo is being led to degradation is probably in play. There are reports that proteasome inhibition might lead to activation of autophagy mechanisms [77, 78], so a closer look into this process might help explain Gαo decreased expression.

Our work unraveled a new potential way by which Gαo can be targeted to degradation, the chaperone-mediated autophagy (CMA) pathway. Contrary to the more classical view of autophagy, where organelles and other membranar compartments containing different types of proteins are fused to lysosomes, resulting in the degradation of their contents [79], CMA consists on the targeting of specific cytosolic proteins to the lysosomes. Proteins with KFERQ motifs, also known as CMA-targeting motifs, are recognized by Hsc70 and then targeted for lysosomal degradation [61]. Our findings show that not only does Gαo possess a KFERQ-like motif (Figure B2.6), but also that SA APP overexpression increases Gαo co-localization with Hsc70 (Figure B2.7), giving strength to the hypothesis that Gαo can be degraded through CMA. Nevertheless, further testing is needed to demonstrate this pathway. The presence of a KFERQ motif does not necessarily implies that Hsc70 can recognize it, it also needs to be exposed to the protein exterior. A look into Gαo's 3D structure might answer this question, while binding assays, such as co-immunoprecipitation, will also verify if Gαo and Hsc70 can bind each other, and if phosphorylation of APP at its S655 residue affects this binding.

The complete mechanism by which APP influences Gαo levels is still not completely clear. We have shown that APP S655 dephosphorylation increases Gαo lysosomal degradation, which is accompanied by an increase in Gαo co-localization with the chaperone Hsc70. Also, APP dephosphorylated at S655 (SA APP mutant) decreases APP interaction with Gαo (Chapter B1) and also increases APP targeting to the lysosome [47, 48]. By combining these findings one possible mechanism emerges: the decreased binding of Gαo to APP results in the unmasking of the Gαo's KFERQ motif [61]. This in turns leads to the recognition of the motif by Hsc70, thus activating chaperone-mediated autophagy and Gαo lysosomal degradation. In this hypothesis, APP would serve has a hub to bring together certain factors, such as Hsc70, that can also bind APP [62, 80], to bind and target Gαo to degradation.

The fact that SA APP, Gαo, and Hsc70 are rarely co-localized in SH-SY5Y cells argues that these proteins are being targeted for degradation separately. Nevertheless, since Gαo CA also affects APP

levels (Figure B2.2A), and appears to be even more degraded than Gαo itself by SA APP (data not shown), both proteins might be co-targeted for degradation. Hence, another potential mechanism could be occuring: APP could bind and activate Gαo, upon APP phosphorylation, targeting it to the PM; upon APP dephosphorylation, APP would be endocytosed with Gαo still bound to it, and Hsc70 would bind to both APP and Gαo; since the dephospho APP avidity to Gαo is small, the Gαo-Hsc70 dimer could free itself and bind to LAMP2 for Gαo to be uptake to the lysosome. Indeed, Gαo activation produces a negative feedback upon APP protein levels; however, this effect seems to be highly dependent on the levels of Gαo activity (Figure B2.2). While high levels of transfection of the constitutively active Gαo decreased APP levels, low levels of transfection of the constitutively active Gαo increased APP levels. Since expression of wild-type Gαo also causes a slight increase in APP levels, this could mean that expression of Gαo might act as a stimulus to increase APP expression, or decrease its degradation, and thus initiate a signaling pathway. Gαo increased activation would then cause a feedback mechanism, triggering downregulation of APP in order to shut down the signaling event. However, due to the high variability between experiments, it is unclear what it is occurring. Overactivation of Gαo using other method other than transfection of a constitutively active mutant, such as treatment with Mastoparan [81], will help us understand the effect of Gαo activation on APP.

Further, the effect of Gαo activity was also assessed by inhibiting it with Pertussis Toxin (PTX). As previously described, Gαo inhibition after treatment with PTX leads to the downregulation of its protein levels [29]. Our results corroborate this and show that this decrease is at least partially caused by proteasomal degradation under basal conditions (Figure B2.8 and Figure B2.9). We have also detected that APP presence apparently did not change the PTX effect; however, it did block Gαo recovery upon proteasomal inhibition. Although this could be expected for SA APP, since we now know that it is targeting Gαo to the lysosome, it also occurs for both Wt and SE APP. Moreover, these two forms are also downregulated when PTX is presence. These effects could somehow be connected to how APP and Gαo interact and how PTX affects this interaction. PTX mechanism of action consists on the ADP-ribosylation of the cysteine present in 4th residue of the Gαo C-terminal, the region where GPCRs and APP bind [28]. While ADP-ribosylation is described to cause the disruption of the interaction between GPCRs and Gαo, a study has described that PTX treatment in *Manduca sexta* increases Gαo binding to the APP-like protein [18]. If a similar effect occurs with mammalian APP and Gαo, it might result in the strengthening of the Gαo interaction with Wt and SE APP, the two forms to which Gαo preferentially binds. This could lead to both proteins being downregulated together. However, the exact mechanisms by which this occurs are still not clear.

Further testing with inhibition of both the proteasome and the lysosome, under PTX treatment, might shed some light on these questions. Interaction assays of APP and Gαo after PTX treatment are also required to determine the exact impact of ADP-ribosylation on this interaction.

The data presented here uncovers new mechanisms by which APP and Gαo are controlled and help understand how APP/Gαo signaling is regulated. This work focused mainly on the degradation pathways of Gαo and APP. Future work should also evaluate possible alterations in the gene expression levels of these proteins, as well as look into alterations on the APP processing, especially the formation of soluble APP, due to its important role on brain function and its reported action with Gαo in cell survival [33, 82].

B2.6. References

[1] Rajagopal S, Shenoy SK. GPCR desensitization: Acute and prolonged phases. *Cell Signal*. Epub ahead of print 2017. DOI: 10.1016/j.cellsig.2017.01.024.

[2] De Vries L, Zheng B, Fischer T, Elenko E, Farquhar MG. The regulator of G protein signaling family. *Annu Rev Pharmacol Toxicol* 2000; 40: 235–271.

[3] Traynor J. Regulator of G protein-signaling proteins and addictive drugs. *Ann N Y Acad Sci* 2010; 1187: 341–352.

[4] Milligan G. Agonist regulation of cellular G protein levels and distribution: mechanisms and functional implications. *Trends Pharmacol Sci* 1993; 14: 413–8.

[5] Wojcikiewicz RJH. Regulated ubiquitination of proteins in GPCR-initiated signaling pathways. *Trends Pharmacol Sci* 2004; 25: 35–41.

[6] Shenoy SK, McDonald PH, Kohout TA, Lefkowitz RJ. Regulation of Receptor Fate by Ubiquitination of Activated β2-Adrenergic Receptor and β-Arrestin. *Science (80-)*; 294.

[7] Shenoy SK, Xiao K, Venkataramanan V, Snyder PM, Freedman NJ, Weissman AM. Nedd4 mediates agonist-dependent ubiquitination, lysosomal targeting, and degradation of the beta2-adrenergic receptor. *J Biol Chem* 2008; 283: 22166–76.

[8] Xiao K, Shenoy SK. Beta2-adrenergic receptor lysosomal trafficking is regulated by ubiquitination of lysyl residues in two distinct receptor domains. *J Biol Chem* 2011; 286: 12785–95.

[9] Marchese A, Benovic JL. Agonist-promoted ubiquitination of the G protein-coupled receptor CXCR4 mediates lysosomal sorting. *J Biol Chem* 2001; 276: 45509–12.

[10] Shenoy SK. Seven-transmembrane receptors and ubiquitination. *Circ Res* 2007; 100: 1142–1154.

[11] Petaja-Repo UE, Hogue M, Laperriere A, Bhalla S, Walker P, Bouvier M. Newly synthesized human delta opioid receptors retained in the endoplasmic reticulum are retrotranslocated to the cytosol, deglycosylated, ubiquitinated, and degraded by the proteasome. *J Biol Chem* 2001; 276: 4416–23.

[12] Wang Y, Dohlman HG. Regulation of G protein and mitogen-activated protein kinase signaling by ubiquitination: Insights from model organisms. *Circ Res* 2006; 99: 1305–1314.

[13] Torres M. Chapter Two - Heterotrimeric G Protein Ubiquitination as a Regulator of G Protein Signaling. In: *Progress in Molecular Biology and Translational Science*. 2016, pp. 57–83.

[14] Torres MP, Lee MJ, Ding F, Purbeck C, Kuhlman B, Dokholyan N V., Dohlman HG. G protein mono-ubiquitination by the Rsp5 ubiquitin ligase. *J Biol Chem* 2009; 284: 8940–8950.

[15] Ogasawara J, Sakurai T, Rahman N, Kizaki T, Hitomi Y, Ohno H, Izawa T. Acute exercise alters Galphai2 protein expressions through the ubiquitin-proteasome proteolysis pathway in rat adipocytes. *Biochem Biophys Res Commun* 2004; 323: 1109–15.

[16] Milligan G, Unson CG, Wakelam MJ. Cholera toxin treatment produces down-regulation of the alpha-subunit of the stimulatory guanine-nucleotide-binding protein (Gs). *Biochem J* 1989; 262: 643–9.

[17] Shah BH. Enhanced degradation of stimulatory G-protein (Gs alpha) by cholera toxin is mediated by ADP-ribosylation of Gs alpha protein but not by increased cyclic AMP levels. *Adv Exp Med Biol* 1997; 419: 93–7.

[18] Ramaker JM, Swanson TL, Copenhaver PF. Amyloid precursor proteins interact with the heterotrimeric G protein Go in the control of neuronal migration. *J Neurosci* 2013; 33: 10165–81.

[19] da Rocha JF, da Cruz E Silva OAB, Vieira SI. Analysis of the amyloid precursor protein role in neuritogenesis reveals a biphasic SH-SY5Y neuronal cell differentiation model. *J Neurochem* 2015; 134: 288–301.

[20] Pinho AC, Dias R, Cerqueira AR, da Cruz e Silva OAB, Vieira SI. APP and its secreted fragment sAPP in SH-SY5Y neuronal-like migration. *Microsc Microanal* 2015; 21: 36–37.

[21] He JC, Gomes I, Nguyen T, Jayaram G, Ram PT, Devi LA, Iyengar R. The G alpha(o/i)-coupled cannabinoid receptor-mediated neurite outgrowth involves Rap regulation of Src and Stat3. *J Biol Chem* 2005; 280: 33426–34.

[22] Kim SH, Kim S, Ghil SH. Rit contributes to neurite outgrowth triggered by the alpha subunit of Go. *Neuroreport* 2008; 19: 521–5.

[23] Ma'ayan A, Jenkins SL, Barash A, Iyengar R. Neuro2A differentiation by Galphai/o pathway. *Sci Signal* 2009; 2: cm1.

[24] Traver S, Bidot C, Spassky N, Baltauss T, De Tand MF, Thomas JL, Zalc B, Janoueix-Lerosey I, Gunzburg JD. RGS14 is a novel Rap effector that preferentially regulates the GTPase activity of galphao. *Biochem J* 2000; 350 Pt 1: 19–29.

[25] Brown NE, Goswami D, Branch MR, Ramineni S, Ortlund EA, Griffin PR, Hepler JR. Integration of G protein α (Gα) signaling by the regulator of G protein signaling 14 (RGS14). *J Biol Chem* 2015; 290: 9037–49.

[26] Slep KC, Kercher M a, Wieland T, Chen C-K, Simon MI, Sigler PB. Molecular architecture of Galphao and the structural basis for RGS16-mediated deactivation. *Proc Natl Acad Sci U S A* 2008; 105: 6243–8.

[27] Busconi L, Guan J, Denker BM. Degradation of Heterotrimeric Gαo Subunits via the Proteosome Pathway Is Induced by the hsp90-specific Compound Geldanamycin. *J Biol Chem* 2000; 275: 1565–1569.

[28] Mangmool S, Kurose H. Gi/o protein-dependent and -independent actions of pertussis toxin (ptx). *Toxins (Basel)* 2011; 3: 884–899.

[29] Li X, Mumby SM, Greenwood A, Jope RS. Pertussis toxin-sensitive G protein alpha-subunits: production of monoclonal antibodies and detection of differential increases on differentiation of PC12 and LA-N-5 cells. *J Neurochem* 1995; 64: 1107–17.

[30] Zhang Y, Xu H. Molecular and Cellular Mechanisms for Alzheimers Disease:Understanding APP Metabolism. *Curr Mol Med* 2007; 7: 687–696.

[31] O'Brien RJ, Wong PC. Amyloid precursor protein processing and Alzheimer's disease. *Annu Rev Neurosci* 2011; 34: 185–204.

[32] da Cruz e Silva OAB, Fardilha M, Henriques AG, Rebelo S, Vieira S, da Cruz e Silva EF. Signal transduction therapeutics: relevance for Alzheimer's disease. *J Mol Neurosci* 2004; 23: 123–42.

[33] Milosch N, Tanriöver G, Kundu A, Rami A, François J-C, Baumkötter F, Weyer SW, Samanta A, Jäschke A, Brod F, Buchholz CJ, Kins S, Behl C, Müller UC, Kögel D. Holo-APP and G-protein-mediated signaling are required for sAPPα-induced activation of the Akt survival

pathway. *Cell Death Dis* 2014; 5: e1391.

[34] Hoe HS, Lee KJ, Carney RS, Lee J, Markova A, Lee JY, Howell BW, Hyman BT, Pak DT, Bu G, Rebeck GW. Interaction of reelin with amyloid precursor protein promotes neurite outgrowth. *J Neurosci* 2009; 29: 7459–7473.

[35] van der Kant R, Goldstein LSB. Cellular Functions of the Amyloid Precursor Protein from Development to Dementia. *Dev Cell* 2015; 32: 502–515.

[36] Wang S, Bolós M, Clark R, Cullen CL, Southam KA, Foa L, Dickson TC, Young KM. Amyloid β precursor protein regulates neuron survival and maturation in the adult mouse brain. *Mol Cell Neurosci* 2016; 77: 21–33.

[37] da Cruz e Silva EF, da Cruz e Silva OA. Protein phosphorylation and APP metabolism. *Neurochem Res* 2003; 28: 1553–1561.

[38] Nishimoto I, Okamoto T, Matsuura Y, Takahashi S, Murayama Y, Ogata E. Alzheimer amyloid protein precursor complexes with brain GTP-binding protein G(o). *Nature* 1993; 362: 75–79.

[39] Brouillet E, Trembleau A, Galanaud D, Volovitch M, Bouillot C, Valenza C, Prochiantz A, Allinquant B. The amyloid precursor protein interacts with Go heterotrimeric protein within a cell compartment specialized in signal transduction. *J Neurosci* 1999; 19: 1717–27.

[40] Okamoto T, Takeda S, Murayama Y, Ogata E, Nishimoto I. Ligand-dependent G protein coupling function of amyloid transmembrane precursor. *J Biol Chem* 1995; 270: 4205–4208.

[41] Yamatsuji T, Okamoto T, Takeda S, Murayama Y, Tanaka N, Nishimoto I. Expression of V642 APP mutant causes cellular apoptosis as Alzheimer trait-linked phenotype. *Embo J* 1996; 15: 498–509.

[42] Okamoto T, Takeda S, Giambarella U, Murayama Y, Matsui T, Katada T, Matsuura Y, Nishimoto I. Intrinsic signaling function of APP as a novel target of three V642 mutations linked to familial Alzheimer's disease. *EMBO J* 1996; 15: 3769–77.

[43] Sola Vigo F, Kedikian G, Heredia L, Heredia F, Anel AD, Rosa AL, Lorenzo A. Amyloid-beta precursor protein mediates neuronal toxicity of amyloid beta through Go protein activation. *Neurobiol Aging* 2009; 30: 1379–1392.

[44] Shaked GM, Chauv S, Ubhi K, Hansen LA, Masliah E. Interactions between the amyloid precursor protein C-terminal domain and G proteins mediate calcium dysregulation and amyloid beta toxicity in Alzheimer's disease. *FEBS J* 2009; 276: 2736–2751.

[45] Ramelot TA, Nicholson LK. Phosphorylation-induced structural changes in the amyloid precursor protein cytoplasmic tail detected by NMR. *J Mol Biol* 2001; 307: 871–84.

[46] Vieira SI, Rebelo S, Domingues SC, da Cruz e Silva EF, da Cruz e Silva OA. S655 phosphorylation enhances APP secretory traffic. *Mol Cell Biochem* 2009; 328: 145–154.

[47] Vieira SI, Rebelo S, Esselmann H, Wiltfang J, Lah J, Lane R, Small SA, Gandy S, da Cruz ESEF, da Cruz ESOA. Retrieval of the Alzheimer's amyloid precursor protein from the endosome to the TGN is S655 phosphorylation state-dependent and retromer-mediated. *Mol Neurodegener* 2010; 5: 40.

[48] Tam JHK, Rebecca Cobb M, Seah C, Pasternak SH. Tyrosine binding protein sites regulate the intracellular trafficking and processing of amyloid precursor protein through a novel lysosome-directed pathway. *PLoS One* 2016; 11: 1–24.

[49] Jordan JD, He JC, Eungdamrong NJ, Gomes I, Ali W, Nguyen T, Bivona TG, Philips MR, Devi LA, Iyengar R. Cannabinoid receptor-induced neurite outgrowth is mediated by Rap1 activation through G(alpha)o/i-triggered proteasomal degradation of Rap1GAPII. *J Biol Chem* 2005; 280: 11413–11421.

[50] Antonelli V, Bernasconi F, Wong YH, Vallar L. Activation of B-Raf and regulation of the mitogen-activated protein kinase pathway by the G(o) alpha chain. *Mol Biol Cell* 2000; 11: 1129–42.

[51] Ram PT, Horvath CM, Iyengar R. Stat3-mediated transformation of NIH-3T3 cells by the constitutively active Q205L Galphao protein. *Science (80-)* 2000; 287: 142–144.

[52] da Cruz e Silva OA, Iverfeldt K, Oltersdorf T, Sinha S, Lieberburg I, Ramabhadran T V, Suzuki T, Sisodia SS, Gandy S, Greengard P. Regulated cleavage of Alzheimer beta-amyloid precursor protein in the absence of the cytoplasmic tail. *Neuroscience* 1993; 57: 873–7.

[53] da Cruz E Silva OAB, Vieira SI, Rebelo S, da Cruz e Silva EF. A model system to study intracellular trafficking and processing of the Alzheimer's amyloid precursor protein. *Neurodegener Dis* 2004; 1: 196–204.

[54] Rebelo S, Vieira SI, Esselmann H, Wiltfang J, da Cruz e Silva EF, da Cruz e Silva OAB. Tyr687 dependent APP endocytosis and Abeta production. *J Mol Neurosci* 2007; 32: 1–8.

[55] Schindelin J, Arganda-Carreras I, Frise E, Kaynig V, Longair M, Pietzsch T, Preibisch S, Rueden C, Saalfeld S, Schmid B, Tinevez J-Y, White DJ, Hartenstein V, Eliceiri K, Tomancak P, Cardona A. Fiji: an open-source platform for biological-image analysis. *Nat Methods* 2012; 9: 676–82.

[56] Bolte S, Cordelières FP. A guided tour into subcellular colocalization analysis in light microscopy. *J Microsc* 2006; 224: 213–32.

[57] Romero-Calvo I, Ocon B, Martinez-Moya P, Suarez MD, Zarzuelo A, Martinez-Augustin O, de Medina FS. Reversible Ponceau staining as a loading control alternative to actin in Western blots. *Anal Biochem* 2010; 401: 318–320.

[58] Ramaker JM, Copenhaver PF. Amyloid Precursor Protein family as unconventional Go-coupled receptors and the control of neuronal motility. *Neurogenes (Austin, Tex)* 2017; 4: e1288510.

[59] Brabet P, Pantaloni C, Bockaert J, Homburger V. Metabolism of two Go alpha isoforms in neuronal cells during differentiation. *J Biol Chem* 1991; 266: 12825–8.

[60] Dice JF. Peptide sequences that target cytosolic proteins for lysosomal proteolysis. *Trends Biochem Sci* 1990; 15: 305–9.

[61] Kaushik S, Cuervo AM. Chaperone-mediated autophagy: a unique way to enter the lysosome world. *Trends Cell Biol* 2012; 22: 407–417.

[62] Park J-S, Kim D-H, Yoon S-Y. Regulation of amyloid precursor protein processing by its KFERQ motif. *BMB Rep* 2016; 49: 337–42.

[63] Dinkel H, Van Roey K, Michael S, Kumar M, Uyar B, Altenberg B, Milchevskaya V, Schneider M, Kühn H, Behrendt A, Dahl SL, Damerell V, Diebel S, Kalman S, Klein S, Knudsen AC, Mäder C, Merrill S, Staudt A, Thiel V, Welti L, Davey NE, Diella F, Gibson TJ. ELM 2016—data update and new functionality of the eukaryotic linear motif resource. *Nucleic Acids Res* 2016; 44: D294–D300.

[64] Bonifacino JS, Traub LM. Signals for sorting of transmembrane proteins to endosomes and lysosomes. *Annu Rev Biochem* 2003; 72: 395–447.

[65] Opresko LK, Chang CP, Will BH, Burke PM, Gill GN, Wiley HS. Endocytosis and lysosomal targeting of epidermal growth factor receptors are mediated by distinct sequences independent of the tyrosine kinase domain. *J Biol Chem* 1995; 270: 4325–33.

[66] Boll W, Rapoport I, Brunner C, Modis Y, Prehn S, Kirchhausen T. The mu2 Subunit of the Clathrin Adaptor AP-2 Binds to FDNPVY and YppO Sorting Signals at Distinct Sites. *Traffic* 2002; 3: 590–600.

[67] Lai A, Sisodia SS, Trowbridge IS. Characterization of sorting signals in the ??-amyloid precursor protein cytoplasmic domain. *Journal of Biological Chemistry* 1995; 270: 3565–3573.

[68] Stricher F, Macri C, Ruff M, Muller S. HSPA8/HSC70 chaperone protein. *Autophagy* 2013; 9: 1937–1954.

[69] Mumby S, Pang IH, Gilman AG, Sternweis PC. Chromatographic resolution and immunologic identification of the alpha 40 and alpha 41 subunits of guanine nucleotide-binding regulatory proteins from bovine brain. *J Biol Chem* 1988; 263: 2020–6.

[70] Rothman S. How is the balance between protein synthesis and degradation achieved? *Theor Biol Med Model* 2010; 7: 25.

[71] Copenhaver PF, Kögel D. Role of APP Interactions with Heterotrimeric G Proteins: Physiological Functions and Pathological Consequences. *Front Mol Neurosci* 2017; 10: 3.

[72] Van Dyke RW. Heterotrimeric G protein subunits are located on rat liver endosomes. *BMC Physiol* 2004; 4: 1.

[73] Chandrasekaran P, Buckley M, Moore V, Wang LQ, Kehrl JH, Venkatesan S. HIV-1 Nef impairs heterotrimeric G-protein signaling by targeting Gα(i2) for degradation through ubiquitination. *J Biol Chem* 2012; 287: 41481–98.

[74] Pratt JM, Petty J, Riba-Garcia I, Robertson DHL, Gaskell SJ, Oliver SG, Beynon RJ. Dynamics of Protein Turnover, a Missing Dimension in Proteomics. *Mol Cell Proteomics* 2002; 1: 579–591.

[75] Kim W, Bennett EJ, Huttlin EL, Guo A, Li J, Possemato A, Sowa ME, Rad R, Rush J, Comb MJ, Harper JW, Gygi SP. Systematic and quantitative assessment of the ubiquitin-modified proteome. *Mol Cell* 2011; 44: 325–40.

[76] Tenbaum S, Arqués O, Chicote I, Tenbaum S, Puig I, G. Palmer H. Standardized Relative Quantification of Immunofluorescence Tissue Staining. *Protoc Exch*. Epub ahead of print 2 April 2012. DOI: 10.1038/protex.2012.008.

[77] Agholme L, Hallbeck M, Benedikz E, Marcusson J, Kågedal K. Amyloid-β secretion, generation, and lysosomal sequestration in response to proteasome inhibition: involvement of autophagy. *J Alzheimers Dis* 2012; 31: 343–58.

[78] Lilienbaum A. Relationship between the proteasomal system and autophagy. *Int J Biochem Mol Biol* 2013; 4: 1–26.

[79] Ciechanover A. Proteolysis: from the lysosome to ubiquitin and the proteasome. *Nat Rev Mol Cell Biol* 2005; 6: 79–87.

[80] Chakrabarti A, Mukhopadhyay D. Novel adaptors of amyloid precursor protein intracellular domain and their functional implications. *Genomics Proteomics Bioinformatics* 2012; 10: 208–16.

[81] Ramírez VT, Ramos-Fernández E, Inestrosa NC. The Gαo Activator Mastoparan-7 Promotes Dendritic Spine Formation in Hippocampal Neurons. *Neural Plast* 2016; 2016: 4258171.

[82] Gakhar-Koppole N, Hundeshagen P, Mandl C, Weyer SW, Allinquant B, Muller U, Ciccolini F. Activity requires soluble amyloid precursor protein alpha to promote neurite outgrowth in neural stem cell-derived neurons via activation of the MAPK pathway. *Eur J Neurosci* 2008; 28: 871–882.

B2.7. Supplementary Material

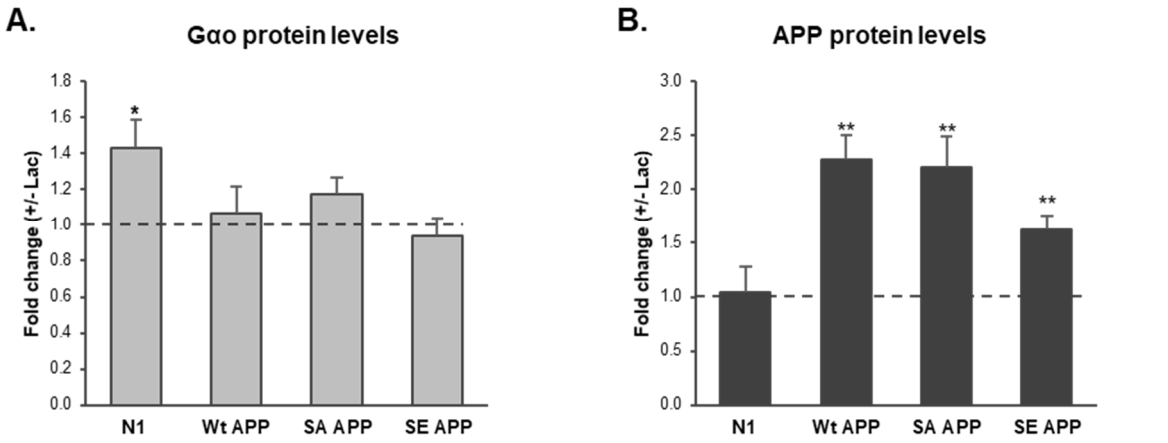

Supplementary Figure B2.1. Effect of proteasome inhibition on PTX treatment. SH-SY5Y cells were transfected with 2 µg of either pEGFP-N1 empty vector, Wt APP-GFP, SA APP-GFP or SE APP-GFP. After 6h of transfection, PTX was added to the cell media to a final concentration of 100 ng/mL, for an additional 18 hours. To test the role of the proteasome on PTX treatment, the proteasome inhibitor Lactacystin (Lac) was added to cells in combination with PTX. The effect of proteasome inhibition on **A.** Gαo and **B.** APP protein levels was evaluated by calculating the ratio between cells treated with PTX+Lac and cells treated just with PTX, and the results are presented as fold changes between both conditions (+/- Lac). The '*' symbol represents statistical significance of cells treated with PTX+Lac relative to PTX alone (dashed line). *, $p<0.05$; **, $p<0.0$

B3. NeuronRead, a semi-automated tool for morphometric analysis of phase contrast and fluorescence neuronal images

Roberto A. Dias[1,2]*, Bruno P. Gonçalves[1,2]*, Joana F. Rocha[1,2], Odete A.B. da Cruz e Silva[2], Augusto M.F. da Silva[3#], Sandra I. Vieira[1,2#]

[1]Cell Differentiation and Regeneration group, Institute of Biomedicine (iBiMED), Department of Medical Sciences, Universidade de Aveiro, Aveiro, Portugal.

[2]Neurosciences and Signalling group, Institute of Biomedicine (iBiMED), Department of Medical Sciences, Universidade de Aveiro, Aveiro, Portugal.

[3]Instituto de Engenharia Electrónica e Telemática (IEETA), Departamento de Electrónica e Telecomunicações (DETI), Universidade de Aveiro, Aveiro, Portugal.

*,# equally contributing authors

Part of this work has been accepted for publication on the journal "Molecular and Cellular Neuroscience"

Acknowledgements

This work was supported Fundação para a Ciência e Tecnologia (Portuguese Ministry of Science and Technology), the COMPETE program, QREN, and the European Union (FEDER): Centre for Cell Biology CBC Pest-OE/SAU/UI0482/2014; Institute for Biomedicine iBiMED UID/BIM/04501/2013; PTDC/SAU-NMC/111980/2009, SFRH/BD/90996/2012, SFRH/BD/78507/2011. We would like to acknowledge Prof. Dr. Pedro Quelhas (INEB, Porto) for his valuable advice on cell body detection; Dr. Sandra Rebelo and Ana Gabriela Henriques (iBiMED, UA), and Dr. Ivan Lalanda and Dr. Carlos Duarte (CNC, Universidade de Coimbra), for helping to establish the neuronal cultures. The authors have no conflict of interest to declare.

B3.1. Abstract

Neurons are specialized cells of the Central Nervous System whose function is intricately related to the neuritic network they develop to transmit information. Morphological evaluation of this network and other neuronal structures is required to establish relationships between neuronal morphology and function, and may allow monitoring physiological and pathophysiologic alterations. Fluorescence-based microphotographs are the most widely used in cellular bioimaging, but phase contrast (PhC) microphotographs are easier to obtain, more affordable, and do not require invasive, complicated and disruptive techniques. Despite the various freeware tools available for fluorescence-based images analysis, few exist that can tackle the more elusive and harder-to-analyze PhC images. To surpass this, an interactive semi-automated image processing workflow was developed to easily extract relevant information (e.g. total neuritic length, average cell body area) from both PhC and fluorescence neuronal images. This workflow, named 'NeuronRead', was developed in the form of an ImageJ macro. Its robustness and adaptability were tested and validated on rat cortical primary neurons under control and differentiation inhibitory conditions. Validation included a comparison to manual determinations and to a golden standard freeware tool for fluorescence image analysis. NeuronRead was subsequently applied to PhC images of SH-SY5Y neuroblastoma cells differentiated with retinoic acid and brain-derived neurotrophic factor, which were maintained in normal differentiating conditions, or treated with Pertussis Toxin, a known Gαo/i inhibitor. Data obtained allowed the correlation of morphological alterations occurring during differentiation with changes in Gαo protein levels. It also further validated NeuronRead as a time- and cost-effective useful tool for monitoring differentiation of both primary neurons and neuronal-like cells.

B3.2. Introduction

The highly specialized neuronal morphology is intimately interconnected with its role, and the function of neuronal networks depends on their complex connections at both regional and single cell level [1–3]. Morphometric analyses are thus applied to neuronal images to study correlations between neuronal structure and function. Neuronal morphometric analyses help to assess network distortions associated with neurological disorders and injury, and can assist high throughput screens of neuronal differentiation and regeneration [4–6]. However, neuronal images typically acquired from primary cultures [7] can be difficult to image and analyze. Even when grown in a 2D environment, neurons present significant morphological variations throughout the culture resulting in highly heterogeneous images. Problems as uneven illumination are relatively common and derive from e.g. unevenly distributed neurons, out-of-focus neurites, and the lower height of neuronal cells [8]. Other imaging problems may occur when working with living cells, such as artifacts arising from dead cells and debris. Although still having to deal with some of these noisy features, fluorescence imaging against a dark background has resolved some of the problems and led to a scarcer use of phase contrast (PhC) images. Processing tools freely available for neuronal cultures analysis are thus usually devoted to fluorescence and not PhC microphotographs [8–10]. PhC images are nevertheless easier to obtain, almost cost-free (just requiring a properly equipped imaging equipment), and may be easily used to image live cells, besides fixed ones. This brightfield microscopy technique explores alterations in the cells' refraction index and circumvents the need for staining reagents, being used to improve the contrast of unlabeled and unprocessed biological samples, such as live cells [11]. PhC microscopy is thus a cost-effective solution that can simultaneously assure imaging of entire populations and live cells. This optical contrast technique is widely used in cellular migration and morphology studies [12, 13], including studies in neuronal differentiation [14–16]. It has been used to create solutions in cell biology for cell tracking and automation of cell counting (via deep learning methodologies and newly developed segmentation algorithms) [17, 18].

Nevertheless, and although they are useful, almost no freeware tools dedicated to the automatic or semi-automatic analysis of PhC neuronal images are available. Currently, NeuronGrowth [19] and NEMO [20] were the only tools retrieved by our survey. NeuronGrowth is a program that automatically quantifies the extension and retraction of neurites and filopodia in time-lapse sequences of two-dimensional images. NeuronGrowth was implemented as a free ImageJ plug-in, in Java language, being an independent multi-platform system that contains entire digital image

pre-processing and processing modules [19]. In PhC images this program can be used to track and measure neurites, and in fluorescence images, it can be used to track filopodia. Unfortunately, NeuronGrowth can only be applied to images obtained from time-lapse experiments where the same sample field is imaged through time. NEMO [20] is also designed to handle and process large quantities of data on single neuronal cells as they evolve over time. This freeware is written in MATLAB code, can handle fluorescence and brightfield images of neuronal 2D cultures and organotypic slices, and uses 3-way principal component analysis (PCA) for variables analysis. NEMO performs morphological analysis using local and global variables; local variables are related to the dendritic tree, while global variables are related to the whole cell structure and include features as radial extension, soma area and cone angle [20]. This program is more dedicated to the automated analysis of images in batch, which has the benefit of time but may result in less accurate measures. When used in a semi-automated manner NEMO can be very efficient; the downside it that images must be correctly labeled before analysis and the tool is relatively complex.

The work here described addresses the need for a simple and straightforward tool that could work in the widely-used ImageJ platform, which could handle not only PhC but also fluorescence images, in a semi-automated manner in order to minimize error in cell segmentation and improve accuracy in morphological features' extraction. We have therefore developed NeuronRead, an ImageJ macro that is capable of analyzing both types of images. PhC/fluorescence pair images of primary neurons at 4 days in vitro (DIV) were used to validate NeuronRead by comparison to manual determinations and to a recognized golden standard for neuronal images, NeuriteQuant [21]. NeuronRead was subsequently applied to a scientific question in order to assess its applicability. SH-SY5Y neuroblastoma cells were differentiated with a combination of retinoic acid (RA) and brain-derived neurotrophic factor (BDNF) [22], and the morphological changes occurring during differentiation were evaluated with NeuronRead. Moreover, changes in morphology were correlated with alteration in the protein levels of two neuronal markers, GAP-43 and βIII-tubulin [23], and of two proteins highly associated with neurite outgrowth, Gαo and APP [24, 25]. Cells were further treated with Pertussis Toxin (PTX), a known inhibitor of Gαo/i proteins, and its effect on SH-SY5Y differentiation was also assessed with NeuronRead. This experiment further demonstrated the usefulness and reliability of NeuronRead in the analysis of the differentiation of both primary neuronal cultures and neuronal-like cells, such as SH-SY5Y neuroblastoma cells.

B3.3. Materials and Methods

B3.3.1. Antibodies

Primary antibodies used in Western Blot (WB) and Immunocytochemistry (ICC) assays: mouse 22C11 monoclonal anti-APP N-terminus (Chemicon; WB-1:250); rabbit anti-Gαo/GNAO1 polyclonal (Thermo; WB-1:2000; ICC-1:200); rabbit anti-βIII-tubulin (abcam; WB- 1:10000; ICC-1:250), rabbit anti-GAP-43 (Millipore; WB-1:1000). Secondary antibodies used: horseradish peroxidase-labeled goat antibodies (GE Healthcare) for enhanced chemiluminescence (ECL) detection; Alexa Fluor 594-conjugated goat antibody (Molecular Probes) for ICC analysis. Antibodies were prepared in 3% BSA in phosphate buffer saline (PBS) for ICC, and in either 3-5% milk or BSA for WB, per the manufacturers' instructions.

B3.3.2. Rat cortical neuronal and SH-SY5Y neuroblastoma cell cultures

Rat cortical primary neurons were established by dissociation of E18 embryonic cortices, as described in [26]. Briefly, upon euthanize the mothers, the embryo cortices were dissociated for 5–10 min/37°C with 0.23 mg/mL trypsin/0.15 mg/mL deoxyribonuclease I-supplemented Hank's balanced salt solution. Dissociated cells were plated at $1.0x10^5$ cells/cm2 onto poly-D-lysine-coated dishes in B27/0.5 mM glutamine/60 μg/mL gentamicin-supplemented Neurobasal medium (GIBCO, Invitrogen), and maintained at 5% CO_2/37ºC for 4 days before being imaged. A minimum number of pregnant female Wistar rats (9-12 weeks; Harlan Interfaune Ibérica, SL) was used, and all steps were taken to ameliorate animal suffering. All experimental procedures complied the ARRIVE guidelines, observed the European legislation for animal experimentation (EU Directive 2010/63/EU) and were approved and supervised by our Institutional Animal Care and Use Committee: Comissão Responsável pela Experimentação e Bem-Estar Animal, CREBEA).

Primary neuronal cultures were treated for 18h (from 3 to 4 DIV) with 10 μM of PD168393 (Sigma-Aldrich), a drug inhibitor of the known neuritic promotor epidermal growth factor receptor (EGFR) [27, 28]. After treatment, neurons were fixed with 4% paraformaldehyde (PFA) in PBS for ICC.

Human neuroblastoma SH-SY5Y cells (ATCC CRL-2266) were grown in Minimal Essential Medium supplemented with F-12, 10% FBS, 0.5 mM L-glutamine, 100 U/ml penicillin and 100 mg/ml streptomycin (Gibco, Invitrogen) at 37°C/5% CO_2.

SH-SY5Y cells were differentiated using a protocol adapted from Encinas et al, 2000 [22]. Briefly, cells were seeded at an initial density of $1x10^5$ cells per 35mm plate. After 24h (day 0), retinoic acid (RA, Sigma-Aldrich) was added to the cells to a final concentration of 10 μM. Cells were maintained

in RA for 5 days, after which RA was removed and brain-derived neurotrophic factor (BDNF) was added in serum-free medium, to a final concentration of 10 ng/mL. Cells were then maintained for further 7 days (to day 12); medium was changed every 2-3 days. Differentiating cells were also treated with 100 ng/mL Pertussis Toxin (PTX) from either day 0 or day 5 of differentiation to day 12. Undifferentiated cells were maintained as control throughout the 12 days. Cells were collected at day 3, 5, 6, 9 and 12 with 1% SDS.

B3.3.3. Immunocytochemistry and Image acquisition

Fixed rat 4 DIV cortical neurons were permeabilized with 0.2% Triton/in PBS, washed with PBS, and blocked with 3% BSA/in PBS for 1h. Neurons were incubated for 2h with a primary antibody (1:200) against Gαo, a protein highly abundant in the inner side of the neuronal plasma membrane [29], allowing for the visualization of the complete neuronal network. Following washing with PBS, cells were incubated with an anti-rabbit secondary antibody for 1h, washed with PBS and deionised water, and mounted onto glass slides using a Vectashield mounting medium (Vector Labs).
Digitized images (n = 30 images) of fixed cortical primary neurons at 4 DIV were acquired by PhC illumination using a LCPlanFl20x/0.40 objective in an Olympus IX-81 widefield epifluorescence inverted microscope equipped with a 12 bit CCD monochromatic 1376 x 1032 pixel digital camera, binning 1x (F-view II, Soft Imaging System) [12, 13, 15]. Paired fluorescence images of the same areas, labeled with an anti-Gαo antibody, were also acquired [filtersets: DAPI (BP 330-385/FT 400/LP 420); GFP/FITC (BP 450-480/FT 500/LP 515); TexasRed/TRICT (BP 510-550/FT 570/LP 590); exposure time for Gαo: around 100-200 ms]. Live differentiated SH-SY5Y neuroblastoma cells were also imaged under the Olympus IX microscope using PhC techniques, at 3, 5, 6, 9 and 12 days of differentiation. Image acquisition was performed in the LiM facility of iBiMED, a node of PPBI (Portuguese Platform of BioImaging).

B3.3.4. SDS-PAGE and Western Blot

Mass-normalized (BCA protein assay; Pierce) cell aliquots were subjected to SDS-PAGE and WB. Ponceau-S staining of the transferred proteins was used as loading control, as an alternative to actin or tubulin, since these proteins vary with our experimental conditions [15, 30]. For this, nitrocellulose membranes were immersed in Ponceau-S solution (Sigma-Aldrich; 0.1 % [w/v] in 5% acetic acid), further washed with distilled water, and scanned (GS-800 calibrated densitometer, Bio-Rad). Following their wash with TBS-T, membranes were subject to WB analysis. Briefly, membranes were blocked with 5% milk or BSA in TBS-T, incubated with primary antibodies (2h or overnight),

and with horseradish peroxidase-linked secondary antibodies (2h), and subject to ECL detection using the ChemiDoc™ Imaging System (Bio-Rad).

B3.3.5. The NeuronRead algorithmic workflow

NeuronRead is a macro script designed to use image processing techniques and to run within the ImageJ environment, which supports semi-automated quantitative analysis of bioimages [31, 32]. A tutorial explaining how to install the macro can be found as a supplementary data at the end of this chapter. Also, the NeuronRead macro can be downloaded from http://www.sciencedirect.com/science/article/pii/S1044743117300866. It was developed focusing on PhC images but can also process fluorescence images. The processing workflow and the major settings are described below (Figures B3.1 and B3.2). The whole computational procedure integrates image enhancement, segmentation and feature extraction steps that provide robust quantitative descriptors of the neuronal images. The algorithm first deals with cell body segmentation, which subsequently drives the neuritic network recognition steps. The algorithm implementation relies both on native ImageJ functionalities and on companion plugins such as MorphoLibJ v1.2.0 [33], Skeletonize3D and AnalyzeSkeleton [34]. A great majority of the operations are automated, and the interactive steps are clearly indicated.

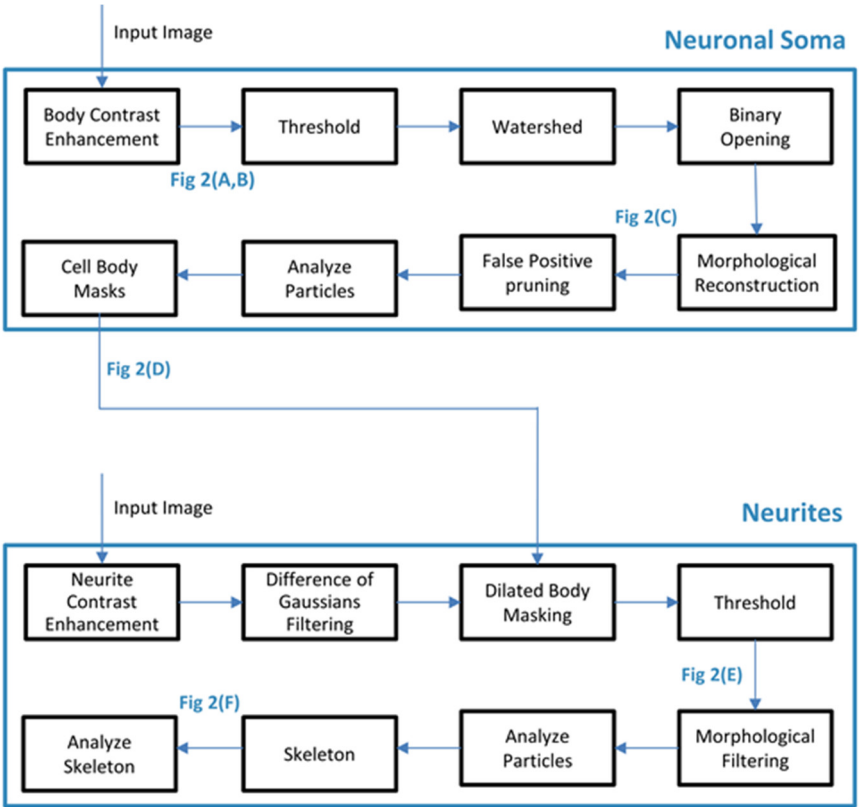

Figure B3.1. Processing workflow of the NeuronRead macro. Schematic flowchart detailing each step of the NeuronRead Macro taken during neuronal soma segmentation (upper part) and neurite segmentation (lower part).

1. Cell body segmentation. Generally, PhC (and Fluorescence) raw images are not compatible with straightforward automated image analysis approaches, impairing the estimation of reliable quantitative features. Our cell-body segmentation strategy assumes that cell bodies and neuritic structures may be considered as tiny objects of interest within a large background comprising mid-range gray level values that clearly dominate the global or regional intensity-based statistics. Noise, intrinsic artifacts and the need to handle rather thin objects were the immediate driving factors determining the chain of pre-segmentation steps that provide thresholding "friendly" images as shown in Figure B3.2B from the input raw images shown in Figure B3.2A.

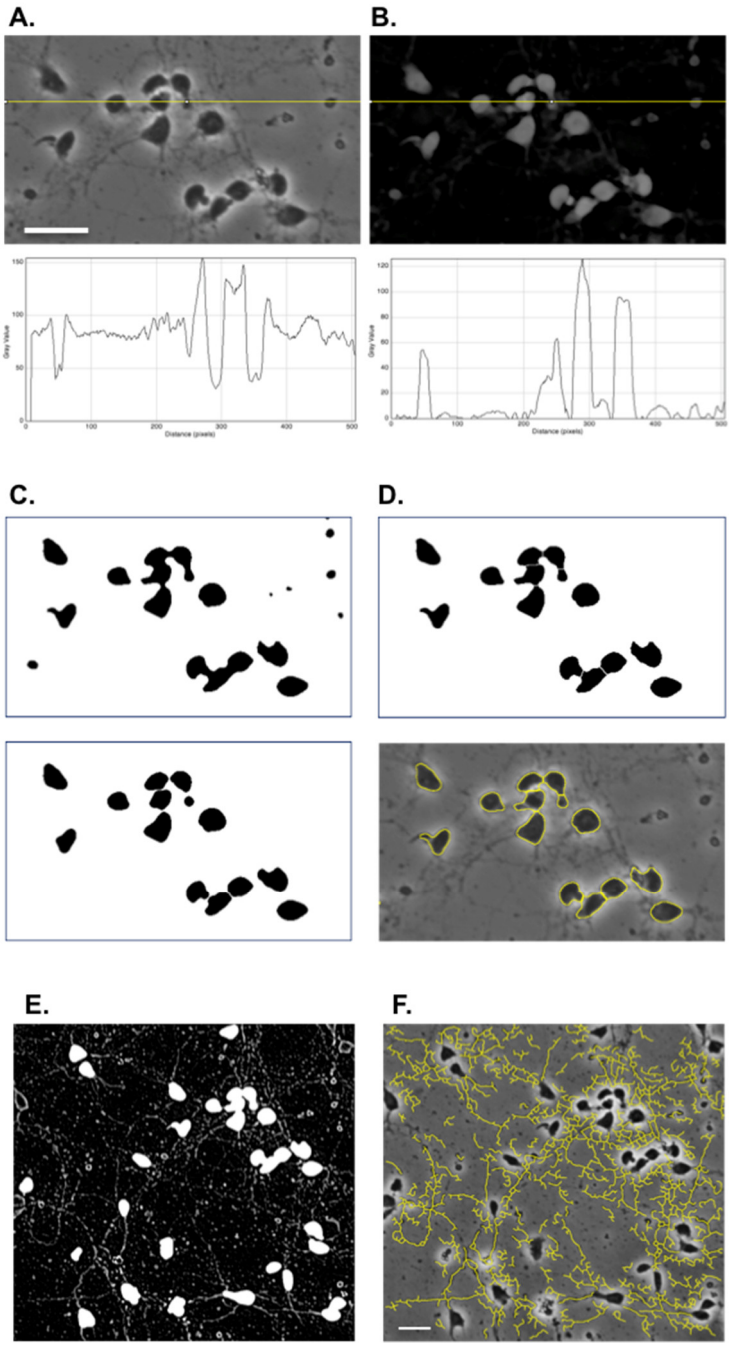

Figure B3. 2. Details of the NeuronRead workflow, applied to Phase Contrast Images. A-D: Cell body segmentation. A. Raw PhC neuronal image. Mid-range values of background gray levels clearly dominate (yellow line), as suggested by the example intensity profile shown below. **B.** Resulting image after grey-level 'bottom-hat' filtering. As shown in the intensity profile, the background is almost removed. Only objects with shape and size fitting the structuring element (SE) stand out more clearly (yellow line). **C.** Automatic threshold (upper image) and subsequent morphological opening (image below). **D.** The original shape of cell bodies, as recovered after morphological reconstruction (upper image). Final result with refinements obtained with watershed segmentation (image below). **E-F: Neuritic segmentation. E.** The difference of Gaussians image masked with cell body areas. **F.** Skeletonized neuritic pathways superimposed on the original image. Structures attached to the image boundaries are not measured. Scale bar = 50 µm.

The main idea is to make our target objects stand out relative to the background and other objects whose shape and size do not qualify them as cell bodies. Given the very nature of neuronal images, our choice to obtain an appropriate tradeoff between noise and contrast enhancement relied upon grey-scale morphological operators [35, 36]. Mathematical morphology provides the conceptual basis for these operators. The basic idea is to express formally how well a small probing object fits the appearance of the target objects. The probing object, normally called the structuring element (SE), may assume any shape but often regular shapes such as disks, squares or lines are used.

Binary erosion and dilation operators that are straightforwardly perceived using set-theoretic definitions are the fundamental building blocks of more complex morphological operations recurrently applied in this work. Most of the binary morphological operators are fully extensible to grey-level image analysis tasks. Erosion and dilation operators applied to grey-scale images can be looked at as regional minimum and maximum filters, respectively, considering the regions restricted by the chosen SE. The opening operator is defined as an erosion followed by a dilation, and the closing operator is defined as a dilation followed by an erosion. For a thorough overview of mathematical morphology techniques and their applications in image analysis please refer to [35, 36].

Our approach to obtain contrast enhanced images for reliable cell body segmentation, consisted of a bottom-hat operation preceded by median filtering. This preliminary step removes the effect of the corpuscular spots. The bottom-hat operation (or 'black top-hat') is formally defined as the difference image of the closed and original versions of the image. Since the closing operation emphasizes the darker valleys, most of them matching our target cell bodies, the result of the bottom-hat clearly promotes the conspicuousness of the cell bodies. This filtering approach practically removes the background clutter and leaves out, for further processing, only the cell body candidate regions. For the sake of visibility Figure B3.2B shows the complement of the bottom-hat image. Notice that the neuritic networks are almost faded and the effect of the white halo surrounding the cell bodies is practically negligible. The image is now ready for proper cell body segmentation. The size and shape of the SE are critical parameters for successful segmentation. Given the acquisition setup, heuristic arguments suggest that the best performance is achieved with disk-shaped SE with a radius of 5 to 10 pixels.

Cell body segmentation consists of thresholding the bottom-hat filtered image and its subsequent binary morphological filtering. Most of the time, the automatically computed threshold level is acceptable. However, the user can optimize the results with minimal manual adjustments. The binary images still undergo morphological opening to remove the tiny regions whose size prevents

them to be considered as live cell bodies. The opening filters with the above-mentioned SE's impose considerable damage to the original body shapes (Figure B3.2C). In this phase, border objects that are only partially visible are also removed. A morphological reconstruction is then used to recover the original body shapes, as shown in Figure B3.2D (upper). An extra refinement in cell body delineation is provided by watershed techniques [37] that often succeed in separating visually overlapped cell bodies. The binary processing phase in body segmentation concludes as shown in Figure B3.2D (lower).

The user may still mark for removal the few miss-segmented cell body components, or add any cell body that was left unrecognized by the macro, by visual inspecting the superposition of the candidate masks to the raw grey-scale image. The end result of this process is a body cell mask image that is ready to be labeled and measured using native ImageJ functionalities. Each cell body (binary object) in each image will thus be numerically labeled, making it possible to measure its morphological features, such as area or perimeter.

2. Neuritic segmentation. To emphasize the tiny neuritic structures, contrast enhancement and differential filtering were applied. Contrast-limited adaptive histogram equalization (CLAHE) and Difference of Gaussians (DoG) filtering provide a good compromise between structural emphasis and noise impact in the subsequent thresholding phase. DoG parameters were matched to the neurite expected width range. We empirically determined that standard deviations for each Gaussian of 1 and 3-pixels were appropriate choices. As shown in Figure B3.2E, this intermediate image is then automatically masked with a dilated version of the cell bodies' image, making then a band-pass interactive threshold to easily identify the neuritic components. Again, image labeling enabled the identification and removal of disconnected structures with an area smaller than 200 pixels. This threshold was previously experimentally determined, with smaller areas leading to the recognition of image artifacts as neurites.

The last step consisted of user-supervised skeletonizing, branch identification and length estimation, by using the AnalyzeSkeleton plugin. To visually validate the neuritic skeleton composed by the segmented neuritic components, the skeleton was automatically superimposed on the original image as shown, resulting in Figure B3.2F.

The NeuronRead macro was developed on images taken under a 20X/0.4 objective (3.1 pixels/µm scale), but can work on different amplification settings (such as a 10X objective - 1.55 pixels/µm) with little user intervention, showing NeuronRead robustness in dealing with images with different scales. To work with other scales/magnifications, some parameters might require user attention, including 1) the radius of different morphological filters that are applied during the macro; as well

as 2) the areas used during “Analyze Particles” to remove unwanted objects from the image. As a rule, higher magnifications used during image acquisition will require higher values for these parameters, while lower magnifications will require lower values. Further, the macro is easily customizable, and some features such as the SE radius and the image scale are asked and can be altered while the macro is running. Noteworthy, the macro alters the scale at two different time points: 1) at the beginning, it removes any previous scale associated with the image or software, so that it does not impair any of the morphological operations the macro performs; 2) near the end, the macro asks for the image scale (number of pixels per micrometer) and applies it to the image being analyzed, so that every extracted feature comes at the desirable unit, normally µm, instead of pixels.

3. Extracted Morphological Features. The quantitative features of the population become available in the “Log” window at the end of the macro. These include Neuritic Parameters (Total Neuritic Length) and Cell Body Parameters (Cell body count, Average Area, Circularity, Roundness, and Perimeter). Individual shape features are also available under the windows “Cell bodies” and “Branch information”. They can be saved as column based “.txt” files for further analysis in a software of choice. The macro does not retrieve neuritic length per cell, but this is easily obtained by dividing the total neuritic length by the number of cells scored in that image. A tutorial explaining how to install and run the NeuronRead macro can be found as supplementary data, at the end of the chapter.

B3.3.6. Data analysis and Statistics

All data is expressed as mean ± standard error of the mean of at least three independent experiments. For NeuronRead validation, statistical significance analysis was conducted by the Bland-Altman method (comparison between NeuronRead and NeuriteQuant) and by the unpaired Student’s t-test (control versus EGFR-inhibitor cultures). In the differentiation assay, statistical analysis was conducted using the one-sample t-test (Control conditions defined as 1).

All tests were performed on the GraphPad Prism® software. Three levels of significance were used, depending if the p-value was under 0.05, 0.01 or 0.001.

B3.4. Results

B3.4.1. The NeuronRead workflow and Cell Body recognition

The image processing workflow based on the ImageJ environment was applied to PhC and fluorescence neuronal 2D-images, with the intent of extracting quantitative morphological details. This workflow (Figure B3.1 and B3.2), named NeuronRead, was first developed and optimized using PhC images taken at living primary cultured neurons. Images of cultures at various differentiation days (days in vitro, DIV) were used to assure that NeuronRead could efficiently extract information from increasingly complex neuritic networks (*in* Dias and Gonçalves et al., accepted). The developed macro returns several primary parameters, such as cell number; cell body area, perimeter, circularity, roundness, and total neuritic length. Secondary parameters such as 'neuritic length per cell' can be obtained by dividing primary parameters by the number of cells. NeuronRead runs in a semi-automatic manner, requiring user-interaction on 4 occasions: first to input if the image to be analyzed is a PhC or fluorescence image; second, to improve cell body recognition (if necessary); third, to improve neuritic detection; and fourth, to input the scale. If wanted, this last step can be surpassed and the conversion from pixels to micrometers only performed by the user in another software of choice after gathering all information from all the images.

A comparison between the raw NeuronRead output and a manual evaluation of the number of cell bodies showed a percentage difference of 5.8%, and the values obtained were not significantly different (paired t-test analysis). This error mainly arises from the presence of large cell clusters (resulting in false negatives), or from the presence of debris in the live cells preparation (resulting in false positives). However, since the macro allows the user to add cell bodies or remove false positives (2nd user interaction step), this minor error can be easily corrected. At this step NeuronRead also allows the user to alter the automatic threshold set for the cell body, further improving cell body recognition and optimizing the "cell body area" value retrieved with NeuronRead. This parameter is nevertheless greatly optimized, with no significant differences between the macro and manual analysis (Figure B3.3). Naturally, close attention must be paid to threshold values. A low threshold value may increase the number of false positives, while high threshold values can lead to missed cell bodies. The same is particularly true for the neuritic detection threshold. While a lower threshold allows a more sensitive neuritic detection, in preparations with a high amount of debris this can lead to an overestimated neuritic length. Our macro was tested in both fixed and live neuronal cultures that did not have their culture media changed, and was able to deal with both types of cultures.

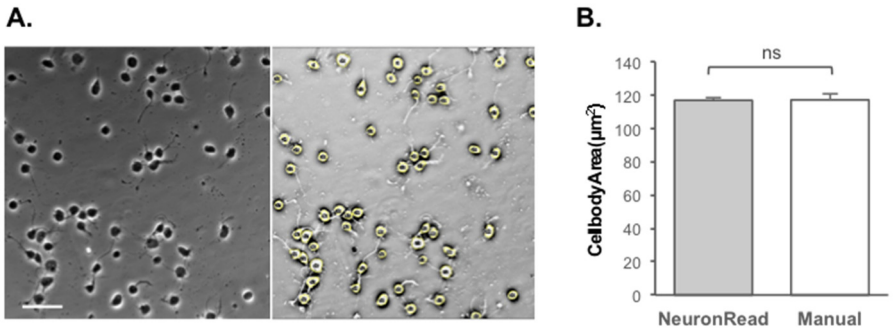

Figure B3.3.NeuronRead versus manual detection of neuronal cell bodies areas. A. Neuronal cell body recognition with NeuronRead in PhC microphotographs of neuronal cultures at 4 days in vitro. Raw data on the left, automatic cell body recognition on the right (halos surrounding cell bodies, in yellow). Scale bar = 50 µm. **B.** Graphical comparison of the average neuronal cell body areas determined by NeuronRead and by manual analysis of the PhC images. There were no statistical differences (ns) between both measurements. n= 10 images, in a total of ca. 300 cell bodies.

B3.4.2. Validation of NeuronRead neuritic segmentation

Our macro is able to extract morphometric data not only from PhC but also from neuronal fluorescence images. Its efficacy was first demonstrated by comparison to an established freeware tool, NeuriteQuant. This golden standard was chosen by its accuracy in neuritic network evaluation of fluorescence images [21]. To validate NeuronRead efficacy, the macro was applied to the same fluorescence images analyzed with NeuriteQuant. These were images of 4 DIV neuronal cultures immunolabeled against Gαo, a highly abundant neuronal protein that clearly stains and delineates the neuritic network [29] (Figure B3.4A upper panel). Results show that NeuronRead is as efficient in analyzing fluorescence images as NeuriteQuant, with 95% of the results having a difference less than 5% (Figure B3.4B, Bland-Altman Plot). NeuronRead also performed as NeuriteQuant in 4 DIV neurons fluorescently immunolabeled against the cytoskeleton marker acetylated beta-tubulin (data not shown). Afterward, using paired neuronal PhC/fluorescence images (Figure B3.4A), the data extracted with NeuronRead from PhC images was compared to the data extracted with NeuriteQuant from paired fluorescence images. The Bland-Altman plot of Figure B3.4C shows that quantitative data extracted from PhC images with NeuronRead was on average 27% lower than the ones obtained from fluorescence with NeuriteQuant.

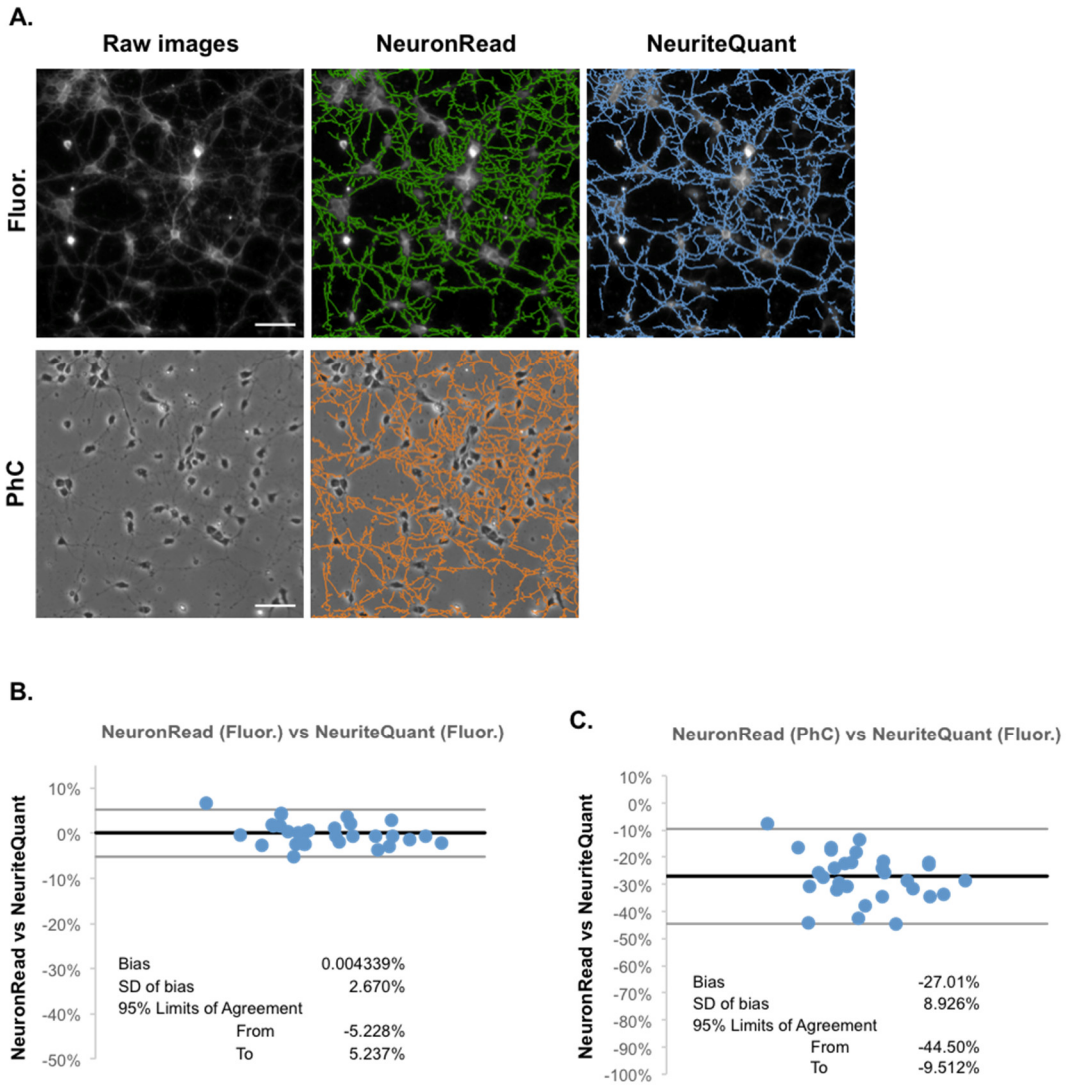

Figure B3.4. NeuronRead validation in PhC and fluorescence neuronal images. A. A set of 30 pairs of fluorescence ('Fluor.')-phase contrast ('PhC') microphotographs of neurons at 4 days in vitro (raw images at the left) were analyzed with the NeuronRead macro (middle images) leading to the neuritic tracing in NeuronRead-Fluor images (in green) and NeuronRead-PhC images (in orange). The fluorescence images were additionally analyzed with the NeuriteQuant plugin, resulting in the NeuriteQuant-Fluor tracing (right image, in blue). Scale bar = 100 µm. **B.** Bland-Altman plot of the comparison between NeuronRead and NeuriteQuant analyses of fluorescence images. The plot shows an average difference between both methods of almost 0%, with 95% of the results differing less than 5%. **C.** Bland-Altman plot of the comparison between phase contrast image analysis with NeuronRead and fluorescence image analysis with NeuriteQuant. The plot shows an average difference between NeuronRead and NeuriteQuant of -27.01%, demonstrating that there is less information available in PhC images than in fluorescence images.

The same was observed when comparing NeuronRead analysis of PhC images with NeuronRead analysis of fluorescence images (Supplementary Figure B3.1). Overlay of the resulting neuritic skeleton onto the original PhC image (Figure B3.4A, lower panel) shows that the macro is running as expected: generally detecting the entire neuritic network present in the image. Together with the previous results on fluorescence images (Figure B3.4B), this indicates that the main reason for the difference in the neuritic length found in fluorescence versus PhC images is the poorer signal-to-noise ratio of raw PhC images, and the higher contrast of the fluorescence ones. These results demonstrate that 1) NeuronRead can be used as a reliable alternative to NeuriteQuant to analyze fluorescence images, while 2) also being able to analyze neuronal PhC images. However, results also highlight the fact that PhC images normally exhibit less detail than fluorescence images regarding the neuritic network and should not be used for 'absolute' determinations. When aiming for absolute values, one should use fluorescence images where the neuronal cytoskeleton or cytosol has been thoroughly labeled to highlight the maximum morphological details, as occurs by immunolabelling the highly abundant Gαo protein, or other neuronal markers such as βIII-tubulin.

We have also tested NeuronRead efficacy in the analysis of neuronal cultures at 12DIV, a time point at which the neuritic network has reached a high density. Comparison of the results obtained with NeuronRead and NeuriteQuant showed a difference of around 1% between both analyses, meaning that NeuronRead is efficient in analyzing both low (4DIV) and high (12DIV) density neuronal cultures (Supplementary Figure B3.2).

NeuronRead robustness and sensitivity were also evaluated by using a similar approach as the one described in [38]. Briefly, by using the ImageJ "Noise" function, two different types of noise (Salt and Pepper, and Gaussian noises) were incrementally added to both PhC and Fluorescence images (Supplementary Figure B3.4). Quantitative analyses of these images showed that NeuronRead's ability to extract cell bodies morphometric data is extremely resistant to noise levels, with no significant changes detected, even when noise was visually noticeable. NeuronRead ability of extracting neuritic data was also resistant to the addition of Salt and Pepper noise to PhC images, while only a high noise level affected its neuritic analysis of fluorescence images (Supplementary Figure B3.3A). Moreover, NeuronRead also effectively extracted neuritic data in the presence of low-to-medium levels of Gaussian noise (Supplementary Figure B3.3B).

The next step was to evaluate if neuronal PhC images, analyzed with NeuronRead, could be used to detect relative alterations in the neuritic network. For that, we tested if the macro could accurately quantify alterations in the neuritic network in PhC images of neurons exposed to an inhibitor of the

epidermal growth factor receptor (EGFR). EGFR translates signals from the pro-survival and pro-neuritogenic EGF and is involved in neuritic outgrowth [27, 28]. Differentiating neurons that were under 18h of EGFR inhibition should thus yield a decrease in their total neuritic length per cell, when compared to control conditions (Figure B3.5A). The analysis of neuronal PhC images using NeuronRead showed a significant reduction of 13.0% in neuritic length per cell when compared to control neurons, virtually identical to the difference obtained when analyzing fluorescence images (13.2%) (Figure B3.5B). These results thus show that both types of images can be analyzed and used to evaluate differences in neuritic length between experimental conditions.

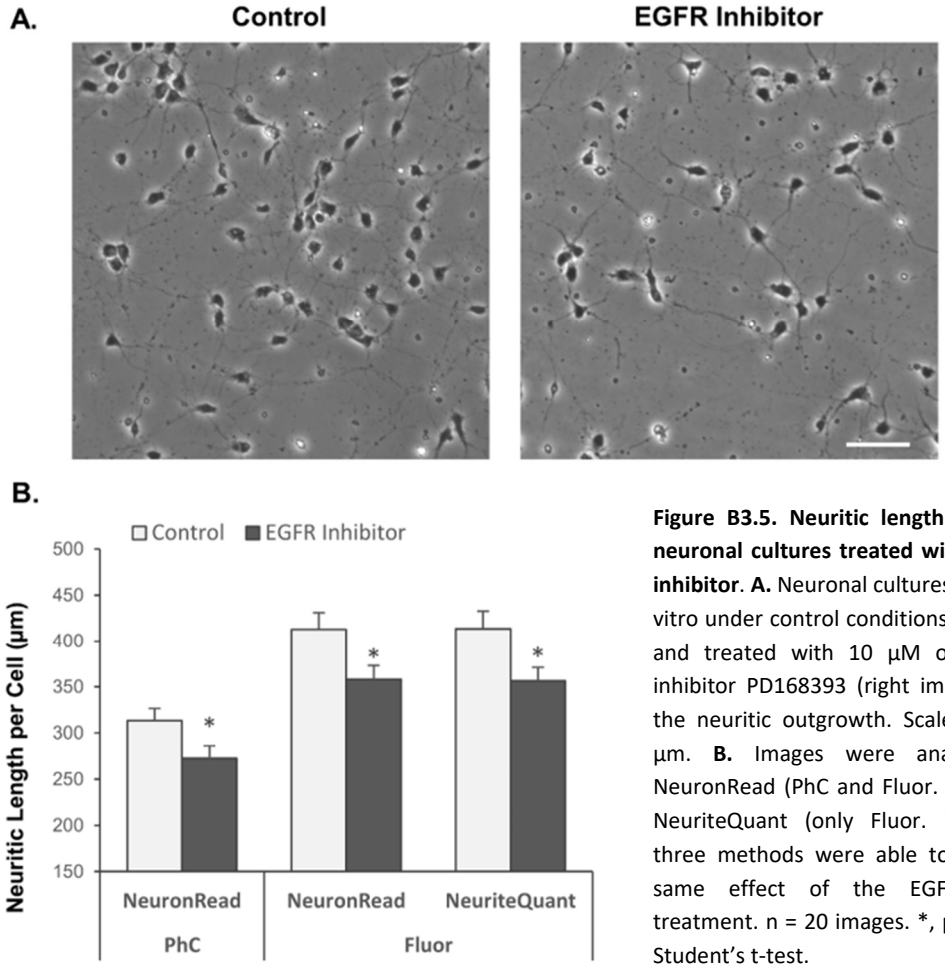

Figure B3.5. Neuritic length analysis of neuronal cultures treated with the EGFR inhibitor. **A.** Neuronal cultures at 4 days in vitro under control conditions (left image) and treated with 10 µM of the EGFR inhibitor PD168393 (right image) to stall the neuritic outgrowth. Scale bar = 100 µm. **B.** Images were analyzed with NeuronRead (PhC and Fluor. images) and NeuriteQuant (only Fluor. images). All three methods were able to detect the same effect of the EGFR inhibitor treatment. n = 20 images. *, $p<0.05$ using Student's t-test.

Regarding some of the performance characteristics of both methods, in a standard PC (eg. Intel® Core™ i5-5200 Dual Core 2.2 GHz, 8GB RAM, 500GB Hard Drive and Intel® HD Graphics 5500) NeuriteQuant took considerably more time analyzing each image (1-2 minutes with NeuronRead vs 8-10 minutes with NeuriteQuant). Another advantage in using NeuronRead was its accurate detection of cell bodies in PhC images, which we did not find as reliable when using NeuriteQuant.

The type of images analyzed also contributes for this difference, most probably due to how the fluorescent probe used stains the cellular body. Indeed, NeuronRead applied to fluorescence images also lost some accuracy in automated detecting the cell bodies, although this was easily corrected manually. Also, while both software programs require some user intervention, NeuronRead allows this while the macro is running, whereas NeuriteQuant requires a more laborious set up before the plugin starts the analysis [39]. NeuronRead is thus highly versatile and robust, and can be applied to neuronal PhC and fluorescence images, and also to PhC images of neuronal-like cell models, such as differentiated SH-SY5Y neuroblastoma cells (Supplementary Figure B3.4).

B3.4.3. Monitoring SH-SY5Y differentiation upon modulation of Gαo activity

As previously described, NeuronRead was successful in analyzing images of both neuronal and neuronal-like cells. NeuronRead was thus used as a tool to monitor neuritogenesis in SH-SY5Y cells, in a study aiming to evaluate Gαo protein levels during BDNF-induced neuronal differentiation, and to assess the effect of modulating Gαo activity during this period.

SH-SY5Y cells were differentiated using a protocol adapted from Encinas et al, 2000 [22]. This protocol uses a sequential treatment of 10 µM RA for 5 days, followed by 10 ng/mL BDNF for additional 7 days (total of 12 days of differentiation), to obtain a culture of fully differentiated cells expressing several neuronal markers, such as GAP-43 and MAP2. Cells differentiated with this protocol were live-imaged at 3, 5, 6, 9 and 12 days ("D3, D5, D6, D9, and D12"), and the images were analyzed with NeuronRead (Figure B3.6A-B). As expected, results show an increase in neuritic length per cell with time when compared to undifferentiated cells. Interestingly, while an increase in neuritic length was already detected at day 3, it only became significantly different after adding BDNF to the medium (51±8 µm at D6-Diff vs 11±2 µm at D6-Ctrl, p-value<0.05). From D6 to D9 there was a burst in neuritic outgrowth (51±8 µm to 94±19 µm at D9-Diff), which then stabilized in the last 3 days of differentiation (94±19 µm to 100±18 µm at D12-Diff). We also checked the expression of two differentiation markers, βIII-tubulin and GAP-43, by western blot (Figure B3.6C). The levels of each protein in the differentiated condition, at a given day, were compared to its levels in the undifferentiated condition at the same day. The differences were plotted with time (Figure B3.6C graphs). This type of analysis excludes possible changes in protein levels that were caused by time-in-culture rather than by the differentiation itself.

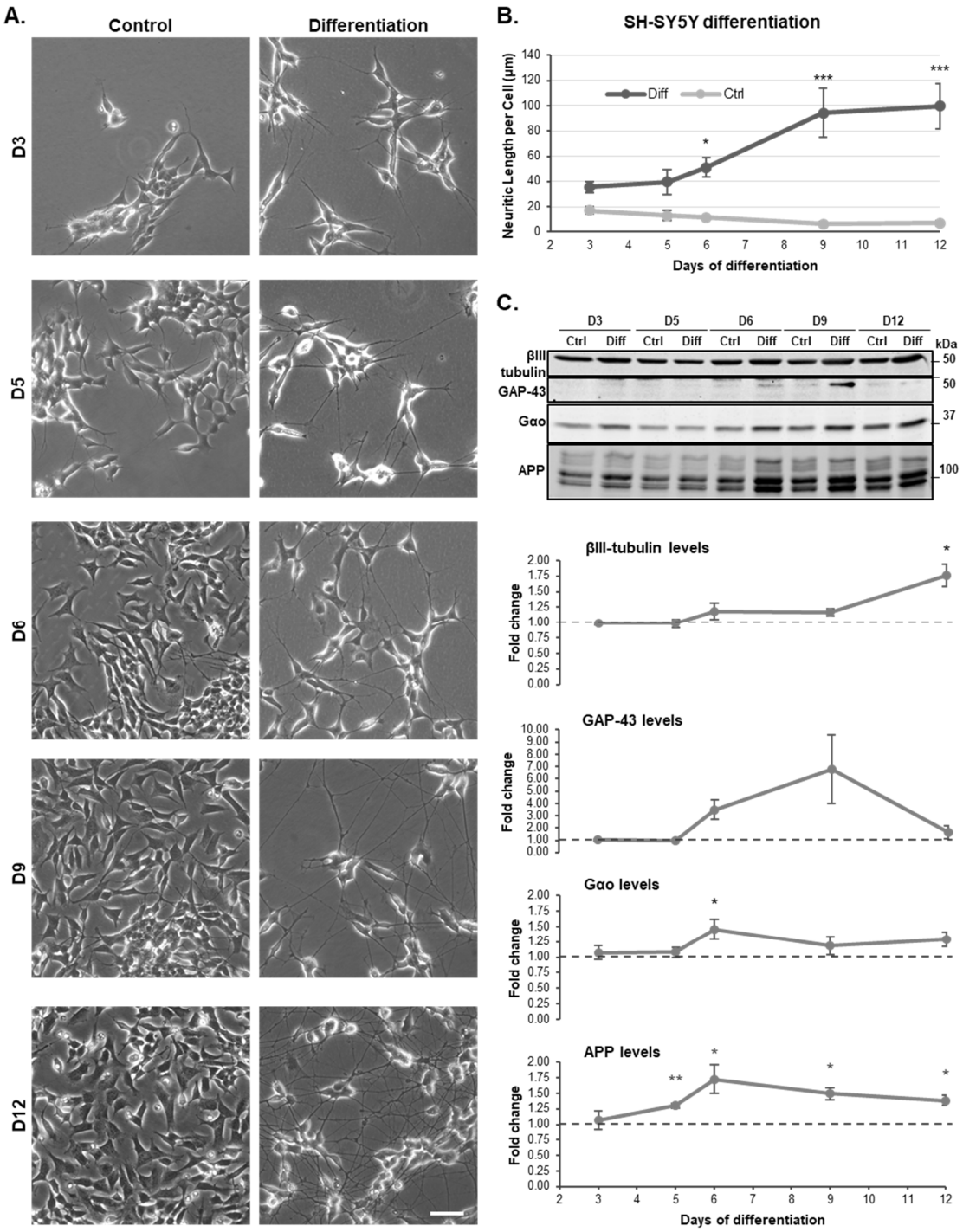

Figure B3.6. Differentiation of SH-SY5Y cells with RA and BDNF. A. Microphotographs acquired of live SH-SY5Y cells at 3, 5, 6, 9 and 12 days in culture, in an undifferentiated state ("Control"), or undergoing the differentiation treatment ("Differentiation"). Differentiation was achieved by treating cells with 10µM RA for 5 days and 10 ng/mL BDNF for additional 7 days. Scale bar: 50 µm **B.** Quantification of the neuritic length per cell during differentiation. Ctrl, undifferentiated cells; Diff, differentiated cells. The neuritic length of each day was compared between Ctrl and Diff with the two-way ANOVA test. **C.** Upper: Immunoblots with the alterations in βIII-tubulin, GAP-43, Gαo, and APP protein levels during differentiation. Of note, all the lanes are from the same blot, but were rearranged to the presented order. Lower: Differences between Diff and Ctrl conditions were plotted with time. At each day, protein levels of the differentiation condition ("Diff") were compared to the ones in control condition ("Ctrl"), and the results presented as fold changes. N=5. The '*' symbol represents statistical significance relative to control (1.0). *, p<0,05; **, p<0,01; ***, p<0,001.

βIII-tubulin is already expressed in undifferentiated SH-SY5Y cells, but its protein levels started to slightly increase when BDNF was added to the culture medium (at D6). A significant increase could be observed at D12 (1.76±0.18-fold change over undifferentiated cells, p-value<0.05). GAP-43 was almost absent from control and RA plus conditions, and increased at 6 and 9 days of differentiation (D6, D9), returning to values close to the control at D12. A similar pattern had been described in the original work by Encinas et al, with GAP-43 levels increasing with the addition of BDNF and then returning to control levels in the subsequent days [22]. The expression of βIII-tubulin and GAP-43, together with the morphological analysis, shows that SH-SY5Y cells were successfully differentiated.

We further evaluated the expression profile of Gαo, a protein highly enriched in neuronal cells that has been strongly associated with neuronal differentiation [24, 40]. In our experimental conditions (Figure B3.6C), we observed that Gαo levels remained close to the control levels during the first 5 days of differentiation (1.07±0.12 at D3 and 1.08±0.08 at D5). However, when BDNF was added to the cells, a significant increase in Gαo levels was detected (1.46±0.16, p-value<0.05). Gαo levels remained high in the subsequent days, but the difference lowered, as undifferentiated control levels slightly increased with time in culture. The protein levels of APP, a known interactor and activator of Gαo [41, 42], and also strongly associated with neuronal differentiation [25, 43] (Chapter B1), were also monitored. The protein levels of APP followed a pattern similar to Gαo, with APP levels (and their difference to control) peaking at D6 of differentiation (1.73±0.24, p-value<0.05), although a significant increase could already be detected at D5 of differentiation (1.30±0.04, p-value<0.01) (Figure B3.6C). APP levels remain higher thereafter, but the difference to the control also decreases, since APP increases with time in culture (Figure B3.6C immunoblot, D9-D12).

Since the peak in Gαo levels at day 6 correlated with a significant increase in neuritic outgrowth, as well as an increase in both GAP-43 and APP, we further evaluated the role of Gαo effect in BDNF-induced SH-SY5Y differentiation by modulating Gαo activity. Cells were exposed to RA for 5 days, after which cells were either allowed to differentiate in the presence of BDNF alone (Figure B3.7A - “Differentiation”), or treated with both BDNF and Pertussis toxin (PTX), a known inhibitor of Gαo and Gαi proteins (Figure B3.7A – “Differentiation + PTX”).

Evaluation of neuritic length showed that from D6 to D9, neuritic growth was roughly the same in untreated cells (“Diff”) and cells treated with PTX (“Diff+PTX”) (Figure B3. 7B). At day 12, cells treated with PTX presented a higher neuritic length than untreated cells, although this difference was not significant (136±18 µm in Diff+PTX vs 107±23µm in Diff). PTX treatment also affected the

protein levels of neuronal markers, βIII-tubulin and GAP-43. βIII-tubulin levels remained lower in cells treated with PTX for the entire duration of the treatment (0.71, 0.78, and 0.80 at D6, D9, and D12, respectively), when compared to the control differentiating cells. Alternatively, GAP-43 protein levels increased with PTX treatment, especially at D6 and D12.

Analysis of Gαo itself also showed a reduction in its protein levels with PTX treatment, at all time points. Further, inhibition of Gαo via ADP-ribosylation by PTX can be visually confirmed, as the Gαo protein migrates slowly through the SDS-PAGE gel (asterisk in Figure B3.7C immunoblot). A PTX-induced reduction in Gαo levels, and the migration shifts, have already been described during differentiation of LA-N-5 neuroblastoma cells [44]. Finally, APP protein levels were only affected by PTX at D12 of differentiation, showing an increase in comparison to untreated cells.

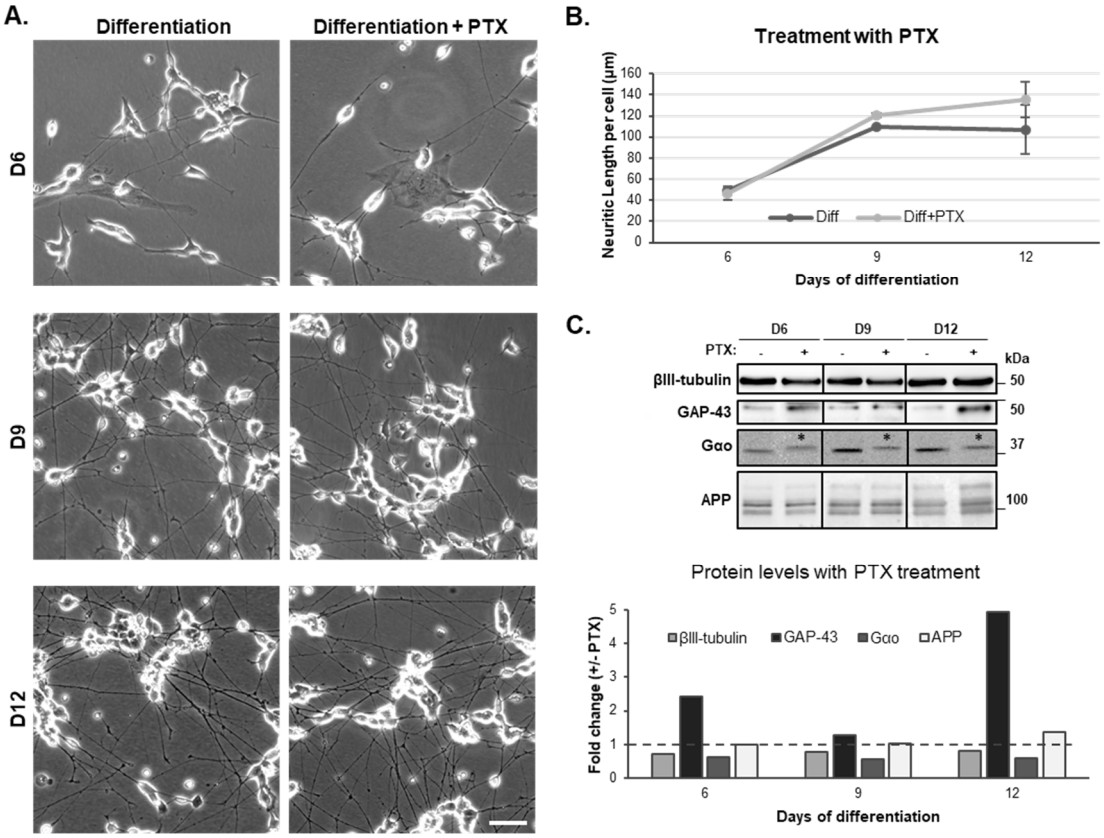

Figure B3.7. Treatment of differentiating SH-SY5Y cells with Pertussis Toxin (PTX). A. Microphotographs acquired of live SH-SY5Y cells at 6, 9 and 12 days of differentiation, with or without PTX treatment. Differentiation was achieved by treating cells with 10 µM RA for 5 days and 10 ng/mL BDNF for additional 7 days. PTX was added at 5 days of differentiation, at a concentration of 100 ng/mL, and it was maintained until the end of the differentiation. Scale bar: 50 µm **B.** Quantification of the neuritic length per cell during differentiation, with or without PTX treatment. Diff, differentiated cells without PTX treatment; Diff+PTX, differentiated cells with PTX treatment. No statistical differences were found between conditions. **C.** Immunoblots of βIII-tubulin, GAP-43, Gαo, and APP protein levels during differentiation in the presence of PTX. At each day, protein levels of cells treated with PTX were compared to the untreated differentiating cells; results were graphically presented as fold changes (+PTX/- PTX). Of note, all the lanes are from the same blot, but were rearranged into the presented order. ADP-ribosylation by PTX results in a slower migration of the Gαo protein through the SDS-PAGE gel (***** in the immunoblot). N=2.

B3.5. Discussion

Quantitative analyses of neuronal morphologic characteristics are widely used to study correlations between morphology and function for various applications, including therapeutic drug development for neuroregeneration [6]. Neuronal features more relevant for quantitative assessment include cell body area and roundness, and neuritic-related parameters such as neuritic length and branching [4, 5, 45]. Although fluorescence microphotographs are nowadays more widely used in cellular imaging, partially due to the high number of freeware tools dedicated to them, PhC images are easier to obtain and more affordable. For example, these PhC images of neuronal cultures can provide valuable and easy-to-obtain morphological data regarding alterations induced by drugs to neuronal cells and their network. Since PhC images are potentially inexpensive in terms of imaging reagents (antibodies or dyes), sample preparation or staining, they are less time-consuming. Another advantage of this technique is its non-invasiveness so that neurons can be imaged alive. As downsize, these images have intrinsic lower contrast, resulting in less absolute information and in a higher difficulty in their analysis. Technical difficulties of PhC images include the low contrast between objects and background (low signal-to-noise ratio), uneven illumination resulting from shining light on 2D-objects, vignetting (darkening of the image corners), and shade-off and halo patterns characteristic of the PhC optical system [11]. However, these last two are considered minor obstacles, and the halo effect can emphasize contrast differences in the less contrasting negative PhC images.

Despite these issues and the potential of PhC images, there are few freeware tools capable of analyzing PhC neuronal images in an automatic or semi-automatic manner [7]. Our search for freeware tools for automatic or semi-automatic analysis of PhC neuronal images only retrieved NeuronGrowth [19] and NEMO [20]. NeuronGrowth cannot be applied to images as the ones herein presented since these were not obtained from time-lapse experiments; it would thus be necessary to mark all the neurites manually if this program was to be used. NEMO [20] performs various morphological analyses and, although very efficient, it is more dedicated to the automated analysis of single cells in images in batch, as time-lapse images, and is more time consuming (e.g. the images need to be correctly labeled before analysis).

In our institute, we perform multiple analyses of neuronal differentiation and regeneration processes in 2D-cultures. This requires a customized image processing workflow that can handle very specific imaging contexts and is able to tackle the processing problems of both types of neuronal images. A sequence of processes and analyzing steps using the ImageJ platform was thus

established and optimized, and termed 'NeuronRead'. The workflow developed is able to quantify parameters such as the cell number, cell body area, and total neuritic length, in a semi-automatic manner. It requires little user-interaction, in order to supervise cell body identification and to reduce noise before neuritic detection. Further, similar to NeuronGrowth and NEMO, NeuronRead can be applied to both PhC and fluorescence images. Validation of our macro was based on various comparative experiments. The robustness of NeuronRead in detecting cell somas and correctly extracting their area was tested by comparison with manual determinations. Indeed, the average cell body areas of 4 DIV neurons retrieved by NeuronRead were not significantly different to our manual evaluation performed with the help of ImageJ tools (Figure B3.3). The macro's ability to extract and quantify the neuritic network in PhC and fluorescence images was compared to the widely used tool NeuriteQuant, applied to fluorescent images (Figure B3.4 and Figure B3.5). There was no statistical significance between the results obtained with both methods (NeuronRead and NeuriteQuant) when these were applied to fluorescence images, either in basal conditions or in conditions of neuritic growth inhibition (Figure B3.4 and Figure B3.5). The macro could also accurately detect the neuritic network of PhC images, but the absolute values taken from PhC images were always below the ones obtained using the paired fluorescence ones (around 25% lower). This results from the fact that PhC images possess a poorly differentiated background where thick and thin, bright and dim neurites coexist, while good fluorescent probes can increase the signal-to-noise ratio and enhance smaller or thinner structures that are almost invisible in PhC images. Nevertheless, although PhC images render less absolute neuritic information, they are very useful to compare experimental conditions, and can be used to accurately detect alterations imposed to the neuritic network by variables external or internal to the culture.

In line with this idea, NeuronRead was successfully applied to track morphological changes occurring during the differentiation of SH-SY5Y neuroblastoma cells (Figure B3.6). As demonstrated in previous work by Encinas et al [22], the treatment of SH-SY5Y cells with RA followed by treatment with BDNF resulted in cells presenting a morphological appearance close to mature neurons (Figure B3.6A-B). Moreover, this was accompanied by the increased expression of two neuronal markers, GAP-43 and βIII-tubulin (Figure B3.6C). The expression of these markers confirm this method of differentiating SH-SY5Y cells as a reliable tool to evaluate the role of certain proteins or drugs in neuronal differentiation. Other protocols for the differentiation of SH-SY5Y cells, such as the treatment with only RA, while being able to induce neurite outgrowth in these cells, do not significantly alter the expression of neuronal markers [23]. These biochemical differences between methods could explain why we detected an increase in Gαo levels with BDNF differentiation, while

other works using SH-SY5Y cells only differentiated with RA did not detect any increase [46, 47]. Indeed, Gαo protein levels were observed to augment during rat's brain development [48], and during the *in vitro* differentiation of other cell lines, such as N1E-115 and PC12 cells [49, 50]. It is interesting to observe that Gαo levels increase after the addition of BDNF, and that it correlates with the increase of both GAP-43 and APP expression, two proteins that are known interactors and activators of Gαo. Moreover, APP increased expression during SH-SY5Y differentiation had already been described in multiple settings, either it be differentiation with RA-only or in combination with BDNF [15, 51, 52]. Some of the GAP-43 and APP roles in the brain have been linked to their association with Gαo. GAP-43 and Gαo are highly enriched in neuronal growth cones, and activation of Gαo by GAP-43 has been shown to modulate neurite outgrowth [53, 54]. Regarding APP, although initial work on its interaction with Gαo focused on its relevance for the Alzheimer's Disease [55, 56], APP-Gαo interaction also seems to have a physiological role in the brain, such as in the control of neuronal migration [57, 58] and in the regulation of neuronal differentiation (Chapter B1). The paralleled increase of Gαo with APP and GAP-43 at D6 could indicate a possible interplay between these proteins at this stage of neuronal differentiation, during which a burst of neurite outgrowth is occurring [22].

To our knowledge, no previous association between BDNF action and Gαo has been reported. Our results showing an increase in Gαo levels after the addition of BDNF points to a possible role for Gαo in the mediation of BDNF neuritogenic functions. Indeed, some of the main pathways activated by BDNF during neuronal differentiation are also known to be modulated by Gαo. BDNF-induced neuritogenesis in SH-SY5Y cells is accompanied by an increase in ERK1/2 activation, which if inhibited leads to a significant decrease in neurite outgrowth and GAP-43 expression [59]. Moreover, BDNF-ERK1/2 activation has also been reported in differentiation of neural stem cells [60, 61]. Different studies, including our own research (Chapter B1), have identified a correlation between Gαo-induced neuritogenesis and ERK1/2 activation [62, 63]. To further understand the meaning of the Gαo role in SH-SY5Y differentiation, cells were treated with PTX, a Gαo/i inhibitor, at the same time BDNF was added to the cells (Figure B3.7). This treatment completely inhibited Gαo, confirmed by the slower migration of Gαo through the SDS-PAGE, a consequence of its ADP-ribosylation (Figure B3.7C) [44]. Gαo inhibition did not produce significant effects on the average neuritic length per cell, only slightly increasing it at later time points, but it significantly altered the protein levels of GAP-43 and βIII-tubulin (Figure B3.7). This shows that Gαo might not be essential for some of the morphological alterations occurring during neuronal differentiation, but that it plays a significant role in the biochemical maturation of neuronal cells. It is not clear how inhibiting

Gαo leads to the alterations in GAP-43 and βIII-tubulin. Since GAP-43 is thought to act upstream Gαo, its increased expression could be a cellular feedback response to try to overcome Gαo inhibition. The same could be thought of APP, although its protein levels were not so affected by PTX, only increasing at D12. Increased GAP-43 could also be a sign of deregulation of proper neuronal differentiation and function [64, 65], thus explaining the reduction in βIII-tubulin levels. An evaluation of the phosphorylation status of GAP-43 will be important to help us understand if this increased expression is also accompanied by an increased activation [66]. Further studies could also monitor potential differences in the subcellular distribution of these proteins, as well as look to other neuronal markers, such as MAP2, tau, and PSD95. It is also imperative to check signaling pathways that might be affected by Gαo inhibition, specially the MAPK/ERK signaling. Finally, although this study shows promising results concerning the role of Gαo in BDNF-induced neuronal differentiation, since PTX is not a specific inhibitor of Gαo, it is important to also evaluate the role of Gαi in this process. Specific targeting of Gαo during BDNF treatment, either by its downregulation or overexpression, will improve our understanding of Gαo role on neuronal differentiation.

In conclusion, NeuronRead proved to be a flexible, practical and useful tool in bioimaging analysis of PhC and fluorescence microphotographs of primary neurons in neuronal cultures. It does not need manual tracing of the neurites as in other neuronal analysis software programs, it requires minor user-interaction to increase its accuracy in morphological detection, and the errors associated with its automated detection are minor, particularly for comparative analyses. The macro is also easily customizable, with the user being able fit the macro to its needs (e.g. batch processing and analysis). In synthesis, this ImageJ Macro is reliable, fast, easy to apply, and considerably robust in extracting morphometric data from the easier, faster and affordable PhC images, with the plus of also being applicable to the neuritic analysis of fluorescence images. It can thus be easily used in routine operations involving morphometric analyses of neuronal cultures.

B3.6. References

[1] Purves D, Augustine G, Fitzpatrick D, Hall M, LaMantia A, McNamara J, White L. *Neuroscience*. 4th ed. Massachusetts: Sinauer Associates, Inchttp://www.sinauer.com/neuroscience-621.html (2008, accessed 3 May 2016).

[2] Kapitein LC, Hoogenraad CC. Which way to go? Cytoskeletal organization and polarized transport in neurons. *Mol Cell Neurosci* 2011; 46: 9–20.

[3] Rolls MM, Satoh D, Clyne PJ, Henner AL, Uemura T, Doe CQ. Polarity and intracellular compartmentalization of Drosophila neurons. *Neural Dev* 2007; 2: 7.

[4] Costa L da F, Manoel ETM, Faucereau F, Chelly J, van Pelt J, Ramakers G. A shape analysis framework for neuromorphometry. *Network* 2002; 13: 283–310.

[5] Ho S-Y, Chao C-Y, Huang H-L, Chiu T-W, Charoenkwan P, Hwang E. NeurphologyJ: an automatic neuronal morphology quantification method and its application in pharmacological discovery. *BMC Bioinformatics* 2011; 12: 230.

[6] Mitchell PJ, Hanson JC, Quets-Nguyen AT, Bergeron M, Smith RC. A quantitative method for analysis of in vitro neurite outgrowth. *J Neurosci Methods* 2007; 164: 350–62.

[7] Carter M, Shieh JC. *Guide to Research Techniques in Neuroscience*. Elsevier. Epub ahead of print 2010. DOI: 10.1016/B978-0-12-374849-2.00017-3.

[8] Xiong G, Zhou X, Degterev A, Ji L, Wong STC. Automated neurite labeling and analysis in fluorescence microscopy images. *Cytometry A* 2006; 69: 494–505.

[9] Ascoli GA. Neuroinformatics grand challenges. *Neuroinformatics* 2008; 6: 1–3.

[10] Meijering E. Neuron tracing in perspective. *Cytometry A* 2010; 77: 693–704.

[11] Shaked N, Zalevsky Z, Satterwhite L. *Biomedical Optical Phase Microscopy and Nanoscopy*https://books.google.pt/books/about/Biomedical_Optical_Phase_Microscopy_and.html?id=qMbrqw7VDLEC&pgis=1 (2012, accessed 13 May 2016).

[12] Serra V, Camões F, Vieira S, Faustino M, Tomé J, Pinto D, Neves M, Tomé A, Silva A, da Cruz e Silva E, Cavaleiro J. Synthesis and Biological Evaluation of Novel Chalcone-Porphyrin Conjugates. *Acta Chim Slov* 2009; 56: 603–611.

[13] Pinho AC, Dias R, Cerqueira AR, da Cruz e Silva OAB, Vieira SI. APP and its secreted fragment sAPP in SH-SY5Y neuronal-like migration. *Microsc Microanal* 2015; 21: 36–37.

[14] Raghavan S, Bitar KN. The influence of extracellular matrix composition on the differentiation of neuronal subtypes in tissue engineered innervated intestinal smooth muscle sheets. *Biomaterials* 2014; 35: 7429–40.

[15] da Rocha JF, da Cruz E Silva OAB, Vieira SI. Analysis of the amyloid precursor protein role in neuritogenesis reveals a biphasic SH-SY5Y neuronal cell differentiation model. *J Neurochem* 2015; 134: 288–301.

[16] Kim H, Kim S, Song Y, Kim W, Ying QL, Jho EH. Dual function of Wnt signaling during neuronal differentiation of mouse embryonic stem cells. *Stem Cells Int* 2015; 2015: 459301.

[17] Chalfoun J, Kociolek M, Dima A, Halter M, Cardone A, Peskin A, Bajcsy P, Brady M. Segmenting time-lapse phase contrast images of adjacent NIH 3T3 cells. *J Microsc* 2013; 249: 41–52.

[18] Wang Y, Zhang Z, Wang H, Bi S. Segmentation of the Clustered Cells with Optimized Boundary Detection in Negative Phase Contrast Images. *PLoS One* 2015; 10: e0130178.

[19] Fanti Z, Martinez-Perez ME, De-Miguel FF. NeuronGrowth, a software for automatic quantification of neurite and filopodial dynamics from time-lapse sequences of digital images. *Dev Neurobiol* 2011; 71: 870–81.

[20] Billeci L, Magliaro C, Pioggia G, Ahluwalia A. NEuronMOrphological analysis tool: open-source software for quantitative morphometrics. *Front Neuroinform* 2013; 7: 2.

[21] Dehmelt L, Poplawski G, Hwang E, Halpain S. NeuriteQuant: an open source toolkit for high content screens of neuronal morphogenesis. *BMC Neurosci* 2011; 12: 100.

[22] Encinas M, Iglesias M, Liu Y, Wang H, Muhaisen A, Ceña V, Gallego C, Comella JX. Sequential treatment of SH-SY5Y cells with retinoic acid and brain-derived neurotrophic factor gives rise to fully differentiated, neurotrophic factor-dependent, human neuron-like cells. *J Neurochem* 2000; 75: 991–1003.

[23] Dwane S, Durack E, Kiely PA. Optimising parameters for the differentiation of SH-SY5Y cells to study cell adhesion and cell migration. *BMC Res Notes* 2013; 6: 366.

[24] Nakata H, Kozasa T. Functional characterization of Galphao signaling through G protein-regulated inducer of neurite outgrowth 1. *Mol Pharmacol* 2005; 67: 695–702.

[25] Hoe HS, Lee KJ, Carney RS, Lee J, Markova A, Lee JY, Howell BW, Hyman BT, Pak DT, Bu G,

Rebeck GW. Interaction of reelin with amyloid precursor protein promotes neurite outgrowth. *J Neurosci* 2009; 29: 7459–7473.

[26] Henriques AG, Vieira SI, Crespo-López ME, Guiomar de Oliveira MA, da Cruz e Silva EF, da Cruz e Silva OAB. Intracellular sAPP retention in response to Abeta is mapped to cytoskeleton-associated structures. *J Neurosci Res* 2009; 87: 1449–61.

[27] Tsai N-P, Tsui Y-C, Pintar JE, Loh HH, Wei L-N. Kappa opioid receptor contributes to EGF-stimulated neurite extension in development. *Proc Natl Acad Sci U S A* 2010; 107: 3216–21.

[28] Evangelopoulos ME, Weis J, Krüttgen A. Mevastatin-induced neurite outgrowth of neuroblastoma cells via activation of EGFR. *J Neurosci Res* 2009; 87: 2138–44.

[29] Brabet P, Dumuis A, Sebben M, Pantaloni C, Bockaert J, Homburger V. Immunocytochemical localization of the guanine nucleotide-binding protein Go in primary cultures of neuronal and glial cells. *J Neurosci* 1988; 8: 701–8.

[30] Romero-Calvo I, Ocon B, Martinez-Moya P, Suarez MD, Zarzuelo A, Martinez-Augustin O, de Medina FS. Reversible Ponceau staining as a loading control alternative to actin in Western blots. *Anal Biochem* 2010; 401: 318–320.

[31] Schneider CA, Rasband WS, Eliceiri KW. NIH Image to ImageJ: 25 years of image analysis. *Nat Methods* 2012; 9: 671–5.

[32] Schindelin J, Arganda-Carreras I, Frise E, Kaynig V, Longair M, Pietzsch T, Preibisch S, Rueden C, Saalfeld S, Schmid B, Tinevez J-Y, White DJ, Hartenstein V, Eliceiri K, Tomancak P, Cardona A. Fiji: an open-source platform for biological-image analysis. *Nat Methods* 2012; 9: 676–82.

[33] Legland D, Arganda-Carreras I, Schindelin J. MorphoLibJ: MorphoLibJ v1.2.0. Epub ahead of print 2016. DOI: 10.5281/ZENODO.50694.

[34] Arganda-Carreras I, Fernández-González R, Muñoz-Barrutia A, Ortiz-De-Solorzano C. 3D reconstruction of histological sections: Application to mammary gland tissue. *Microsc Res Tech* 2010; 73: 1019–29.

[35] Soille P. *Morphological image analysis : principles and applications*. Springer, 2013.

[36] Dougherty ER, Lotufo RA, Society of Photo-optical Instrumentation Engineers. *Hands-on morphological image processing*. SPIE, 2003.

[37] Vincent L, Soille P. Watersheds in digital spaces: an efficient algorithm based on immersion

simulations. *IEEE Trans Pattern Anal Mach Intell* 1991; 13: 583–598.

[38] Pani G, De Vos WH, Samari N, de Saint-Georges L, Baatout S, Van Oostveldt P, Benotmane MA. MorphoNeuroNet: an automated method for dense neurite network analysis. *Cytometry A* 2014; 85: 188–99.

[39] Dehmelt L, Poplawski G, Hwang E, Cho C, Halpain S. NeuriteQuanthttp://www.ccb.tu-dortmund.de/groups/CB/bastiaens/dehmelt/NeuriteQuant/ (accessed 6 November 2015).

[40] He JC, Gomes I, Nguyen T, Jayaram G, Ram PT, Devi LA, Iyengar R. The G alpha(o/i)-coupled cannabinoid receptor-mediated neurite outgrowth involves Rap regulation of Src and Stat3. *J Biol Chem* 2005; 280: 33426–34.

[41] Nishimoto I, Okamoto T, Matsuura Y, Takahashi S, Murayama Y, Ogata E. Alzheimer amyloid protein precursor complexes with brain GTP-binding protein G(o). *Nature* 1993; 362: 75–79.

[42] Brouillet E, Trembleau A, Galanaud D, Volovitch M, Bouillot C, Valenza C, Prochiantz A, Allinquant B. The amyloid precursor protein interacts with Go heterotrimeric protein within a cell compartment specialized in signal transduction. *J Neurosci* 1999; 19: 1717–27.

[43] Gakhar-Koppole N, Hundeshagen P, Mandl C, Weyer SW, Allinquant B, Muller U, Ciccolini F. Activity requires soluble amyloid precursor protein alpha to promote neurite outgrowth in neural stem cell-derived neurons via activation of the MAPK pathway. *Eur J Neurosci* 2008; 28: 871–882.

[44] Li X, Mumby SM, Greenwood A, Jope RS. Pertussis toxin-sensitive G protein alpha-subunits: production of monoclonal antibodies and detection of differential increases on differentiation of PC12 and LA-N-5 cells. *J Neurochem* 1995; 64: 1107–17.

[45] Baxes GA. *Digital image processing : principles and applications*. Wiley, 1994.

[46] Ammer H, Schulz R. Retinoic acid-induced differentiation of human neuroblastoma SH-SY5Y cells is associated with changes in the abundance of G proteins. *J Neurochem* 1994; 62: 1310–8.

[47] Korecka JA, van Kesteren RE, Blaas E, Spitzer SO, Kamstra JH, Smit AB, Swaab DF, Verhaagen J, Bossers K. Phenotypic Characterization of Retinoic Acid Differentiated SH-SY5Y Cells by Transcriptional Profiling. *PLoS One*; 8. Epub ahead of print 2013. DOI: 10.1371/journal.pone.0063862.

[48] Asano T, Kamiya N, Semba R, Kato K. Ontogeny of the GTP-binding protein Go in rat brain and heart. *J Neurochem* 1988; 51: 1711–6.

[49] Brabet P, Pantaloni C, Rodriguez M, Martinez J, Bockaert J, Homburger V. Neuroblastoma differentiation involves the expression of two isoforms of the alpha-subunit of Go. *J Neurochem* 1990; 54: 1310–20.

[50] Asano T, Morishita R, Sano M, Kato K. The GTP-binding proteins, Go and Gi2, of neural cloned cells and their changes during differentiation. *J Neurochem* 1989; 53: 1195–8.

[51] Ruiz-León Y, Pascual A. Induction of tyrosine kinase receptor B by retinoic acid allows brain-derived neurotrophic factor-induced amyloid precursor protein gene expression in human SH-SY5Y neuroblastoma cells. *Neuroscience* 2003; 120: 1019–1026.

[52] Holback S, Adlerz L, Iverfeldt K. Increased processing of APLP2 and APP with concomitant formation of APP intracellular domains in BDNF and retinoic acid-differentiated human neuroblastoma cells. *J Neurochem* 2005; 95: 1059–68.

[53] Strittmatter SM, Valenzuela D, Kennedy TE, Neer EJ, Fishman MC. Go is a major growth cone protein subject to regulation by GAP-43. *Nature* 1990; 344: 836–41.

[54] Strittmatter SM, Igarashi M, Fishman MC. GAP-43 amino terminal peptides modulate growth cone morphology and neurite outgrowth. *J Neurosci* 1994; 14: 5503–5513.

[55] Okamoto T, Takeda S, Giambarella U, Murayama Y, Matsui T, Katada T, Matsuura Y, Nishimoto I. Intrinsic signaling function of APP as a novel target of three V642 mutations linked to familial Alzheimer's disease. *EMBO J* 1996; 15: 3769–77.

[56] Yamatsuji T, Matsui T, Okamoto T, Komatsuzaki K, Takeda S, Fukumoto H, Iwatsubo T, Suzuki N, Asami-Odaka A, Ireland S, Kinane TB, Giambarella U, Nishimoto I. G protein-mediated neuronal DNA fragmentation induced by familial Alzheimer's disease-associated mutants of APP. *Science* 1996; 272: 1349–52.

[57] Ramaker JM, Swanson TL, Copenhaver PF. Amyloid precursor proteins interact with the heterotrimeric G protein Go in the control of neuronal migration. *J Neurosci* 2013; 33: 10165–81.

[58] Ramaker JM, Copenhaver PF. Amyloid Precursor Protein family as unconventional Go-coupled receptors and the control of neuronal motility. *Neurogenes (Austin, Tex)* 2017; 4: e1288510.

[59] Encinas M, Iglesias M, Llecha N, Comella JX. Extracellular-regulated kinases and phosphatidylinositol 3-kinase are involved in brain-derived neurotrophic factor-mediated survival and neuritogenesis of the neuroblastoma cell line SH-SY5Y. *J Neurochem* 1999; 73: 1409–1421.

[60] Lim JY, Park SI, Oh JH, Kim SM, Jeong CH, Jun JA, Lee K-S, Oh W, Lee J, Jeun S. Brain-derived neurotrophic factor stimulates the neural differentiation of human umbilical cord blood-derived mesenchymal stem cells and survival of differentiated cells through MAPK/ERK and PI3K/Akt-dependent signaling pathways. *J Neurosci Res* 2008; 86: 2168–78.

[61] Liu F, Xuan A, Chen Y, Zhang J, Xu L, Yan Q, Long D. Combined effect of nerve growth factor and brain-derived neurotrophic factor on neuronal differentiation of neural stem cells and the potential molecular mechanisms. *Mol Med Rep* 2014; 10: 1739–45.

[62] Kim SH, Kim S, Ghil SH. Rit contributes to neurite outgrowth triggered by the alpha subunit of Go. *Neuroreport* 2008; 19: 521–5.

[63] Cotta-Grand N, Rovère C, Guyon A, Cervantes A, Brau F, Nahon J-L. Melanin-concentrating hormone induces neurite outgrowth in human neuroblastoma SH-SY5Y cells through p53 and MAPKinase signaling pathways. *Peptides* 2009; 30: 2014–24.

[64] Holahan MR, Honegger KS, Tabatadze N, Routtenberg A. GAP-43 gene expression regulates information storage. *Learn Mem* 2007; 14: 407–15.

[65] Tanner DC, Qiu S, Bolognani F, Partridge LD, Weeber EJ, Perrone-Bizzozero NI. Alterations in mossy fiber physiology and GAP-43 expression and function in transgenic mice overexpressing HuD. *Hippocampus* 2008; 18: 814–823.

[66] Nordman JC, Kabbani N. An interaction between α7 nicotinic receptors and a G-protein pathway complex regulates neurite growth in neural cells. *J Cell Sci* 2012; 125: 5502–13.

B3.7. Supplementary Material

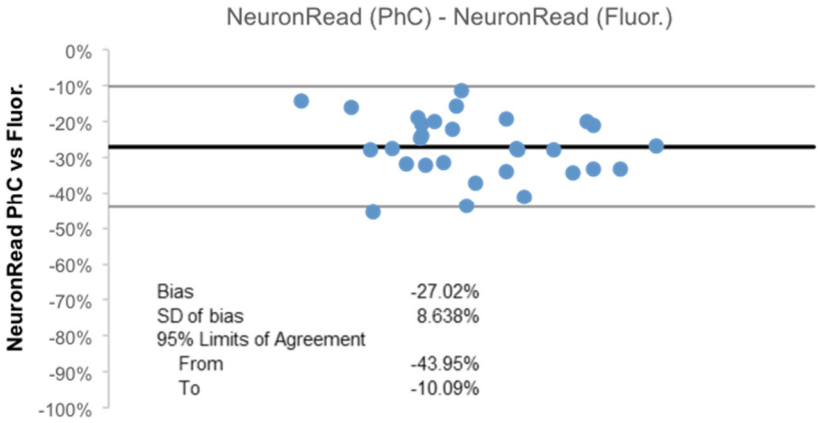

Supplementary Figure B3.1. Comparison between NeuronRead analyses of phase contrast images and fluorescence images. A set of 30 pairs of fluorescence ('Fluor.')-PhC microphotographs of neurons at 4 days in vitro were analyzed with the NeuronRead macro. Data extracted from both types of images were compared via **the** Bland-Altman plot, which shows an average difference between both methods of almost -27.02%, again indicating that neuronal PhC images have lower amount of neuritic information.

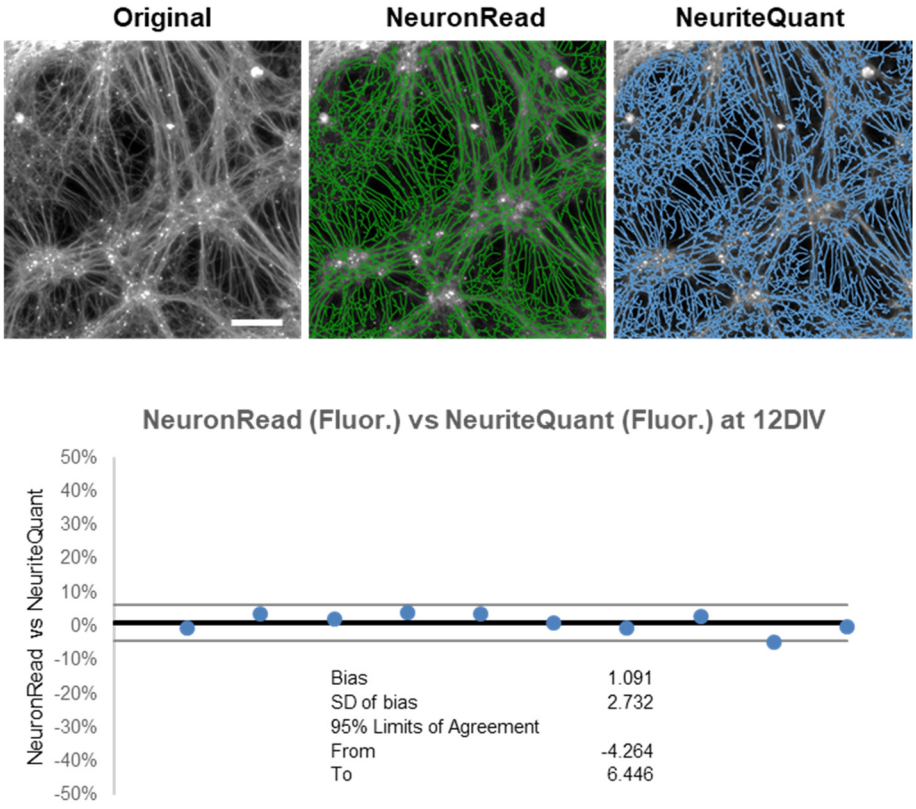

Supplementary Figure B3.2. Analysis of rat cortical primary neuronal cultures. Upper: Fluorescence images of 12DIV (days in vitro) neuronal cultures, labeled with an antibody against β-III tubulin, were analyzed with NeuronRead and NeuriteQuant. Bar: 50 µm. Bellow: Bland-Altman plot of the comparison between NeuronRead and NeuriteQuant show an average difference between both methods of around 1%. n = 10.

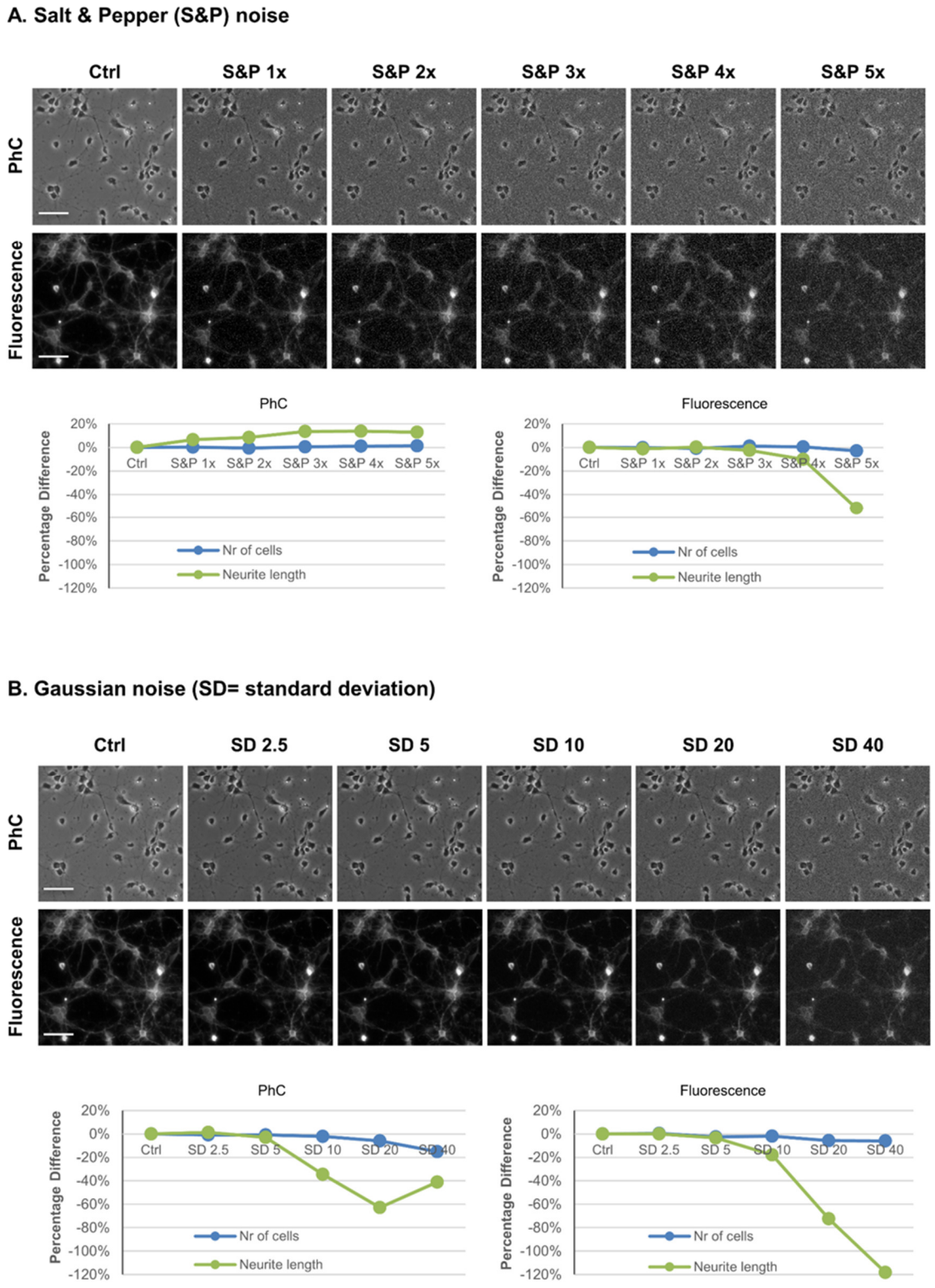

Supplementary Figure B3.3. Testing NeuronRead robustness and sensitivity to noises. Salt and Pepper (A.), and Gaussian noises (B.) were incrementally added to PhC and Fluorescence images, using the ImageJ. NeuronRead's ability of extract the number of cell bodies and total neuritic length was tested in these conditions. n = 5. Bar = 50 µm. S&P, Salt and Pepper; SD, Standard Deviation.

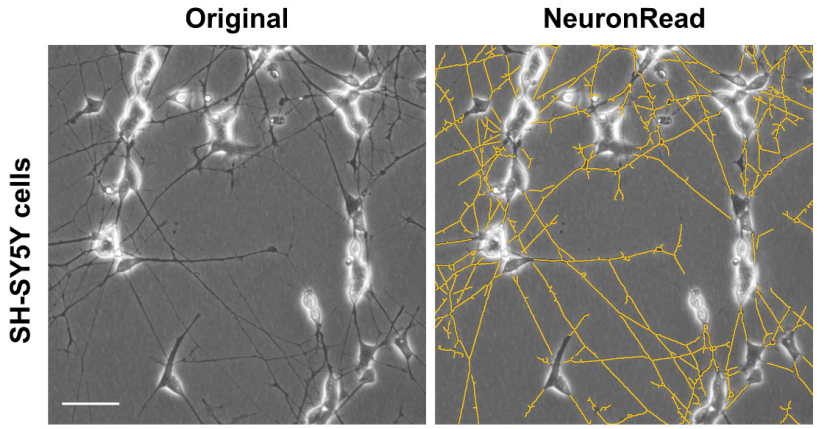

Supplementary Figure B3.4. Differentiated SH-SY5Y cells analyzed with NeuronRead. SH-SY5Y cells were differentiated for 12 days in vitro (DIV) using a protocol adapted from Encinas et al (2000) using 10 μM retinoic acid (first 5 days) and 10 ng/mL of brain-derived neurotrophic factor (BDNF; in the further 7 days). Photos were taken to living cells at 12 DIV (raw image at the left), and cells' neuritic network was analyzed with NeuronRead (right image, tracing in orange). Scale bar = 100 μm.

NeuronRead Tutorial

Setup

The NeuronRead macro runs on ImageJ software and is supported by three main plugins: MorphoLibJ, Skeletonize3D and Analyze Skeleton. For the smoothest and fastest application of the macro we recommend installing the most recent FIJI package, an ImageJ bundle that already includes the Skeletonize3D and Analyze Skeleton plugin (https://imagej.net/Fiji/Downloads). After installing FIJI, the MorphoLibJ must be added manually. Detailed instructions on how to install this plugin can be found on http://imagej.net/MorphoLibJ. NeuronRead was built around version 1.3.2 of MorphoLibJ, which means that compatibility problems may arise when using older versions.

There are 3 ways to install and run NeuronRead on ImageJ:

1. Open ImageJ, select Plugin → Macro → Install, and then select NeuronRead. This way each time the user wants to run the macro he only needs to go to the Plugin → Macro and select NeuronRead at the bottom of the tab. This install is not permanent, so the user has to repeat these steps each time ImageJ is opened.
2. Open ImageJ, go to Edit → Options → Startup… and add the following code: run("Install...", "install = /FullPath/macroname.ijm"); where "FullPath/macroname.ijm" must be replaced by the user actual path to the macro. This way, each time ImageJ is opened NeuronRead is installed automatically.
3. Open ImageJ, select Plugin → Macro → Run and then select NeuronRead, which will start immediately.

Running NeuronRead

1. Run NeuronRead. This step assumes the user performed the installation of NeuronRead as described in steps 1) or 2) of the previous section.

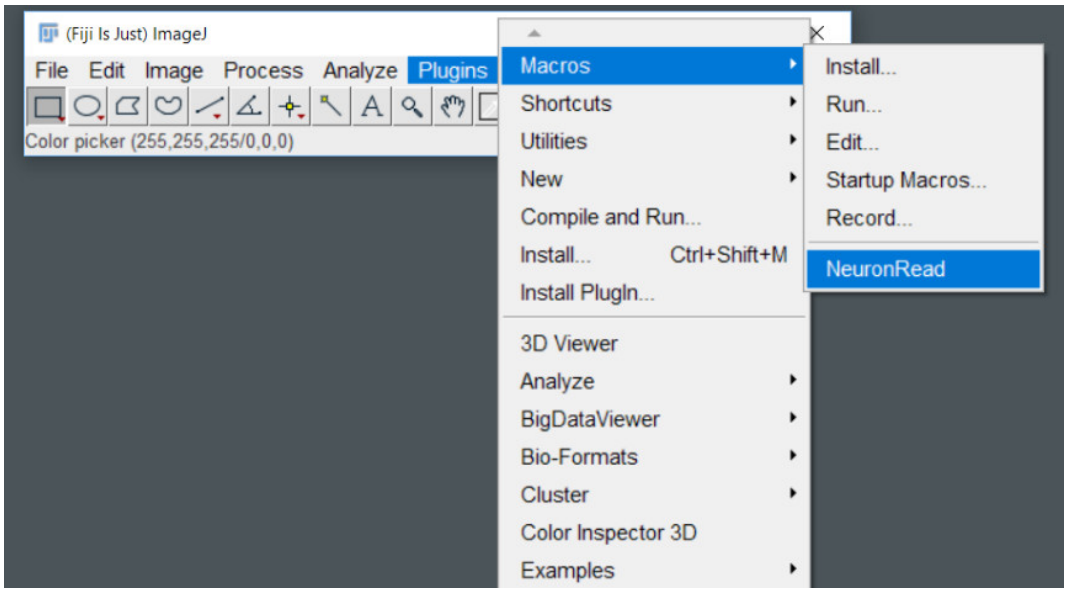

2. A new window opens. Search for the folder where the images are saved and select the image to be analyzed.

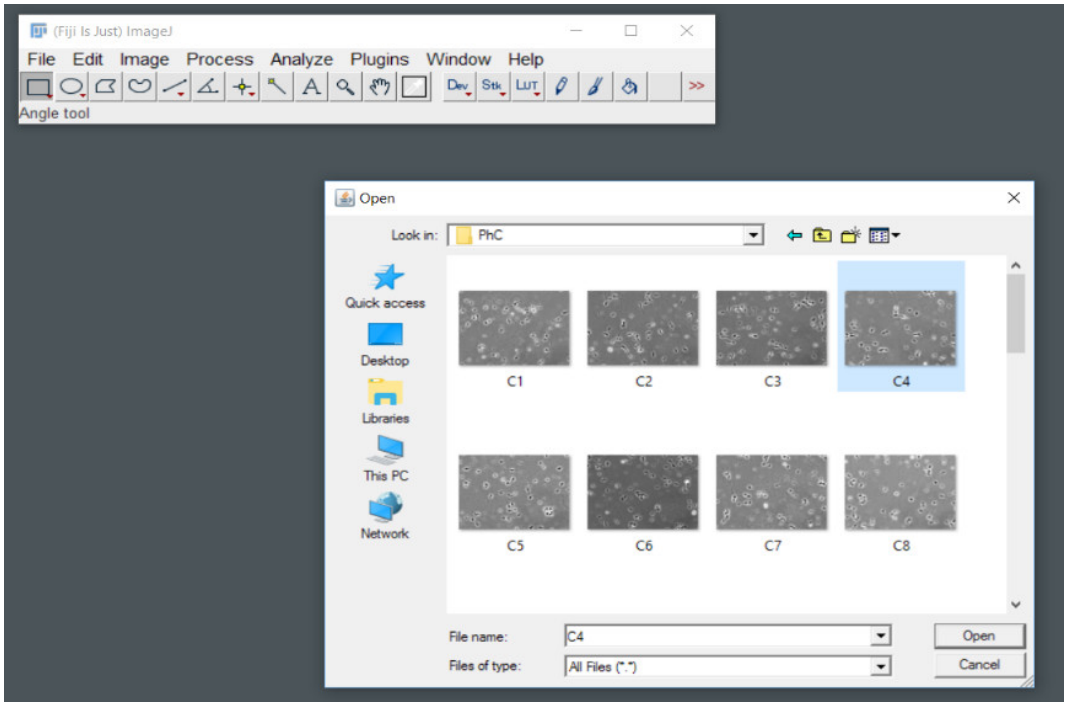

3. The analysis starts. The first stop (user dialog box) is for defining if the image being analyzed is a phase contrast image. If so, leave the checkbox ticked. If you are analyzing a fluorescence image untick the checkbox.

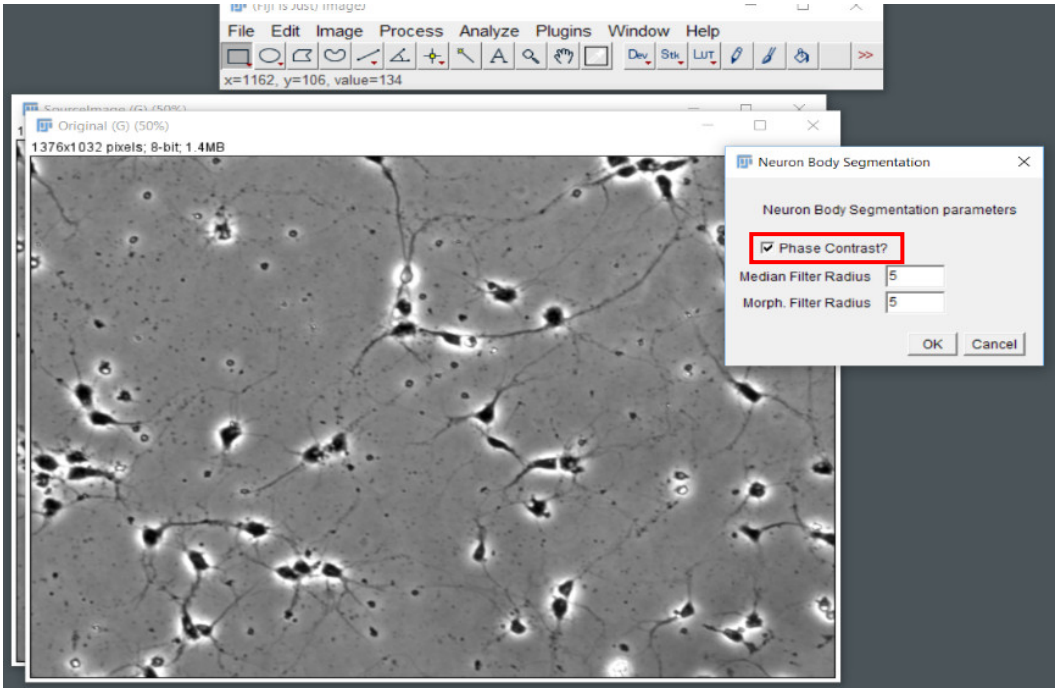

4. On the same box, the user can change some segmentation parameters to improve cell body recognition. These parameters are dependent on the magnification used for the images acquisition. Higher magnifications will require the application of filters with larger radius, while lower magnifications will require smaller radius. A filter of 5 is set as default; it was applied for images taken with a 20x objective, but it may change with the resolution of the camera.

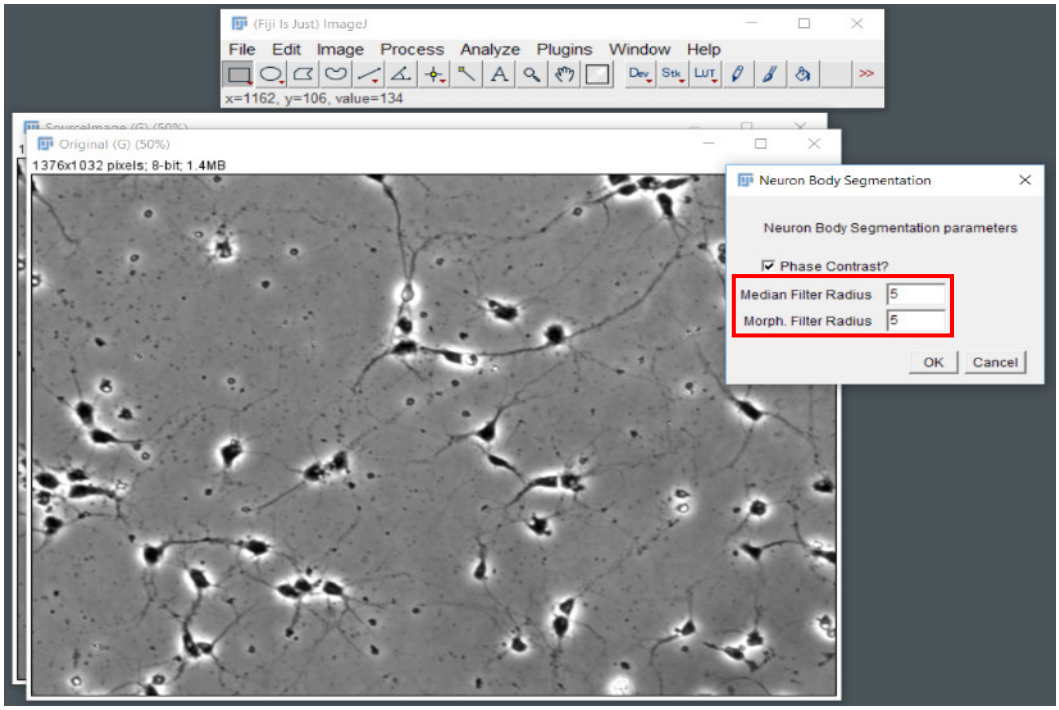

5. The next step asks for defining the appropriate threshold for cell body recognition. Increasing the threshold will remove small debris present in the image, but it can also remove some cell bodies. Apply the threshold and, if you find it to be correctly adjusted, then click OK the “Soma Thresholding” box.

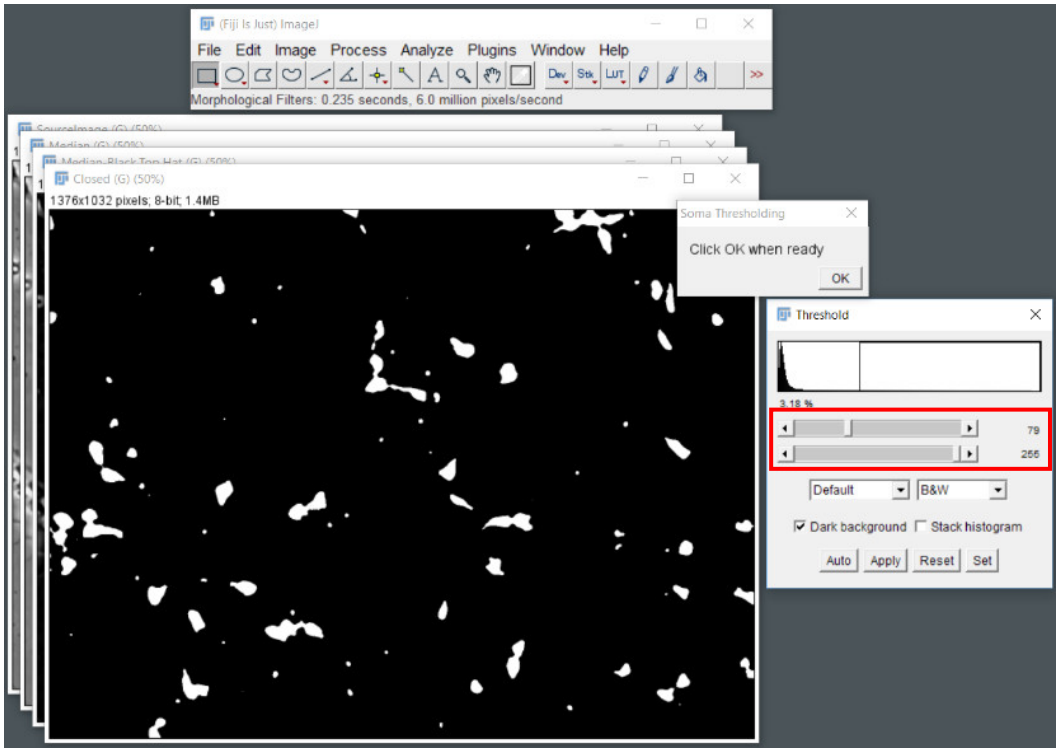

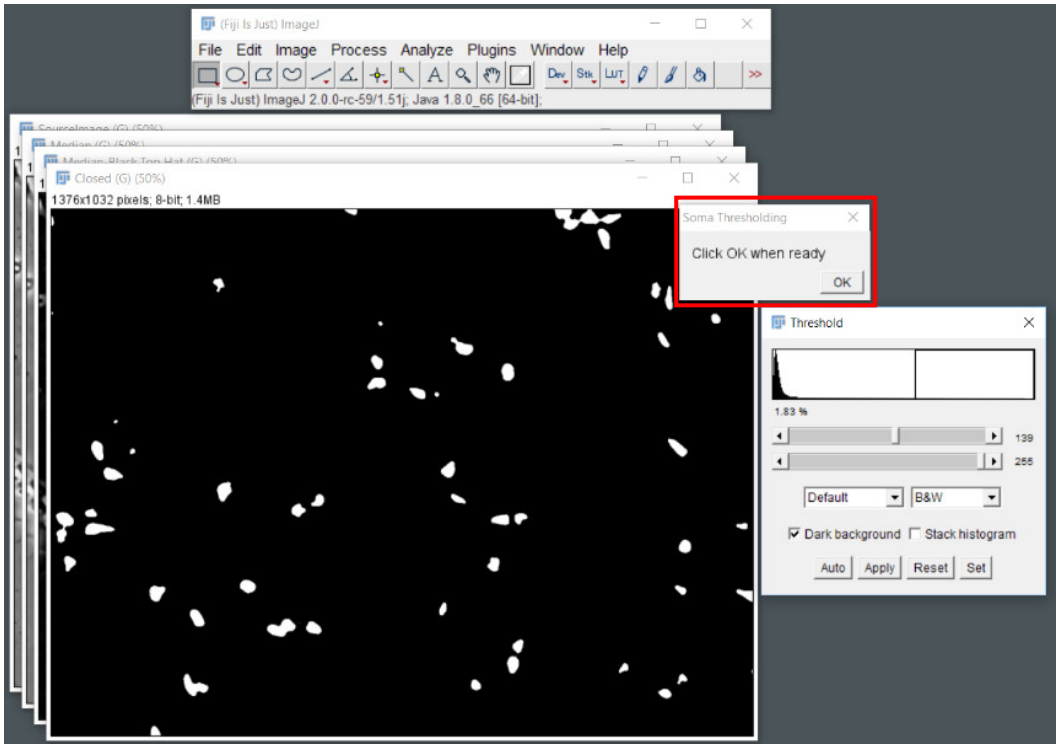

6. If any cell body is missing you can add it by using the selection tools of ImageJ and pressing “T” afterwards. You can also remove misidentified cell bodies by selecting them in the “ROI manager” and deleting them.

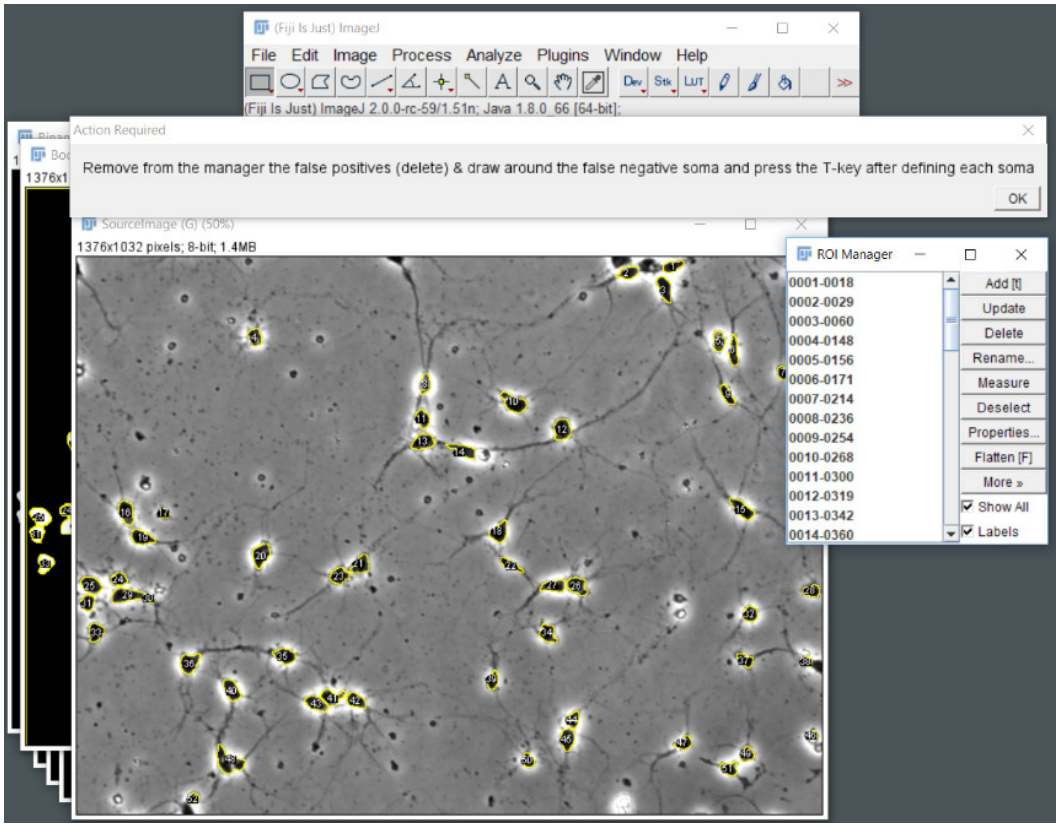

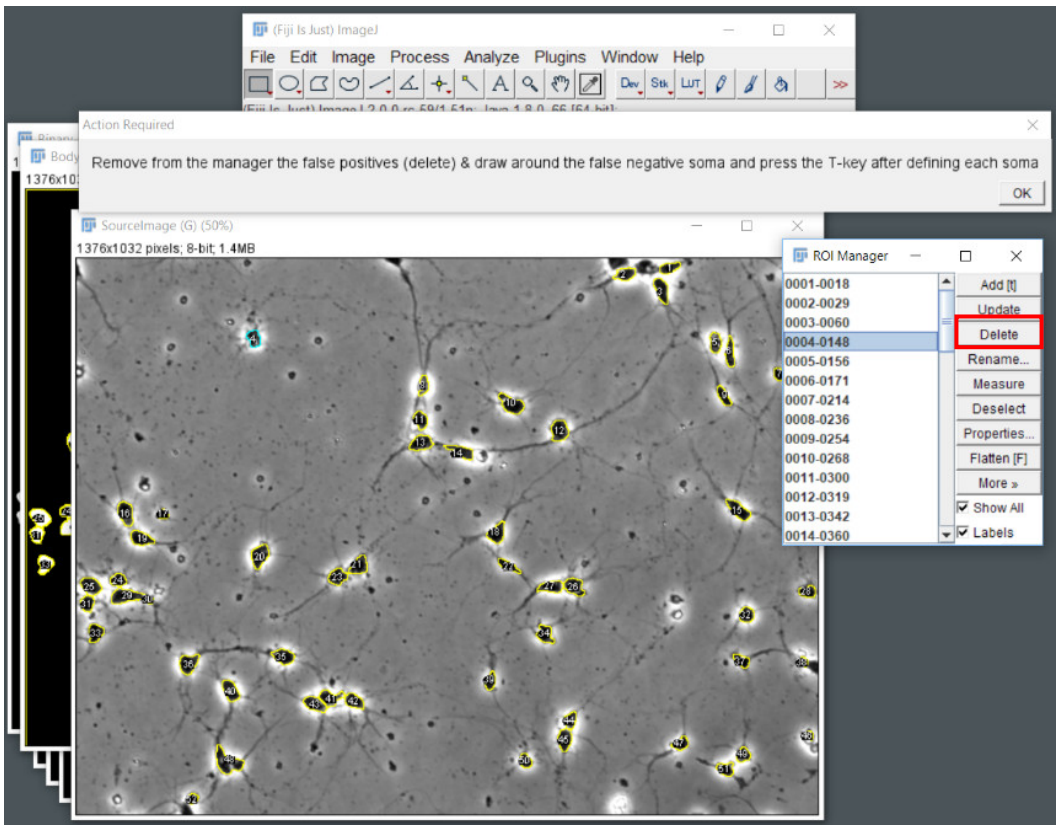

7. Proceed with neurite thresholding. The same principle that was mentioned before applies here to the threshold. Higher threshold limits will eliminate debris, but will also obscure neurites, while lower threshold limits can insert artifacts into neurite recognition.

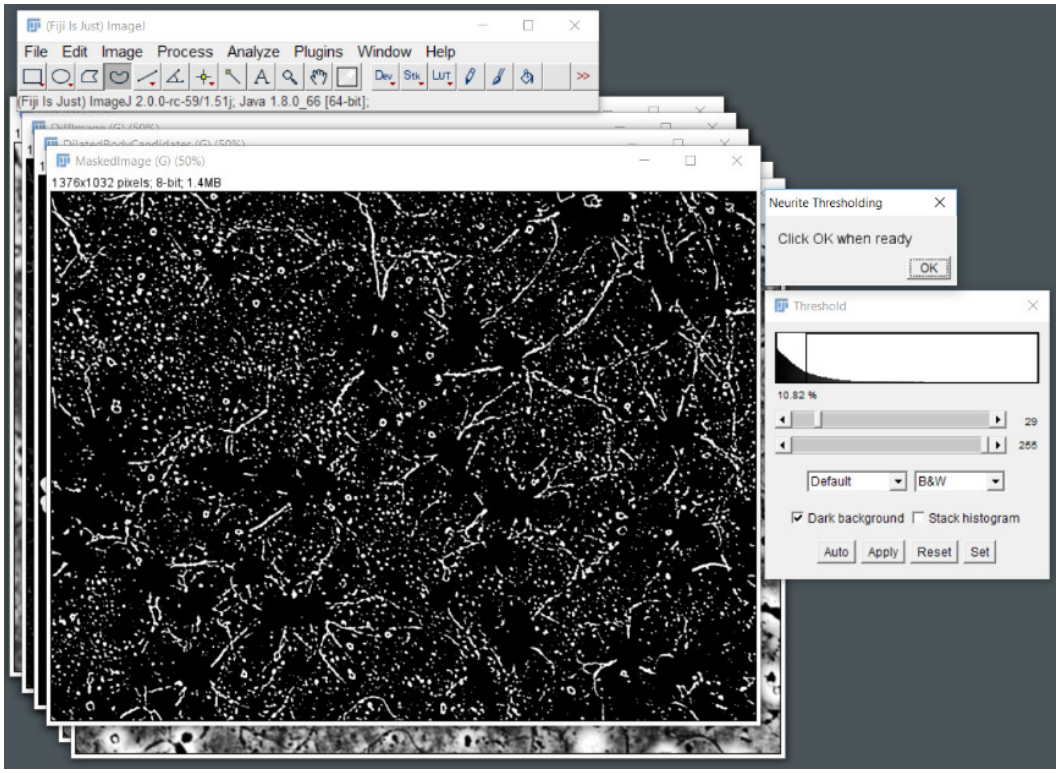

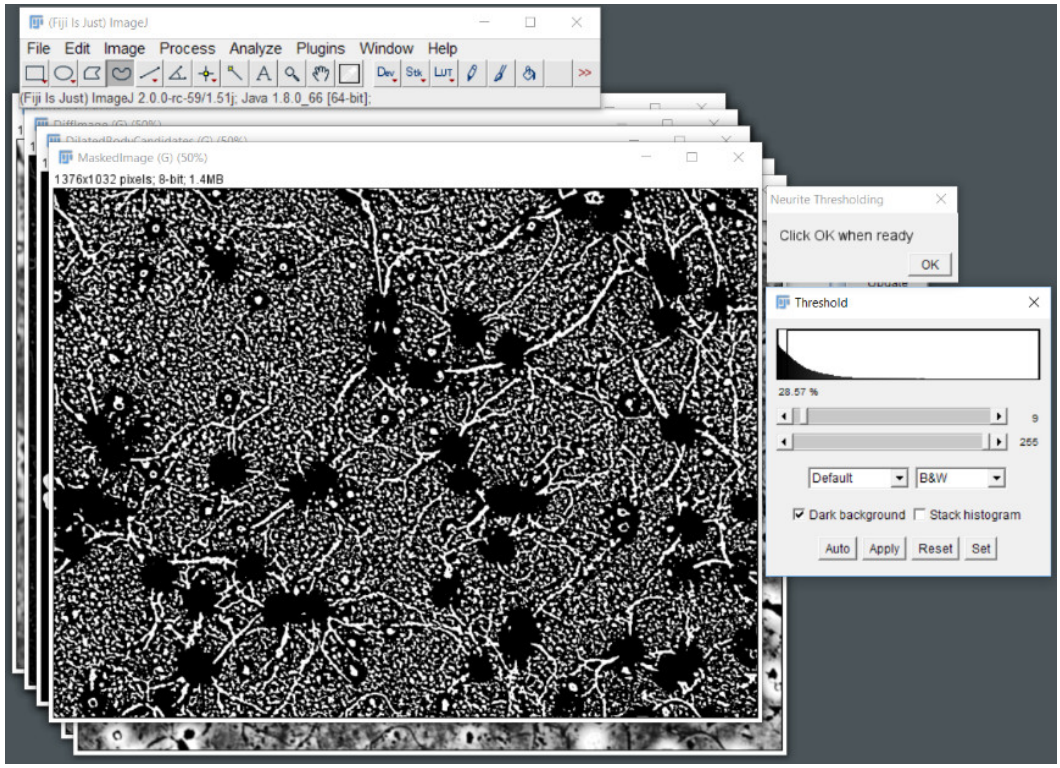

8. The final user interaction stop is “Set scale”. For the data to be retrieved in µm, the user must input the image scale according to the acquisition settings used. This step can be ignored, in which case the results will be presented as pixels. Image scale can be obtained from the images’ information or from the scale bar, if available.

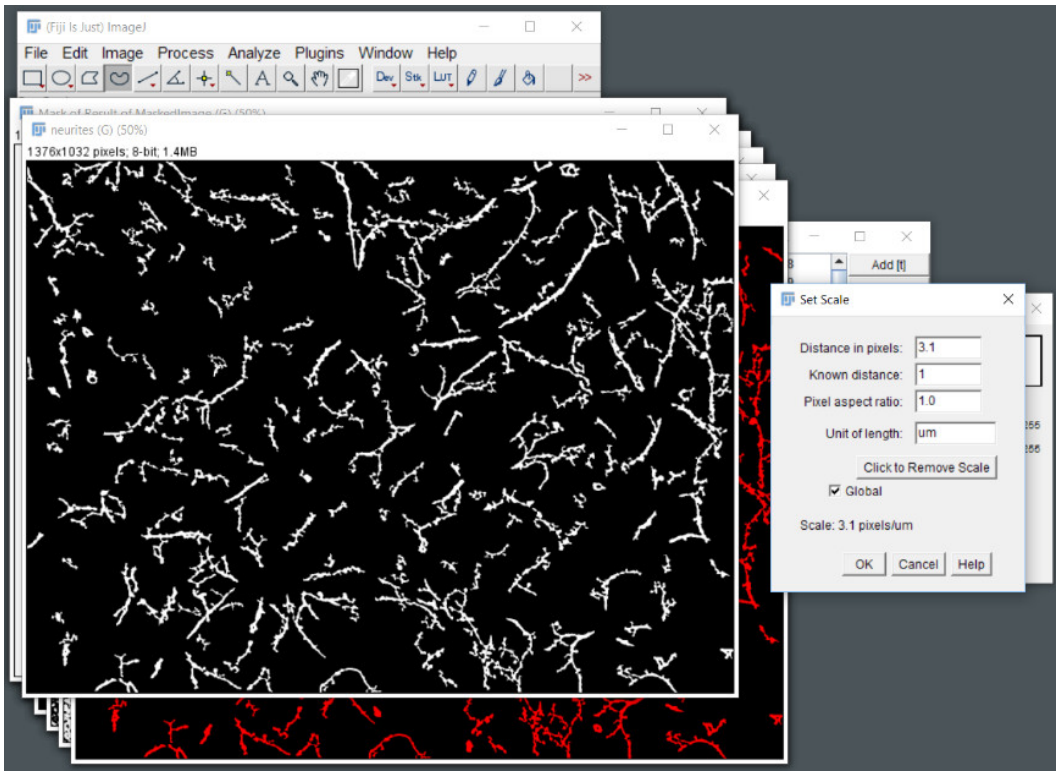

9. The macro ends by presenting the “Log” window with the morphological data extracted from the analysis.

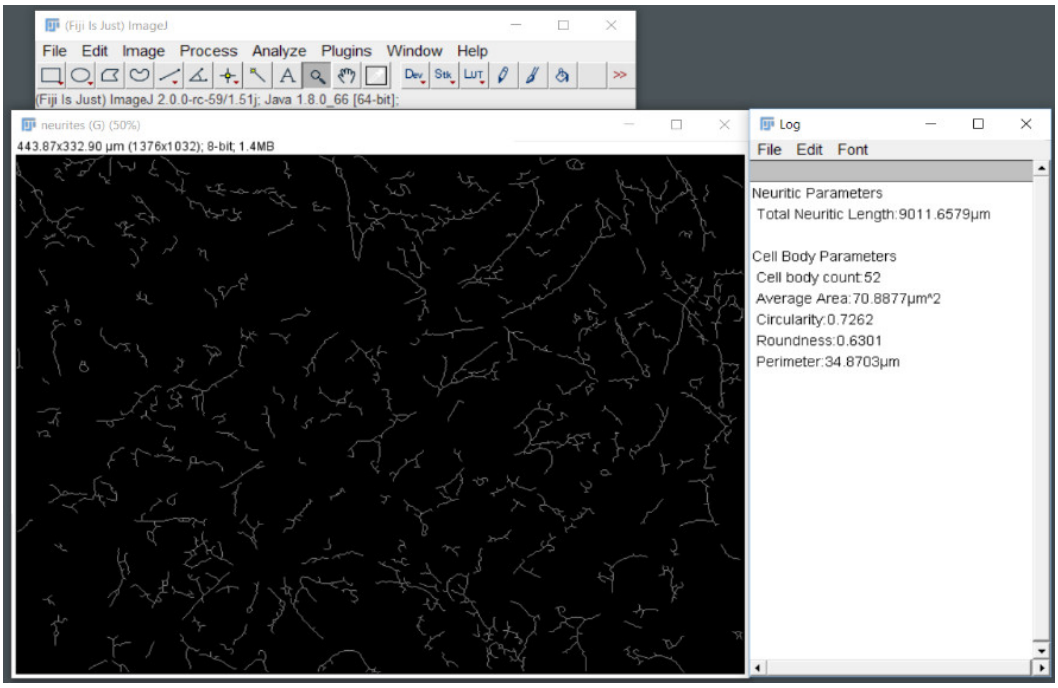

C. General Discussion

C1. Main findings and future work

The Gαo protein is the most expressed Gα subunit in the brain. Discovered over 3 decades ago, Gαo specific function in neurophysiology has remained unclear so far. Several studies point to neuronal differentiation as one of the main mechanisms in which Gαo is involved: Gαo expression increases during rat brain development, as well as during the neuronal-like differentiation of different cell lines, such as PC12 and N1E-115 [1–3]; several signaling pathways activated by Gαo lead to neuritogenic alterations, such as the Src-STAT3, ERK1/2, and GRIN1-cdc42 pathways [4–8]; and activation of Gαo promotes synaptogenesis [9–11], a mechanism not only necessary during brain development but also extremely important during adulthood, especially for memory and learning.

The main goal of this work was to further characterize the role of Gαo during neuronal differentiation by focusing on Gαo interaction with the Amyloid Precursor Protein (APP). APP, like Gαo, has been strongly associated with neuronal differentiation. Its expression suffers critical changes during neuritogenesis [12–14], and it has also been described as a modulator of at least two of the signaling pathways that Gαo is involved, such as STAT3 and ERK1/2 [15–17]. The combined knowledge that APP binds and activates Gαo [18, 19], and that these two proteins share similar neuritogenic functions, led us to hypothesize that the APP-Gαo interaction could play a role in neuritogenesis.

Our work started by evaluating if APP phosphorylation affected the APP-Gαo binding (Chapter B1). Phosphorylation of Serine 655 is known to induce conformational changes in the APP's C-terminal region to which Gαo binds [20]. By using APP phosphomutants mimicking constitutive dephospho/phosphorylation of S655 (SA APP and SE APP, respectively), we demonstrated that Gαo bound preferentially to wild-type (Wt) APP and SE APP. Moreover, phosphorylation of APP also increased Gαo activation. This is the first time that it was described a connection between APP phosphorylation and its binding to Gαo. Furthermore, APP phosphorylation is an important modification that induces crucial alterations on APP interactome and functions [21, 22]. Phosphorylation of Thr668 increases with differentiation of PC12 cells and expression of an APP mutant mimicking Thr668 phosphorylation affects NGF-induced differentiation of these cells [23]. However, it is still not known what is the profile of S655 phosphorylation with neuronal differentiation. It will be important to study this profile, and to see how it relates to the alterations we have detected on Gαo expression during BDNF-induced differentiation of SH-SY5Y cells, and in differentiating cells upon Gαo inhibition (Chapter B3). It is also important to keep in mind that the Gαo activation induced by SE APP might not mimic exactly what happens *in vivo*. On one hand, SE

APP phosphomutant is mimicking a state of constant phosphorylation, while *in vivo* APP phosphorylation exists in a cyclic state due to the combined action of kinases and phosphatases [24]. On the other hand, the substitution of an amino acid to mimic phosphorylation (in this case substituting serine by a glutamate to mimic a phosphorylated serine) is not able to completely mimic the phosphorylated residue. In the case of glutamate, this residue only possesses one negative charge in its side-chain, while the addition of a phosphate group adds two negative charges to the phosphorylated residue, which can then lead to subtle but important variations of the protein conformation [25]. These differences in conformation might account for some of the differences detected in SE APP activation of Gαo. Activation of G proteins can induce a shift on the localization of the Gα subunit from the plasma membrane, where it normally rests and is activated, to the cytosol, where it binds to various effector proteins [26, 27]. However, when we transfected SH-SY5Y cells with SE APP-GFP we observed an increase of Gαo localization on the plasma membrane compared to the cytosol. This could indicate that SE APP, due to its different conformation, is "locking" Gαo with it in the plasma membrane of the cell body and cell processes, where these proteins interact. The APP-Gαo complex at the plasma membrane might thus interact with a smaller and specific subset of Gαo effectors related to neuritic elongation. This could then explain some of the morphological features we detected, such as the increased in neurite elongation already at 6h after transfection. Still, these observations are based on a qualitative analysis of SE APP-GFP transfected cells. More detailed experiments, such as colocalization studies with a plasma membrane marker and fractionation assays, will demonstrate if SE APP is indeed increasing Gαo membrane localization.

We then tried to decipher the morphological consequences of this interaction and possible signaling pathways that would underlie these alterations and would be modulated by the APP-Gαo complex. We detected a sequential activation of STAT3 and the ERK1/2 pathway by Gαo, with STAT3 being involved in the formation of new processes, while ERK1/2 increased activation correlated more with an increase in neuritic elongation. Another study has reported an involvement of ERK1/2 in neuritic elongation rather than neurite formation [28], while an interplay between STAT3 and ERK1/2 activation in neurite outgrowth is also known (discussed in more detail further ahead). However, some questions remain regarding this biphasic mechanism. One is if STAT3 initial activation is required for ERK1/2 activation. This does not seem the case since co-transfection of SE APP with Gαo was able to activate ERK1/2 without a previous phase of STAT3 activity. However, since we only evaluated specific time-points, and phosphorylation events can occur in a matter of minutes or even seconds, SE APP-Gαo activation of STAT3 might have occurred without we being

able to detect it. So, to answer this question time-courses with shorter time-points should be performed, or STAT3 phosphorylation could be inhibited for longer periods of time (up to 24h) and ERK1/2 activation monitored during that time. It will also be important to confirm if ERK1/2 activation is indeed necessary for the neuritic elongation by directly modulating ERK1/2 activity with MEK1/2 inhibitors.

APP effect on Gαo-induced neuritogenesis also seemed to develop throughout two phases. At 6h of transfection, Wt APP augmented Gαo-induced STAT3 activation, which resulted in the highest increase in the number of processes formed. This increase must thus result not only from cycles of Wt APP-induced Gαo activation, but Wt APP must also serve as bridge to an important Gαo effector in the STAT3 pathway (such as Rap1GAP) or other involved in generation of new processes (such as GRIN1, activator of Cdc42 and its subsequent filopodia formation). Also at 6h of transfection, SE APP-Gαo expression promoted the elongation of pre-existing neurites, with no visible early alterations on STAT3 and ERK1/2 signaling.

At 24h of transfection, APP potentiator effects on Gαo-induced neurite formation and elongation seem to be lost, with Gαo alone being able to elongate neurites to the same extent than Gαo-Wt and SE APP co-transfected conditions. At this time point, Gαo alone is more efficient in neuritic elongation than when co-overexpressed with the Wt APP. This suggests that the potential Wt APP effect of activating and bridging Gαo to an effector more involved in new processes formation is 1) sequestering part of the Gαo pool from being involved in elongation and/or 2) per se not sufficient to induce/maintain novel processes formation in a period of major neuritic elongation and no STAT3 activation. It could also mean that the overexpression of these two proteins might induce pathological effects due to excessive Gαo activation. We detected a significant increase in ERK1/2 activation when SE APP-Gαo were co-transfected with no increase in neuritic elongation over Gαo alone. EGFR-ERK1/2 activation is important for neuritic elongation, as observed in the EGFR inhibitor assays but overactivation of ERK1/2 by APP has already been associated with Alzheimer's Disease [29], and Gαo overactivation induced by mutant APP has also been reported in cases of Familial Alzheimer's Disease [30, 31]. Thus, one has to consider that overactivation of Gαo by SE APP might also lead to cell damage in the long run. An evaluation of cell viability should provide us some answers regarding these effects. Surprisingly, SA APP co-expression with Gαo was able to further increase the number of cells with pre-neurites, without alterations in the Gαo-induced ERK1/2 signaling. One can speculate that this increased neuritogenesis might be related to the increased Gαo degradation detected in the second part of this thesis (Chapter B2). Protein overexpression can have detrimental effects on normal cell function, even by the simple fact that

when a transfected protein exists in overabundance when compared to physiological conditions, it can be mistargeted to the wrong subcellular compartments, and can be improperly folded [32]. Furthermore, as we are talking about a signaling protein, it is important to properly control its periodic signaling. Since we have detected that SA APP was able to control Gαo by targeting it to lysosomal degradation, this could be a mechanism by which APP is controlling Gαo function with time and thus promote a more efficient neuritogenesis. Nevertheless, this could be a short-term effect in these in vitro conditions, since SA APP transfection results in a higher production of Aβ [33], one of the main elements of Alzheimer's Disease. Differences between the effects of the different APP forms on Gαo-induced neuritogenesis might also be explained by alterations of the Gαo interactome. In our lab we have evaluated the differential phospho S655 (pAPP) interactome, and observed that while SE APP binds more to signaling-related moelcules, SA APP binds (among other) to a group of proteins that relate to actin remodeling (data not published). A study evaluating the Gαo interactome in the presence or absence of APP overexpression might thus provide us with new molecular players involved in APP-Gαo signaling at this stage of neuritic elongation.

Our results on rat primary neurons showed that Gαo and APP promote dendritogenesis in detriment of axonal growth at 4 days *in vitro*. After 24h of (co-)transfection no significant increase in the STAT3 and ERK1/2 ratios was detected, although the levels of both phospho and total STAT3 and ERK1/2 were increased over control conditions. Further, Src and EGFR inhibitors hindered Gαo positive effects on dendritogenesis. This means that these two pathways are connected to Gαo dendritogenic function on rat primary neurons, directly or not. Interestingly, APP transfection overcomed Src and EGFR inhibitory effects on dendritogenesis. This seems to indicate that, in neurons, APP is able to activate mechanisms that are independent of these two proteins (Src and EGFR). However, it is not clear if Gαo participates on such mechanisms. Future experiments should evaluate the effect of APP single transfections on this time-point, and inhibit Gαo on these conditions. Moreover, APP-Gαo effects should also be evaluated at earlier time-points (0-2 DIV), where the formation of new neurites is more pronounced [34, 35].

The second part of this work focused on the effects that APP and Gαo have on each other's protein levels (Chapter B2). We identified two degradation mechanisms by which Gαo can be eliminated: Lysosomal degradation in response to SA APP overexpression; and proteasomal degradation after Gαo inhibition with PTX treatment.

As mentioned above, lysosomal degradation could be a mechanism activated to control APP-Gαo signaling. One hypothetical signaling event would thus be initiated by APP phosphorylation. Gαo

binds to the phosphorylated APP, is activated and initiates downstream signaling (potentially through STAT3 and ERK1/2, and other effectors). If APP is maintained in a phosphorylated state, it can reactivate Gαo after GTP-hydrolysis. Subsequent APP dephosphorylation, however, stops the signaling, not only by being unable to reactivate Gαo but also by enhancing its degradation. Lysosomal degradation would thus act as a feedback mechanism to stop APP-Gαo signaling. This targeting to lysosomal degradation probably takes other factors into account: e.g. the localization of APP and Gαo inside the cell. It is unlikely that APP dephosphorylation would directly deliver Gαo for degradation. It might instead act has a hub for other molecular players that will be involved in this mechanism, such as Hsc70, and Adaptor Proteins [22, 33, 36, 37]. Indeed, we discovered that Gαo, like APP, possesses a KFERQ-motif, a signaling sequence involved in chaperone-mediated autophagy (CMA). We also observed an increased co-localization of Gαo with Hsc70, one of the main players of CMA, in SA APP transfected cells. Further, in these cells Gαo also co-localizes more with LAMP2, another CMA major player. Future work should focus on trying to understand if Gαo does interact with Hsc70 and if the co-localization between both proteins is directly correlated with Gαo lysosomal degradation.

Proteasomal degradation of Gαo as a result of PTX treatment could be a response of the cell to eliminate ADP-ribosylated proteins, similar to the mechanism it uses to eliminate misfolded proteins. However, at this point, it is still unclear how ADP-ribosylation of Gαo causes its degradation. One hypothesis is that ADP-ribosylation causes a conformational change in Gαo that makes it recognizable by ubiquitin ligases, and thus prone to be ubiquitinated and targeted to the proteasome. Another hypothesis is that the ADP-ribosyl group itself might be recognized by the proteasome. This seems to occur in cases of poly-ADP-ribosylation, however, it is unclear if it also occurs in mono-ribosylated proteins [38, 39]. Also, the fact that APP also seems to be co-degraded with Gαo in response to PTX treatment needs to be further investigated.

During our experiments with primary neuronal cultures we felt the need to evaluate neuronal differentiation with time without having to fix and immunostain the neuronal cells. The easiest and fastest way to visualize a same live cell population is by phase contrast (PhC) imaging. However, while several software exist to analyze fluorescence images of 2D neuronal cultures, such as NeuriteQuant and MorphoNeuroNet [40, 41], we could not find any reliable tool to analyze random fields of PhC images. So, the third and final part of this work focused on the development of NeuronRead, an ImageJ macro capable of analyzing both PhC and Fluorescence neuronal images (Chapter B3). NeuronRead is able to extract information regarding the cell body morphology (number of cells, average area, circularity) and neuritic network (total neuritic length, average

neuritic length per cell) with high accuracy, demonstrated by the comparison with manual analyses, as well as by using NeuriteQuant, a proved tool used to analyze neuritic networks in fluorescence images [40]. Also, NeuronRead proved to be reliable in the analysis of images acquired from primary neuronal cultures, as well as images from neuronal-like cells, such as differentiated SH-SY5Y neuroblastoma cells.

Following, NeuronRead was used successfully to relate morphological alterations induced by RA-BDNF differentiation of SH-SY5Y cells [42] with alterations in Gαo protein levels. Moreover, it also detected alterations in total neuritic net length caused by PTX treatment. Future work will also use secondary parameters obtained with Neuron Read (through “Skeletonize” and “Analyze Skeleton”, two plugins integrated into NeuronRead), such as the number of branches detected in each image, to further evaluate the role of Gαo activity in SH-SY5Y differentiation.

Our initial approach was already able to detect significant biochemical alterations as a result of Gαo inhibition, such as the decrease in βIII-tubulin and the increase in GAP-43 levels, two neuronal markers. While further work is required to determine the real meaning of these alterations, it does strengthen the idea that Gαo is a fundamental player in proper neuronal differentiation.

C2. Potential role of APP-Gαo signaling during brain development

Most of the analysis and discussion of our results was performed in light of the applied methodology, such as the use of SH-SY5Y cells as our main cell model, and the use of protein overexpression as a way to determine potential physiological effects. But can we now fit this data with the already described mechanisms involved in neuronal differentiation, as well with what is known about APP and Gαo functions?

One of the main signaling pathways associated with neuronal differentiation is the MAPK/ERK signaling [43–46]. As mentioned above, Gαo is able to induce ERK1/2 activation, with APP potentiating this effect. Interestingly, this activation occurred after an initial phase of STAT3 activity. An interplay between ERK1/2 and STAT3 during neuritogenesis has already been described. Neuronal differentiation of mice embryonic stem cells with retinoic acid is accompanied by an increase in ERK1/2 and STAT3 activity. Inhibiting ERK1/2 results in a decrease of STAT3 activity, and a decrease in the expression of neuronal markers [44]. Another study has shown that activation of the CB1 receptor (CB1R) and IL-6 receptor (IL-6R) act synergistically to promote neurite outgrowth via activation of STAT3 and ERK1/2 [47]. Interestingly, this study showed that a peek in ERK1/2 activation occurred early (first 15 min of stimulation), while STAT3 activity peaked later (around 6h after initial treatment). In both these studies, ERK1/2 activation preceded STAT3, which seems to contradict our results. However, there are studies showing that ERK1/2 activation can occur in a biphasic mechanism. The first phase of ERK1/2 activation is reportedly extremely fast, between 1-15 min after stimulation, while the second phase seems to vary accordingly to the stimuli/environment, ranging from 15 min [48] to several hours [49, 50] after the initial phase. Even in the work regarding the cooperation between CB1R and IL-6R signaling, results show that after the initial ERK1/2 activation there was a second activation phase around 4-6 hours after treatment. Taking together, these results could mean that the Gαo-ERK1/2-STAT3 signaling described in our work could be following a similar pattern, but since the first phase of ERK activation occurs extremely fast we were unable to detect it. Future work following ERK activity immediately after transfection will be necessary to answer this question. ERK1/2 activation detected in our experiments could be an outcome of crosstalk with other signaling pathways that were meanwhile activated, or because of activation of gene transcription during the first phase of signaling. Thus, inhibiting the STAT3 for longer periods of time (24h) will allow us to check if this activation needs to occur prior to ERK1/2, or if both signaling pathways happen in parallel.

Interestingly, one of the studies describing the biphasic ERK1/2 activation demonstrated that activation of Gαi/o proteins was required for the second phase of the process [48]. Moreover, the overall ERK1/2 activation mechanism started with the stimulation of CB1R, a receptor that can induce neuritogenesis by activating Gαo-Src-STAT3 [5, 6]. This could mean that APP activates a signaling pathway similar to the one downstream of CB1R. It would also be interesting to explore the role of APP as a participant in the CB1R pathway. The first phase described by Asimaki and Mangoura [48] involves PKC, which is the main in vivo kinase able to phosphorylate APP at Serine 655 [51, 52]. One could hypothesize that the signaling initiated by CB1R would lead to PKC activation that would consequently lead to the phosphorylation of APP. pAPP would then be one of the initiators of the second phase of ERK1/2 signaling, by prolonging the cycles of Gαo activation. However, one must take close consideration the model in which to study this kind of signaling. While CB1R has be seen to activate ERK1/2 by different studies, the exact upstream pathways involved are not clear, with certain kinases, such as PI3K and Src, being either required or unnecessary for ERK1/2 activation [53, 54]. Also, to our knowledge, no direct crosstalk between CB1R and APP signaling has been described so far.

APP and Gαo neuritogenic actions have both been independently associated with Reelin [55, 56]. Reelin is an extracellular factor involved in neuronal polarization [46, 57]. Reelin interaction with the extracellular domain of APP was detected *in vitro*, and knockdown of endogenous APP in rat hippocampal neurons blocked Reelin neuritogenic effects on these cells [56]. Another study showed that Gαo inhibition with PTX or knockdown using siRNA also blocked Reelin neuritogenic effects on hippocampal neurons, in a Src-dependent mechanism [55]. However, no receptor was identified in this mechanism. One could then speculate that APP might act as an unconventional receptor for Reelin, which upon binding stimulates a downstream pathway involving Gαo. APP functioning as a receptor has been for long proposed, however, the identity of natural ligands is not well established. Treatment of APP-Gαo vesicles with the 22C11 antibody has shown that binding of the antibody to APP modulates Gαo activation [19, 58]. Authors hypothesized that 22C11 could be acting as a possible not yet identified extracellular ligand of APP, and Reelin could be such a ligand. Another of Reelin main biological roles is to control neuronal migration, and hence a possible link between Reelin action and APP-Gαo known co-function in neuronal migration should also be investigated [57, 59, 60].

Our work has also brought up a possible connection between BDNF and Gαo signaling in neuronal differentiation, with Gαo being important for the biochemical maturation of neuronal-like cells *in vitro*. So far, Gαo has never been described as a possible downstream effector of BDNF. However,

there is some work showing that BDNF release is significantly inhibited in AtT-20 cells upon treatment with PTX [61]. Combining both results, Gαo could potentially act in a positive feedback loop during *in vivo* neuronal polarization. BDNF release would stimulate neurite elongation and branching accompanied by an increase in Gαo activation, what, in turn, would promote BDNF release, further promoting neurite elongation and branching.

This thesis' main focus was on the role of Gαo on neuritogenesis, and the modulation of this function by APP. However, the formation and growth of dendrites and axon are only part of neuronal differentiation, with synaptogenesis being a crucial step for the full maturation of neuronal cells. There are already a few studies implying Gαo on synapse formation. In *Drosophila*, Gαo translates the signal from Frizzled receptors to the microtubule cytoskeleton during the formation of the neuromuscular junction (NMJ) [9]. Insect APP, like Gαo, is also involved in the proper formation of NMJ [62]. In hippocampal rat neurons, Gαo acts downstream of Wnt5-Frizzled9 signaling to regulate the formation of dendritic spines, a mechanism that also involves the activation of CaMKII, JNK, and PKC [10, 11]. Since we detected an increase in dendritic elongation and branching when overexpressing both Gαo and APP, it is possible that this complex is also important for the formation of dendritic spines and synaptogenesis.

Finally, the lysosomal and proteasomal degradation that Gαo is subjected to, and the fact that APP plays an important part on this control, could be important features of normal neuronal differentiation. The ubiquitin-proteasome-system plays several important functions during brain development and function, including the control of axonal growth and guidance, neuronal migration, dendritic morphogenesis, and synaptic plasticity [63–65]. Likewise, several reports exist showing that lysosomal degradation plays an essential role in the nervous system, especially in the regulation of synaptogenesis and synaptic plasticity [66–68]. Also, Gαo increased levels during neuronal development have been associated with both an increase in its synthesis and a decrease in its degradation [69]. Further studies focusing on the regulation of Gαo turnover might provide vital clues regarding its function in the human brain.

C3. Conclusion

This work had as its main goal to investigate Gαo role in neuronal differentiation, and we achieved it by focusing on the study of Gαo interaction with one of its activator proteins, the amyloid precursor protein. By doing this, we defined a mechanism by which Gαo induces neurite outgrowth by the sequential activation of the STAT3 and ERK1/2 pathway, and demonstrated that APP modulates this mechanism in a phosphoAPP-dependent manner; we identified proteasomal and lysosomal degradation as important mechanisms for the control of APP-Gαo interaction; and we described Gαo as a potential important player in BDNF-induced differentiation. Furthermore, we developed an ImageJ macro to analyze Phase Contrast and Fluorescence neuronal images, thus adding a tool that the scientific community can use freely to study neuronal cells.

This work thus adds new data regarding the function of Gαo on the human brain and unravels new potential mechanisms involved in neuronal differentiation.

References

[1] Asano T, Kamiya N, Semba R, Kato K. Ontogeny of the GTP-binding protein Go in rat brain and heart. *J Neurochem* 1988; 51: 1711–6.

[2] Brabet P, Pantaloni C, Rodriguez M, Martinez J, Bockaert J, Homburger V. Neuroblastoma differentiation involves the expression of two isoforms of the alpha-subunit of Go. *J Neurochem* 1990; 54: 1310–20.

[3] Mullaney I, Milligan G. Identification of two distinct isoforms of the guanine nucleotide binding protein G0 in neuroblastoma X glioma hybrid cells: independent regulation during cyclic AMP-induced differentiation. *J Neurochem* 1990; 55: 1890–8.

[4] Nakata H, Kozasa T. Functional characterization of Galphao signaling through G protein-regulated inducer of neurite outgrowth 1. *Mol Pharmacol* 2005; 67: 695–702.

[5] He JC, Gomes I, Nguyen T, Jayaram G, Ram PT, Devi LA, Iyengar R. The G alpha(o/i)-coupled cannabinoid receptor-mediated neurite outgrowth involves Rap regulation of Src and Stat3. *J Biol Chem* 2005; 280: 33426–34.

[6] Jordan JD, He JC, Eungdamrong NJ, Gomes I, Ali W, Nguyen T, Bivona TG, Philips MR, Devi LA, Iyengar R. Cannabinoid receptor-induced neurite outgrowth is mediated by Rap1 activation through G(alpha)o/i-triggered proteasomal degradation of Rap1GAPII. *J Biol Chem* 2005; 280: 11413–11421.

[7] Won JH, Park JS, Ju HH, Kim S, Suh-Kim H, Ghil SH. The alpha subunit of Go interacts with promyelocytic leukemia zinc finger protein and modulates its functions. *Cell Signal* 2008; 20: 884–91.

[8] Jiang M, Bajpayee NS. Molecular mechanisms of go signaling. *Neurosignals* 2009; 17: 23–41.

[9] Lüchtenborg A-M, Solis GP, Egger-Adam D, Koval A, Lin C, Blanchard MG, Kellenberger S, Katanaev VL. Heterotrimeric Go protein links Wnt-Frizzled signaling with ankyrins to regulate the neuronal microtubule cytoskeleton. *Development* 2014; 141: 3399–409.

[10] Ramírez VT, Ramos-Fernández E, Inestrosa NC. The Gαo Activator Mastoparan-7 Promotes Dendritic Spine Formation in Hippocampal Neurons. *Neural Plast* 2016; 2016: 4258171.

[11] Ramírez VT, Ramos-Fernández E, Henríquez JP, Lorenzo A, Inestrosa NC. Wnt-5a/Frizzled9 Receptor Signaling through the Gαo-Gβγ Complex Regulates Dendritic Spine Formation. *J*

Biol Chem 2016; 291: 19092–107.

[12] Apelt J, Schliebs R, Beck M, Roiner S, Bigl V. Expression of amyloid precursor protein mRNA isoforms in rat brain is differentially regulated during postnatal maturation and by cholinergic activity. *Int J Dev Neurosci* 1997; 15: 95–112.

[13] Holback S, Adlerz L, Iverfeldt K. Increased processing of APLP2 and APP with concomitant formation of APP intracellular domains in BDNF and retinoic acid-differentiated human neuroblastoma cells. *J Neurochem* 2005; 95: 1059–68.

[14] da Rocha JF, da Cruz E Silva OAB, Vieira SI. Analysis of the amyloid precursor protein role in neuritogenesis reveals a biphasic SH-SY5Y neuronal cell differentiation model. *J Neurochem* 2015; 134: 288–301.

[15] Venezia V, Nizzari M, Repetto E, Violani E, Corsaro A, Thellung S, Villa V, Carlo P, Schettini G, Florio T, Russo C. Amyloid precursor protein modulates ERK-1 and -2 signaling. *Ann N Y Acad Sci* 2006; 1090: 455–65.

[16] Kwak YD, Dantuma E, Merchant S, Bushnev S, Sugaya K. Amyloid-beta precursor protein induces glial differentiation of neural progenitor cells by activation of the IL-6/gp130 signaling pathway. *Neurotox Res* 2010; 18: 328–338.

[17] Rama N, Goldschneider D, Corset V, Lambert J, Pays L, Mehlen P. Amyloid precursor protein regulates netrin-1-mediated commissural axon outgrowth. *J Biol Chem* 2012; 287: 30014–30023.

[18] Nishimoto I, Okamoto T, Matsuura Y, Takahashi S, Murayama Y, Ogata E. Alzheimer amyloid protein precursor complexes with brain GTP-binding protein G(o). *Nature* 1993; 362: 75–79.

[19] Okamoto T, Takeda S, Murayama Y, Ogata E, Nishimoto I. Ligand-dependent G protein coupling function of amyloid transmembrane precursor. *J Biol Chem* 1995; 270: 4205–4208.

[20] Ramelot TA, Nicholson LK. Phosphorylation-induced structural changes in the amyloid precursor protein cytoplasmic tail detected by NMR. *J Mol Biol* 2001; 307: 871–84.

[21] Tamayev R, Zhou D, D'Adamio L. The interactome of the amyloid beta precursor protein family members is shaped by phosphorylation of their intracellular domains. *Mol Neurodegener* 2009; 4: 28.

[22] Chakrabarti A, Mukhopadhyay D. Novel adaptors of amyloid precursor protein intracellular domain and their functional implications. *Genomics Proteomics Bioinformatics* 2012; 10: 208–16.

[23] Ando K, Oishi M, Takeda S, Iijima K, Isohara T, Nairn AC, Kirino Y, Greengard P, Suzuki T. Role of phosphorylation of Alzheimer's amyloid precursor protein during neuronal differentiation. *J Neurosci* 1999; 19: 4421–7.

[24] Tian Q, Wang J. Role of serine/threonine protein phosphatase in Alzheimer's disease. *Neurosignals*; 11: 262–9.

[25] Sieracki N, Komarova Y. Studying Cell Signal Transduction with Biomimetic Point Mutations. In: Figurski D (ed) *Genetic Manipulation of DNA and Protein - Examples from Current Research*. InTech. Epub ahead of print 5 February 2013. DOI: 10.5772/35029.

[26] Svoboda P, Novotny J. Hormone-induced subcellular redistribution of trimeric G proteins. *Cell Mol Life Sci* 2002; 59: 501–12.

[27] Hynes TR, Hughes TE, Berlot CH. Cellular localization of GFP-tagged alpha subunits. *Methods Mol Biol* 2004; 237: 233–246.

[28] Zhang K, Duan L, Ong Q, Lin Z, Varman PM, Sung K, Cui B. Light-mediated kinetic control reveals the temporal effect of the Raf/MEK/ERK pathway in PC12 cell neurite outgrowth. *PLoS One* 2014; 9: e92917.

[29] Kirouac L, Rajic AJ, Cribbs DH, Padmanabhan J. Activation of Ras-ERK Signaling and GSK-3 by Amyloid Precursor Protein and Amyloid Beta Facilitates Neurodegeneration in Alzheimer's Disease. *Eneuro* 2017; 4: ENEURO.0149-16.2017.

[30] Yamatsuji T, Matsui T, Okamoto T, Komatsuzaki K, Takeda S, Fukumoto H, Iwatsubo T, Suzuki N, Asami-Odaka A, Ireland S, Kinane TB, Giambarella U, Nishimoto I. G protein-mediated neuronal DNA fragmentation induced by familial Alzheimer's disease-associated mutants of APP. *Science* 1996; 272: 1349–52.

[31] Yamatsuji T, Okamoto T, Takeda S, Murayama Y, Tanaka N, Nishimoto I. Expression of V642 APP mutant causes cellular apoptosis as Alzheimer trait-linked phenotype. *Embo J* 1996; 15: 498–509.

[32] Gibson TJ, Seiler M, Veitia RA. The transience of transient overexpression. *Nat Methods* 2013; 10: 715–721.

[33] Tam JHK, Rebecca Cobb M, Seah C, Pasternak SH. Tyrosine binding protein sites regulate the intracellular trafficking and processing of amyloid precursor protein through a novel lysosome-directed pathway. *PLoS One* 2016; 11: 1–24.

[34] Dotti CG, Sullivan CA, Banker G a. The establishment of polarity by hippocampal neurons in culture. *J Neurosci* 1988; 8: 1454–68.

[35] Takano T, Xu C, Funahashi Y, Namba T, Kaibuchi K. Neuronal polarization. *Development* 2015; 142: 2088–93.

[36] Park J-S, Kim D-H, Yoon S-Y. Regulation of amyloid precursor protein processing by its KFERQ motif. *BMB Rep* 2016; 49: 337–42.

[37] Kaushik S, Cuervo AM. Chaperone-mediated autophagy: a unique way to enter the lysosome world. *Trends Cell Biol* 2012; 22: 407–417.

[38] Locht C, Antoine R. A proposed mechanism of ADP-ribosylation catalyzed by the pertussis toxin S1 subunit. *Biochimie* 1995; 77: 333–340.

[39] Kalisch T, Amé J-C, Dantzer F, Schreiber V. New readers and interpretations of poly(ADP-ribosyl)ation. *Trends Biochem Sci* 2012; 37: 381–390.

[40] Dehmelt L, Poplawski G, Hwang E, Halpain S. NeuriteQuant: an open source toolkit for high content screens of neuronal morphogenesis. *BMC Neurosci* 2011; 12: 100.

[41] Pani G, De Vos WH, Samari N, de Saint-Georges L, Baatout S, Van Oostveldt P, Benotmane MA. MorphoNeuroNet: an automated method for dense neurite network analysis. *Cytometry A* 2014; 85: 188–99.

[42] Encinas M, Iglesias M, Liu Y, Wang H, Muhaisen A, Ceña V, Gallego C, Comella JX. Sequential treatment of SH-SY5Y cells with retinoic acid and brain-derived neurotrophic factor gives rise to fully differentiated, neurotrophic factor-dependent, human neuron-like cells. *J Neurochem* 2000; 75: 991–1003.

[43] Aouadi M, Binetruy B, Caron L, Le Marchand-Brustel Y, Bost F. Role of MAPKs in development and differentiation: lessons from knockout mice. *Biochimie* 2006; 88: 1091–8.

[44] Li Z, Theus MH, Wei L. Role of ERK 1/2 signaling in neuronal differentiation of cultured embryonic stem cells. *Dev Growth Differ* 2006; 48: 513–23.

[45] Samuels IS, Saitta SC, Landreth GE. MAP'ing CNS Development and Cognition: An ERKsome

Process. *Neuron* 2009; 61: 160–167.

[46] Funahashi Y, Namba T, Nakamuta S, Kaibuchi K. Neuronal polarization in vivo: Growing in a complex environment. *Curr Opin Neurobiol* 2014; 27: 215–223.

[47] Zorina Y, Iyengar R, Bromberg KD. Cannabinoid 1 receptor and interleukin-6 receptor together induce integration of protein kinase and transcription factor signaling to trigger neurite outgrowth. *J Biol Chem* 2010; 285: 1358–70.

[48] Asimaki O, Mangoura D. Cannabinoid receptor 1 induces a biphasic ERK activation via multiprotein signaling complex formation of proximal kinases PKCε, Src, and Fyn in primary neurons. *Neurochem Int* 2011; 58: 135–44.

[49] Wu H, Li H, Wu X, Zhao J, Guo J. Reactive oxygen species mediate ERK activation through different Raf-1-dependent signaling pathways following cerebral ischemia. *Neurosci Lett* 2008; 432: 83–7.

[50] Joo D, Woo JS, Cho K-H, Han SH, Min TS, Yang D-C, Yun C-H. Biphasic activation of extracellular signal-regulated kinase (ERK) 1/2 in epidermal growth factor (EGF)-stimulated SW480 colorectal cancer cells. *BMB Rep* 2016; 49: 220–5.

[51] da Cruz e Silva EF, da Cruz e Silva OA. Protein phosphorylation and APP metabolism. *Neurochem Res* 2003; 28: 1553–1561.

[52] Vieira SI, Rebelo S, Domingues SC, da Cruz e Silva EF, da Cruz e Silva OA. S655 phosphorylation enhances APP secretory traffic. *Mol Cell Biochem* 2009; 328: 145–154.

[53] Galve-Roperh I, Rueda D, Gómez del Pulgar T, Velasco G, Guzmán M. Mechanism of extracellular signal-regulated kinase activation by the CB(1) cannabinoid receptor. *Mol Pharmacol* 2002; 62: 1385–92.

[54] Derkinderen P, Valjent E, Toutant M, Corvol J-C, Enslen H, Ledent C, Trzaskos J, Caboche J, Girault J-A. Regulation of extracellular signal-regulated kinase by cannabinoids in hippocampus. *J Neurosci* 2003; 23: 2371–82.

[55] Cho S-K, Choi J-M, Kim J-M, Cho JY, Kim S-S, Hong S, Suh-Kim H, Lee Y-D. AKT-independent Reelin signaling requires interactions of heterotrimeric Go and Src. *Biochem Biophys Res Commun* 2015; 467: 1063–9.

[56] Hoe HS, Lee KJ, Carney RS, Lee J, Markova A, Lee JY, Howell BW, Hyman BT, Pak DT, Bu G, Rebeck GW. Interaction of reelin with amyloid precursor protein promotes neurite

outgrowth. *J Neurosci* 2009; 29: 7459–7473.

[57] Lee GH, D'Arcangelo G. New Insights into Reelin-Mediated Signaling Pathways. *Front Cell Neurosci* 2016; 10: 122.

[58] Brouillet E, Trembleau A, Galanaud D, Volovitch M, Bouillot C, Valenza C, Prochiantz A, Allinquant B. The amyloid precursor protein interacts with Go heterotrimeric protein within a cell compartment specialized in signal transduction. *J Neurosci* 1999; 19: 1717–27.

[59] Ramaker JM, Swanson TL, Copenhaver PF. Amyloid precursor proteins interact with the heterotrimeric G protein Go in the control of neuronal migration. *J Neurosci* 2013; 33: 10165–81.

[60] Ramaker JM, Copenhaver PF. Amyloid Precursor Protein family as unconventional Go-coupled receptors and the control of neuronal motility. *Neurogenes (Austin, Tex)* 2017; 4: e1288510.

[61] Gunther EC, Von Bartheld CS, Goodman LJ, Johnson JE, Bothwell M. The G-protein inhibitor, pertussis toxin, inhibits the secretion of brain-derived neurotrophic factor. *Neuroscience* 2000; 100: 569–579.

[62] Nicolas M, Hassan BA. Amyloid precursor protein and neural development. *Development* 2014; 141: 2543–8.

[63] Tuoc TC, Stoykova A. Roles of the ubiquitin-proteosome system in neurogenesis. *Cell Cycle* 2010; 9: 3174–80.

[64] Hamilton AM, Zito K. Breaking it down: the ubiquitin proteasome system in neuronal morphogenesis. *Neural Plast* 2013; 2013: 196848.

[65] Alvarez-Castelao B, Schuman EM. The Regulation of Synaptic Protein Turnover. *J Biol Chem* 2015; 290: 28623–30.

[66] Yamamoto A, Yue Z. Autophagy and its normal and pathogenic states in the brain. *Annu Rev Neurosci* 2014; 37: 55–78.

[67] Shehata M, Inokuchi K. Does autophagy work in synaptic plasticity and memory? *Rev Neurosci* 2014; 25: 543–57.

[68] Shen D-N, Zhang L-H, Wei E-Q, Yang Y. Autophagy in synaptic development, function, and pathology. *Neurosci Bull* 2015; 31: 416–26.

[69] Brabet P, Pantaloni C, Bockaert J, Homburger V. Metabolism of two Go alpha isoforms in neuronal cells during differentiation. *J Biol Chem* 1991; 266: 12825–8.